This dissertation has been microfilmed exactly as received 65-4676

ROWAN, Lawrence Calvin, 1933-
STRUCTURAL ANALYSIS OF THE QUAD-WYOMING-LINE CREEKS AREA, BEARTOOTH MOUNTAINS, MONTANA-WYOMING.

University of Cincinnati, Ph.D., 1964
Geology

University Microfilms, Inc., Ann Arbor, Michigan

STRUCTURAL ANALYSIS OF THE QUAD-WYOMING-LINE CREEKS AREA, BEARTOOTH MOUNTAINS, MONTANA-WYOMING

A dissertation submitted to
The Graduate School
of the University of Cincinnati

in partial fulfillment of the
requirements for the degree of

DOCTOR OF PHILOSOPHY

1964

by

Lawrence C. calvin Rowan

B.A. University of Virginia, 1955
M.S. University of Virginia, 1957

UNIVERSITY OF CINCINNATI

JULY 31, 19 64

I hereby recommend that the thesis prepared under my supervision by LAWRENCE CALVIN ROWAN

entitled STRUCTURAL ANALYSIS OF THE QUAD-WYOMING-LINE CREEKS AREA, BEARTOOTH MOUNTAINS, MONTANA-WYOMING

be accepted as fulfilling this part of the requirements for the degree of DOCTOR OF PHILOSOPHY

Approved by:

Harvey C. Sunderman

Form 668—Grad. Sch.—1M—4-61

Abstract

The Beartooth Mountains are one of several Precambrian blocks uplifted in the Middle Rocky Mountains during the Laramide Revolution. Quartzites, para-amphibolite and iron-silicate rocks are interlayered with granitic gneisses and migmatites. Granitization of the metasediments has been dated at 2.7 b.y., while zircons with detrital characteristics yield 3.1 b.y. as a minimum date.

The Quad-Wyoming-Line Creeks area is located in the northeastern portion of the Beartooth Range and consists mainly of migmatites, granitic gneisses, amphibolites and quartzites. Mica schists, granitic pegmatites, iron-silicate rocks, ultramafic rocks and mafic dikes are subordinate. Laramide felsic porphyries occur as dikes, sills and small plugs.

Detailed mapping, scale 1:2400, and statistical structural analysis has demonstrated two large N-S to NE-SW trending folds; the Quad Creek synform and the Wyoming Creek antiform. These are later (F_2) folds and plunge S-SW. They are slightly non-cylindrical and non-plane. An earlier, F_1, synform trends E-W in the nose of the F_2 Quad Creek synform adjacent to a metanorite body. No other undoubted large F_1 folds have been observed in the map area. Agmatite is especially widespread in the Wyoming Creek antiform nose. The major F_2 synform is more appressed than the antiform, and the general fold style is "similar".

Mesoscopic statistical structural analysis of the Quad-Wyoming-Line Creeks tectonite has been conducted by measuring axial planes and axes of F_1 and F_2 small folds, hornblende lineations and skialith elongations at 12 structure stations. Stations homogeneous with respect to a particular penetrative fabric element have been combined into macroscopic subareas.

Refolding of small F_1 folds by F_2 folds is common. In general, F_1 folds are isoclinal with an amplitude to wave length ratio of 2:1 or greater. Small F_2 folds are generally more open than F_1 folds and have 1:1 amplitude to wave length ratio. Contrasting mean ductilities are influential in F_1 and F_2 fold styles. Passive flow folds are common in ductile migmatites, granitic gneisses and micaceous rocks, while flexural flow folds are prevalent in relatively non-ductile quartzites and para-amphibolite. Axes of F_1 small folds, B_1, and hornblende elongations, L_1, are folded by F_2 folds. B_1- and L_1-subfabrics reflect F_2 fold geometries in rocks of variable mean ductilities. "Similar" F_2 folds in ductile migmatites, granitic gneisses and micaceous rocks have dispersed B_1 and L_1 along planes, which are great circle girdles on lower hemisphere equal area projections. Slightly "concentric" F_2 folds have formed in relatively non-ductile quartzites and para-amphibolite, dispersing these linear elements along curviplanar surfaces.

B_1 and F_2 small fold axes, B_2, are generally parallel throughout the map area but have different plunges. L_1 lies in the major compositional plane, S_0, and therefore, changes strike progressively around F_2 fold noses. B_1 and L_1 are generally concordant, except in the Wyoming Creek antiform nose. F_2 small folds appear to be parasitically related to the major F_2 folds.

Constructed β S_1-axes are generally coincident with B_2-axes. The mesoscopic S_0-subfabric symmetry is generally triclinic in the map area, while it has been found to be monoclinic on the mesoscopic and macroscopic scales in the Lonesome Mountain area (Larsen, Poldervaart, and Kirchmayer, in preparation). F_2 axial plane foliation (S_2) is well developed in migmatites, and pre-granitization axial shearing has been demonstrated also.

Deformation of L_1 by F_2 folds precludes the possibility that the Quad-Wyoming-Line Creeks area is a B-tectonite, i.e. only one fold set is present. Triclinic S_0-subfabric symmetry supports this conclusion. Concordance of B_1 and L_1 suggests a temporal and genetic relation between formation of the F_1 folds and the crystallization of hornblende. B_1, L_1 and B_2 change strike progressively around the nose of the Quad Creek synform adjacent to the metanorite body. The writer believes that this body has acted as a protective block during granitization preserving the large F_1 fold here. Pre-granitization shearing and S_2 axial plane foliation has destroyed large F_1 folds elsewhere. The metanorite body was probably emplaced prior to F_2 folding, causing divergence of B_2 adjacent to the body.

Acknowledgements

This study has been financed by the National Science Foundation (Grant GP-1386 to L.H. Larsen). The writer has held National Science Foundation Summer Fellowships during 1962 and 1963 and a Cooperative Graduate Fellowship during 1963-64. The Sigma Xi Society provided funds also.

The writer is indebted to Professor Leonard H. Larsen for his guidance throughout this study. Professor William F. Jenks made helpful suggestions after reading the manuscript. Professor D.U. Wise, Franklin and Marshall College, guided the writer in the initial phases of the field work. Use of the Yellowstone-Bighorn Research Association's facilities near Red Lodge, Montana are greatly appreciated also.

Curtis Larsen and Richard Ellis served ably as field assistants during the summer of 1963. Special thanks are due Jack Richard of Cody, Wyoming for his excellent aerial photographic work. The aid in map preparation provided by George S. Meadors, Charlottesville, Virginia is greatly appreciated.

CONTENTS

ILLUSTRATIONS

FIGURE Page

FIGURE Page

MAP

APPENDIX Page

INTRODUCTION

Location and Regional Setting

The Beartooth Mountains are one of several Precambrian blocks uplifted in the Middle Rocky Mountain Region during the Laramide Revolution (Figure 1). The larger blocks typically have major frontal thrusts and gravity tectonic features associated with the uplifts. Vertical uplift ranges from approximately 10,000 to 35,000 feet. Numerous hypotheses have been presented to explain the nature of the uplifting and associated faulting (Bucher et al., 1933; Thom, 1957; Foose et al., 1961; Eardley, 1963; and Wise, 1963).

The Beartooth uplift is located along the Montana-Wyoming border between longitude 109°20'W and 110°40'W and latitude 44°45W to 45°30'N. It is bordered on the north-east by the Bighorn Basin and by the Tertiary volcanics of the Absaroka-Shoshone Mountains on the southwest (Figure 2). The uplift is archlike and asymmetrical. The range is bordered by the Beartooth Thrust on the northeast and by the Gardner fault on the southwest. Laramide uplift has elevated the basement 10,000-12,000 feet above mean sea level and 20,000 feet above its level in the Bighorn Basin (Bucher et al., 1933). The segment southeast of the Stillwater River was thrust northwestward during the Laramide Revolution, while thrusting was to the south-

Figure 1. Location map of the Beartooth Mountains and surrounding Precambrian uplifted blocks (after Eardley, 1963, p. 3).

Figure 2. Location of the Beartooth Mountains. (after Eckelmann and Poldervaart, 1957, p. 1228).

west northwest of this point (Bucher et al., 1933, p.689; 1934, p.173; Foose et al., 1961, p.1152).

Detailed petrological and structural studies have not been conducted in most of the surrounding Precambrian terrains. However, similarities in structural relations, age dates, and metamorphic mineral assemblages in some of the areas suggest that brief comparison here may be beneficial in later discussions.

The Precambrian of the Big Horn Mountains consists primarily of pink to grey granitic gneisses and migmatites with relatively minor pegmatites, amphibolites, ultramafic rocks and mafic dikes (Hoppin, 1961, p.356). While the gneisses and migmatites are regarded by Hoppin (p.360) as metamorphic, no undoubted metasedimentary rocks analagous to the quartzites and iron-silicate rocks of the Beartooth Mountains have been found. Mineral assemblages are characteristic of the almandine amphibolite facies (Fyfe, Turner and Verhoogen, 1958, p.229). Detailed structural analysis has been confined to fracture analysis, and Hoppin (p.356-357) regards the two conspicuous s-surfaces as products of shearing. Gast et al. (1958, p.331) report an age date of 2700 m.y.±150 for these rocks. Pegmatites associated with the youngest granitic rocks in the northern Teton range yield a similar age date (Giletti, 1960). Reed (1963, p.62) reports two Precambrian fold sets in this area and regards the compositional banding as a transposed surface, rather than original sedimentary layering.

The Pony metamorphic rocks in the northern Tobacco Root Mountains consist primarily of gneiss and amphibolitic granulite, while the Cherry Creek series is composed of gneiss, amphibolite, quartzite, marble and anthophyllite schist (Reid, 1963, p.293). He considers the Pony series as lying conformably over the Cherry Creek sequence, in contrast to Tansley's (1933, 57p.) conclusions. The entire sequence is believed by Reid (p.299-300) to have been isoclinally folded about northeast trending axes under granulite facies conditions, producing axial plane schistosity. Metasomatic feldspathization and metamorphic differentiation accompanied formation of these recumbent, isoclinal folds. He further postulates intrusion of basaltic dikes and sills followed by two periods of horizontal shearing, first under granulite facies conditions, then under amphibolite facies conditions. These movements largely destroyed the hinge zones of the isoclinal folds. Broad, concentric folds deformed the earlier sheared flexures and all fold axes plunge north. Rubidium-strontium ages of 1500 m.y. from the Pony and Cherry Creek rocks are suspect, since ages become progressively younger towards Cretaceous intrusives (Giletti, 1960). Zircons from the Little Belt rocks yield $\geq$ 2500 m.y., while their metamorphism is dated at 1900 m.y. (Catanzaro and Kulp, 1964, p. 115).

Metamorphic rock types and age dates are similar in these Precambrian complexes, but structural relations in the Beartooth Range are somewhat anomalous as interpreted by Eckelmann and Poldervaart (1957, p.1230). Multiple folding is characteristic in the Tobacco Root Mountains, the Black Hills (Noble et al., 1949) and in the northern Teton Range, whereas only one system of south plunging folds has been identified in the Beartooth Range (Eckelmann and Poldervaart, 1957, p.1230). Quartzites and iron-silicate rocks in the northeastern Beartooth Mountains are similar to those in the Cherry Creek series in the northern Tobacco Root Mountains. Anthophyllite- and cummingtonite-rich rocks have been reported from both ranges. However, Catanzaro and Kulp (1964, p.18) have dated zircons from quartzites and granitic gneisses from the Beartooth Range at $\gtrsim$ 3100 b.y., and the granitization has been dated at 2700 m.y. $\pm$150 (Gast et al., 1958).

General Geology of the Eastern Beartooth Mountains:

Topographic contrasts between the eastern interior of the Beartooth range and the area near the frontal thrusts are significant. The latter area is characterized by U-shaped valleys, cirques and hanging valleys and a felsenmeer plateau surface stripped of Paleozoic sediments. The former area is less intensely dissected by Alpine glaciation and streams, hence steep U-shaped valleys are not common. Glaciation here was partly of the continental type, producing rolling topography, numerous lakes, roches moutonnées, low relief and generally good exposures. The plateau approximates the original surface between the basement and the Lower Cambrian Flathead sandstone (Hughes, 1933b, p.321). Generally, only a few Paleozoic remnants are preserved, such as Beartooth Butte. Paleozoic sediments reappear in the frontal thrust zone.

Granitic gneisses, migmatites and metasediments are found throughout the Beartooth range, and no single area of 5 square miles has been found which consists exclusively of uniform granitic gneiss (Poldervaart and Bentley, 1958, p.8). Proportions of granitic gneisses, migmatites and metasediments vary somewhat from the peripheral zone to the interior. Metasediments are widespread in the Stillwater area in the northern peripheral zone and are common in the northeastern area. These rock types occur as remnants and skialiths in the interior of the range. Orbicular gneisses constitute large portions of some exposures in the Lonesome Mountain area (Leveson, 1963). Gray to white sodic granitic gneisses are reportedly abundant north of Cooke City and along the northeastern boundary, whereas pink potassic gneisses are widely ditributed in the interior. Mineralogically simple acid pegmatites are widespread and appear as ductless, lensoidal or irregular bodies. Other metamorphic and igneous rock types are para-amphibolites, small ultramafic bodies, dolerite and meta-dolerite dikes, and Laramide felsic porphyries.

Metasediments were formerly argillites, with minor siltites, arenites and banded ironstones (Poldervaart and Bentley, 1958, p.9). Interbedded lavas, tuffs or calcarenites have not been found. Schists and gneisses in the range containing mineral assemblages with muscovite, sillimanite, kyanite and andalusite are believed to have been derived from aluminous argillites. Metamorphism to the amphibolite facies of dolomitic shales or graywackes has produced banded para-amphibolites. Quartzites and banded ironstones are interbedded and grade into para-amphibolite. The ironstones form thin lenses, but quartzites are occasionally thick and persistent units (Map 1). Although recrystallization of the quartzites has produced coarse, pure orthoquartzites similar to vein-type quartz, their high detrital zircon content proves their sedimentary origin (Poldervaart and Eckelmann, 1957, pp.1242-44; Harris, 1959, Plate 4). No stratigraphic marker unit has been recognized, but the thickness of the metasediments is believed to exceed 10,000 feet (Poldervaart and Bentley, 1958, p.10).

Ultramafic rocks and ortho-amphibolites have been studied in detail by Poldervaart (in preparation) in the Highline Lakes area (Fig. 3) and Bentley (unpublished Ph.D. thesis, 1964, Columbia University) in the Question Mark Lake area. Ultramafics usually form lenticular bodies there. Pods show rotation internally, and complex folding is evident in the intervening rocks. Poldervaart and Bentley (1958, p.10) have described a swarm of small ultramafic lenses in the Highline Lakes area which follow the trend of an antiform axis, and each pod plunges in the same direction as the antiformal axis, but at a steeper angle. These pods appear to have formed by disruption of sills or sheets of ultramafic rocks. Ortho-amphibolite bodies are usually small but widespread. However, thick sheets of generally unbanded, homogeneous ortho-amphibolite have been reported north of Beartooth Butte (Poldervaart and Bentley, 1958, p.10).

Detailed mapping by Poldervaart and his students and Wise (1957, unpublished Ph.D. thesis, Princeton University) have outlined a series of broad, open synforms and antiforms which trend generally N-S and plunge 20-40 degrees S. Wise (1957) has recognized the Yellow Gulch antiform, Cyclone synform, Deep Lake anti-

Figure 3. Location map of recent studies in the Beartooth Mountains, (after Poldervaart and Bentley, 1958, p. 4).

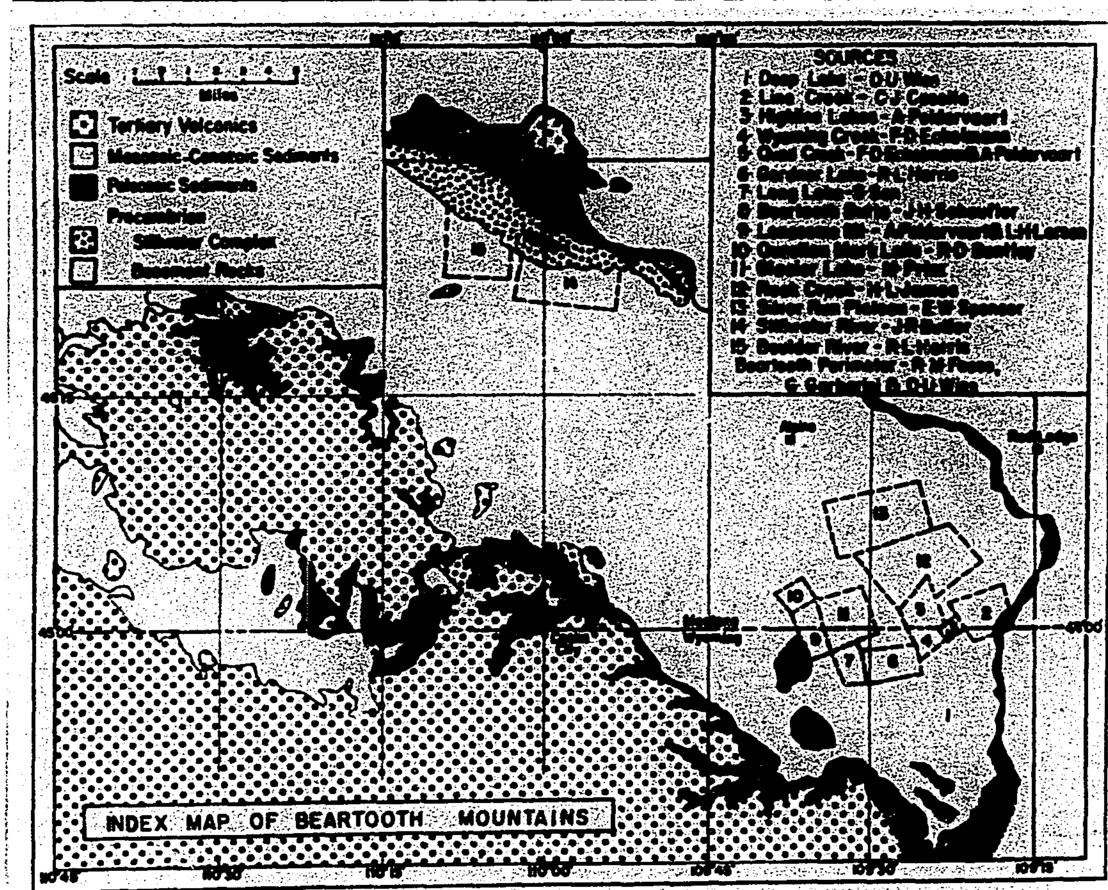

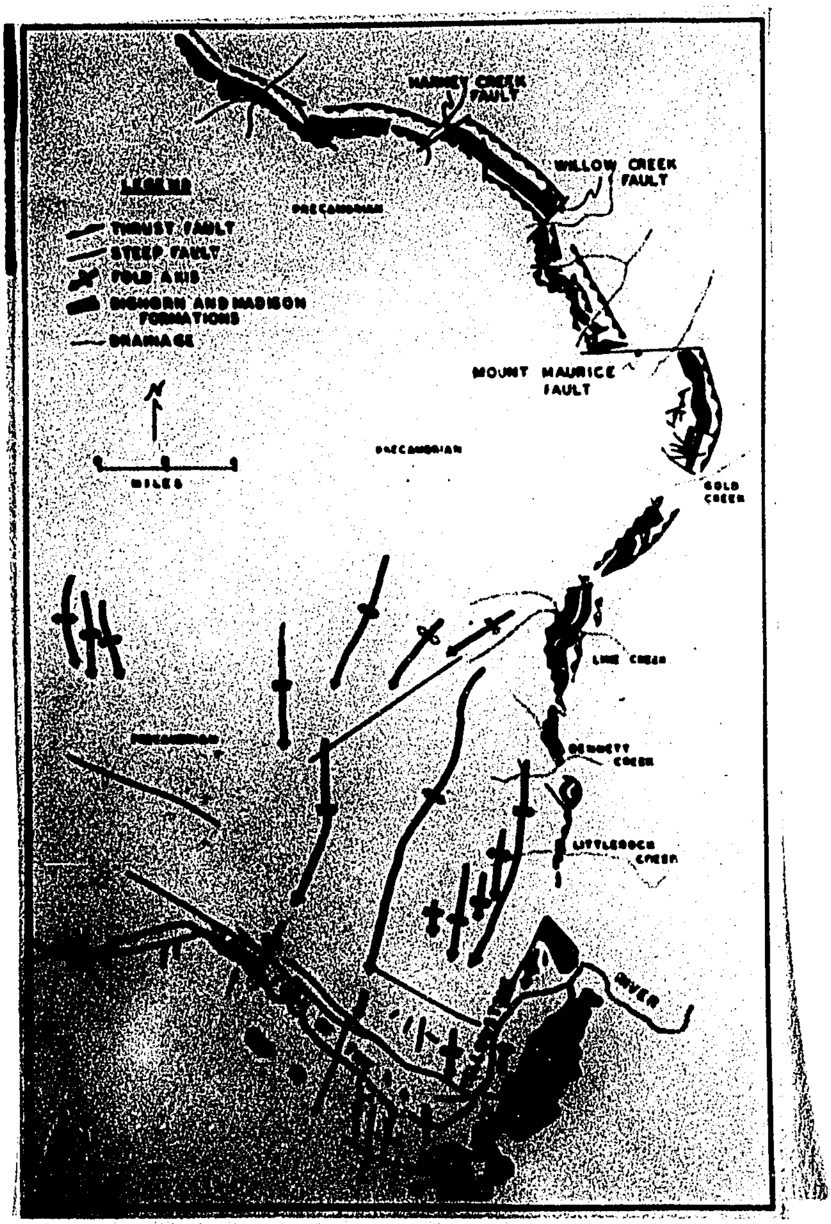

Figure 4. Map showing major fold trends in the Beartooth Mountains (after Foose et al., 1961, modified by the writer and Casella)

form and the Sawtooth synform in the southeast Beartooth range (Fig. 4). The Sawtooth synform continues through the Gardner Lake area (Harris, 1959, Plate 5) into the Quad Creek area (Map 1; Eckelmann and Poldervaart, 1957, Plate 5). The Deep Lake anticline extends towards Line Creek where it is offset by a fault and swings northeast (Poldervaart and Bentley, 1958, p.11). Fold geometries have been defined by outcrop patterns and statistical treatment of compositional foliations. Generally, the fold geometry does not vary from the more granitic areas to the metasedimentary-migmatite areas. Small folds are common in the latter areas but have not been treated in detail prior to this report. Casella (in press), Harris (1959, pp.1195-1196) and Larsen, Poldervaart, and Kirchmayer (in preparation) measured minor fold axes but did not analyze their axial planes. Small fold axes form maxima which are closely coincident with constructed β-axes. However, in the Christmas Lake area axes of small folds lie in a nearly vertical N-S striking plane in the east flank (Harris, 1959, p.1196), and no south plunging statistical maximum corresponding to the regionally defined β-axis is suggested. Major folds plunge gently north in the Cathedral Peaks area near the Stillwater complex in contrast to the regional south plunge (Butler, 1964, unpublished Ph.D. thesis, Columbia University). The writer has found pronounced deviations in the Quad-Wyoming-Line

Creeks area from the regional trend of small fold axes.

Fracture analysis by Spencer (Figure 5) (1959, pp. 467-508) on a regional scale indicates the following dominant trends; N15°W, N45°W, N45°E and N65°W. Other trends are N55°-60°E, N15°-20°E, N-S to N5°E and N85°E to E-W. All of these fractures are nearly vertical. Low dipping fractures occur in the northeast part of the uplift and result from more intense deformation in the overthrust part of the uplift. Five groups of dikes have trends parallel to fractures: (1) Ortho-amphibolite dikes are the oldest dikes and appear to be pregranitization in age. (2) Archean metabasaltic dikes. (3) Unmetamorphosed late Precambrian quartz dolerites. (4) Olivine dolerite dikes, probably Tertiary. (5) Laramide porphyry dikes. Prinz (1964, unpublished Ph.D. thesis, Columbia University) has made additional petrologic studies of the mafic dikes.

The Quad Creek metanorite (Map 1) is one of a few metanorite plugs located along the eastern boundary. Eckelmann and Poldervaart (1957, p.1257) suggest intrusion of this body late in the granitization cycle. However, structural relations suggest emplacement prior to metamorphism, folding and granitization.

The above mentioned quartz dolerite dikes are the thickest and most continuous dikes in the range. They are unmetamorphosed and show little evidence of cata-

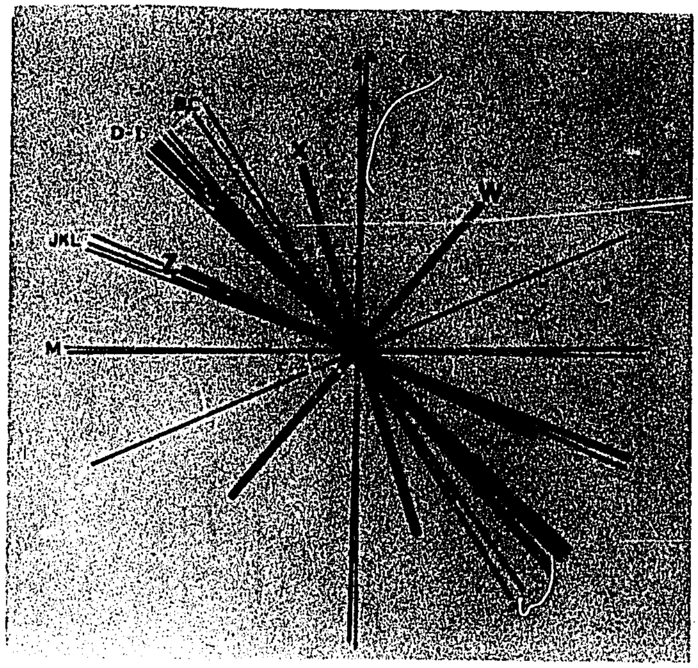

Figure 5. Major fracture trends in the Beartooth Mountains (after Spencer, 1959, figure 7).

clastic deformation. Small off-shoots intruding joints in the country rocks and transection of faults without displacement date these intrusions as younger than the major joint system in the Archean country rocks. They are unconformably overlain by Flathead sandstone near Beartooth Butte. Poldervaart and Bentley (1958, p.12) conclude that these dikes are "Proterozoic" and were preceded by a major uplift.

Laramide faulting in the Archean rocks generally appears to be dominantly northwest trending and nearly vertical. Precambrian trends have controlled these displacements in some instances. Monzonite and granite porphyries are penecontemporaneous with Laramide faulting.

Scope of Study

Detailed studies by Professor Arie Poldervaart and his students (Eckelmann and Poldervaart, 1957; Poldervaart and Bentley, 1958; Harris, 1959) indicated that the granitic gneisses of the Beartooth Range were formed *in situ*. Broad, open folds in Archean metasediments were considered to have formed prior to granitization (Eckelmann and Poldervaart, 1957, p.1230). Pods of metasediments in granitic gneisses and migmatites (Eckelmann and Poldervaart, 1957, Plate 5) suggested that the series quartzite-granitic gneiss might be defined in this area and studied mineralogically, texturally and chemically. Granitic gneisses frequently have modal quartz contents as high as 38 per cent. Detailed mapping by the writer on oblique aerial photographs in 1962 suggested a more complex structural history. Specifically, the following features indicated the need for further structural studies:

(1) Mapping by the writer in the axial zone of the Quad Creek synform just north of the metanorite body (Map 1) defined an E-W trending synform, suggesting an earlier period of folding.

(2) Outcrops of metasediments are frequently "hook" or "crescent" shaped (Eckelmann and Poldervaart, 1957, Plate 5). Carey (1962, p.101) has shown these patterns to be characteristic of superposition of fold sets. Termination of metasediments in each other and not in granitic gneisses or migmatites cannot be attributed to granitization.

(3) Detailed mapping showed that the quartzites are generally continuous.

Measurement of the following linear and planar structural elements on the megascopic and macroscopic scales have been made where possible throughout the map area:

(1) Small fold axes,

(2) Small fold axial planes,

(3) Hornblende elongations,

(4) Elongation of pods and skialiths, and

(5) Compositional foliations.

Geometrical and kinematic analyses of these penetrative fabric elements are presented in the following pages. Results of these investigations also clarify the petrology of the eastern Beartooth Range.

Methods of Investigation

Field mapping was done on low level oblique aerial photographs taken during the summer of 1962. Low level vertical aerial photographs with an average scale of 1:2400 were taken by Jack Richards of Cody, Wyoming during the summer of 1963 for use in more detailed mapping. A 1960 Federal Bureau of Public Roads survey of U.S. Highway 12 was used as a planimetric horizontal and vertical control in the Quad Creek area. Plane table techniques were used to extend control points to the Wyoming and Line Creeks areas. The final base map was prepared using a Kelsh plotter and U.S. Geological Survey vertical aerial photographs, scale 1:47,400.

Eckelmann and Poldervaart (1957, pl.5) mapped the area indicated in Figure 6, scale 1:6000. Casella (in press) mapped the Line Creek area, scale 1:9000, from the frontal thrust to the Line Creek plateau rim (Figure 6). The former investigations dealt primarily with the petrogenesis of the Archean rocks, while the latter studies emphasized structural relations. The writer has

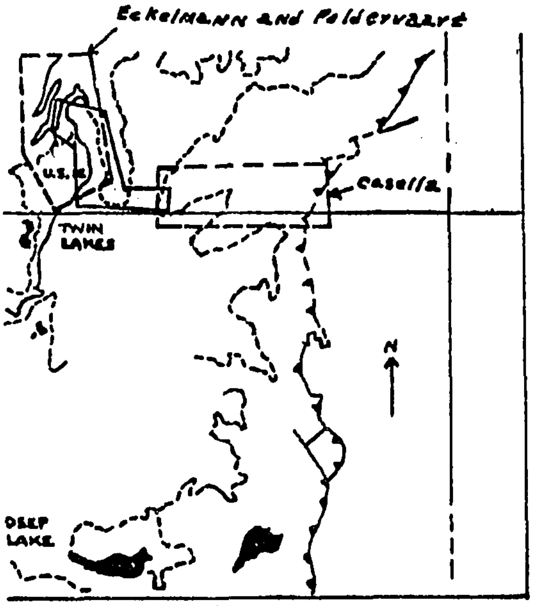

Figure 6. Map locating areas studied by the writer (solid lines) and by Casella and Eckelmann and Poldervaart (broken lines).

mapped the intervening Wyoming Creek area and emphasizes detailed structural analysis. Mapping by Eckelmann and Poldervaart (1957, Plate 5) and Casella (in press) on the scales of 1:6000 and 1:9000 suggests granitization has produced discontinuous bodies of quartzites, para-amphibolite and agmatite in migmatites and granitic gneisses. However, it must be emphasized that unexposed areas are included under leucogranitic gneiss on the former workers' map, and contacts indicated by solid lines are both observed and interpreted. By contrast, Harris (1959, Pl. 5) has shown exposure limits, inferred contacts and observed contacts by different symbols. However, the map gives the impression of being an interpreted outcrop map. The writer has used solid lines for observed contacts only, and dashed lines for inferred and interpreted contacts on Map 1. Dotted line contacts indicate transitional boundaries parts of which have been observed. Areas which are entirely covered are uncolored or no boundary lines are shown between the colors. This method affords the reader a better understanding of the critical exposures and degree of interpretation.

Twelve structure stations (Maps 2a and 2b) were selected for geometrical analysis on the mesoscopic scale. Compositional foliation, S_o, measurements are plotted on Map 1 and have been utilized for statistical purposes also

(Maps 2a and 3a). All available small fold axes and axial planes have been carefully measured within the structure stations, and 75 hornblende elongations have been plotted at each station. Lineations and poles to foliations have been plotted on lower hemisphere equal area projections and contoured using a Duschatko device (Duschatko, 1955). About 20 oriented specimens showing refolding have been sliced and studied using photographs, sketches and selective feldspar staining techniques.

Contoured and uncontoured linear and planar fabric data are keyed to the appropriate mesoscopic sub-domains on Maps 2a and 2b, respectively. Macroscopic fabric subareas and data are shown on Maps 3a and 3b. Mesoscopic structure stations homogeneous with respect to a particular fabric element have been combined to form macroscopic subareas. Detailed analyses of individual diagrams are given in Appendices I, II, III, IV, V and VI.

Previous Investigations

Earlier investigations in the Beartooth Mountains were made on smaller scale maps and emphasized economic or general structural geology. Lovering (1929) reported two intrusive granites, the Goose Creek and the Cooke, from the Cooke City Mining District, the latter being the younger granite. Lammers (1939, unpublished MS. thesis) described the Goose Creek granite as intrusive but regarded the Cooke granite as a product of lit par lit injection, granitization and partial assimilation of hornblende- and biotite-schist by the Goose Creek granite. Foliation was interpreted as platy flow structure. Lenses of biotite-schist, biotite-gneiss, and amphibolite in granitic gneiss were reported as stoped xenolithic blocks. For the Beartooth Range, he distinguished between a core of granitic gneiss nearly free of schist, gneiss and amphibolite lenses, and a mantle of metasediments and migmatites. James (1946) arrived at similar conclusions in his detailed studies of the chromite deposits of the northeast Beartooth Mountains. The quartzites and magnetite-rich rocks of this area were correlated tentatively with the Cherry Creek series by Parsons and Bryden (1952, p.253).

The spectacular eastern frontal thrust received attention in the investigations of Hughes (1933a), Wise (1958; unpublished Ph.D. thesis, 1957, Princeton University), Foose et al. (1961), and Casella (in press). Wise (1958, p.28) reports the intersection of two vertical faults at Clark's Fork Canyon. The N-NE trending faults show a change in dip from vertical at Clark's Fork Canyon to 50 degrees W at Little Rock Creek and nearly horizontal at Bennett Creek. The horizontal displacement is about one mile at this point but is unknown at the northeast corner of the range, where the fault becomes an overthrust. Tear faults are well developed in this area and show the following displacements (Foose *et al.*, 1961, p.1159);

Mount Maurice. . . . . .10,000 feet
Willow Creek . . . . 3,000 feet
Harney Creek . . . . 4,000 feet

Casella (in press) suggests that the Precambrian surface has been displaced about 20,000 feet at Line Creek. This displacement apparently decreases to less than 10,000 feet at the southeast corner of the range.

Control of later structures by Precambrian trends has been suggested by Bucher *et al.* (1933, p.689), Cloos and Cloos (1933), Lammers (1939), Chamberlin (1945), Osterwald (1959, p.41), Foose *et al.* (1961, p.1167) and Wise (1958, p.26). Spencer (1959, pp.497-499, 1958) illustrates parallelism of two Precambrian mafic dike swarms, the major joints in the Archean crystalline rocks and the Laramide faults that border the range.

Investigations conducted as integral parts of the Beartooth Research Project (Figure 3) indicate a complex history for the Beartooth Mountains. The work of Eckelmann and Poldervaart (1957) and Casella (in press) are basic in the writer's study, since portions of the Quad-Wyoming-Line Creeks area were first investigated by them on a smaller scale (Figure 6). This study emphasizes detailed structural analysis of the area as a continuation of investigations in key areas.

The Quad Creek area was the first critical area investigated by the Poldervaart group, and the following geologic history is given by Eckelmann and Poldervaart (1957, p.1225):

> "(1) Original deposition of an Archean sedimentary sequence. (2) Emplacement of metagabbro and ultramafic intrusions, followed by folding; fold axes strike north-northeast. (3) Regional metamorphism and granitization, resulting in a core of granitic gneiss and mantle of migmatites and metasediments with boundaries trending northwest. The last expression of granitization was the production of pegmatites; a few metanorite intrusions were emplaced before pegmatite formation (4) Emplacement of a metabasaltic dike swarm, younger than the pegmatites but probably within the same plutonic cycle, and striking mainly northwest. (5) Emplacement of a younger Precambrian dolerite dike swarm which has the same dominant strike as the older dike swarm. (6) Peneplanation and deposition of Paleozoic sediments. (7) Laramide uplift and thrusting, and emplacement of felsic porphyries early in this cycle. Laramide structures are controlled by basement structures. The dominant northwest trend was established in the Archean cycle of regional metamorphism and granitization, yet the direction of the oldest foldings is unique."

They further conclude that the granitic and tonalitic gneisses and migmatites were formed in situ by migrating alkaline aqueous solutions after open folding about north-

northeast trending axes and metamorphism to the sillimanite-almandine subfacies of the amphibolite facies (1957, p.1249-1250, 1254). The NW trending boundary of granitization intersects the fold axes at about 40°-50° without deflection of the latter structure (1957, p.1249-1250). Parallel interbedding of quartzites, amphibolites, and iron-silicate rocks with migmatites and granitic gneisses was interpreted by them as original sedimentary layering. Studies of growth phenomena of zircons of granitic gneisses, migmatites and quartzites also indicate autochthonous formation of the gneisses (1957, p.1242-1244). Discontinuous bodies of metasediments in gneisses and migmatites were interpreted by Eckelmann and Poldervaart (1957, p.1244) as remnants of progressive feldspathization and granitization.

Fabric analysis by Casella (in press) in the Line Creek area is interpreted by him as indicative of one episode of passive slip folding synchronous with granitization. Although he analyzed compositional banding (S) and various lineations (B), axial planes of small folds were not treated. Figure 7 summarizes his penetrative fabric data. Sub-areas 1, 2 and 3 have been constructed from 19 structure stations. Subarea 1 is located in the northern portion of the area near the frontal thrust, and subarea 2 includes the western portion as well as a small portion of Structure Station 12 in this report (Map 2a).

The fabric in these subareas is monoclinic with coincident B- and β-maxima. Subarea 3 has a triclinic S-fabric and covers the southern portion of the area. He draws an analogy with Prandtl's elongated compression cell (Kanizay, 1962, p.12) and concludes that homogeneity of the fabric varies with position in the cell. Subarea 2 was selected as the cell's center due to its pronounced homogeneity, and the inhomogeneous fabric in Subarea 3 is explained by a possible third dimensional component of flow. Rotation of the data is considered to be a reflection of position of the subareas in the NE trending cell. Small fold sets have not been distinguished, and horizontal lineations are reported in the nose of the SW plunging, upright Line Creek synform.

Additional investigations conducted by the Columbia University group have illuminated the petrogenesis and general geology of the range: Leveson (1963) on orbicular rocks, Skinner (1964, unpublished Ph.D. thesis) on the contact metamorphic zone of the Stillwater complex, and Prinz (1964, unpublished Ph.D. thesis) on the mafic dikes. Poldervaart (in preparation) is studying ultramafic rocks in the Highline Lakes area, and Bentley (1964, unpublished Ph.D. thesis) is investigating similar rocks in the Question Mark Lake area. Butler (1964, unpublished Ph.D. thesis) is completing a study of the Cathedral Peaks area near the

Stillwater complex. The studies of Harris (1959) in the Gardner Lake area and of Larsen, Poldervaart and Kirchmayer (in preparation) are of particular interest, since these are key areas.

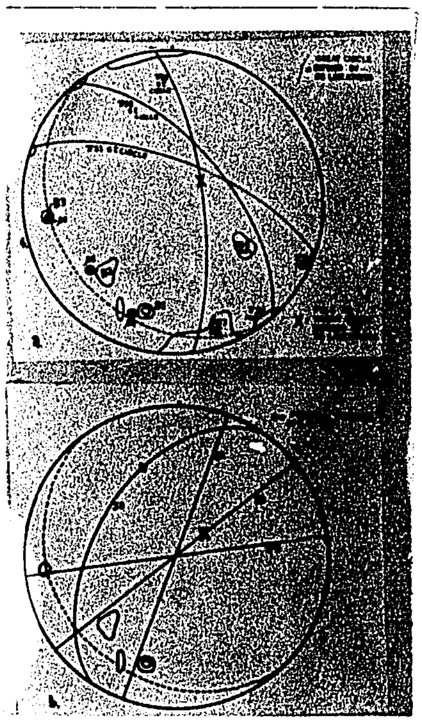

Figure 7. Summary of fabric data from the Line Creek synform area (from Casella, in press).

GENERAL GEOLOGY OF THE QUAD-WYOMING-LINE CREEKS AREA

General Statement:

Excellent exposures occur in the steep canyon walls of Quad and Line Creeks, but outcrops are generally limited to quartzites (Figure 8) and mafic dikes on the felsenmeer plateau surface. The Wyoming Creek area is only moderately dissected, hence outcrops are limited here. Maximum relief in the map area is approximately 1400 feet.

Migmatites are the most abundant rocks in the area, while quartzites, para-amphibolites and granitic gneisses occur in significant and about equal amounts. Ultramafic rocks, ortho-amphibolites, acid pegmatites, ironstones and micaceous schists are subordinate. Precambrian meta-dolerite and relatively unmetamorphosed quartz-dolerite dikes intrude these rocks. Laramide porphyries occur as dikes, sills and small plugs (Map 1).

The Quad Creek synform and the Wyoming Creek antiform are prominent folds with contrasting geometrical properties. Small folds are divisible into two styles and ages, F_1 and F_2. Refolding of F_1 by F_2 has been observed throughout the area but is most prevalent in ductile rocks, such as migmatites, granitic gneisses, micaceous schists and impure quartzites. Location of the Quad Creek metanorite in the axial zone of the major synform (Map 1) is believed by the writer to be structurally

Figure 8. Quartzites in Line Creek canyon and on Line Creek plateau. Wyoming Creek in top portion and Line Creek canyon in bottom portion of photograph.

significant. Age relations of deformation, granitization and emplacement of this body are vital to the geological history of this area and are discussed in the following section. Faulting is of minor importance.

Map Units

General Statement:

Map units are defined according to lithologic variations which are easily recognizable in the field. Many rocks are transitional and are indicated by dotted line contacts on Map 1. Detailed petrographic studies have been made by Eckelmann and Poldervaart (1957, pp.1233-1256) in the Quad Creek area, and the following discussion is intended only to provide an adequate understanding of the rock types to facilitate discussion of the structural geology.

Granitic Gneisses:

Granitic gneisses are characterized by homogeneous distribution of biotite forming a faint or megascopically indistinct foliation. They are widely distributed in the Quad-Wyoming-Line Creeks area. Large portions of the Quad Creek area are underlain by granitic gneisses, but they are more sparsely distributed in the Wyoming and Line Creek areas. Color variations are from pink to gray or white, reflecting variable microcline: plagioclase ratios.

Pink granitic gneisses contain microcline as a major constituent, while gray tonalitic varieties have microcline as an accessory mineral, or it is absent. Moderately sodic plagioclase and quartz are major mineral constituents also. Biotite rarely exceeds 10 per cent by volume. Common accessory minerals are green epidote, chlorite, zircon, apatite, muscovite and opaque minerals. Pink granitic gneisses are more abundant than gray tonalitic gneisses, the latter variety commonly being associated with biotite schists and para-amphibolites.

Pink Granitic Gneiss: Major constituents of pink granitic gneiss are quartz, microcline and oligoclase with accessory amounts of biotite, chlorite, muscovite, apatite, zircon, green epidote and ilmeno-magnetite. Oligoclase is commonly twinned by the albite, Calsbad and pericline laws, but untwinned crystals have been observed. Twin lamellae are frequently bent, cloudy and contain irregular patches of microcline. Evidence of intense cataclasis is rare in these rocks. Rounded grains of quartz are ubiquitous in microcline and andesine. Simultaneous extinction of two or three quartz grains within a single feldspar crystal suggests replacement of quartz by both feldspars. Myrmekitic textures are developed at plagioclase-microcline contacts. Microcline is usually perthitic or shows well-developed gridiron twinning. Eckelmann and Poldervaart (1957, p.1233) cite the following relations as evidence of microcline being later than plagioclase - "The more microcline, the more conspicuous are: (1) turbidity of plagioclase, (2) alteration of biotite to chlorite, (3) myrmekite, and (4) albite rims around plagioclase." Rounded or irregular inclusions of plagioclase in microcline is common also.

Gray Granitic Gneiss: Primary constituents of gray granitic gneiss are quartz and oligoclase. Microcline is a minor constituent as are biotite, epidote, ilmeno-magnetite, sericite, allanite, apatite, chlorite and zircon. Plagioclase crystals are more complexly twinned than in pink granitic gneiss and are often altered to sericite and epidote. Myrmekite is less abundant than in pink granitic gneiss. Gray granitic gneiss is intimately associated with para-amphibolite and biotite schists. Pink granitic gneiss is rarely found in direct contact with these mafic rocks. Microcline becomes progressively less abundant and biotite more abundant upon approaching para-amphibolite and biotite schist contacts.

Migmatites:

Migmatites possess distinct compositional banding as used here. Bands of biotite and occasionally hornblende alternate with quartzo-feldspathic layers and are subparallel or parallel to foliation in interlayered metasediments. Skialiths (Goodspeed, 1948, p.516) of para-amphibolite and biotite schist are common. When the rock appears to contain more than 50 per cent skialiths by volume the term agmatite is used here rather than migmatite. The microcline: plagioclase ratio variation produces colors transitional from pink to gray or white. Gray tonalitic varieties contain biotite, quartz and plagioclase as major constituents. Microcline is present as an accessory mineral or is entirely absent. Pink varieties contain microcline as well as quartz, plagioclase, and biotite, as major components. Plagioclase in these types is somewhat less calcic than in the gray migmatites, where it is oligoclase. Plagioclase is complexly twinned, altered and often forms small porphyroblasts around which biotite wraps. Actinolite, sericite and epidote may be prominent components, and muscovite is rare (Eckelmann and Poldervaart, 1957, p.1237).

Numerous small flow folds occur in migmatites. Axial plane orientations suggest that within these highly ductile units axial plane foliation has transposed the original sedimentary layering, S_o.

Para-amphibolite:

The writer has attempted to distinguish between ortho- and para-amphibolites. Para-amphibolite is generally melanocratic, delicately banded, and interlayered with other metasediments. Ortho-amphibolite shows a more homogeneous texture. This criterion may be insufficient in some cases.

Para-amphibolite is decidedly more abundant than ortho-amphibolite and forms thicker, more consistent layers (Map 1). Chemical composition is variable, especially with respect to hornblende (Eckelmann and Poldervaart, 1957, pp.1234-1235, Table 1). Banding in the para-amphibolite is usually parallel or subparallel to the foliation in adjacent metasediments and migmatites. Ultramafic bodies, ironstones and ortho-amphibolites are commonly associated with para-amphibolite layers (Map 1).

Major constituents are twinned or untwinned oligoclase and green hornblende which may be accompanied by pyroxene. Quartz is commonly a major constituent. Accessory minerals are epidote, microcline, chlorite, apatite, sphene, sericite, allanite, garnet, calcite and ilmeno-magnetite.

Agmatite:

The term agmatite (Sederholm, 1926, p.136) is used here for migmatites containing blocks and lenses of amphibolite and biotite schists in excess of 50 per cent by volume. Anastomosing quartzo-feldspathic veinlets (Figure 9) become more numerous and thicker near migatite and granitic gneiss contacts, finally isolating blocks of amphibolite (Fig. 10) forming agmatite. Skialiths of para-amphibolite become less densely concentrated in the granitic gneiss or migmatite further from the para-

Figure 9. Anastomosing quartzo-feldspathic veinlets in para-amphibolite.

Figure 10. Agmatite in Wyoming Creek.

amphibolite contact. Agmatite is particularly well-developed in the Wyoming Creek antiform nose. Foliation in amphibolite blocks is frequently slightly oblique to that of the surrounding rocks (Figure 11). This may be due to rotation of relatively non-ductile, brittle amphibolite blocks and lenses. Fractured blocks are frequently transected by quartz-feldspathic veins which may have been derived locally through metasomatic processes or intruded into open fissures by plastic flow of the more ductile acid material. In some instances, the para-amphibolite block becomes progressively poorer in plagioclase and correspondingly richer in hornblende from the core of the block to the peripheral portion adjacent to the surrounding gneiss or migmatite. These relations suggest that at least some of the quartzo-feldspathic material has been derived metasomatically from the enclosed blocks. Intermediate rock types show various degrees of development at granitic gneiss-para-amphibolite contacts in the Lonesome Mountain area, yielding the series - biotite amphibolite, biotite-hornblende-epidote-schist, and biotite-epidote-chlorite-schist (Larsen, Poldervaart and Kirchmayer, in preparation). Hornblende-biotite gneiss is widespread in the Wyoming Creek area and may be representative of a similar series in this area.

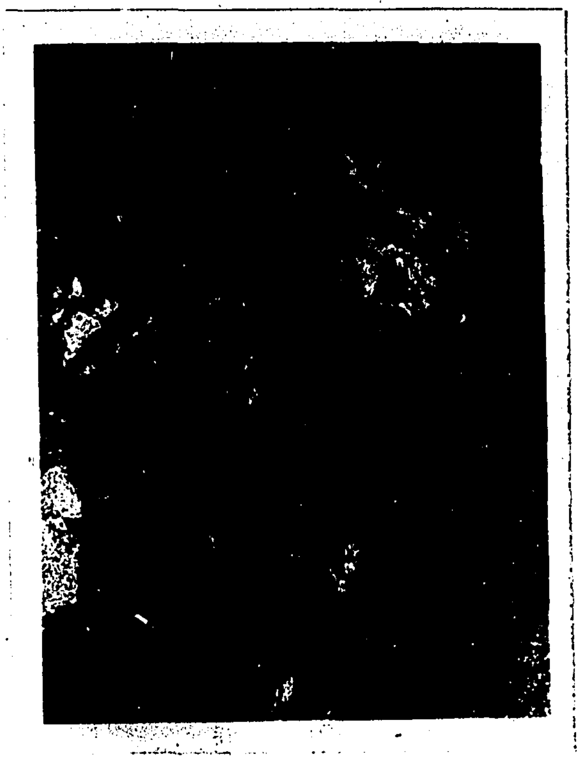

Figure 11. Oblique foliation in rotated para-amphibolite block in grey granitic gneiss from Wyoming Creek.

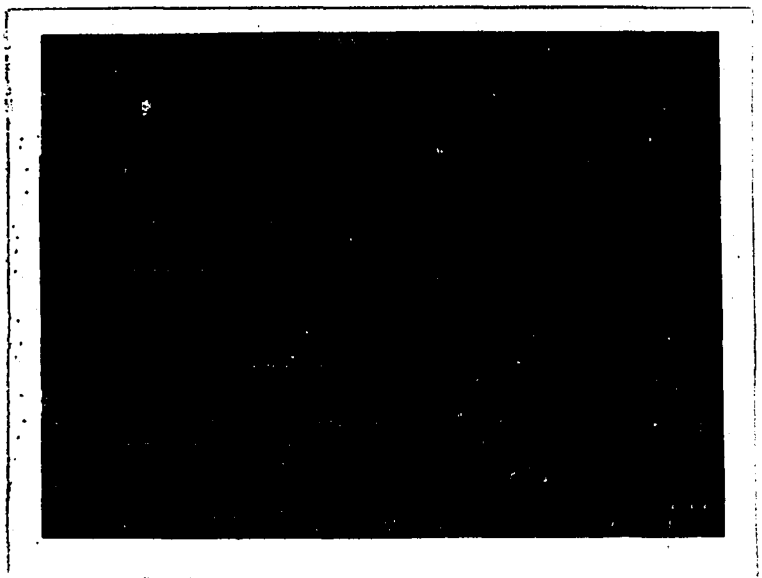

Figure 12. Feldspathized quartzite on the left in contact with pure quartzite on the right.

Ironstones:

Banded ironstones are closely associated with para-amphibolites and consist of light bands of quartz or quartz plus magnetite and dark bands of highly variable composition, usually of magnetite, pink garnet and green hornblende (Eckelmann and Poldervaart, 1957, p.1238). The bodies are generally lenticular and grade into para-amphibolite.

Quartzites:

Quartzites form layers which are continuous in the Quad Creek area and around the Wyoming Creek antiform (Map 1). They are frequently interlayered with mica schists, and a maximum width of approximately 1000 feet is measurable in Line Creek canyon. Skialiths are found occasionally in migmatites and granitic gneisses. Quartzites outcrop continuously from Line Creek to Wyoming Creek (Figure 8) and form very low ridges on the Quad Creek plateau. Individual beds range from a few inches to about 10 feet in thickness.

Although usually light gray or tan in color, green quartzites colored by copper-rich mica are especially common in Line Creek canyon. Porphyroblasts of microcline and plagioclase have developed (Figure 12) along planes which are parallel or subparallel to the contacts with granitic gneisses, migmatites and other metasediments.

By progressive feldspathization, rare skialiths of quartzites in the Quad Creek area appear to grade into granitic gneiss. The quartzites are usually completely recrystallized to coarse-grained rocks resembling vein or pegmatite quartz. However, zircon concentrates show that a majority of the grains are rounded with or without later euhedral overgrowths. Quartzites are also intimately interbedded with other metasediments, such as ironstones, biotite schists, and para-amphibolite; hence, the quartzites in the Quad-Wyoming-Line Creeks area appear to be metamorphosed sandstone. Although Eckelmann and Poldervaart (1957, p.1253) report some cross-bedding, this has not been observed by the writer. Color banding parallel to the major compositional foliation (S_o) has been recognized on Line Creek plateau. Small flow folds are more abundant in feldspathized or biotitic quartzites. Quartz-quartz grain boundaries are generally highly serrate. Boehm lamellae and slightly biaxial quartz grains are common in thin sections. Sillimanite, zircon, garnet, rutile and opaque minerals are common accessories.

Biotite Schists and Gneiss:

Biotite schist and gneiss constitute small, thin layers associated with quartzites and para-amphibolite. Eckelmann and Poldervaart (1957, p.1239) report quartz, plagioclase, greenish brown biotite, with or without epidote, and bluish-green hornblende as major constituents where these rocks are associated with para-amphibolite. Minor minerals are magnetite and ilmenite, sphene, epidote, clinozoisite, zircon, chlorite, sericite, apatite, calcite and allanite. Biotite schists associated with quartzites contain primary amounts of quartz, plagioclase and brown biotite and accessory almandine, garnet, magnetite and ilmenite and microcline. Some of the schists contain significant cordierite and sillimanite and occasionally bronzite and anthophyllite.

Meta-Igneous Rocks

Ultramafic Bodies:

Small, discontinuous ultramafic bodies have been mapped by the writer (Map 1). Mineralogical compositions are quite variable, and the form is usually that of ellipsoidal lenses from about one to several feet in length or small dikes. The foliation of the surrounding rocks bends around the discontinuous lenses, and banding in the ultramafics is commonly oblique to that of the host rocks. These basic bodies are associated with banded para-amphibolite units and contain different combinations of the following minerals: olivine, pleochroic bronzite, pale-green actinolite, colorless or pale-yellow serpentine, talc, phlogopite, chlorite, spinel and magnetite (Eckelmann and

Poldervaart, 1957, p.1240). Casella (in press) reports two ultramafic schists interbedded with para-amphibolites; anthophyllite-orthopyroxene-phlogopite schist and cummingtonite-actinolite-cordierite-phlogopite schist. Detailed studies of the ultramafic rocks have been made by Schafer (1937), James (1946), Poldervaart (1958) and Poldervaart and Bentley (1958).

Quad Creek Metanorite:

Major mineral constituents of the metanorite are plagioclase (An 50-60), bronzite and hornblende. Accessory constituents are quartz, biotite, augite, magnetite and ilmenite, sulfides and apatite. Eckelmann and Poldervaart (1957, p.1240) state that plagioclase poikilitically encloses pleochroic bronzite prisms, and that the amount of plagioclase increases towards the margin of the body. Interstital sulfides occur in lower exposed portions of the intrusive. Metanorite pegmatite veins are transected by discontinuous granite pegmatites. Coarse plagioclase with minor biotite forms small, irregular zones in the upper regions of the body which are essentially anorthosite. A fine-grained border about 5-12 feet thick has been mapped (Map 1). It is absent on the north side where shearing is evident, and biotite gneiss and grey granitic gneiss are immediately adjacent to the metanorite. Major constituents of the fine-grained border rock are altered plagioclase and actinolite. Banding is occasionally detectable and is nearly vertical in all cases. Light bands are composed primarily of plagioclase, whereas the dark layers are dominantly bronzite. The sides of the intrusive may be vertical as shown by Eckelmann and Poldervaart (1957, Plate 5) or dipping steeply towards the center of the body.

Granitic Pegmatite Dikes:

Granitic pegmatites are composed primarily of quartz and microcline and are rarely more than three feet wide. Accessory minerals are biotite, muscovite, and albite; minerals such as tourmaline, beryl and topaz are absent. The bodies are usually lenticular or irregular patches. Most of the dikes are crosscutting and have walls coated with biotite, epidote and chlorite. Gradational contacts with host rocks have been observed in Wyoming Creek.

Mafic Dikes:

Three Precambrian dike swarms have been identified which consist of Archean ortho-amphibolite, Archean metadolerite, and late Precambrian dolerite. The petrology of the dikes has been studied in detail by Prinz (1964, unpublished Ph.D. thesis, Columbia University).

Igneous Rocks

Laramide Porphyry:

Dikes, plugs and sheets of felsic porphyry are widely distributed throughout the area. Contacts follow irregular joints or smooth curved planes. The phenocrysts are orthoclase, sodic plagioclase, biotite, quartz and hornblende of variable size and number, enclosed in a dense tan or greenish groundmass. The dike situated in the fault zone at the head of Line Creek canyon (Map 1) has numerous xenoliths of migmatite, dolerite and quartzite. It is also highly brecciated in a narrow zone which parallels the trend of the fault zone.

Structural Features

Large Folds:

Large scale (1:2400) mapping (Map 1) and statistical structural analysis by the writer has demonstrated two large folds in the Quad-Wyoming-Line Creeks area; the Quad Creek synform and the Wyoming Creek antiform. A synform is defined by Ramsay (1958, p.274) as a fold which closes downward and for which there is no top or bottom criteria; an antiform closes upward. Both major structures are outlined by the outcrop pattern and foliation (S_o) trends in quartzites, para-amphibolite, granitic gneisses and migmatites (Map 1). Eckelmann and Poldervaart (1957, p.1230) state that "in the Quad Creek area the structure is continuous across the gradational boundary zone between migmatites and metasediments to the northeast and granitic gneiss to the southwest." This boundary is not defined within the limits of the writer's area (Map 1). Transection of this boundary by the synform without deflection implies that the folding is pre- or syn-granitization in age. A general paucity of cataclasis in the granitic gneisses and migmatites supports this conclusion. Figure 22 contains slip surfaces, but the feldspars along these zones are not sheared.

Contrasting geometrical relations are evident from inspection of Map 1 and statistical structural analysis (Maps 2a, 2b, 3a and 3b). The Wyoming Creek antiform is open and approximately 3 miles in breadth. Parasitic folds (F_2) have plunges from 40°-55° to S20°-40°W and are slightly asymmetrical to the southeast. Therefore, in contradiction of Eckelmann and Poldervaart's (1957, p.1230) statement that 10°-30° S-SW "is the overall plunge of the folds in the Quad Creek area and in adjacent areas," the Wyoming Creek antiform is slightly non-cylindrical (Turner and Weiss, 1963, p.108). Variation in the plunge of the adjacent Line Creek synform from 30° to 40° supports the writer's conclusion (Casella, in press). The Wyoming Creek fold was not known to exist by Eckelmann and Poldervaart (1957, p.1230) and Casella (in press). In contrast, the Quad Creek synform trends N10°E and plunges about 10°-15° S-SW and is more appressed than the adjacent antiform. The limbs dip at steep angles, generally between 60° and 75°, and the breadth is about 2 miles. The macroscopic subfabric symmetry with respect to linear and planar structural features is triclinic, while it is monoclinic for the Wyoming Creek antiform. The axial plane of the Quad Creek synform appears to be nearly vertical.

Geologic mapping and statistical structural analysis in the nose of the Quad Creek synform (Map 1) has defined an east-west trending synform which is folded by the major north-south trending fold. Therefore, the east-west trending synform is earlier than the Quad Creek synform and is designated F_1. In referring to the north dipping foliations on the south limb of this F_1 fold, Eckelmann and Poldervaart (1957, p.1230) state "locally the plunge steepens, as it does just north of the Quad Creek metanorite."

Small parasitic F_1 fold axes (B_1) and hornblende lineations (L_1) rotate around the major nose and converge on the axial zone (Map 2b). The F_1 synform has an estimated wave length of 400 feet and a nearly vertical warped axial plane. The eastern F_1 nose is outlined by quartzites and para-amphibolite, showing the isoclinal form of this fold. The anticipated western F_1 nose at the quartzite termination has not been located by the writer. Complex, tight folding of the quartzite nearly adjacent to the metanorite suggest that the south F_1 limb may not continue to the western nose. However, the sequence of rock types in the road cuts of upper and lower Quad Creek are nearly identical (Map 1). The writer concludes that the western nose exists but is covered. Granitization of the generally resistant quartzite has been considered as an explanation of this western termination, but there is little to recommend it. Most significantly, no quartzite or para-amphibolite skialiths have been found in the surrounding granitic gneiss. Sudden disappearance of resistant rock types without remnants in the granitic gneiss is not plausible to the writer. Although the quartzite-granitic gneiss contact bears evidence of Laramide shearing (Figure 13), sharp, undisturbed contacts in the same area render shearing as a local feature. Pre-granitization shearing has been noted just south of this area and may explain the disappearance of the quartzites in the western outcrop. An original sedimentary discontinuity is also a plausible hypothesis for the quartzite termination here. However, there is no evidence in the immediate area for these last two hypotheses.

The Quad Creek metanorite is located in the nose of the Quad Creek synform and is elongated parallel to the axial trend. As previously mentioned, shearing is evident around the northern periphery but not around the southern border (Map 1). Gray granitic gneiss and biotite gneiss occur in the northern area adjacent to the metanorite, and the compositional foliation (S_o) is complexly swirled. The age date derived from biotite in the metanorite is 2700 m.y. ±150 (Poldervaart, personal communication), which agrees with the date of granitization derived from granitic gneiss biotite (Gast et al., 1958, p.331). The age date from the metanorite biotite may be the date of recrystallization and granitization and therefore, be only a minimum date for the biotite. F_1 and F_2 fold axes rotate[1] around the Quad Creek synform nose (Map 2b) and converge on the axial zone, while they strike parallel to the axis of Wyoming Creek antiform in the nose. The metanorite body has apparently influenced the orientation of these small fold axes in the major synform nose. Post-F_1 and F_2 emplacement might be anticipated to have deflected these lineations. However, these relations do not preclude intrusion synchronous with the early stages of F_1 folding. Granite pegmatites in the metanorite appear to have formed under the influence of the synformal shape and its attitude (Figure 17). Therefore, the metanorite

---

[1]Rotation of lineations is used here to denote a progressive change of strike around later fold noses. Lineations on opposing sides of a later axial zone converge where their plunges steepen inward or downward towards this axial zone. They diverge when their plunges steepen away from the axial zone. The plunges are opposite in direction on opposing sides of the later axial trace.

body does not appear to be younger than the present form and attitude of the Quad Creek synform. The writer believes that the metanorite was emplaced prior to F_1 folding and has acted as a structural buttress during deformation. Shearing on the north side of the body may be due to a shouldering effect upon intrusion of a partially crystallized body.

Structural relations have influenced the distribution and continuity of quartzites, para-amphibolite and agmatite. Although tightly folded in the nose, quartzites are continuous throughout the Wyoming Creek antiform (Map 1). Para-amphibolite is also continuous throughout the antiform, but intense disjointing and formation of anastámosing quartzo-feldspathic veins in the para-amphibolite has produced agmatite in the nose. The quartzite and para-amphibolite layers thicken slightly in the nose, suggesting flowage into this zone. In general, both rock types are less continuous in the Quad Creek synform nose (Map 1). However, agmatite is not abundantly developed there, and F_1 folds are represented on the mesoscopic and macroscopic scales, while no large F_1 folds have been identified elsewhere. The writer believes that refolding of these F_1 folds by the later (F_2) in the Quad Creek synform explains the lower outcrop continuity of para-amphibolite and quartzites here relative to the remainder of the area.

The association of lensoidal, banded ironstones with para-amphibolite is demonstrated in the Quad Creek area (Map 1). Although the bodies are discontinuous, they occur around the Quad Creek synform nose in association with the para-amphibolite and quartzites. They also are found with these rock types in the west flank of the major synform (Map 1). Similarities between the sequence in the nose and the west flank suggest that the folds in the latter locality are F_1 folds. This may be the F_1 antiform adjacent to the F_1 synform in the Quad Creek synform nose.

Ortho-amphibolite and chromite-bearing ultramafic rocks occur as small lensoidal bodies throughout the area in association with para-amphibolite, but relatively large bodies occur in the Quad Creek area and in Line Creek canyon (Map 1). The outcrop pattern in Line Creek canyon demonstrates folding of the ultramafic bodies by S-SW plunging F_2 folds. The bodies here and in the Quad Creek chromite mine appear to be discontinuous along strike due to plastic flowage of the ultramafic rocks. Individual ultramafic pods are rotated, possess highly variable magnetic directions, and folding in intervening para-amphibolite rocks is highly complex. Parasitic F_1 folds in the Quad Creek area fold the ultramafic units (Map 1). Therefore, the writer concludes that these rocks were emplaced as sills prior to F_1 folding. The largest ortho-amphibolite body occurs in association with para-amphibolite and ironstone in the larger F_1 fold (Map 1). It is only about 3-4 feet thick and appears to be a discontinuous sill.

Micaceous schists are associated with quartzites and para-amphibolite as thin layers in which F_1 passive flow folds are abundant (Map 1). Although they are most prominent in the excellently exposed quartzites of Line Creek and Quad Creek, thin layers have been found throughout the map area.

Granitic pegmatites are widespread as irregular or lensoidal bodies which transect the Archean rocks except metadolerite, "Proterozoic" quartz-dolerite dikes, and Laramide porphyries. Bodies nearly concordant with the major compositional banding, S_0, appear to be more abundant than discordant pegmatites. Concordant pegmatites occasionally have gradational contacts with granitic gneisses, migmatites and quartzites (Wyoming Creek, Map 1). Although some of the bodies appear to be folded, such as in the Wyoming Creek area, this may be due to selective replacement of a folded bed. Acid pegmatites are especially abundant in the agmatized Wyoming Creek antiform nose (Map 1), suggesting a possible genetic and temporal relationship between formation of the major fold, agmatization and pegmatization.

Faults:

No major faults have been observed in the Quad-Wyoming-Line Creeks area. Northwest trending faults with small, apparent horizontal displacements have been mapped in the west flank of the Wyoming Creek antiform and at the southwest head of Line Creek canyon. The latter area has been mapped carefully by the writer (Map 1), and the relations are; (1) The southwest quartzite-mica schist block has apparently been displaced horizontally about 200 feet to the northwest. (2) A Precambrian mafic intrusion lies approximately in the major compositional plane (S_0) and shows little or no offset. (3) Laramide porphyry intrudes the migmatites, quartzites and mafic dike and contains xenoliths of these rocks. (4) The porphyry is sheared, but no offset was discerned. Small porphyry bodies located in the southeast portion of the fault zone are not intensely sheared. Casella (in press) suggests that the age of faulting is Upper Cretaceous, since the Lower Cretaceous porphyry is involved. Alternately, it is possible that the faulting took place prior to intrusion of the mafic dike or sill; hence, the dike shows no offset. Reactivation of faulting during Upper Cretaceous time with little or no displacement would produce shearing in the porphyry.

Sheared and mylonitized zones have been noted in the Quad Creek and Line Creek areas. The plane of slippage and shear is parallel to compositional banding, S_o. Eckelmann and Poldervaart (1957, pp.1230-1231) suggest that Laramide thrusting to the northeast has been translated partly in the major folds into compression at right angles to the Quad Creek synform axis.

Dike Trends:

The writer has not studied dike trends in the Quad-Wyoming-Line Creeks area. Figures 14 and 15 summarize the data of Eckelmann and Poldervaart (1957, p.1231). Low dipping mafic dikes are not common in the southern Beartooth uplift, but Laramide porphyry dikes usually have low dips. In the Quad Creek area, the large porphyry dikes trend N30°-40°W and dip 25°-35°E. They appear to be controlled by Laramide trends. The spread of poles to small porphyry dikes is large in Figure 14, but the maxima attitudes are N15°W, 36°E and N35°E, 48°NW. Eckelmann and Poldervaart (1957, p.1230) point out that the acute angle between these two planes is bisected by the Quad Creek synform axis, N10°E. They report (p.1231) that of 22 dikes on the east limb 13 dip east, 9 dip west. Hence, orientation of the smaller porphyry dikes appears to be strongly influenced by the synformal structure. These dikes show a northeast trend and dip at low angles northwest in the Line Creek area (Figure 16) (Casella, in press). The data are sparse, but they may be controlled

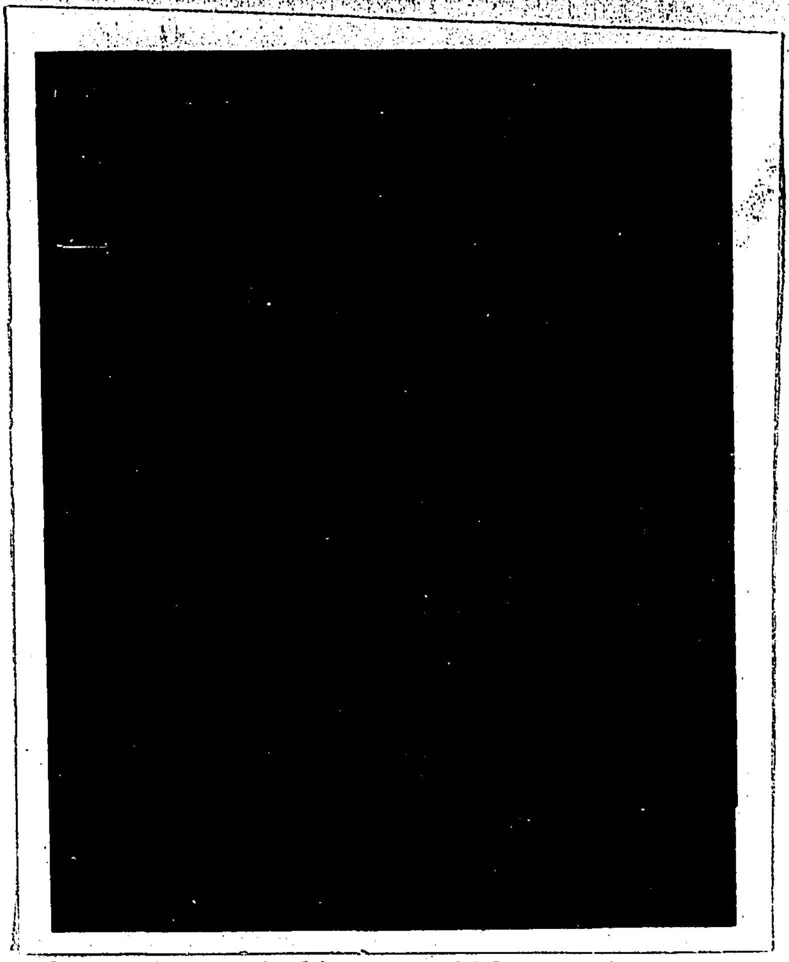

Figure 13. Sheared quartzite-granitic gneiss contact in the Quad Creek area.

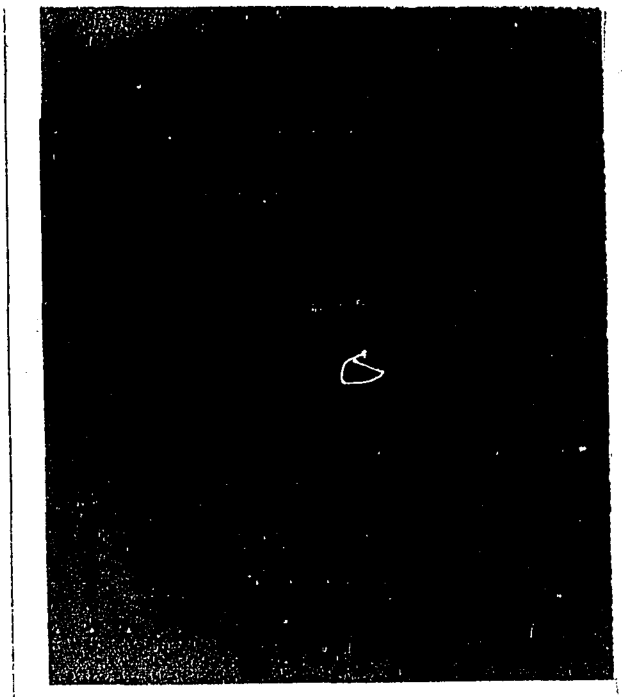

Figure 14. Plotted poles to 89 Laramide felsic porphyry dikes in the Quad Creek area (after Eckelmann and Poldervaart, 1957, p. 1231, figure 3).

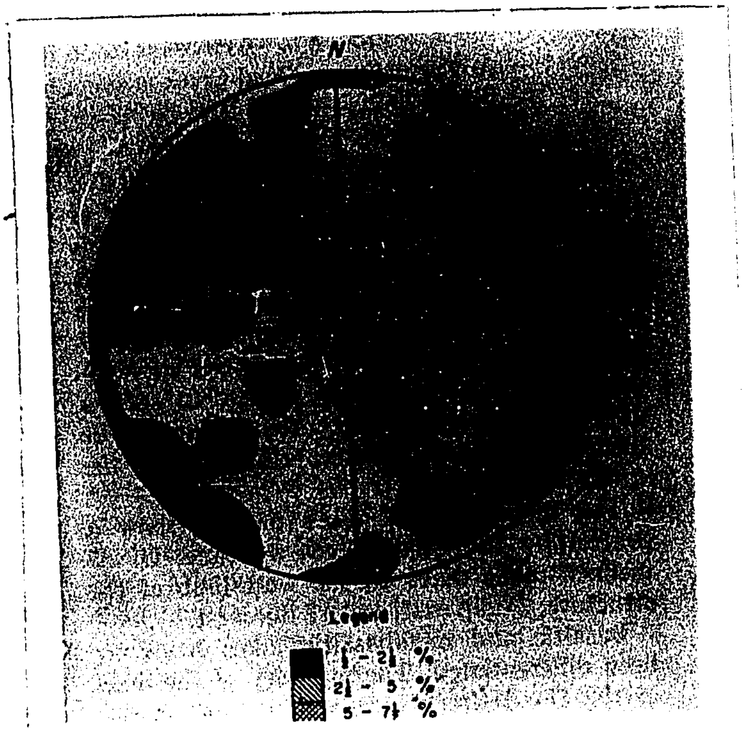

Figure 15. Plotted poles to 89 Precambrian mafic dikes in the Quad Creek area (after Eckelmann and Poldervaart, 1957, p. 1231, figure 5).

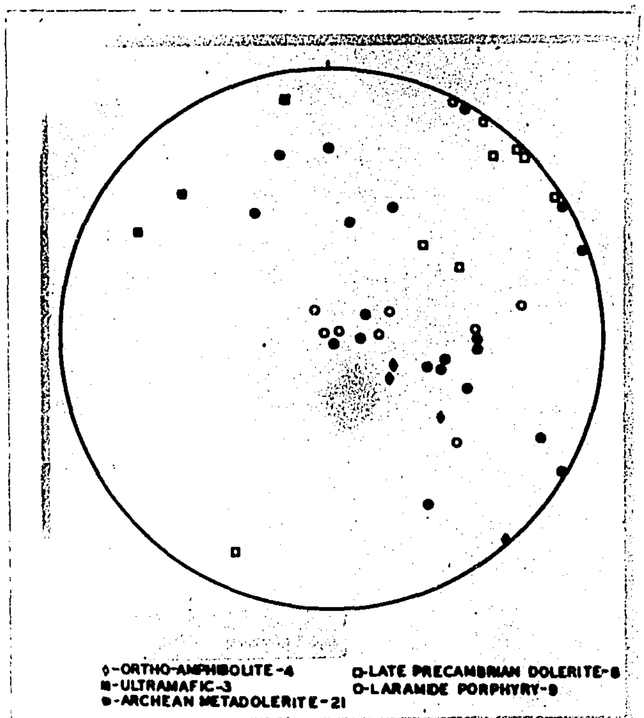

Figure 16. Plotted poles to 45 Precambrian mafic dikes from the Line Creek area (after Casella, in press).

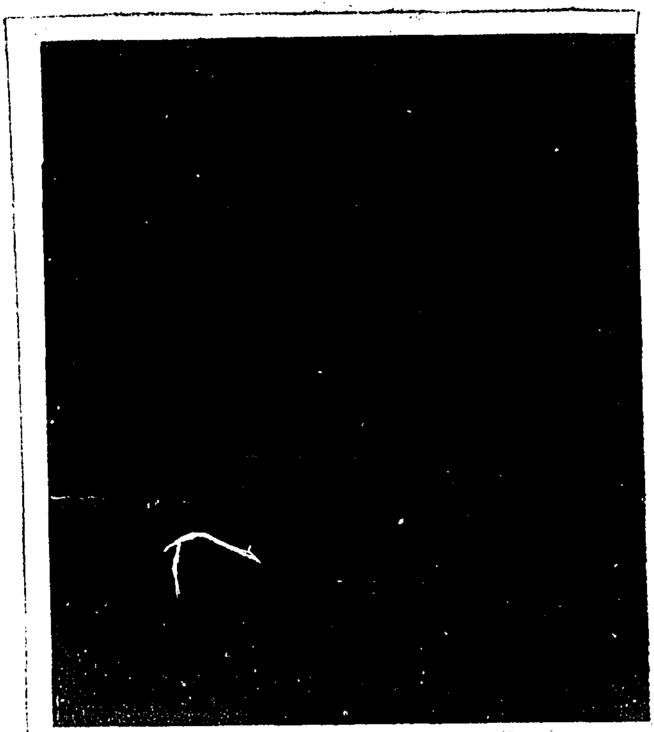

Figure 17. Attitude of Precambrian pegmatite dikes in Quad Creek metanorite and in granitic gneisses and metasediments (after Eckelmann and Poldervaart, 1957, p. 1232, figure 6A).

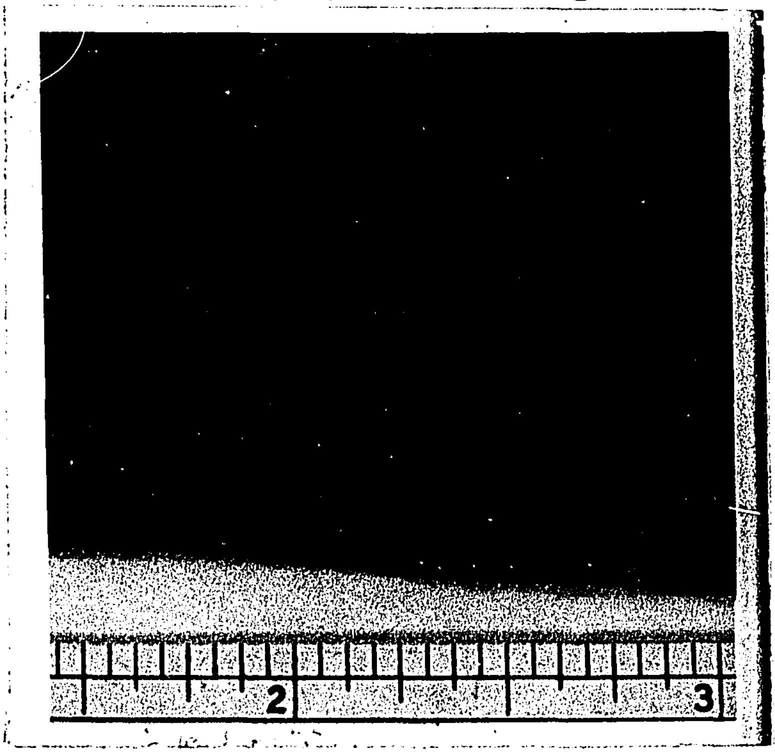

Figure 18. Stained F_1 passive flow fold with large wave length to amplitude ratio. Alkali feldspar appears white. Scale is in inches.

by Laramide trends.

Pegmatite dikes (Figure 17) show similar controls by the Quad Creek synform (Eckelmann and Poldervaart, 1957, p.1232). These workers state that the 13 Archean acid pegmatites in the metanorite body show random orientation (p.1233). Although scatter is slightly greater than for pegmatites in metasediments, migmatites and granitic gneisses, the writer does not feel that the pegmatites in the metanorite are randomly oriented. The dips and overall pattern is very similar to that of the pegmatites outside the intrusion. This may be corroborating evidence that the metanorite was intruded prior to folding (F_2).

Casella (in press) has shown that "Proterozoic" dolerite dikes trend northwest and dip steeply (Figure 16). Ortho-amphibolite and Archean metadolerites have dominant northeast trends and dip northwest at low to moderate angles. Unmetamorphosed and metamorphosed dikes are not differentiated in the Quad Creek area (Eckelmann and Poldervaart, p.1232), so the northwest trending vertical dikes may be predominantly late dolerite dikes. The N50°W and N45°E trends correspond closely with prominent Beartooth fracture trends (Spencer, 1959, p.494).

<u>Small Folds</u>

<u>General Statement</u>: Small folds occur abundantly in migma-

tites, impure quartzites, granitic gneisses, mica schists and para-amphibolite throughout the Quad-Wyoming-Line Creeks area. Although transitional types are common, two principal fold styles can be recognized: (1) Highly appressed, isoclinal folds, referred to as F_1. (2) Non-isoclinal, open folds which have rounded and thickened hinge zones. These folds frequently refold F_1 folds and are designated F_2. "Hook" and "crescent" outcrop patterns characteristic of refolding (Carey, 1962, p.101) and contrasting fold styles in F_1 and F_2 facilitate identification of these folds. Fold axes and axial planes have been carefully measured in the field and laboratory and analyzed statistically. Refolded samples have been studied to ascertain geometrical and mineralogical relations of earlier and later small fold events.

<u>Small Appressed Isoclinal Folds, F_1</u>: Small F_1 folds are generally most abundant in rocks of high mean ductilities (Donath and Parker, 1964, p.50), such as migmatites, granitic gneisses, impure quartzites and micaceous schists. They have an amplitude to wave length ratio of 2:1 or greater (Figure 18). In more ductile rocks, such as migmatites, hinges are sharp and the axial plane thickness is nearly constant, thus suggesting passive flow, <u>i.e.</u> the layering has not controlled the fold geometry and has acted passively (Donath and Parker, 1964, p.56). Less ductile rock types,

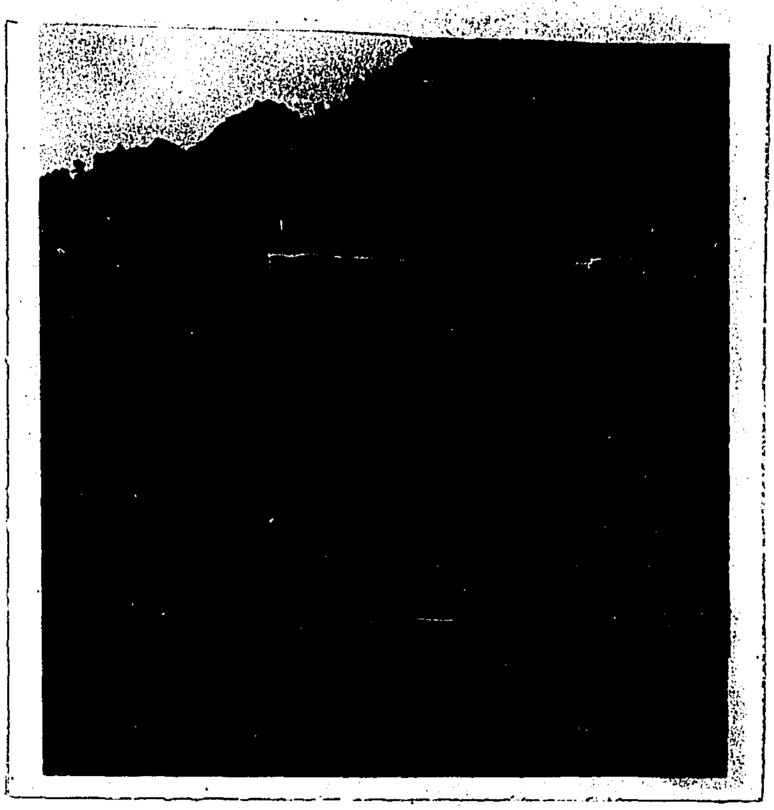

Figure 19. F_1 fold in relatively non-ductile para-amphibolite.

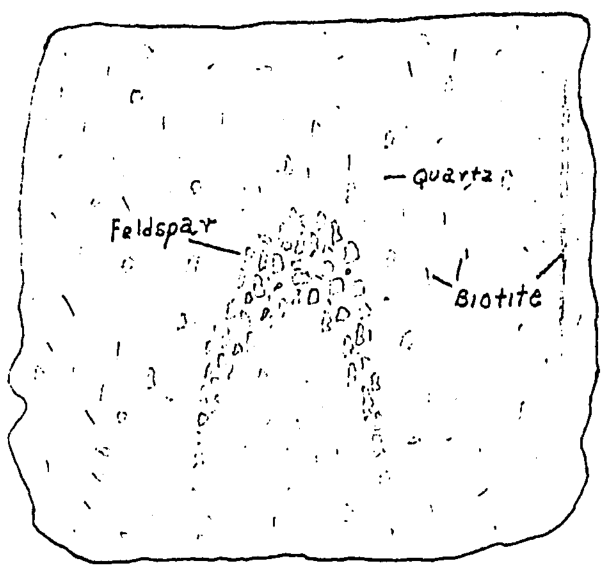

Figure 20. Feldspars concentrated in the nose of an F_1 fold in quartzite. 1/4 natural size.

such as pure quartzites and para-amphibolite, tend to have folds with variable axial plane thickness and rounded hinges (Figure 19). Folding in these cases appears to be partially flexural. In general, small F_1 folds are more abundant in the Quad Creek synform than in the Wyoming Creek antiform. F_1 folds formed by passive flow generally have wave lengths of 3-5 inches. F_1 folds are usually non-plane and non-cylindrical on the mesoscopic scale (Turner and Weiss, 1963, p.108).

F_1 folds with 4-5 foot wave lengths are parasitically related to the E-W trending F_1 synform in the Quad Creek area (Map 1). They have rounded crests and troughs and are generally "similar" in style. These folds are folded by open F_2 small folds which are overturned to the N-NE. Mapping and statistical structural analysis shows convergence of these F_1 fold axes on the major Quad Creek axis (Map 2b). Therefore, geometrical analysis in this area has deomonstrated that these isoclinal appressed F_1 folds are distinctly older than the Quad Creek synform. Additionally, they are warped by small F_2 folds which rotate around the major synform nose also. These geometrical relations suggest that both F_1 and F_2 folds are older than the major synform. Evidence from the remainder of the area indicates that F_2 folds are parasitically related to the larger folds but F_1 small folds are older than F_2. Therefore, the writer concludes that the rotation of F_2

folds around the Quad Creek synform nose is due to a buttressing effect of the metanorite body. Statistically, structural data presented in the next section support this conclusion.

No axial plane foliation has been observed in F_1 folds, suggesting that it has been destroyed by recrystallization if it ever existed. Although Reid (1963, p.294) has described axial plane folding (Scotford, 1956, pp.1155-1198) of earlier isoclinal, appressed folds which show axial plane foliation in the Cherry Creek and Pony series in the Tobacco Root Mountains, these rocks are not granitized to the extent of the older Archean rocks in the Beartooth Range. S_0 in the map area may be axial plane foliation formed by refolding of F_1 by F_2 folds. This point will be discussed in detail in a later section. Figure 20 shows both feldspars concentrated in the nose of an F_1 small fold from the Quad Creek synform area with no evidence for development of feldspar in the axial plane direction.

<u>Small Open Folds, F_2</u>: These occur in migmatites, granitic gneisses and metasediments throughout the area. These folds are plane and cylindrical on the mesoscopic scale (Turner and Weiss, 1963, p.108). Their amplitude to wave length ratio is approximately 1:1, and the wave length range from about 4 inches to 20 feet. Axes and axial planes of only

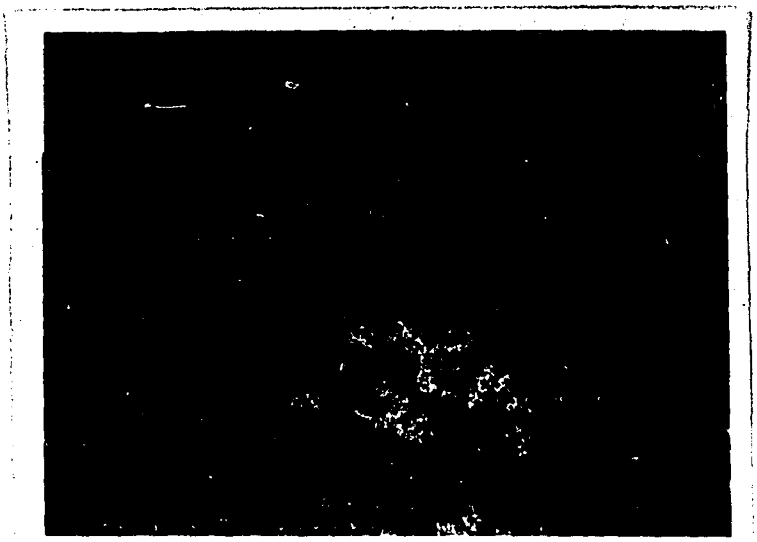

A

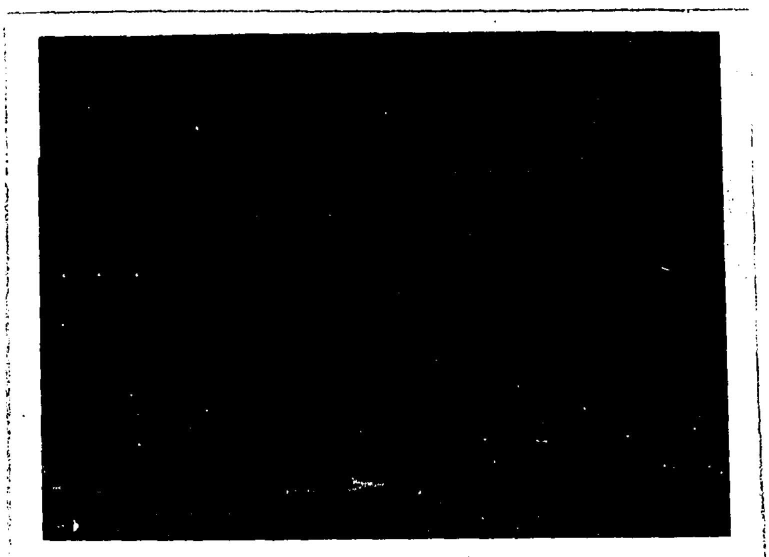

B

Figure 21. F_2 flexural flow folds in quartzite from Structure Station 12.

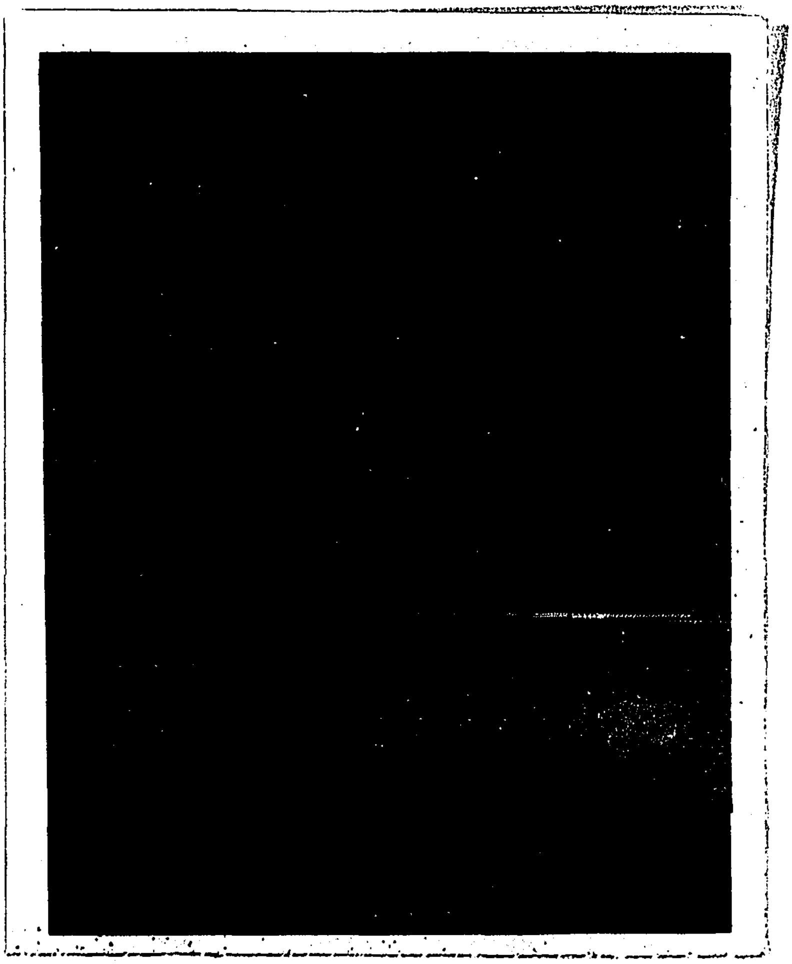

Figure 22. Disharmonic folding in biotite gneiss.

the smaller folds have been measured directly. Structural position with respect to the major antiform and synform (F_2) and rock type appear to affect the style of F_2 somewhat less than F_1 folds. However, F_2 folds in relatively non-ductile rocks, such as pure quartzites and para-amphibolite, appear to be more open (Figure 21b), and the folding mechanism is primarily by flexural flow (Donath and Parker, 1964, p.53). The axial plane thickness increases progressively towards the hinge area in these cases. F_2 folds in ductile rocks, such as migmatites, are occasionally nearly isoclinal and suggest folding by a mechanism approaching passive flow folding. In general, F_2 folds are open, have rounded hinges and exhibit crestal thickening. F_2 folds in migmatite are particularly appressed in the east limb of the Quad Creek synform (Map 1) and are open in quartzites in the southeast flank of the Wyoming Creek antiform. Axial plane foliation has been observed by the writer in several F_2 folds (Figures 23 and 26) and has been reported by Casella (in press) in the Line Creek area.

F_2 folds are occasionally quite open and disharmonic (Figure 22). A décollement appears to have formed between the rigid mafic layer and the ductile quartzo-feldspathic band. The mechanism of folding appears to have been a combination of flowage in the more ductile layers and slip

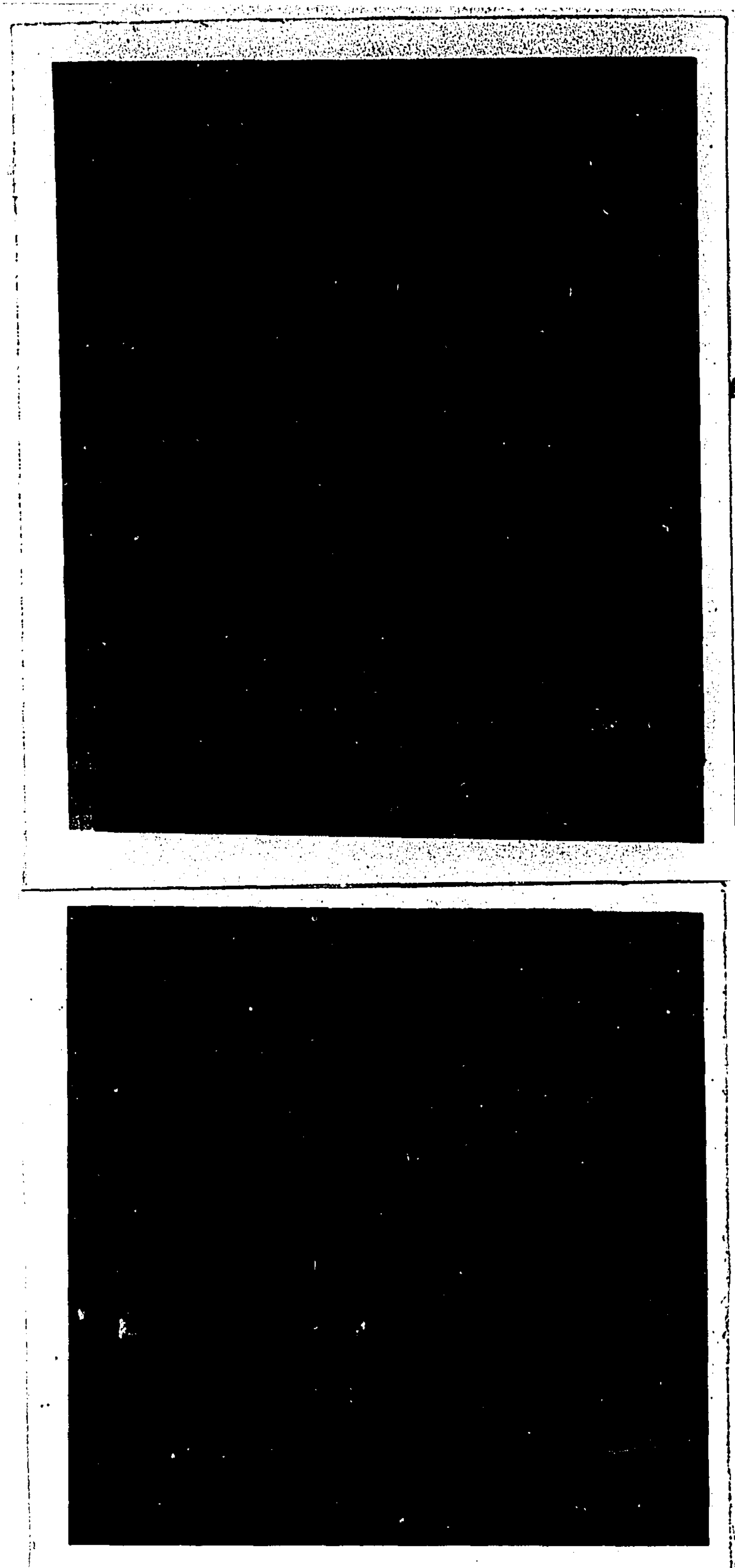

A

B

Figure 23. A-refolding of F_1 fold by F_2 fold in feldspathized quartzite. B- axial plane foliation (S_2) developed by biotite and plagioclase - enlargement of outlined portion in A. Both feldspars are stained and alkali feldspar appears white.

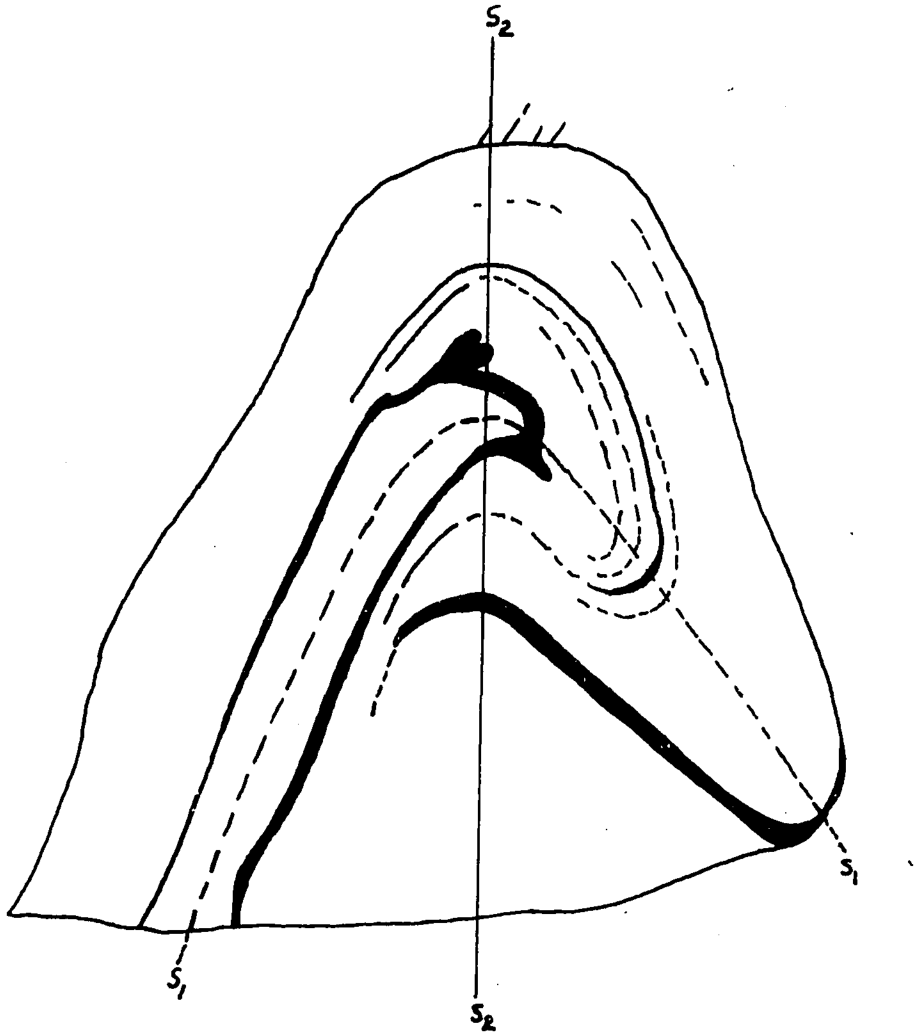

Figure 24. Sketch from Figure 23 showing refolding of an F_1 fold by F_2 fold. S_1 and S_2 are axial planes. B_2 is perpendicular to the page.

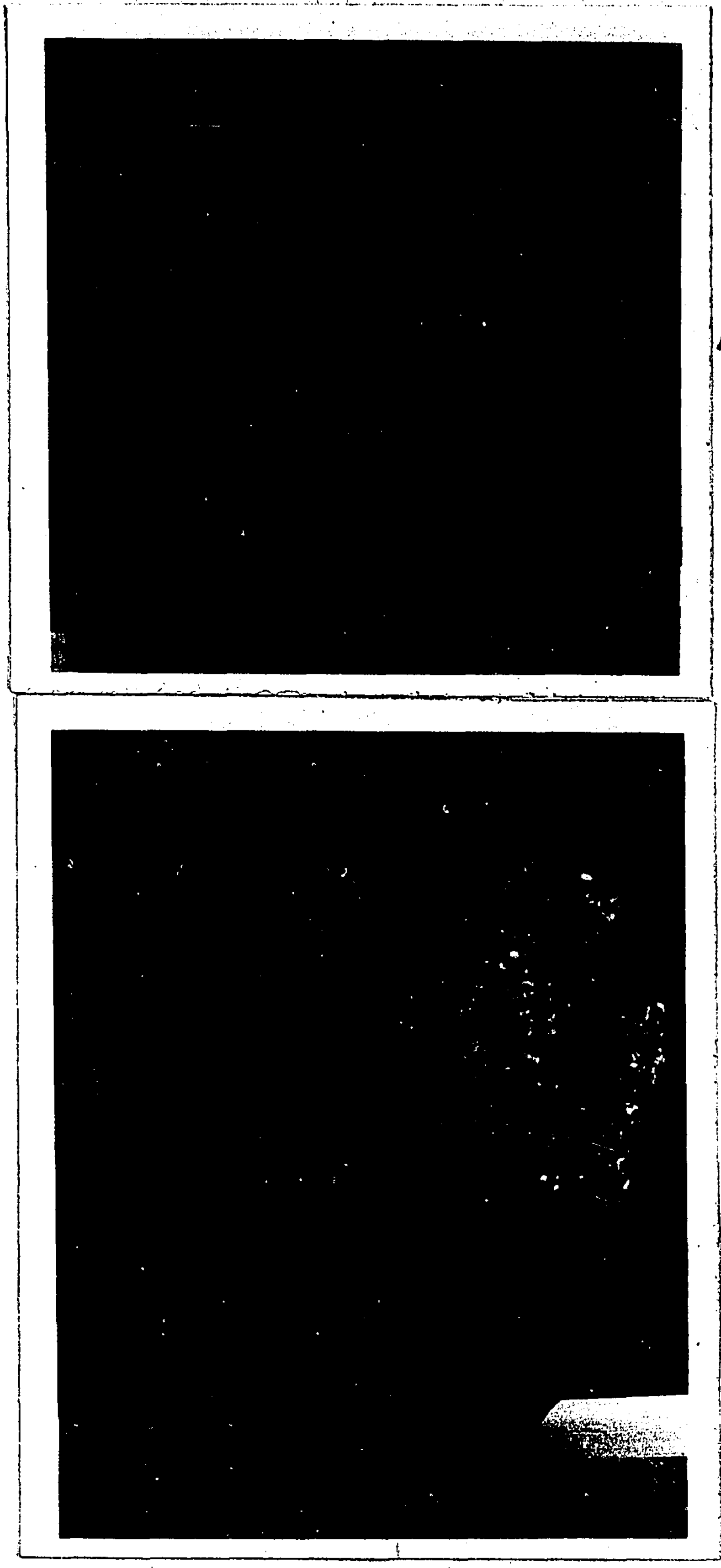

A

B

Figure 25. Refolded F_1 folds in banded migmatite from Structure Station 2.

along the less ductile beds.

Refolding:

Refolded folds have been observed in migmatites, quartzites, granitic gneisses, para-amphibolite and micaceous schists throughout the area. They are somewhat more prevalent in the Quad Creek area, where refolding of F_1 by F_2 exists on the mesoscopic and macroscopic scales. No large refolded F_1 folds have been observed in the Wyoming and Line Creek areas, although they may have existed and been destroyed by shearing and granitization. Statistical structural analysis of F_1 axes and axial planes (Maps 2a, 2b, 3a and 3b) demonstrate refolding of F_1 by F_2 also. Figures 24 and 23A show refolding of an appressed F_1 fold and axial foliation developed by biotite and plagioclase in an F_2 fold from Structure Station 5 (Maps 2a and 2b). The F_1 fold is defined by biotite and slightly feldspathized quartzite layers, forming a hook at the F_1 hinge zone. Intersection of the F_2 axial plane (S_2) and the major compositional banding (S_0) produces a lineation coincident with the F_2 fold axis (B_2). Grooving in the hinge zone of F_2 parallels B_2 also. The F_1 axial plane (S_1) is defined by the curviplanar S_0 surface. Figure 25 illustrates refolding of F_1 by F_2 in slightly banded granitic gneiss from Station 2.

No biotite or feldspar is developed along S_2.

Generally F_1 and F_2 small folds are distinct according to the following criteria:

(1) F_1 and F_2 have generally different fold styles in a particular rock type and structural position in the major folds (F_2).

(2) Orientations of F_2 folds determined from samples showing refolding afford distinctive geometrical differences on the mesoscopic scale.

(3) F_2 fold axial planes (S_2) are frequently homogeneous on the mesoscopic scale and aid differentiation of F_1 from F_2 folds.

All available small folds were sampled at each structure station, noting fold styles, rock type and whether the axial surface was plane or non-plane. The writer has found these to be adequate bases for separation of the two small fold sets at all stations except those located in the flanks of the Quad Creek synform where intense appression and recrystallization has rendered these criteria nearly useless (Stations 1, 6, 7, 8 and 9). Figure 26 shows the hook pattern which is characteristic of the migmatites in this area. Carey (1962, p.101) points out that this pattern is typical of refolding when axes are nearly parallel but have different plunges.

Paucity of specimens displaying measurable refolding has necessitated placing greater reliance on constructed β-axes in these areas, where refolding is manifested only as hook patterns, than in areas where geometrical relations can be measured directly.

These relations do not necessarily indicate formation of F_1 and F_2 during separate phases of deformation. Geometrical relations described in statistical analysis of the linear and planar structural elements suggest that these fold sets are part of one extended sequence of deformational movements.

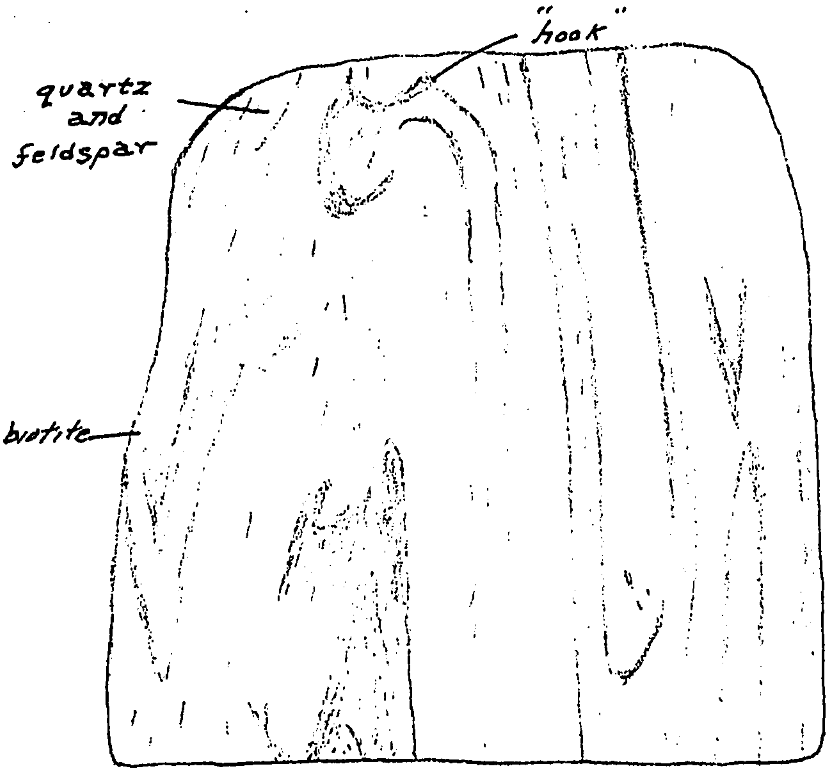

Figure 26. Sketch showing hook pattern due to refolding of F_1 by F_2 in migmatite. Natural size.

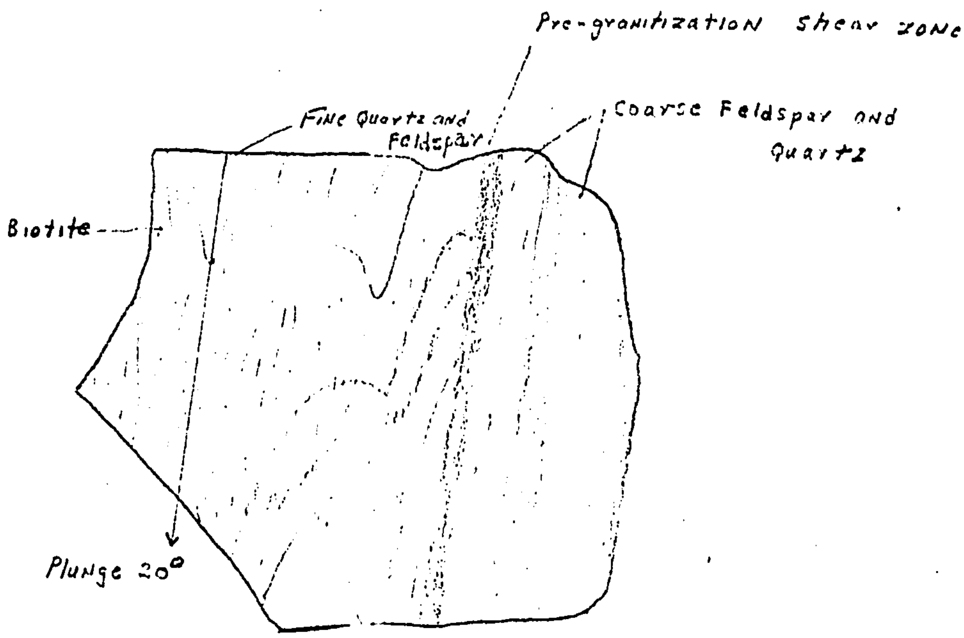

Figure 27. Pre-granitization shearing sub-parallel to the axial plane. Natural size.

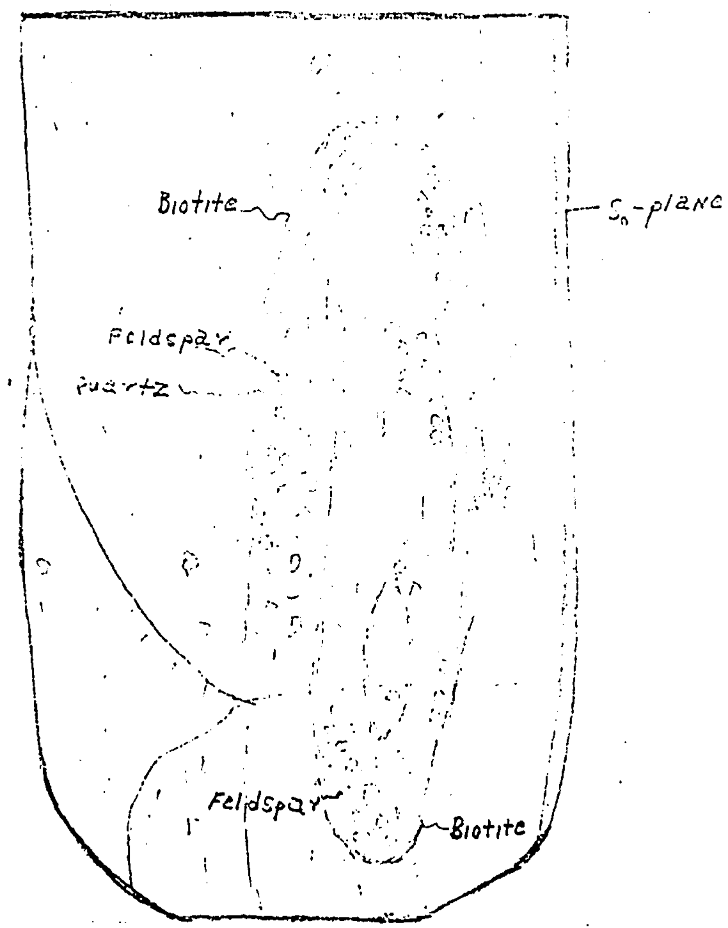

Figure 28. F_1 fold with feldspars developed in the nose and flanks. Natural size.

STRUCTURAL ANALYSIS

Structural analysis of a tectonite is usually conducted in three phases: (1) geometrical, (2) kinematic, and (3) dynamic. Tectonites containing one set of cylindrical, plane folds can usually be treated kinematically and dynamically with a minimum of geometrical data. Superposition of fold sets and high ductility contrasts in tectonites require detailed geometrical analysis on the microscopic, mesoscopic and macroscopic scales. Investigation of the Quad-Wyoming-Line Creeks tectonite is confined to the mesoscopic and macroscopic scales. Therefore, kinematic and dynamic analyses are generalized. Emphasis is placed on geometrical relations of linear and planar structural features.

The geometrical terminology used is that of Turner and Weiss (1963, pp.76-143):

S - foliation planes

L - lineations

F - fold set on all scales

B - fold axes

β - statistical maximum of intersections of measured s-surfaces of one type or normal to a constructed π-circle.

π - closest great circle approximation to poles of measured segments of S. β is axis of the π-circle.

<u>a</u> - Kinematic axis of slip or flow

<u>b</u> - Kinematic axis perpendicular to <u>a</u> in the plane of slip or flow and is an axis of rotation

<u>c</u> - Kinematic axis perpendicular to the ab plane.

Chronological subscripts relate penetrative fabric elements to corresponding fold sets.

Geometrical Analysis

Geometrical analysis has been conducted on the mesoscopic and macroscopic scales to ascertain domains of statistical structural homogeneity with respect to the following penetrative fabric elements;

1. <u>Foliations</u>:
    - a. compositional foliations
    - b. small fold axial planes
2. <u>Lineations</u>:
    - a. axes of small folds
    - b. mineral elongations
    - c. skialith and mullion elongations

Mesoscopic structures are defined (Turner and Weiss, 1963, p.76) as fabric elements visible in hand specimens and single, continuous outcrops. Mesoscopic structure stations have been constructed using exposure limits as arbitrary boundaries (Maps 2a and 2b). Structure stations homogeneous with respect to a particular fabric element are combined on Maps 3a and 3b to give macroscopic subareas. Non-penetrative structures, such as faults and fractures, are not considered in detail here. All data are plotted on lower hemisphere equal area projection, and L_1, B_1, S_0 and S_1 data have been contoured using a Duschatko device (Duschatko, 1955).

The statistical significance of fabric diagrams with preferred orientations have been treated extensively in the literature (Flinn, 1958, pp.526-539). Fabrics with weak preferred orientations have been considered suspect in many cases. However, rather strong preferred orientation is shown (Maps 2a, 2b, 3a and 3b) by the subfabrics in the Quad-Wyoming-Line Creeks area. Measurements may be subject to considerable error in slumped areas or due to exposure controlled by very prominent joint sets. Particular penetrative fabric elements may be subject to other errors also:

(1) Fold axes probably possess a high degree of accuracy, because the true axis or hinge line is usually easily defined. Accuracy may be somewhat lower in slightly non-cylindrical F_1 folds and open F_2 folds.

(2) Although axial planes (S_1 and S_2) were measured in reasonably plane folds only, open, slightly "concentric" folds present

some difficulty in locating the axial surface accurately.

(3) Compositional foliation, S_0, measurements are believed by the writer to be accurate, since no measurements have been taken in slumped areas or near magnetic rock types. However, the mesoscopic sub-domains are usually large in many cases, and homogeneity is not common with respect to the S_0-subfabric. These relations may indicate that the sub-domains are too large, or that superposition of F_2 on F_1 is intense and prevalent on the mesoscopic scale. Smaller sub-domains (Stations 2 and 5, Map 2a) show pronounced inhomogeneity due to superposition of F_2 on F_1, and ductile rocks, such as banded migmatites, show intense refolding. Although this tectonite is essentially homogeneous and shows monoclinic symmetry on the macroscopic scale, S_0 is typically triclinic and heterogeneous on the mesoscopic scale. Subdivision of larger sub-domains has not produced significantly greater homogeneity. Therefore, emphasis has been placed on analysis of the S_1-subfabric.

The writer believes that hornblende lineations, L_1, are especially subject to errors and bias. In addition to slumping and jointing, personal bias, areal extent of the sample area and the time of day when measurements are taken may also be significant. Measurements from areas of obvious slumping and agmatization have been avoided. Personal bias has been checked by taking two independent sets of 75 L_1 readings at Stations 1 and 8. Measurements were taken by different workers from slightly different areas within the same sub-domain. The two L_1-subfabric patterns are nearly identical. Therefore, the writer does not consider personal bias to be significant. Although L_1 frequently plunges more gently than B_1, differences in F_2 fold styles in migmatites and para-amphibolite appear to explain this difference. Limited outcrop area occasionally confined L_1 measurements to a relatively small area. It appears that this has produced a pattern at Station 3 which is divergent from those in adjacent sub-domains (See page 117).

Statistical sampling of penetrative fabric elements cannot be successfully subjected to vigorous statistical theory. Efforts have been made to maintain relatively constant numbers of measurements in each sub-domain. This has been done with respect to L_1, but B_1 and S_1 vary rather widely. Figure 30 shows the effect of having a larger number of S_1 measurements on the west flank of the

Wyoming Creek antiform than on the southeast flank. The east maximum suggests that this fold is overturned to the east. However, S_2 data show that the degree of overturning is actually slight (20°-30°).

Foliations, S

Major compositional foliation in the Quad-Wyoming-Line Creeks area consists of interlayering migmatites, granitic gneisses and metasediments (Map 1). Interlayering of ironstones with para-amphibolites and quartzites, and zircon studies (Eckelmann and Poldervaart, 1957, pp. 1242-1244) suggest a sedimentary origin for these rocks. Rock types resistant to granitization and flow, such as quartzites and para-amphibolite, outcrop with a high degree of continuity around major folds (Map 1). The banding appears to be original sedimentary layering on this scale (1:2400) and is referred to by the writer as S_o. Eckelmann and Poldervaart (1957, p.1230) state that:

> "Two criteria show that the beds are right-side up, and thus that the overall structure of the Quad Creek area is a true syncline: (1) cross-bedding in quartzites and (2) graded bedding as shown by gradual increase upward of hornblende and biotite and corresponding decrease of quartz and feldspar in individual beds of para-amphibolite or biotite schist and gneiss."

Casella refers to "apparent crossbedding" in migmatite in the Line Creek area (in press). The writer has not observed cross-bedding in the quartzites or migmatite. The writer has attempted no stratigraphic correlation in this area of intense granitization and multiple folding. Warping around boudins and skialiths frequently occurs. As previously mentioned, S_o of amphibolite blocks in agmatite is frequently oblique to that of the surrounding gneisses and migmatites (Figure 11).

Careful examination of S_o on the hand specimen scale shows that banding within some ductile layers is not parallel to the major compositional banding. Figure 28 illustrates development of feldspar porphyroblasts along the limbs of a small F_1 flow fold. The fold lies in the plane of S_o, i.e. the axial plane parallels the S_o-plane. Although the fold is nearly isoclinal, the trend of the limbs is not parallel to S_o. Biotite in flow folds (F_1) commonly exhibits subparallelism to S_o also. Mineral alignment in small folds occasionally suggests two ages of biotite and feldspar, although the temporal hiatus may be small. Figure 23 shows refolding of an F_1 fold by a relatively open F_2 fold in feldspathized quartzite. F_1 is tightly appressed, and S_1 is warped into the form of the later F_2 flexure. F_1 is defined clearly by small bands of biotite. Preferred orientation of biotite and, to a lesser, extent, plagioclase parallel to S_2 defines a later axial plane foliation. This example comes from the nose of the Quad Creek synform (Maps

2a and 2b, Structure Station 5) where F_1 and F_2 have nearly parallel strikes but plunge at different angles (Maps 2a and 3a). These geometric relations are reasonably consistent throughout the area. Refolding in migmatites from Structure Station 2 (Figure 25) (Maps 2a and 2b) shows folding of biotite about B_2, but neither later biotite nor plagioclase are developed parallel to S_2. The structural positions of the two examples do not differ greatly. The writer suggests that rock type, and consequently degree of ductility, might be the principal controlling factor. The later minerals may have developed only in rocks which reacted to stress by fracturing, as in quartzites, and not by flow as in ductile migmatites.

Migmatites in the flanks of the Quad Creek synform show abundant evidence of extensive flowage. No significant difference in fold style is generally apparent; both F_1 and F_2 are isoclinal and appressed. F_1 folds are frequently obliterated by recrystallization and refolding, and refolding is reflected as hook and crescent outcrop patterns (Figure 26). Crestal thickening and limb attenuation is more pronounced in the migmatites than in the less ductile quartzites and para-amphibolite. Although refolding is usually difficult to demonstrate in the field at these structure stations (1, 6, 7, and 8), the B_1- and S_1-subfabric patterns (Maps 2a and 2b) strongly suggest refolding.

Axial planes dip more steeply at these structure stations than the S_0-planes (Map 2a). Harris (1959, pp.1195-1196) shows small fold axial planes in the east and west flanks of the south plunging Christmas Lake synform trending about N-S and dipping at an angle which generally exceeds 83 degrees W. In contrast, S_0 dips do not usually exceed 70 degrees. The outcrop pattern suggests that this is an open and upright major fold. Hence, axial plane foliation appears to be locally developed in migmatitic layers in this area, since biotite shows a preferred orientation parallel to the flow fold axial planes. Biotite in the migmatite layers of the Quad Creek synform flanks warps around the F_2 hinges and is also developed in an axial plane direction (Figure 26). These relations have not been observed in non-ductile quartzite and para-amphibolite in this flank. The writer concludes that axial plane foliation (S_2) is developed locally in the banded migmatite layers. Fabric data (S_0 and S_1) suggest that the angle between the axial plane foliation and S_0 is small. Although axial plane foliation (S_2) may be developed in the quartzites and para-amphibolites also, it is not readily detectable.

Large F_1 folds have not been identified outside the Quad Creek synform nose (Subarea 2, Map 3a). These folds may not have developed elsewhere, or they may have been rendered inconspicuous by shearing. In this way, hinge areas would be destroyed. One north plunging fold with a wave length of about 5 feet has been found in Subarea 4. No evidence of shearing parallel to the axial plane was noted. Shear zones in these areas may have been destroyed by subsequent granitization and recrystallization. Figure 27 illustrates apparent shearing in pink migmatite from Subarea 1. The shear plane is subparallel to the axial plane of the fold shown in the sample. Since mineral grains are not fractured in the shear zone, shearing must have been pre-granitization. Shearing at the appropriate angle to the hinge would produce geometrical relations which might be misinterpreted as cross-bedding.

S_o-subfabric

<u>Mesoscopic</u>:

The mesoscopic S_o-subfabric is complicated by overprinting of F_1 and F_2 fold sets. The symmetry ranges from monoclinic to triclinic, the lowest order of symmetry being in the major F_2 fold noses. Measurements at the structure stations number from 22 to 92, and the areal extent ranges from about 17,000 to 100,000 square yards. These are unusually large mesoscopic domains, which accounts in part for their complexity. However, attempts to ascertain homogeneity by subdividing these stations has not simplified the S_o-subfabric significantly. Since the S_1-subfabric possesses higher symmetry and is less complex than the S_o-subfabric, emphasis in the geometrical analysis of F_2 folds is placed on the S_1-subfabric and lineation subfabrics. Map 2a shows the S_o-subfabric diagrams. Appendix I contains detailed analyses of individual diagrams.

β S_o-axes at Structure Stations 9, 10, 11 and 12 plunge moderately from SW to SE. Agreement between the β S_o- and β S_1-axes is reasonably good at Station 12. The effects of overprinting of F_1 and F_2 are evident at Stations 9 and 10, since two girdles are plausible and the symmetry is triclinic. Relatively open F_2 folds which are overturned to the east are indicated, but the axial attitude is widely divergent. Structure Stations 9 and 10 show patterns which imply overprinting of S_o data by F_2 and F_1. The symmetry is generally triclinic, and πS_{oa}-girdles trend in directions separated by about 90 degrees. Poles to N-S trending and nearly vertical S_o-planes produce maxima which do not appear to be an integral part of the overall S_o-subfabric.

The S_o-subfabric pattern in the east flank of the Quad Creek synform generally shows a high order of symmetry, but two nearly perpendicular π S_o-girdles are usually suggested. Significantly, Stations 6 and 7 are located in migmatite and para-amphibolite, while quartzites and para-amphibolite dominate at Structure Station 8. As previously discussed, S_2 axial plane foliation appears to have developed at a small angle to the major compositional banding in ductile migmatites and granitic gneisses but is not detectable in quartzites and para-amphibolite. Measurements from these complexly folded rocks yield a βS_o-axis plunging gently S-SW. This attitude only approximates the true B_2 orientation (Map 2a) in these sub-domains. This pattern is not developed in the relatively non-ductile quartzites and para-amphibolite at Station 8, suggesting that F_2 axial plane foliation has not developed or is not detectable here in these rocks on this scale. N-S trending πS_o-girdles at these stations may be due to superposition of F_2 cross-folds. S_1-, L_1- and B_1-subfabrics and the map (1) pattern suggest the existance of these folds also. However, they may be a manifestation of F_2 and F_1 superposition rather than being a distinct fold set.

The S_o-subfabric in the Quad Creek synform nose (Stations 3, 4 and 5) is nearly undecipherable without considering other subfabric data. Overprinting of F_2 on F_1 is intense and exists on all scales studied by the writer. The E-W trending F_1 synform is deformed by F_2 folds of nearly parallel trends (Map 1). The S_o-subfabric at Station 4 defines the gently warped north limb of this F_1 synform, and the deformed south flank is contained in Station 5. The βS_{oa}-axis corresponds to B_1 (Map 2b) at Station 4, while B_2- and βS_{oa}-axes are nearly coincident at Station 5. The strongest πS_0-girdle at Structure Station 3 defines a βS_0-axis roughly corresponding to B_2. The less well-defined πS_0-girdle may be related to F_1 folds which plunge west here (Map 2b).

Stations 1 and 2 are similar to the east flank of the Quad Creek synform with respect to the S_0-subfabric. Migmatites are prevalent in both areas. Axial plane foliation and axial plane shearing (pp.79-80) may explain the patterns at Stations 1 and 2. South plunging βS_0-axes approximate B_2- and βS_1-axes here. However, superposition of broad, open F_2 cross-folds is suggested by mapping (Map 1) and the other subfabric patterns. E plunging βS_0-axes may define the axes of these folds. However, these broad open cross-warps may be due to superposition of S plunging F_2 folds on F_1 folds.

Macroscopic:

Macroscopic analysis of the S_0-subfabric does not appear to be justified, since homogeneity has not been attained on the mesoscopic scale. However, mesoscopic analysis of S_0 does illustrate the significance of scale.

Homogeneity on the macro- and mesoscopic scales in the Lonesome Mountain area (Larsen, Poldervaart and Kirchmayer, in preparation) is the same, but in the Wyoming Creek anticline they are different. In the former case, open, cylindrical folds are suggested on both scales. In the latter case, open, cylindrical folds are suggested on the macroscopic scale only. Figure 29 illustrates the S_0-subfabric relations for the entire Wyoming Creek antiform. βS_0-, βS_1-, B_2- and B_1-axes agree closely also. In contrast, mesoscopic analysis of S_0 displays lower symmetry and general disagreement between βS_0-axes and other subfabric axes. Therefore, S_0 is less homogeneous on the smaller, mesoscopic scale than on the macroscopic scale in the major antiform. The writer believes that S_2 axial plane foliation has developed in migmatites and granitic gneisses. S_0 measurements restricted to the major compositional banding in quartzites and para-amphibolites might yield relations similar to those in the Lonesome Mountain area. However, the S_0 data are insufficient to test this hypothesis in the present study.

S_1-subfabric

Mesoscopic:

S_1 is statistically sampled at all 12 structure stations, and measurements number from 13 to 43. A detailed analysis of each diagram is given in Appendix II.

The S_1-subfabric is particularly significant in the geometric analysis of the Quad-Wyoming-Line Creeks area, because it is not affected by overprinting of both fold sets. S_0 is strongly affected by overprinting of F_1 and

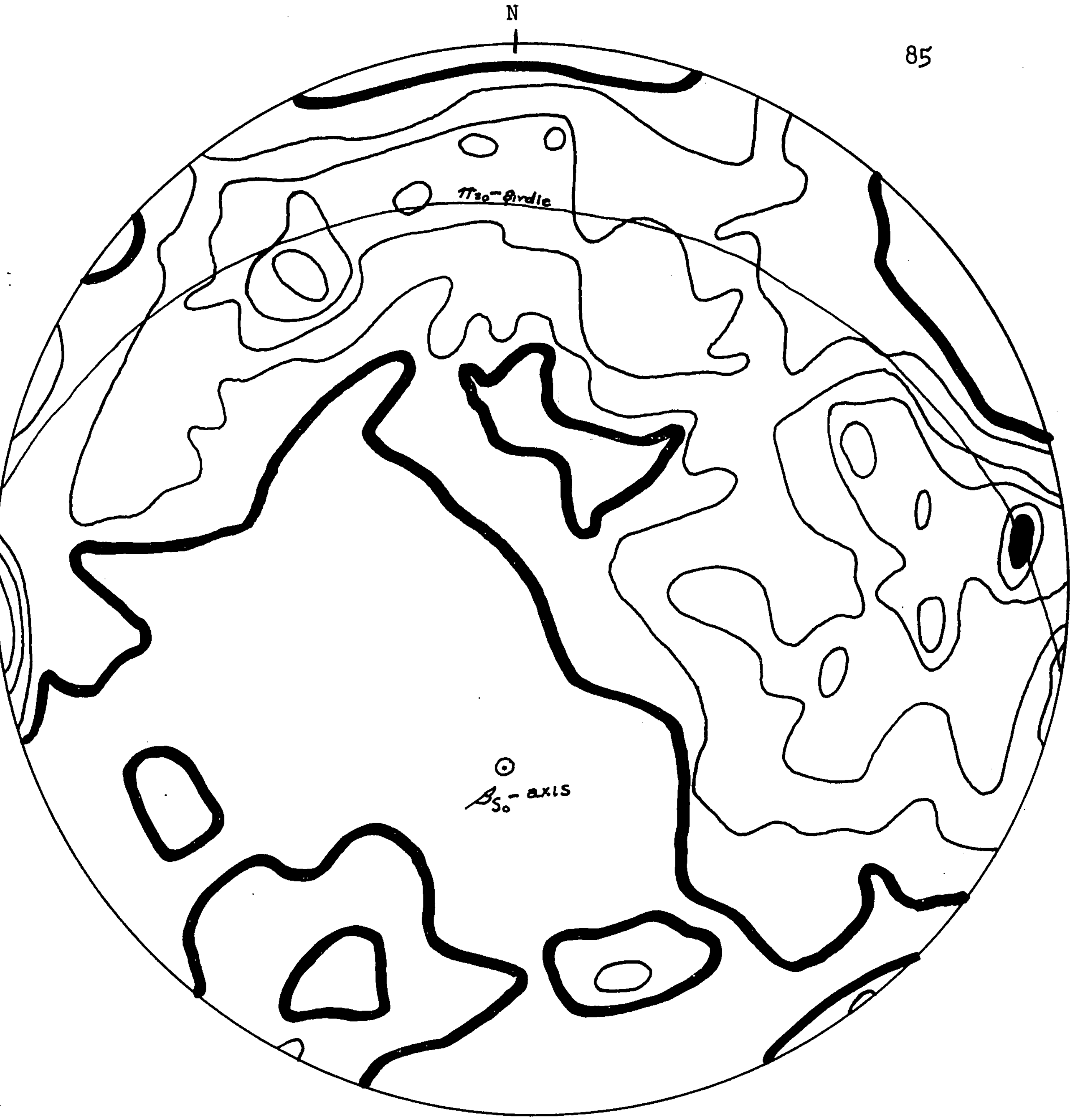

Figure 29. Synoptic S_0 diagram for Stations 6, 7, 8, 9, 10, 11, and 12. Contour interval: 0.2-0.9-1.9-2.9-3.9-4.9%. Based on 352 measurements.

F_2 on the mesoscopic scale and is of limited geometrical use. The following generalized remarks briefly summarize the most pertinent geometrical features of the S_1-subfabric:

(1) S_1 is folded by F_2 folds which are relatively open in non-ductile quartzites and para-amphibolite and isoclinal in ductile migmatites, granitic gneisses and micaceous schists.

(2) The S_1-subfabric symmetry ranges from triclinic to monoclinic, and the highest degree of triclinity occurs in the major fold noses (Structure Stations 2, 3 and 10). S_1-subfabric symmetry is higher than S_o-subfabric symmetry.

(3) S_1 lies in the S_o-plane, i.e. S_1 parallels S_o in strike and dip. Therefore, S_1 and S_o maxima rotate around the major fold noses, but the S_o-subfabric is heterogeneous.

(4) Constructed β S_1-axes agree closely with measured B_2-axes at most structure stations.

The S_1-subfabric is simplest and most clearly defined in the Wyoming Creek antiform nose and southeast flank (Stations 10, 11 and 12; Map 2a). β S_1-axes at these stations plunge moderately S-SW and agree with B_2 measurements (Map 2b). F_2 folds are relatively open and overturned eastward at Station 10. These relations are in agreement with field observations and the map pattern

(Map 1). The dominant rock types at these stations are quartzites and para-amphibolite. The unusually great width of the π S_1-girdles suggests that the F_2 folds are not entirely cylindrical. B_2 shows strike and dip dispersion in Sub-area 3 (Map 3b). This does not necessarily imply that F_2 is refolded, but broad, open flexures have been identified on the west flank of the major antiform. These folds appear to be cross-folds which deform F_2 very gently. However, they may be due to superposition of F_2 on F_1 rather than being a distinct fold set.

The $S_{1,2}$-subfabric in the east flank of the Quad Creek synform is more complex than in the southeast flank of the Wyoming Creek antiform. The subscripts 1,2 are used at these stations, because it was not possible to separate F_1 and F_2 at Structure Stations 6, 7, 8 and 9. Examples of refolding are uncommon, but hook and crescent (Carey, 1962, p.101) outcrop patterns suggest refolding. Crestal thickening and limb attenuation is prevalent in the ductile migmatites. The overall $S_{1,2}$-subfabric pattern indicates broad, open folds plunging steeply east. This trend is perpendicular to the Quad Creek synform axis, so that these appear to be cross-folds related to the major synform. The S_0-subfabric supports the existence of these folds. However, the pattern at Structure Station 6 is exceptional. South plunging isoclinal F_2 folds which are nearly symmetrical are suggested here by the S_1-subfabric. Additionally, lineation subfabric patterns (Map 2b) at these stations are not adequately explained as being deformed by later (F_2) cross-folds only. Continuation of the geometric relations at Stations 10, 11 and 12 through these stations is indicated by the linear elements, which also implies the existence of south plunging, isoclinal F_2 folds at Stations 6, 7, 8 and 9. Therefore, these folds must be highly appressed and overturned in the S_0-plane at these stations. Figure 46 shows an example of this F_2 geometry. F_2 cross-folds may have been superimposed on this geometry and have dispersed the poles to the axial planes. Alternately, the cross-warps may be due only to overprinting of F_2 on F_1. The prominent maxima may represent S_2 poles. Within the Wyoming Creek antiform, F_1 folds appear to have formed primarily in ductile layers, such as migmatites and mica schists. Variation in the F_2 geometry may be related to rock ductility or to greater appression in the Quad Creek fold. The writer believes that open, flexural flow folds (F_2) have formed in the relatively non-ductile quartzite and para-amphibolites, while appressed, isoclinal passive F_2 flow-folds have developed in the migmatites. F_2 folds in the east Quad Creek flank may have been further appressed during formation of the major folds.

Stations 3, 4 and 5 are separated from Station 6 by an area of sparse outcrops. β S_1-axes have rotated approximately 90 degrees in strike from S-SW at Station 6 to E-SE at Stations 3, 4 and 5. The plunge is difficult to ascertain accurately at Station 6 but appears to be 40°-50°S. β S_1-axes plunge gently E-SE at Stations 3, 4 and 5. Therefore, β S_1-axes rotate around the nose of the Quad Creek synform with a corresponding change in plunge. F_2 is overturned to the N-NE and is relatively open. Quartzites and para-amphibolite are the dominant rock types in these sub-domains.

The S_1-subfabric at Structure Stations 1 and 2 indicate that F_2 completes its rotation around the major synform. Most of the measurements were derived from migmatites. The S_1-subfabric at Station 1 is similar to the pattern at Station 6. B_2 measured from refolded samples plunge very gently S-SW at Station 2. The β S_{1a}-axis approximates this attitude. The subfabric at this station is somewhat unique, because two equally well-defined π S_1-girdles are dispersed at Structure Station 1. These features may be due to superposition of broad, open F_2 cross-warps on F_2. These later (F_2) folds correspond to the cross-folds noted in the east flank of the Quad Creek synform but may be due to superposition of F_2 on F_1 and not a distinct later fold set.

Macroscopic Scale:

Treatment of the S_1-subfabric on the macroscopic scale has been conducted by combining structure stations homogeneous with respect to S_1 into subareas. Six subareas have been constructed in this manner and are keyed to the appropriate subareas on Map 3a. Measurements number from 18 to 117. The symmetry for the individual subareas is generally monoclinic. Homogeneity is slightly greater in the Wyoming Creek antiform than in the Quad Creek synform. In general, S_1 is not a penetrative fabric element for the two major folds, because it rotates around the major noses (Turner and Weiss, 1963, pp.144-151).

The S_1 patterns in Subareas 1, 3 and 4 suggest folding of S_1 by isoclinal F_2 folds. The folds are overturned slightly in the S_o-plane. β S_1-axes rotate around the Quad Creek synform nose and converge slightly on the synform axis. β S_1-axes do not rotate around the Wyoming Creek antiform nose. Although the axial attitudes of the isoclinal F_2 folds is difficult to ascertain statistically, they appear to coincide closely with the measured B_2-axes (Map 3b). The dominant rock types in Subareas 1 and 4 are banded migmatites, while quartzites compose Subarea 3.

F_2 folds in Subareas 2, 5 and 6 are relatively open and are overturned variably from NE to E-NE. Asymmetry is more pronounced in Subareas 2 and 5 in the F_2 fold noses than in the southeast flank of the Wyoming Creek antiform (Subarea 6). β S_1-axes and B_2-axes show close agreement in subareas containing open F_2 folds. Quartzites and para-amphibolite are prevalent in Subarea 6. As previously mentioned with respect to the mesoscopic scale, fold style is variable with different rock ductilities. Open flexural flow folds (F_2) occur in non-ductile quartzites and para-amphibolites (Subareas 2, 5 and 6), whereas isoclinal passive flow folds (F_2) are widespread in ductile migmatites, granitic gneisses and mica schists (Subareas 1 and 4). Subarea 3 is anomalous in this respect, but the data are sparse.

S_1-subfabric symmetry is monoclinic for the synoptic diagram shown in Figure 30. These data are from Subareas 4, 5 and 6. The β S_1-axis corresponds closely with B_2 axes from these subareas (Figure 43). Figure 31 is a synoptic S_1 diagram for the entire area. The degree of triclinity with respect to S_1 is higher than for the Wyoming Creek antiform. This is due to rotation of the βS_1- and B_2-axes around the Quad Creek nose but not around the Wyoming Creek nose. Therefore, S_1 is not deformed homogeneously with respect to these major folds.

S_2-subfabric

Mesoscopic:

S_2 measurements are not numerous at any of the 12

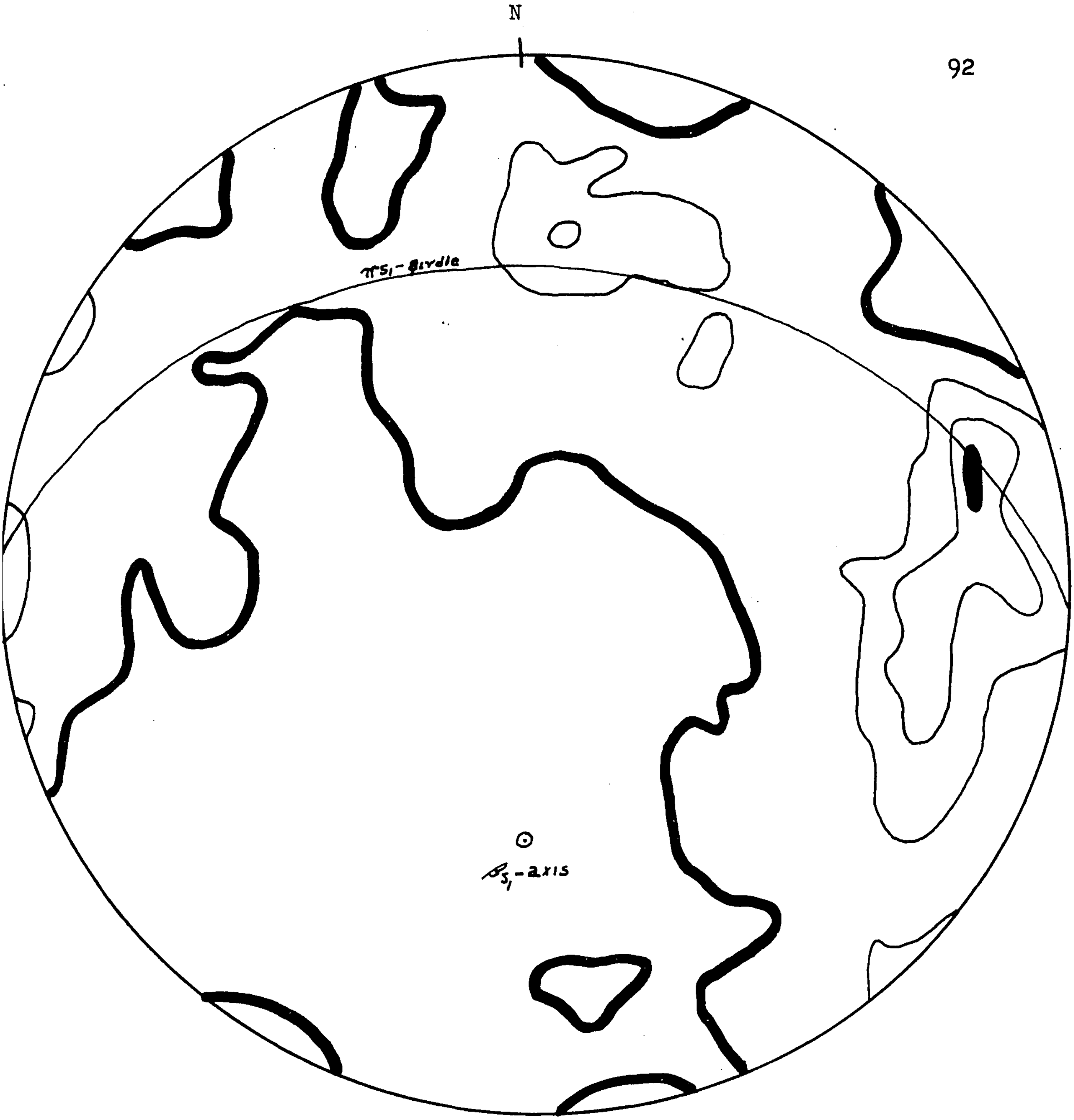

Figure 30. Synoptic S_1 diagram for Subareas 3, 4 and 5. Contour interval: 0.5-2.3-4.2-6.1%. Based on 213 measurements.

Figure 31. Synoptic S_1 diagram for the entire map area. Contour interval: 0.3-0.9-1.9-2.9-3.9%. Based on 308 measurements.

structure stations, because F_1 and F_2 small folds are frequently very similar in style. As previously mentioned, F_1 and F_2 are not distinguishable at Structure Stations 6, 7, 8, 9 and 11. Nearly all of the S_2 measurements were taken from F_2 folds showing refolding at Stations 2, 3 and 5. Uncontoured data are shown on Map 2a and are discussed in Appendix 3. S_2-subfabric symmetry ranges from axial to monoclinic.

The monoclinic S_2-subfabric at Structure Stations 2, 10 and 12 suggests that F_2 folds are non-cylindrical and non-plane in these sub-domains. This does not necessarily imply later folding of the S_2-planes. The orientation of the F_2 folds indicates that they are parasitic on the major Wyoming Creek antiform. Figure 4 shows that the major folds are slightly non-cylindrical on the regional scale. Therefore, small F_2 folds might reflect this geometry on the mesoscopic scale. Formation of this pattern may be related to the nature of the F_2 deformation or to a later deformation. The writer believes that the non-cylindrical nature of small and large F_2 folds may be explained by triaxial strain during their formation. S_2-planes are occasionally difficult to measure accurately, since the F_2 folds at these stations are open and nearly "concentric". Folds later than F_2 have not been found at Structure Stations 10, 11 and 12. The S_2 attitude at

Structure Stations 10 and 12 is generally N-NE and dipping steeply W-NW. Therefore, F_2 folds trend obliquely to the S_0- and S_1-planes and are slightly overturned to the E-SE here. S_2 does not rotate around the Wyoming Creek antiform nose, while S_1 warps around both major noses.

The S_2-subfabric at Structure Stations 3 and 5 have axial or orthorhombic symmetry. S_2 trends parallel to the S_0-plane and therefore, wraps around the Quad Creek synform nose.

Macroscopic:

Three macroscopic subareas have been constructed by combining stations homogeneous with respect to S_2. Although S_1 and S_2 are not separated at Structure Stations 6, 7, 8 and 9, these stations are included in Subarea 3. The pattern at these stations suggests S_2 orientations similar to the attitude at Stations 10 and 12. Map 3a shows the subareas and corresponding uncontoured diagrams.

S_2 is a penetrative fabric element for the Wyoming Creek antiform (Subarea 3), since it is relatively homogeneous throughout the entire structure. In contrast, S_2 rotates around the nose of the Quad Creek synform. F_2 folds are overturned to the north in Subarea 2. Figure 32 is a synoptic S_2-diagram for Subarea 1 and 2, defining a β S_2-axis plunging 18° to S15W. This is a significantly

Figure 32. Poles to S_2-planes from Subareas 1 and 2.

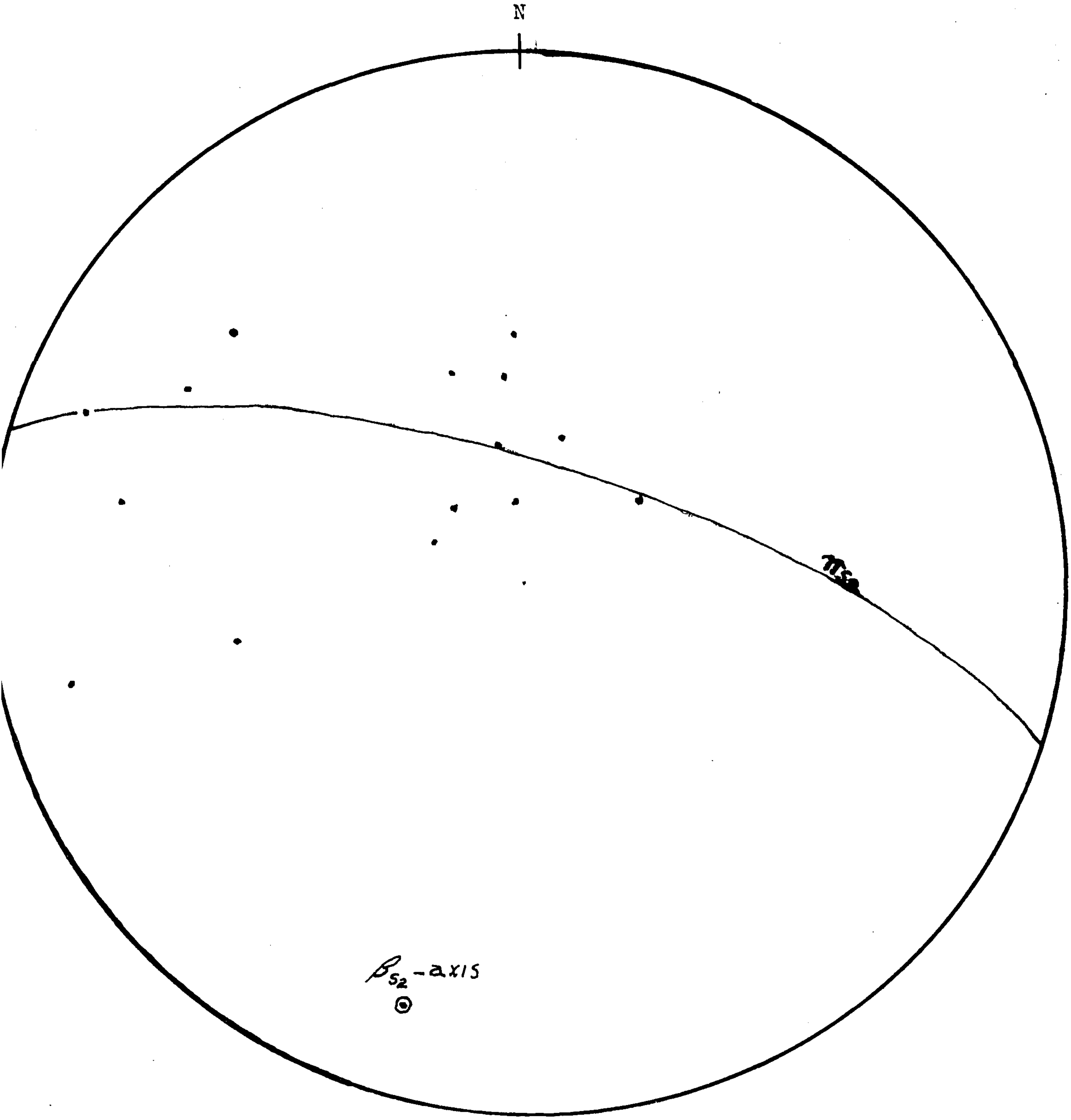

different attitude than that derived for the Wyoming Creek antiform. Therefore, S_2 appears to be older than the major synform. However, the presence of the metanorite body is believed to be significant in these anomalous geometrical relations.

Summary

S_o-subfabric:

The S_o-subfabric is complicated by overprinting of F_2 on F_1 and generally has triclinic symmetry. It defines βS_o-axes which correspond roughly to B_2 and βS_1-axes at Stations 11 and 12, where F_1 has been observed on the scale of small folds only. Constructed βS_o-axes in the flanks of the Quad Creek synform generally define steeply plunging cross-folds related to the major synform. However, the writer believes that these cross-warps are not a distinct fold set but are manifestations of F_2-F_1 superposition. Warping of this type has been observed in the E-W trending F_1 synform in Quad Creek (Map 1). βS_o-axes which plunge in the direction of B_2 only approximate the actual B_2 attitude. Most of the S_o measurements at Stations 1, 6 and 7 are from migmatites in which refolding is intense and S_2 axial plane foliation is evident. The S_o-subfabric patterns at these stations reflect these relations.

F_1 and F_2 folds exist on the small and large scales in the Quad Creek synform nose, so that the S_0-subfabric is very complex here. βS_0-axes generally agree roughly with B_2- and βS_1-axes. The patterns at Stations 4 and 5 substantiate the existence of the F_1 synform in this area. The S_0-subfabric has not been treated on the macroscopic scale, except in the Wyoming Creek antiform. Figure 29 shows the βS_0-axis and πS_0-girdle for this major fold. βS_0-, B_2-, and βS_1-axes agree rather closely. Therefore, the S_0-subfabric is homogeneous on the macroscopic scale but not on the mesoscopic scale.

$\underline{S_1\text{-subfabric}}$:

The S_1-subfabric has been especially useful in determining the F_2 fold geometry. Open F_2 folds are demonstrated by the S_1-subfabric in the southeast flank of the Wyoming Creek antiform, where non-ductile quartzites and para-amphibolite dominate. SW plunging, asymmetrical F_2 folds are defined in the nose of the major antiform. S_1 and S_2 are not separated in the east flank of the Quad Creek synform. However, south plunging, isoclinal, nearly symmetrical F_2 folds are defined at Station 6. This pattern is poorly developed at Stations 7, 8 and 9. The dominant rock types at these stations are migmatites. The writer believes that F_2 folds fold S_1 at these stations, but that they are appressed and overturned in the plane of S_0. The macroscopic S_1-subfabric demonstrates the interpreted F_2 fold geometry in this area. Additionally, the presence of highly ductile migmatites appears to be an influential factor in F_2 fold style. In general, F_2 folds are slightly appressed and "similar" in migmatites and granitic gneisses, while they are generally open and partially flexural in non-ductile quartzites (Figure 21) and para-amphibolite. Although cross-flexures related to the major synform are suggested at Stations 1, 2, 6, 7, 8 and 9, the writer believes that these broad, open warps are manifestations of refolding. β S_1-axes at Stations 6, 10, 11 and 12, as well as in Subareas 3, 4 and 5, are closely coincident with B_2-axes. Figure 30 shows the βS_1-axis for the entire Wyoming Creek antiform. The S_1-subfabric is homogeneous on the macroscopic scale, and the mesoscopic subfabric is significantly more homogeneous than the S_0-subfabric.

The S_1-subfabric at Station 1 is similar to the Station 6 pattern. F_2 folds which are relatively open and are overturned to the N-NE dominate in the Quad Creek synform nose. The constructed βS_1-axes agree closely with measured B_2-axes. βS_1-axes rotate around the Quad Creek synform nose, while little rotation is noted in the Wyoming Creek antiform.

<u>S_2-subfabric</u>:

S_2 measurements are sparse at most stations and are absent in areas where F_1 and F_2 have not been separated. Although S_2 is somewhat dispersed in Subarea 3, the subfabric does not suggest rotation around the Wyoming Creek antiform nose. The writer believes that these F_2 folds are parasitically related to the large SW plunging antiform. The dispersion of S_2 data is attributed to triaxial strain, rather than to a later deformation.

S_2 rotates around the Quad Creek synform nose, suggesting that this major fold is younger than F_2 folds. However, the buttressing effect of the metanorite body is believed to have produced sufficient north directed stress to cause this local change in orientation of small F_2 folds. S_2 is nearly recumbent to the north at Station 5. This is believed to be due to buttressing of the metanorite and not to intrusion of the body. However, the βS_2-axis probably approximates the true Quad Creek synform axial attitude (Fig. 32).

Axial plane foliation (S_2) has developed locally, especially in migmatites of the Quad Creek synform flanks. It has not been detected in the quartzites here, but is well illustrated in quartzites from the Quad Creek synform nose (Fig. 23). The $S_2 \measuredangle S_0$ angle does not appear to exceed 10°-15°.

Lineations, L

Lineation is defined by Cloos (1946, p.1) as "....a descriptive and non-genetic term for any kind of linear structure within or on a rock. It may include striae on slickensides, fold axes, flow lines, stretching, elongated pebbles or ooids, wrinkles, streaks, intersections of planes, linear parallelism of minerals or components, or any other kind of linear structure of megascopic, microscopic or regional dimensions." However, Turner and Weiss (1963, p.101) restrict the term lineation to linear structures which are penetrative in hand specimens or in small exposures. Grooves and striae are not penetrative fabric elements and are excluded by them. Large linear structures such as rods and mullion are treated separately by these workers also. The writer considers each penetrative linear feature separately, in order to ascertain the age and geometrical relations of each. The following lineations are analyzed in this investigation;

(1) Small fold axes, B, are generated by a line parallel to the hinge moving with constant orientation. The hinge line (Figure 33) joins points of greatest curvature. Many of the measurements utilized here are hinge lines. Attitudes of hinge lines and fold axes are difficult to measure accurately in

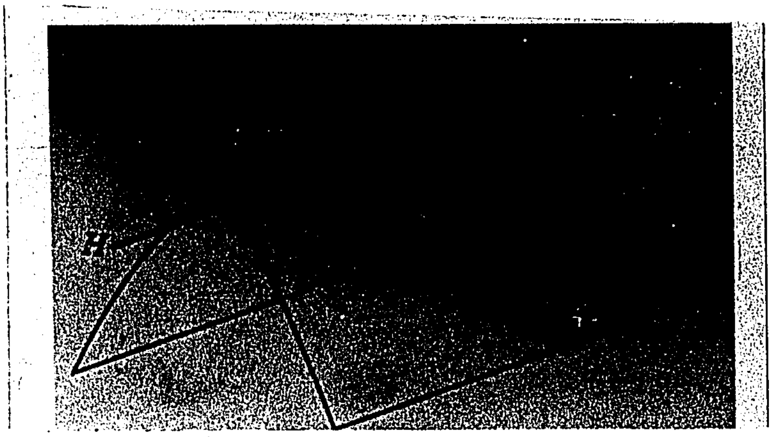

Figure 33. Sketch showing the hinge line of a fold (after Turner and Weiss, 1963, p. 107).

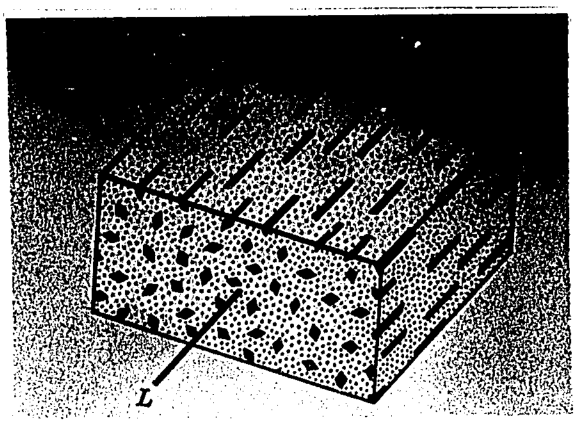

Figure 34. Sketch showing single crystal elongation (after Turner and Weiss, 1963, p. 102).

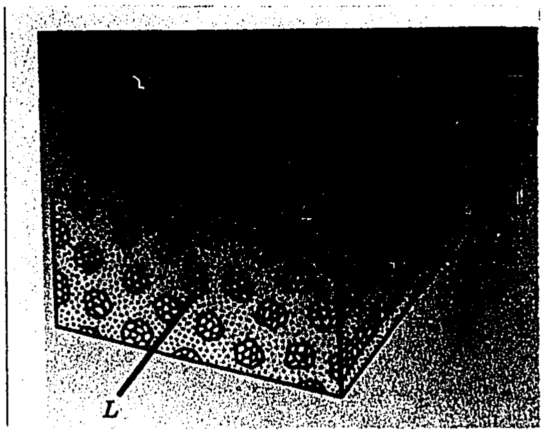

Figure 35. Sketch showing elongation of mineral aggregates (after Turner and Weiss, 1963, p. 102).

Figure 36. Photo showing mullion structure in quartzite.

open and concentric folds.

(2) Mineral lineations, L, are of two types:

a. elongation of single hornblende crystals, L_1 (Figure 34).

b. elongation of mineral aggregates (Figure 35), such as biotite, L_2, on slip surfaces in flexural flow folds.

(3) Elongation of pods and skialiths, L_1, has been measured where the relief is sufficiently great to permit accurate measurements. Para-amphibolite and, occasionally, quartzite skialiths are abundant in areas of agmatization. Figure 36 shows mullions (Wilson, 1953, pp.118-151) in quartzite.

(4) Grooves and crenulations are most commonly associated with F_2 folds (Figure 37). Grooving is usually found in the hinge zone parallel to B_2. Crenulations occur in micaceous layers and are included with measurements of fold axes.

Lineations formed by intersecting planes, feldspar porphyroblast elongations, and the trace of lineations on an obliquely intersecting plane ("apparent lineations", den Tex, 1953, p.59) are not treated here.

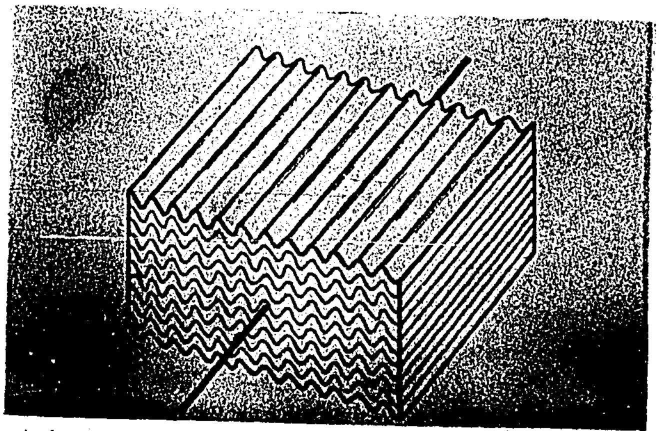

Figure 37. Sketch showing crenulations (after Turner and Weiss, 1963, p. 102).

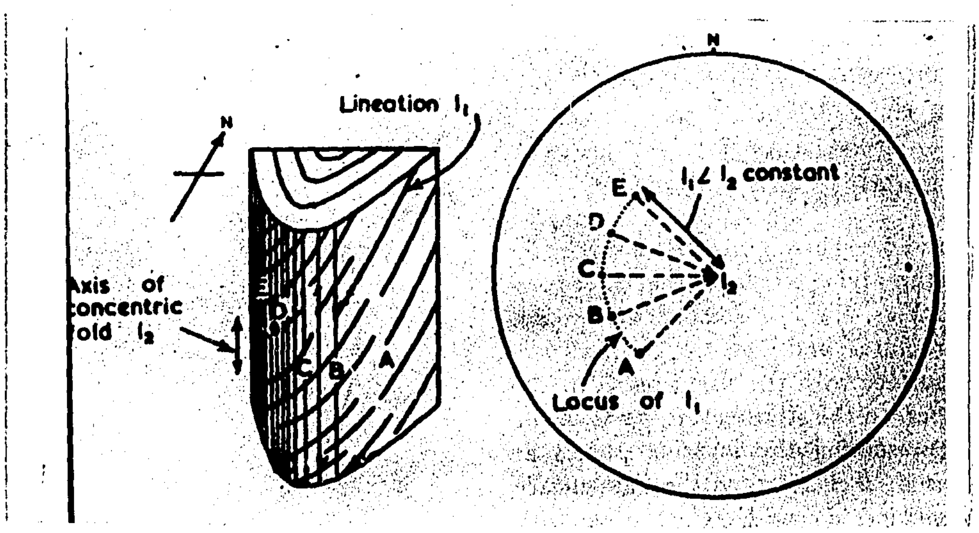

Figure 38. "Concentric" folding of earlier rectilinear lineations (after Ramsay, 1960, p. 77).

Figure 39. "Similar" folding of earlier rectilinear lineations (after Ramsay, 1960, p. 78).

B_1-Subfabric

Mesoscopic:

B_1 measurements are fold axes and hinge lines of small, isoclinal F_1 folds, numbering from 13 at Station 8 to 36 at Station 12. Contoured diagrams are keyed to the corresponding structure stations on Map 2b. It must be emphasized that both B_1 and B_2 measurements are included at Structure Stations 6, 7, 8 and 9, since F_1 and F_2 are not separated in these sub-domains. A detailed analysis of each diagram is given in Appendix IV.

The B_1-subfabric symmetry ranges from monoclinic to triclinic. No significant symmetry variation is evident with respect to position in the major folds. However, the B_1-subfabric varies from a partial great circle girdle (Station 7) to a pattern which approaches a partial small circle girdle (Station 12). Ramsay (1960, pp.75-93) has shown that "concentric" folding disperses earlier rectilinear lineations into a partial cone which forms a partial small circle when projected on an equal area net (Figure 38). In contrast, "similar" folds deform earlier rectilinear lineations along a plane which projects as a partial great circle girdle (Figure 39). Folding in nature is usually intermediate between these idealized styles. F_2 fold style in the Quad-Wyoming-Line Creeks area appears to be influenced by rock types, and consequently, by mean ductility (Donath and Parker, 1964, p.50). Relatively open, "concentric" F_2 folds occur in non-ductile quartzites and para-amphibolites at Structure Stations 3, 4, 10 and 12. The S_1-subfabric reflects this fold style (Map 2b) in these areas. In contrast, "similar" F_2 folds occur in the ductile migmatites and granitic gneisses at Structure Stations 1, 2, 6, 7, 8 and 9. These differences in F_2 fold style due to differential mean ductilities are reflected in the B_1-subfabric. B_1 is dispersed along partial great circle girdles where F_2 folds are "similar" passive flow folds. Partial small circle B_1-girdles are suggested where F_2 is slightly "concentric" and appears to have formed by flexural flow folding. The pattern is intermediate between a partial small circle and a partial great circle girdle, since these F_2 folds are not entirely "concentric" and have not formed through purely flexural slip folding (Donath and Parker, 1964, p.54).

The B_1-subfabric at Structure Stations 6, 7, 8, 9 and 10 suggests that B_1 and B_2 are nearly parallel (Clifford, 1960, p.377, Fig. 9-D9). This relation is confirmed at Station 10 by B_2 attitudes (Map 2b). The patterns at Stations 7 and 8 suggest folding of B_1 by "similar" F_2 folds, since the B_1-girdle is a partial great circle. Primary maxima plunge moderately S-SW. Partial small circle B_1-girdles are approached at Stations 10 and 12, where relatively non-ductile quartzites and para-amphibolites dominate. F_2 folds are nearly "concentric" in these areas. Patterns at Stations 6 and 9 are intermediate between "similar" and "concentric" styles. The S_1-subfabric at Station 6 (Map 2a) indicates that F_2 folds are highly appressed and nearly symmetrical. B_1 measurements were derived from migmatites at Stations 6, 7, 8 and 9. F_2 cross-folds are suggested by the S_o- and S_1-subfabrics at these stations and may explain some of the scatter. However, these broad, open F_2 cross-warps may be only due to superposition of F_2 on F_1 folds. B_1 does not rotate around the Wyoming Creek antiform nose.

F_1 and F_2 are distinguished easily at Structure Stations 2, 3 and 5 in the nose of the Quad Creek synform. Although B_1 and B_2 strike nearly parallel here, they are separated in plunge by about 40° as measured from the horizontal plane (Map 2b, Station 5). It is evident that B_1 begins to rotate around the major synform nose and converges on the axial zone. F_2 folds are relatively open and slightly "concentric" in the non-ductile para-amphibolites at these stations. Therefore, the B_1 pattern is intermediate between a partial small circle and a partial great circle girdle. These F_2 folds are overturned to the north. B_1 has rotated completely around the Quad Creek synform nose at Stations 1 and 2, where the dominant B_1 plunge is N-NE. The partial great circle B_1-girdles indicate that the F_2 folds are "similar". Broad, open F_2 cross-folds suggested by the S_1- and S_o-subfabrics may explain the unusually large scatter of B_1 data here. The S_2-subfabric supports this conclusion. Therefore, rock ductilities control the F_2 style and mechanism at Structure Stations 1, 2, 3, 4 and 5 as they do in the remainder of the area. However, B_1 wraps around the Quad Creek synform nose and converges on the axial zone.

Macroscopic Scale:

Stations homogeneous with respect to B_1 have been combined to form macroscopic sub-areas (Turner and Weiss, 1963, pp.144-151). Five sub-areas are shown on Map 3b with the corresponding subfabric diagrams. Measurements number from 50 to 89. Although B_1 is nearly homogeneous for the Wyoming Creek antiform, sufficient variation exists to necessitate construction of 3 sub-areas here. The subfabric symmetry is generally monoclinic. Homogeneity is significantly greater for the B_1-subfabric than for the S_1-subfabric, especially in the Wyoming Creek antiform.

B_1 and B_2 are nearly parallel in Subareas 3 and 4, producing patterns typical of coaxial folding by flexural flow folding. Flexural slip folding produces a partial small circle girdle, whereas a partial great circle girdle results from coaxial refolding by passive flow or passive slip folding. Small circle B_1-girdles are most conspicuous in Sub-area 4, where F_2 folds are relatively "concentric". B_1 and B_2 are not parallel in Sub-area 5, where F_2 folds are also slightly "concentric" and open. These appear to be flexural flow folds in relatively non-ductile quartzites and para-amphibolites. B_1 and B_2 are not separated in Sub-area 3, but F_2 folds are apparently more appressed and "similar" in this area than in Sub-areas 4 and 5. Broad, open F_2 cross-folds suggested by the S_o- and S_1-subfabrics in Sub-area 3 (Map 3a) probably explain some of the scatter of B_1 data here. Primary B_1-maxima plunge S to SW in Sub-areas 3, 4 and 5, and no rotation around the major fold nose is noted. Figure 40 is a synoptic diagram for B_1 in this area. B_1 and B_2 are nearly parallel (Figure 43).

Sub-areas 1 and 2 illustrate rotation of B_1 around the Quad Creek synform. The NE maximum in Sub-area 1 and the W-NW maximum in Sub-area 2 show convergence of B_1 on the synform axis. However, the two subfabric patterns differ greatly. Quartzites and para-amphibolit compose most of Sub-area 2, while migmatites dominate in Sub-area 1. As discussed above, open, slightly "concentric"

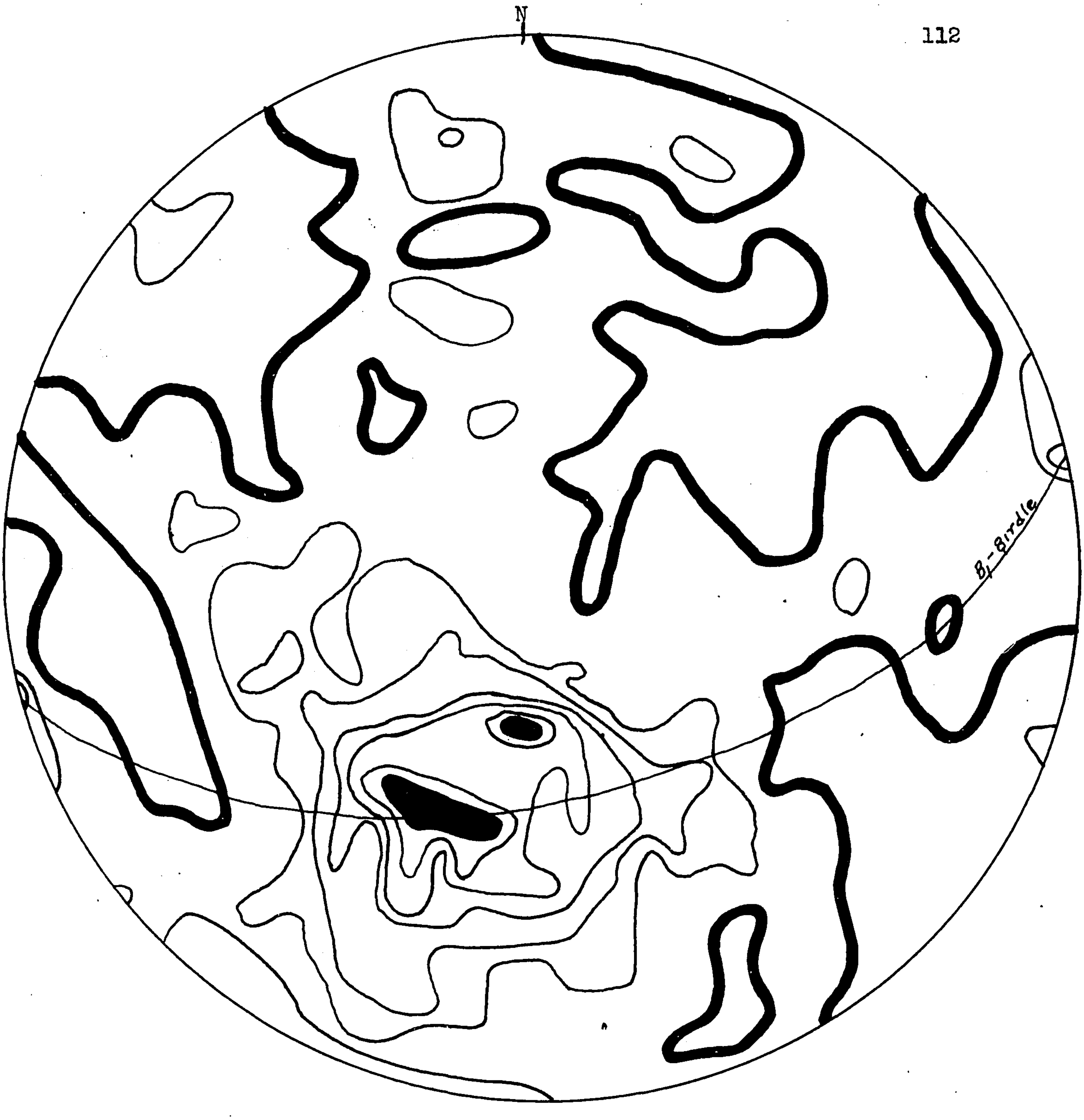

Figure 40. Synoptic B_1 diagram for Subareas 3, 4 and 5. Contour interval: 0.4-1.4-2.4-3.4-4.4-5.4-6.4%. Based on 213 measurements.

F_2 folds formed in relatively non-ductile rocks disperse B_1 into a distorted cone. This projects as a curviplanar surface intermediate between a partial small circle and a partial great circle girdle. Therefore, "similar" F_2 folds have formed on Sub-area 1, while open, slightly "concentric" F_2 folds have formed in the relatively non-ductile quartzites and para-amphibolites in Sub-area 2. The large width of the B_1-girdle in Sub-area 1 is attributed to gentle warping of B_1 by broad, open F_2 cross-folds, which may be due to the non-cylindrical and non-plane nature of small and large F_2 folds.

L_1-Subfabric

Mesoscopic:

Seventy-five (75) hornblende lineations (L_1) have been taken from para-amphibolite at all twelve structure stations. L_1-subfabric diagrams are keyed to the appropriate areas on Map 2b. A detailed analysis is given for each L_1-diagram in Appendix V.

L_1-subfabric symmetry ranges from monoclinic to triclinic, the lowest order of symmetry being in the east flank of the Quad Creek synform. The following are the most significant geometrical features of the L_1-subfabric in the Quad-Wyoming-Line Creeks area;

(1) The L_1-subfabric mimics the B_1-subfabric pattern

except for deviations explicable by contrasting F_2 fold styles due to mean ductility differences. F_2 folds are more "concentric" in relatively non-ductile para-amphibolite than in ductile migmatites.

(2) L_1 strikes approximately parallel to the S_o-plane.

(3) L_1-girdles usually approach partial small circles, so that they trend about perpendicular to the S_o-plane. However, great circle girdles have been constructed on Maps 2b and 3b, because the pattern is scattered and intermediate between great and small circle girdles. Distorted small circle girdles are shown in Appendix V only.

(4) L_1 generally plunges more gently than B_1.

(5) L_1 is widely dispersed in the east flank of the Quad Creek synform.

(6) L_1 rotates around both major noses.

F_2 folds in para-amphibolite have dispersed L_1 into partial small circle girdles with little suggestion of partial great circle girdles. This pattern suggests that F_2 folds are nearly "concentric" in these relatively non-ductile rocks (Ramsay, 1960, pp.75-93). Figure 41 illustrates the writer's interpretation of the geometrical relations of L_1 and B_2 at Structure Station 12. L_1 trends W-SW and was nearly horizontal prior to F_2 folding. Slight overturning to the SE of the SW plunging F_2 folds produces L_1 lineations plunging gently east and dispersion into distorted partial small circle girdles. This interpretation requires only minor revisions to be applicable at Structure Stations 10 and 11 also. The larger scatter of L_1 at the latter station is believed by the writer to be due to agmatization which is extensive here. The L_1 maximum plunges more gently west at the former station than at Station 12. However, limited suitable outcrops confined L_1 measurements to a relatively small area at Structure Station 10. Concentration of these measurements on the SE flank of an overturned, open F_2 fold may be partly responsible for this pattern. Agmatization has produced scatter of the L_1 data at this station also. However, L_1 appears to trend W-SW here, while B_1 trends about N-S.

Although B_1 and B_2 are not separated at Structure Stations 6, 7, 8 and 9, the subfabric suggests B_2 plunges moderately S-SW. Therefore, B_2 strikes slightly more south at these stations that at Stations 10, 11 and 12. Utilizing the interpretation presented in Figure 41, partial small circle L_1-girdles should appear in the S-SW and N-NE near the great circle. However, the girdles (a).

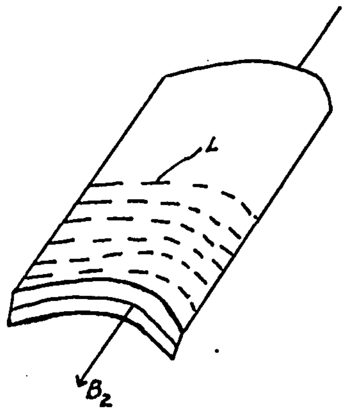

(b).

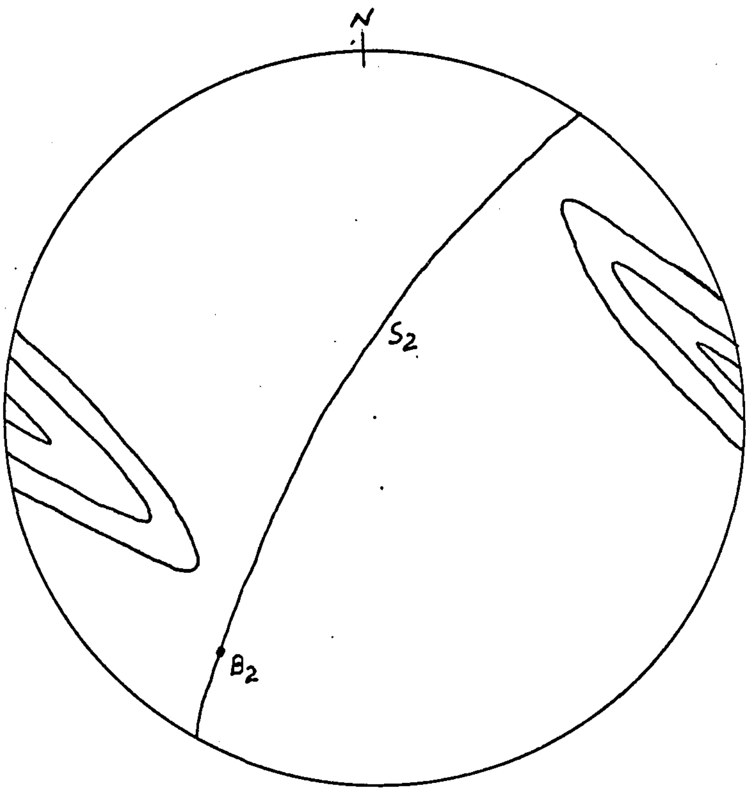

Figure 41. Earlier rectilinear hornblende lineations, L_1, deformed by an open, slightly concentric F_2 fold.

(a). B_2 plunges about 30°SW and L_1 was nearly horizontal prior to F_2 folding.

(b). L_1 is ideally dispersed along partial great circles. S_2 is the axial plane of F_2 and shows slight overturning to the SE.

trend about E-W with maxima plunging gently S. This relation indicates that L_1, B_1 and B_2 very closely approach parallelism in these sub-domains. Agmatization and superposition of broad, open F_2 cross-warps is believed by the writer to explain the scatter and triclinic symmetry. These cross-warps may be due to superposition of F_2 on F_1 rather than being a distinct fold set.

The L_1-symmetry at Stations 4 and 5 are very similar to the B_1-subfabric patterns at Stations 3 and 4. The rocks are dominantly quartzites and para-amphibolites at Stations 4 and 5 and contain slightly "concentric" F_2 flexural flow folds. The subfabric patterns reflect the F_2 folding style by dispersion of earlier rectilinear lineations, B_1 and L_1, into curviplanar surfaces intermediate between partial small circle and partial great circle girdles. Orienation of the maxima at these stations and number 6 show the rotation of L_1 into the Quad Creek synform nose. Structure Station 3 is anomalous, because the entire pattern has rotated about 120 degrees S from Stations 4 and 5. Agmatization is not extensive here, and no faults or shear zones have been noted. B_1 and L_1 are believed to be nearly parallel at all of these stations. The L_1 measurements were confined to a relatively small area. The writer concludes that concentration of L_1 measurements in the hinge of an F_2 fold overturned to the N is the cause of this pattern.

L_1 has rotated completely around the Quad Creek synform nose at Stations 1 and 2. Maxima plunge NE, indicating convergence on the major synformal axis. The L_1-subfabric patterns at these stations suggest relatively "concentric" F_2 folds in the non-ductile para-amphibolite.

Macroscopic:

Mesoscopic stations homogeneous with respect to L_1 have been combined to form homogeneous macroscopic sub-areas. Measurements number from 75 to 300 in the 6 sub-areas which are keyed to the appropriate areas on Map 3b. Detailed analysis of individual diagrams is given in Appendix V. The symmetry is generally monoclinic, with the highest degree of triclinity being in Sub-area 4.

Although L_1 and B_1 appear to be generally parallel and trend approximately parallel to the S_0-plane, the subfabric patterns differ greatly in Sub-areas 1, 2, 4, 5 and 6. L_1 girdles are near the great circle and strike about perpendicular to the S_0-plane. Field observations and consideration of contrasting fold styles in para-amphibolite and migmatites suggest that B_1 and L_1 are nearly parallel throughout the area. The greatest divergence from parallelism is probably in Sub-areas 5 and 6. The writer believes that lower mean ductility in para-amphibolite has produced open, nearly "concentric" F_2 folds, while appressed "similar" F_2 folds deform B_1 in ductile migmatites. Selective L_1 measurements from portions of F_2 folds yield local divergences from the overall L_1 pattern (Sub-area 2).

The previously discussed L_1-subfabric geometry in Sub-area 6 is generally applicable throughout the Wyoming Creek antiform (Sub-areas 4 and 5), but L_1 rotates around the major nose. However, L_1 and B_2 appear to be more nearly parallel in Sub-area 4 than in Sub-areas 5 and 6. Agmatization and possibly superposition of broad, open F_2 cross-folds has produced scatter of the L_1 data in Sub-area 4 also.

L_1- and B_1-subfabrics in Sub-area 3 are strikingly similar in contrast to the widely different L_1 and B_1 patterns in the other subareas. The differences in the mean ductility of para-amphibolite and quartzite are apparently small. Therefore, the writer concludes that similar subfabric patterns are developed here, because F_2 folds are slightly "concentric" and open in both rock types. As previously mentioned, the apparent rotation of the L_1-subfabric in Sub-area 3 is due to selection of L_1 measurements from a small portion of an open F_2 fold.

L_1 has rotated completely around the Quad Creek synform nose in Sub-area 1. B_1 measurements are dispersed into a partial great circle in these ductile migmatites, while L_1-girdles approach partial small circles. F_2 folds are "similar" in the migmatites but "concentric" in the para-amphibolite.

Measurements of skialith elongations (L_1) are not numerous, because measurements were taken only when the attitude was clearly defined. Examination of the attitudes at Stations 2, 3 and 6 (Figures 42a, b and c) suggests that these L_1 measurements are coincident with B_1 rather than B_2. Therefore, these linear elements must have formed during F_1 folding and been refolded during F_2 (Station 6).

As previously mentioned, mica aggregates are occasionally drawn out producing lineations. The attitudes shown in Figure 42d were measured from green mica aggregates on the surfaces of quartzite layers in F_2 folds from Line Creek canyon (Station 12). These measurements correspond only roughly with B_2 (Map 2b). However, they were confined to a small area and are believed by the writer to have formed during F_2 folding by flexural flow. Significantly, these lineations (L_2) indicate transport to the south at a moderate angle. Drawn biotite aggregates are occasionally developed on the surfaces of para-amphibolite layers in the Quad Creek area. They plunge gently S here and are apparently concordant with the major synform axis.

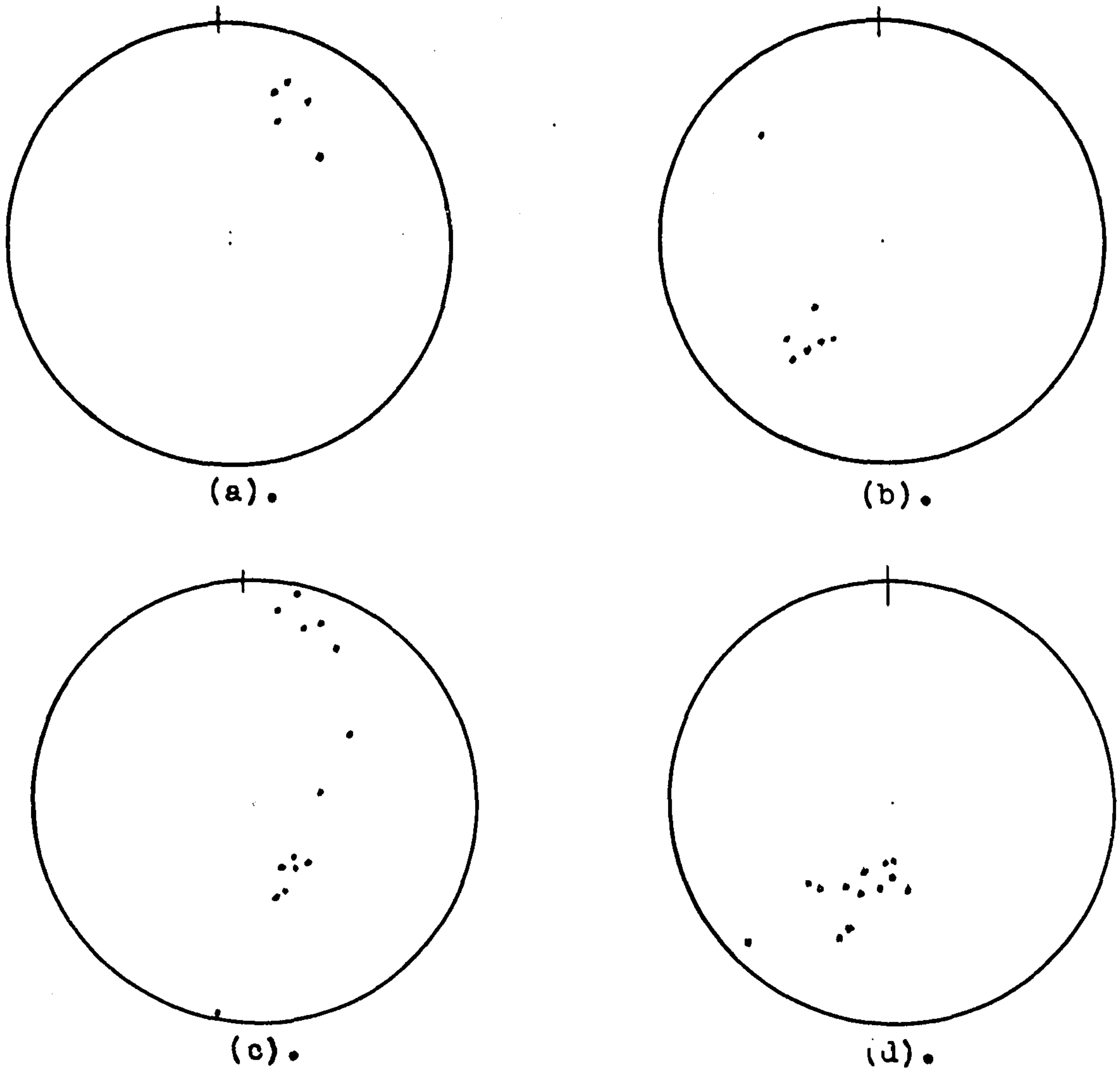

Figure 42. Projections a, b, and c show skialith elongations, L_1, at Structure Stations 2, 3, and 6, respectively. Projection d shows green mica elongations, L_2, at Structure Station 12.

B_2-Subfabric

Mesoscopic:

B_2 measurements number from 3 to 17 at stations where F_1 and F_2 are separable. No B_2 measurements are given for Stations 1, 4, 6, 7, 8, 9 and 11, because F_1 and F_2 are not easily distinguished in these sub-domains. Most of the B_2 axes at Stations 2, 3, and 5 have been derived from samples showing refolding of F_1. Uncontoured data are keyed to the appropriate areas on Map 2b. B_2-subfabric symmetry ranges from axial at Structure Station 3 to monoclinic at Station 10. These data are given in Appendix VI also.

The B_2-subfabric is generally monoclinic at Structure Stations 10 and 12. Turner and Weiss (1963, pp.129-143) have shown that superposition of fold sets yields non-cylindrical later (F_2) folds. However, this effect is slight when later folds are considerably larger than the earlier folds. Although overprinting of F_2 and F_1 may explain some of the B_2 dispersion, consideration of the larger fold attitudes on a regional scale (Figure 4) suggests an alternative explanation. Major folds in the Beartooth range plunge from 10 to 40 degrees to S-SW. Small F_2 folds in the Wyoming Creek antiform appear to be parasitically related to the major structure. Therefore, the writer concludes that the B_2 dispersion is a reflection of the major fold non-cylindrical character. These geometrical relations may be inherent in these Archean folds or due to a later deformation. No later small folds have been identified at Stations 10 and 12. The writer believes that the larger and smaller F_2 folds developed non-cylindrically due to triaxial strain during folding. Although B_1 and B_2 are not separated at Stations 6, 7, 8 and 9, primary $B_{1,2}$-subfabric maxima and two refolded samples, indicate that B_2 plunges moderately S-SW in these areas. B_2- and β S_1-axes are nearly coincident throughout the Wyoming Creek antiform.

B_2 plunges gently E-SE at Structure Stations 3 and 5, agreeing closely with constructed β S_1-axes (Map 2a). Rotation of B_2 around the Quad Creek synform nose is completed at Structure Station 2, where the B_2 trend is about N-S. However, the normal southerly plunge has not been resumed. Assuming a B_2 south plunge in the west Quad Creek flank, B_2 converges slightly on the major synform axis. Scatter of the B_2 data at Station 2 may be due to superposition of F_2 on F_1.

Macroscopic:

Three sub-areas have been constructed by combining stations homogeneous with respect to B_2. Map 3b shows the uncontoured data keyed to the appropriate areas. The macroscopic B_2-subfabric symmetry is axial in Sub-area 2 and monoclinic in Sub-areas 1 and 3. Detailed discussions are given in Appendix VI.

B_2 does not rotate around the Wyoming Creek antiform nose (Sub-area 3) and is, therefore, considered a penetrative fabric element for this major structure. These F_2 small folds are interpreted by the writer as parasitic folds on the major antiform, reflecting the non-cylindrical character of the major structure. B_2 is nearly coincident with the β S_1- and β S_o-axes for the entire fold (Figure 43).

B_2 rotates around the Quad Creek synform nose and assumes a nearly horizontal plunge in Sub-areas 1 and 2. B_2 agrees reasonably well with constructed β S_1-axes here.

Summary

<u>B_1-subfabric</u>:

The axes of isoclinal flow folds, B_1, have been folded by "similar" F_2 folds in migmatites and granitic gneisses throughout the Quad-Wyoming-Line Creeks area. Therefore, B_1 is dispersed into a partial great circle which generally trends perpendicular to the S_o-plane. Slightly "concentric" F_2 folds have deformed B_1 at Stations 3, 4, 5, 9, 10 and 12, where the rocks are

Figure 43 . Synoptic B_2 and S_2 diagram for Subarea 3.

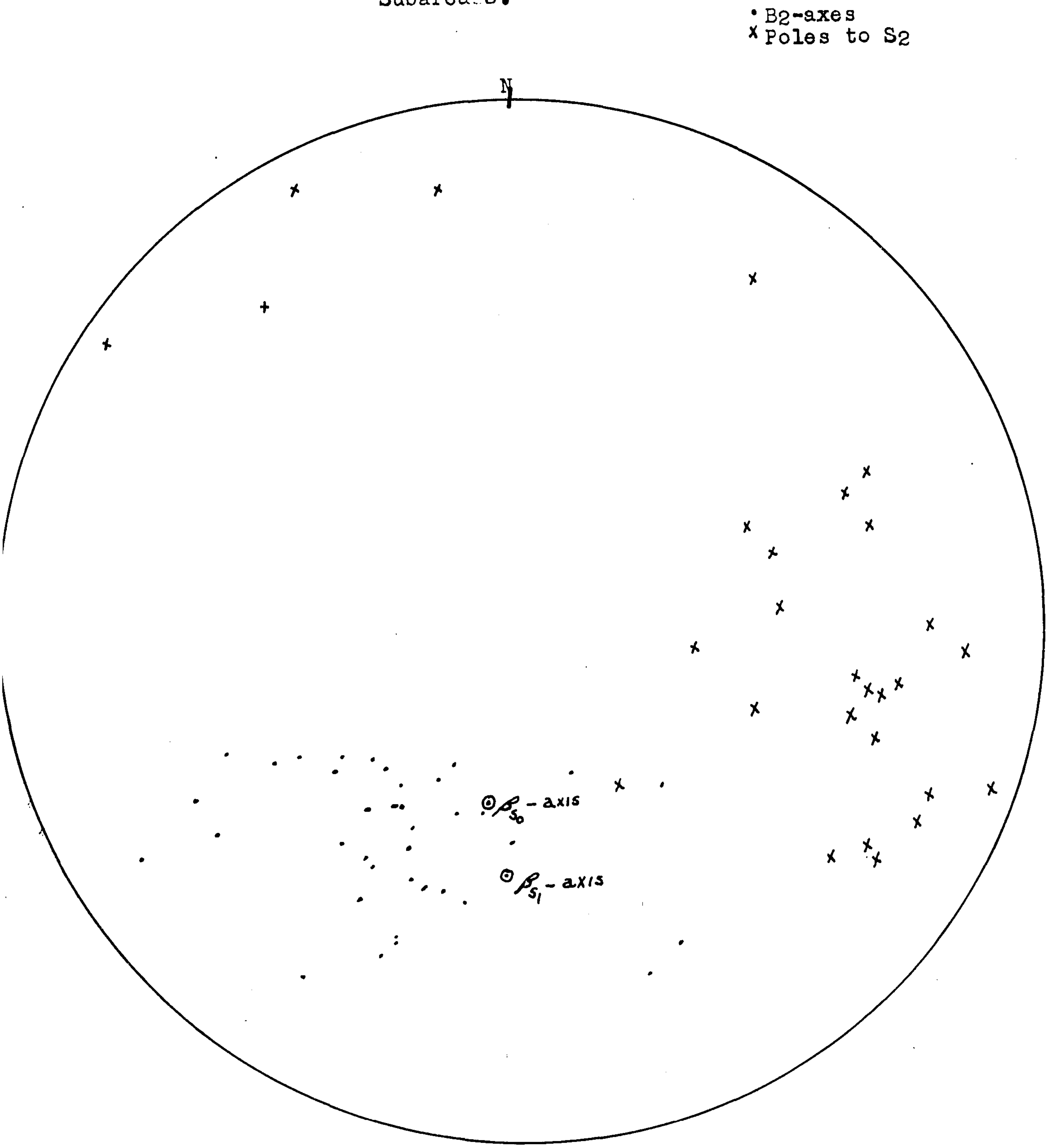

relatively non-ductile quartzites. The B_1-girdle is a curvi-planar surface intermediate between a partial small circle girdle and a partial great circle girdle, suggesting that F_2 folds are intermediate between "similar" and "concentric" styles (Ramsay, 1960, pp.75-93) in these non-ductile rocks. B_1 and B_2 are generally parallel, the greatest divergence being at Stations 11 and 12. B_1 converges on the major Quad Creek synform axis and rotates around the nose. In contrast, B_1 does not converge on the Wyoming Creek antiform axis, nor does it show any significant rotation in strike in the nose. The B_1-girdle for the entire Wyoming Creek antiform is shown in Figure 40.

$\underline{L_1\text{-subfabric}}$:

L_1 is generally parallel to B_1, but nearly "concentric" F_2 folds have formed in the relatively non-ductile para-amphibolite. L_1-girdles generally trend perpendicular to the S_o-plane and the B_1-girdle, because the nearly "concentric" F_2 folds have dispersed L_1 into partial girdles which more nearly approach small circles than great circles. The L_1-subfabric is dispersed by agmatization, especially in the east flank of the Quad Creek synform. L_1 rotates around the Quad Creek synform nose and converges on the major axial zone, while it only rotates around the Wyoming Creek antiform nose. Therefore, the L_1-subfabric mimics the B_1-subfabric when contrasting mean ductilities and F_2 fold styles in para-amphibolite and migmatites are considered, except at Station 10. The two subfabrics are nearly identical at Stations 3, 4 and 5, where B_1 was measured in non-ductile quartzites and para-amphibolite. The writer concludes that the subfabrics are similar here, because B_1 and L_1 measurements have been derived from rocks with similar mean ductilities. The F_2 folds appear to have formed through flexural flow at these stations. The parallelism of L_1 and B_1 suggests synchronous development of these lineations.

Although measurements of skialith elongations are sparse, the data suggest parallelism of these lineations with B_1 and hornblende elongations. It is, therefore, concluded that skialiths assumed their orientation during F_1 folding.

L_2 measurements are from drawn-out green mica and biotite aggregates. Although they are sparse, they are nearly coincident with B_2.

$\underline{B_2}$**-subfabric:**

B_2 measurements are not available at stations where F_1 and F_2 are not separable and are scarce at the other stations. However, the data are sufficient to demonstrate rotation of 90° around the Quad Creek synform nose. In contrast, B_2 strike parallel to the Wyoming Creek antiform axis, and F_2 folds appear to be parasitically related to the major antiform. As previously stated, B_1 and L_1 are generally parallel with B_2, but the largest divergence in strike is approximately 37 degrees at Station 12. The difference in B_1 and B_2 dips may be about 30° here. F_1 and F_2 appear to be nearly coaxial at Stations 6, 7, 8, 9 and 10. Strikes are approximately parallel at Stations 1, 2, 3, 4 and 5, but the B_1-B_2 dip separation is about 35° when measured from the horizontal.

Interpretation of Fabric

Interpretation of the Quad-Wyoming-Line Creeks tectonite is aided by qualitative kinematic analysis. Detailed quantitative kinematic and dynamic analyses are not within the scope of the present study, since petrofabric data are not presently available. Contrasting fold geometries in rocks of different mean ductilities emphasize the importance of rheological properties in the movement picture. Contrasts of this type appear to be important in the present area. Mesoscopic linear and planar penetrative fabric elements are used here for kinematic analysis, primarily following the method developed by Ramsay (1960, pp.75-93).

Much confusion has arisen concerning interpretation of Sander's fabric axes (1948, 215pp.). Futile controversies are still evident in the literature concerning _a_- and _b_-lineations in the Caledonian rocks of Scandinavia and Britain. Weiss (1959, p.26) believes that these controversies have arisen primarily from a lack of appreciation of fabric symmetry and from confusion of fabric axes with kinematic axes. Therefore, Turner and Weiss (1963, p.400) restrict the use of kinematic axes _a_, _b_ and _c_ to movement pictures having monoclinic symmetry expressible in terms of gliding upon a prominent structural discontinuity (an s-surface). The following principles are emphasized for purposes of clarity in the discussion to follow;

(1) Kinematic *a* and *b* lie in the axial plane; *c* is perpendicular to the *ab* plane.

(2) Kinematic *b* corresponds to the B-fold axis in purely flexural slip folding but may be at any angle to B in passive slip, passive flow and flexural folding. *Therefore, B- and constructed β-axes generally do not parallel kinematic b.*

(3) "Similar" folding disperses earlier rectilinear lineations along a partial great circle girdle which contains the *a* direction (Ramsay, 1960, p.89; Turner and Weiss, 1963, pp.482-483). Orientation of this partial great circle is controlled by the direction of *a* and the initial orientation of the earlier lineations. Since *a* is included in the axial plane, *a* is defined by the intersection of the axial plane and the partial great circle girdle. Kinematic *b* lies 90° from *a* in the axial plane, and *c* is perpendicular to the *ab* plane. Deformed lineations are rotated towards *a* (Ramsay, 1960, Figs. 17, 18, and 19).

The Quad-Wyoming-Line Creek area has been divided into two sub-domains on the basis of fabric symmetry; the Quad Creek synform displays triclinic symmetry, whereas the Wyoming Creek antiform is monoclinic. Kinematic analysis is restricted here to the latter area. The general style of the antiform is similar, especially when viewed by the "down-plunge method". Small F_2 folds show contrasting styles in rocks possessing different mean ductilities. Similar F_2 folds are prevalent in the ductile layers, such as migmatites and micaceous schists, while nearly concentric F_2 folds have developed in relatively non-ductile quartzites and para-amphibolite. Deformation of B_1 by both similar and concentric F_2 folds is reflected in the B_1-subfabric patterns in Sub-areas 3, 4, and 5. B_1 and B_2 are nearly parallel in Sub-areas 3 and 4, whereas the $B_1 \measuredangle B_2$ is about 30° with respect to strike in Sub-area 5. B_1 appears to have been nearly horizontal here prior to F_2 folding. It must be emphasized that B_1 and B_2 are not distinguished in Sub-area 3 and in only part of Sub-area 4.

Two nearly perpendicular B_1-girdles are suggested in Sub-areas 3, 4, and 5. Ramsay's method of locating a is restricted to earlier lineations deformed by similar folds. The N-S trending B_1-girdles are due to deformation of B_1 by similar F_2 folds, since B_1 and B_2 are nearly coincident in Sub-areas 3 and 4. This girdle is poorly defined in Sub-area 5, where F_2 folds are nearly concentric. The generally E-W trending B_1-girdles in these Sub-areas are believed by the writer to be due to concentric F_2 folding of B_1 in relatively non-ductile quartzites and para-amphibolites. Block rotation during agmatization may be partially responsible for these B_1-girdles. The N-S trending B_1-girdle for the entire Wyoming Creek antiform has been plotted on Figure 44 with the S_2-plane. Accurate location of the S_2-plane is difficult here, because small F_2 folds are not strictly cylindrical and plane (S_2, Map 3a, Subareas 4 and 5). Therefore, the general trend of the major axial surface has been plotted in Figure 44. Location of a in the SW implies transport in that direction. The generally E-W trending B_1-girdle passes very close by the constructed a. B_2-, βS_1- and βS_0-axes are nearly coincident with a. Casella (in press) obtained a, b, and c orientations in the Line Creek synform similar to the orientations constructed here for the Wyoming Creek antiform. Drawn-out mica aggregates, L_2, at Station 12 (Figure 42) show a maximum plunging moderately S. Although this attitude is slightly discordant with a, it provides independent evidence for transport to the S or SW. The significance of this movement picture will be considered in more detail subsequent to a brief review of the F_1 and F_2 geometrical relations in the two major F_2 folds. L_1 has not been used for kinematic analysis, since it is folded by slightly concentric F_2 folds. Intersection of the S_2-plane and the L_1-girdle would be in the SW also.

Studies by Professor Arie Poldervaart and his students have defined a series of open folds plunging S to SW. In the Lonesome Mountain area (Larsen, Poldervaart and Kirchmayer, in preparation), mesoscopic and macroscopic fabric analysis have demonstrated monoclinic fabric symmetry and generally coincident β- and B-axes. The initial fabric was apparently homotactic here. No kinematic analysis was conducted, and small fold axial planes were not measured.

The present study clearly demonstrates the existence of two fold sets in the Quad Creek synform nose. F_1 fold axes, B_1, as well as skialith and hornblende elongations, rotate around the major synform nose and converge on the axial zone. However, B_2 also rotates around this nose, but convergence in the axial zone is not pronounced. These geometrical relations suggest that the Quad Creek metanorite body has been a significant, but local, factor in the development of these fold sets.

Field observation and statistical structural analysis in the Wyoming Creek antiform have demonstrated refolding of small F_1 folds by F_2 folds. However, no undoubted large F_1 folds have been found by the writer outside the Wyoming Creek area. Additionally, neither B_1 nor B_2 rotate around the Wyoming Creek antiform nose. <u>In significant contrast, L_1 rotates around both major F_2 fold noses</u>.

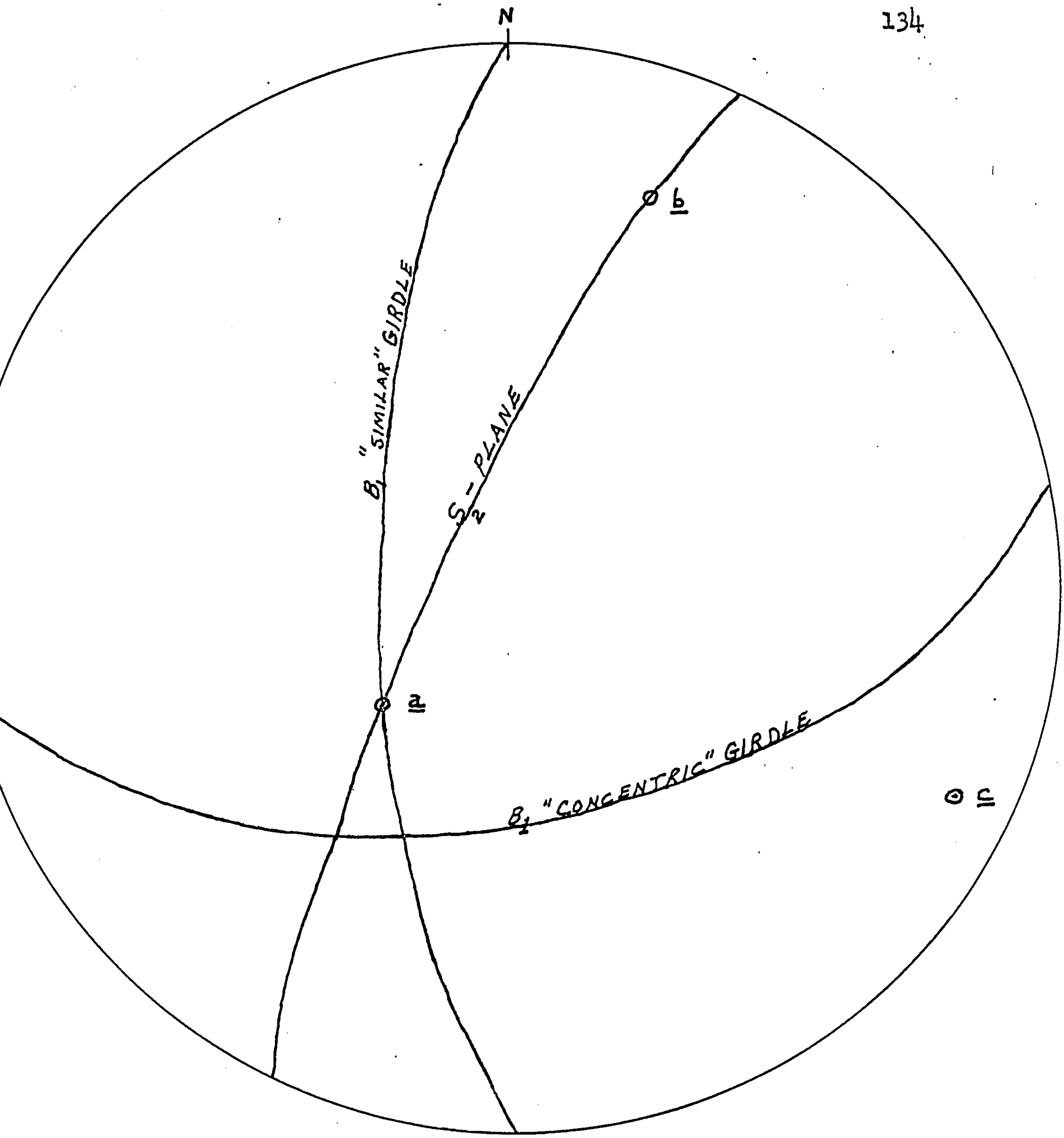

Figure 44. Location of a, b, and c in the Wyoming Creek antiform using the S_2-plane and the B_1-girdle.

Therefore, geometrical data are conflicting from the sub-domains represented by the two major F_2 folds. Briefly stated, two hypotheses appear to be feasible:

(1) The monoclinic fabric of the Wyoming Creek antiform suggests that this is a B-tectonite produced during one period of deformation. In this case, the Quad Creek synform is an anomalous area, since the fabric symmetry here is triclinic. Therefore, the geometrical relations in the Quad Creek synform nose are logically related to the location of the metanorite body in the major F_2 axial zone. However, rotation of L_1 around both F_2 noses is not in agreement with the B-tectonite hypothesis.

(2) Alternately, the entire Quad-Wyoming-Line Creeks area is a $B \wedge B'$ tectonite. In this hypothesis, the metanorite body would have functioned as a protecting block during granitization and, possibly, shearing also. Paucity of large F_1 folds in the Wyoming Creek antiform would be attributed to extensive shearing of earlier F_1 folds and intense granitization. However, B_1 does not rotate around the Wyoming Creek antiform nose.

B-tectonite Hypothesis:

Rotation of L_1 around the Wyoming Creek antiform nose, as well as around the Quad Creek synform nose, presents a very formidable objection to the B-tectonite hypothesis. However, this hypothesis warrants consideration here, because it has been accepted generally by most workers in the Beartooth Mountains. The facts that no large F_1 folds have been found in the Wyoming Creek antiform and that small F_1 folds are generally passive flow folds lying in the S_0-plane of ductile layers strongly support this hypothesis. Additionally, B_1 neither rotates around the major F_2 antiform nor converges on the axial zone. The mesoscopic and macroscopic S_1-subfabrics show that F_1 is deformed by F_2 folds. These geometrical relations do not necessarily require that the F_1 folds be distinctly younger than the F_2 folds, because they may have developed synchronously. Assuming the application of NW-SE directed horizontal stresses to layers possessing high ductility contrasts, flowage in the ductile layers would initiate flexing in the rigid, non-ductile plates. In this sense, the passive flow folds (F_1) would be older than the open, nearly concentric F_2 folds but part of the same sequence. Continued unsteady flow might produce refolding about the initial axis of folding (Wynne-Edwards, 1962, p.30). Intense refolding and synchronous or later granitization might explain the hook outcrop pattern developed on the hand specimen scale in the migmatites in Sub-area 3.

Kinematic a indicates that the direction of flow or transport was towards the Wyoming Creek antiform nose, and the following relations support this conclusion;

(1) Drawn-out mica aggregates, L_2, show a maximum in the south,

(2) Agmatization is extensive in the major antiform nose and

(3) Map 1 shows slight thickening of layers in this nose also.

Therefore, development of passive flow folds (F_1) would be favored in the ductile layers confined between rigid quartzite and para-amphibolite layers.

In this hypothesis, rotation of B_1 and B_2 around the Quad Creek synform nose and the prominence of F_1 folds here are attributed directly to the presence of the metanorite body in the major F_2 synform axial zone. This body might have acted as a structural buttress during one phase of deformation by flexural flow folding. The F_1 fold set would then develop as a manifestation of local triaxial strain. Although these local stresses would be primarily north directed in the formation of the large south plunging F_2 fold, the overall stress distribution would probably be radial from the metancrite body. Geometrical relations suggest that the F_1 folds and the hornblende and skialith elongations are older than the major F_2 synform, although the temporal hiatus may be small. Apparently, the metanorite body was emplaced synchronously with or prior to F_2 folding. The writer believes that the systematic rotation of L_1 and B_1 around the major F_2 nose argues against synchronous intrusion of the metanorite. However, it is feasible that buttressing against this body under high temperatures and pressures might prevent pronounced divergence of these linear features during intrusion of the metanorite.

$B \wedge B'$-Tectonite Hypothesis:

Superposition of two fold sets is considered in some detail in this discussion, because

(1) Hornblende lineations, L_1, rotate around both major F_2 fold noses,

(2) Shearing which is apparently pre-granitization in age has been demonstrated in the west flank of the Quad Creek synform, and axial plane foliation (S_2) is extensively developed in the east flank of the Quad Creek synform,

(3) The deformed small F_1 folds discussed in the above hypothesis may be remnants of an earlier fold set (F_1), and

(4) The deformational histories of surrounding Precambrian terrains, such as the northern Tobacco

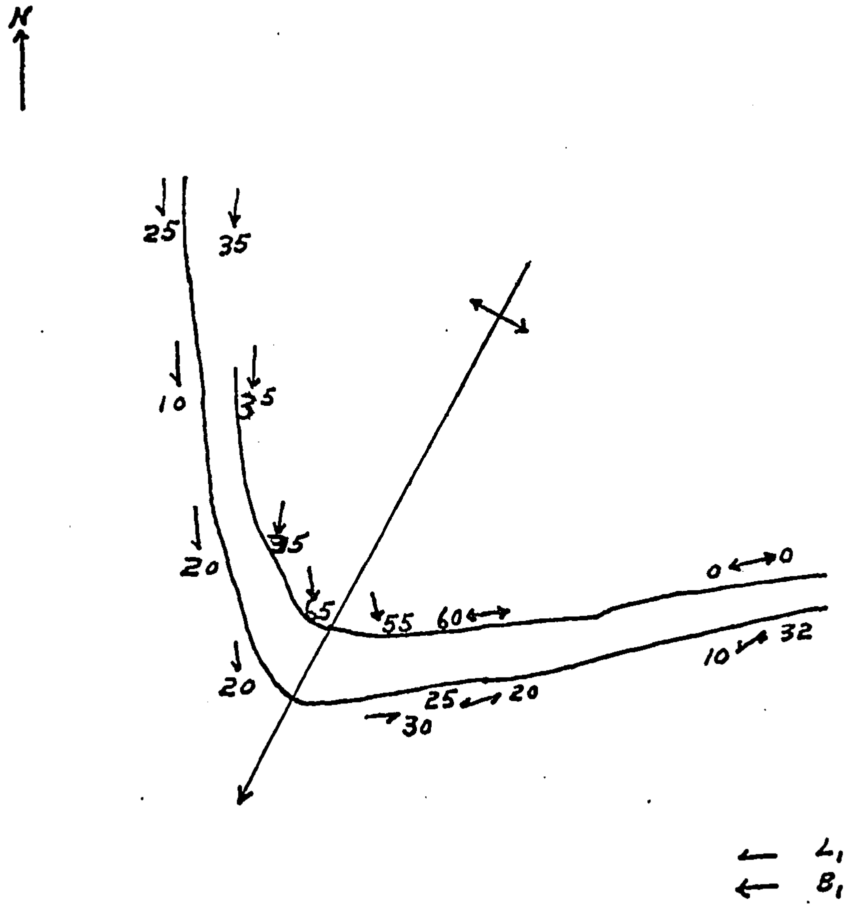

Figure 45. Attitudes of primary L_1 and B_1 maxima in the Wyoming Creek antiform.

Root Mountains, are complex with at least two periods of deformation. Intense recrystallization and granitization in the Lonesome Mountain area (Larsen, Poldervaart and Kirchmayer, in preparation) and the Bighorn Mountains may have destroyed all mesoscopic evidence of an earlier fold set.

The writer concludes that L_1 is distinctly older than the F_2 folds, since it rotates around the major F_2 folds and is dispersed into partial small circle girdles by smaller F_2 folds on the mesoscopic scale. Additionally, Casella (in press) has reported horizontal lineations in the Line Creek synform nose. B_1 and L_1 are generally parallel throughout the Quad-Wyoming-Line Creeks area, except in the Wyoming Creek antiform nose (Maps 2b and 3b). Therefore, L_1 lies in the S_o-plane without exception. Coincidence of these linear elements appears to be more than fortuitous. Attitudes of primary L_1 and B_1 maxima are plotted in Figure 45 for the Wyoming Creek area. Parallelism of the two lineations is evident, except in the major antiform nose where they are nearly perpendicular. Neither faulting nor block rotation during agmatization adequately explains the systematic rotation of L_1 in the S_o-plane. Therefore, L_1 appears to be an earlier lineation deformed by F_2 folds, thus precluding

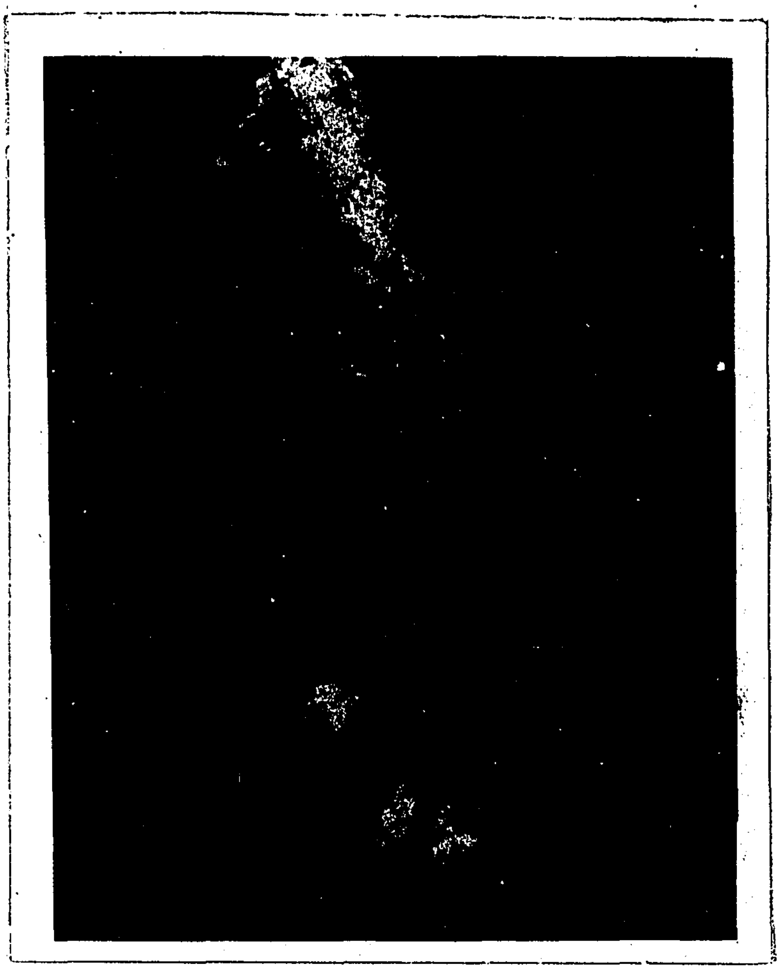

Figure 46. Slightly warped, appressed F_1 fold from the east flank of the Quad Creek synform. Natural size.

the possibility that the Wyoming Creek antiform is a simple B-tectonite.

It is assumed in this hypothesis that all F_1 folds are representative of an earlier fold set, which has been nearly destroyed by shearing and granitization throughout the Wyoming and Line Creeks area but is preserved in the Quad Creek area by the protecting metanorite body. This assumption is not necessary if L_1 is not correlated temporally and genetically with the F_1 folding. Although L_1 may be older than F_1, pronounced parallelism of L_1 and B_1 seems to render correlation of the two lineations as being very plausible. This correlation requires

(1) Destruction of large F_1 fold hinges in the Wyoming Creek antiform,

(2) General rotation of B_1 and S_1 through the major F_2 folds, except in the F_2 antiform nose, and

(3) An adequate explanation for the attitude of small F_1 folds in the Wyoming Creek nose.

Reid (1963, p.294) has described early isoclinal folding of Cherry Creek and Pony rocks in the northern Tobacco Root Mountains, followed by two periods of mafic dike intrusion and shearing parallel to the early axial plane foliation. Hinge zones have been largely destroyed by this shearing. The entire sequence was then deformed into broad, open N-S trending folds. However, these rocks have not been subjected to the intense granitization which is characteristic of the Beartooth Mountain Archean rocks.

Pre-granitization shearing of F_1 folds has been demonstrated in the west flank of the Quad Creek synform. Additionally, the writer believes that the cross-bedding reported (Casella, in press) in the Line Creek migmatites is actually pregranitization shearing of earlier small folds. Shearing of this type is only rarely observed. However, this is probably due to the obscuring effect of later recrystallization and granitization.

No axial plane foliation has been observed in the F_1 folds. This planar element may have been destroyed by later granitization also, if it ever existed. Axial plane foliation (S_2) is commonly developed by biotite in migmatite and, occasionally, in quartzites. This later axial plane foliation has transposed the earlier biotite S-surface nearly completely in migmatites where F_2 folds are intensely appressed (Sub-area 3). Hook outcrop patterns characterize these areas. Field observations and statistical structural analysis indicate that the $S_1 \measuredangle S_2$ angle is small. Although this axial plane foliation (S_2) has probably developed in quartzites, it is not readily detectable megascopically.

The writer believes that quartzites and para-amphibolite have responded to axial plane refolding (Scotford, 1955, p.1614) of isoclinal F_1 folds primarily by shearing. Shearing prior to F_2 folding may have destroyed F_1 fold hinges also. Complete rotation of the F_1 folds would tend to obscure these folds, because B_1 and B_2 are nearly parallel. However, folds have been observed in Sub-areas 1 and 3 which the writer believes are appressed F_1 folds. The smallest of these three folds is shown in Figure 46, and its degree of appression is characteristic of the larger folds in these areas. It is apparent that these structures might go undetected unless the small hinge zones were observed directly. Therefore, the writer believes that F_1 folds have been destroyed by shearing at a small angle to the S_1-surface. Rotation of F_1 has obscured these earlier folds also. There are no data to suggest the wave length and amplitude of the F_1 folds, but they were apparently E-W trending.

One of the most formidable objections to the $B \wedge B'$ hypothesis is the fact that B_1 does not rotate around the Wyoming Creek antiform nose. However, transport of material into this F_2 fold nose during refolding of F_1 and confinement of ductile material between thick, rigid quartzite and para-amphibolite layers may have produced rotation of F_1 passive flow folds here. Knill and Knill (1958, pp.497-510) have described rotated, "discordant" folds which are preserved as remnants only. Apparently, the non-ductile layers would not react in this manner due to their greater rigidity. Turner and Weiss (1963, p.501) point out that small earlier folds are occasionally rotated internally.

The S_0-subfabric provides additional evidence for transportation of an earlier fabric through intense refolding and granitization. Although the S_0-subfabric is monoclinic on the macroscopic scale, it is generally triclinic on the mesoscopic scale. In contrast, the meso- and macroscopic fabric symmetries are both monoclinic in the Lonesome Mountain area (Larsen, Poldervaart and Kirchmayer, in preparation). It is difficult to explain the lower symmetry in the Quad-Wyoming-Line Creeks tectonite unless it is assumed that the original fabric has been almost completely destroyed and is only detectable on the mesoscopic, and probably the microscopic, scales.

Rotation of B_1, L_1 and S_1 in the F_2 folds apparently requires that temperatures and pressures be maintained at a level sufficient to render the entire body relatively mobile. Therefore, it appears that the two fold sets are probably parts of one phase of deformation. However, Turner and Weiss (1963, p.501) suggest that the relative sizes of earlier and later folds controls the survival of the earlier fold set. As previously stated, there is little evidence concerning the magnitude of the F_1 folds.

The E-W trending F_1 synform in the Quad Creek area may either be parasitically related to larger, but obscured, F_1 folds or represent the largest F_1 folds developed. However, interdigiting tongues of granitic gneisses and migmatites in the Quad Creek area (Eckelmann and Poldervaart, 1957, Plate 5) may indicate that the distribution of these rocks might be directly related to refolding of large, isoclinal F_1 folds by N-S trending F_2 folds.

Mineralogical evidence also suggest F_1 and F_2 folding as one extended sequence during metamorphic differentiation and granitization. Concentration of both feldspars in the crests and troughs of F_1 small folds is evident, but this may be due to metamorphic differentiation rather than granitization. Biotite apparently developed prior to F_1 folding, since it is folded by small F_1 flexures. It also developed during F_2 folding, forming S_2 axial plane foliation. Therefore, biotite appears to have crystallized prior to F_1 folding and during F_2 folding. Hornblende elongations, L_1, are generally parallel with F_1 fold axes, B_1, suggesting hornblende crystallization during the early stages of the sequence. Both feldspars have formed in the S_2-plane, occasionally developing pronounced axial plane foliation. However, this is not detectable on the scale of the two large folds.

Although the geometrical data are conflicting, the writer tentatively accepts the $B \wedge B'$ hypothesis. Additional detailed structural analysis, especially on the microscopic scale, will be necessary to test the validity of this hypothesis on a regional scale. Relations of the metanorite body to deformation, metamorphic differentiation, and granitization are still problematical. The writer has stated evidence which may suggest pre-F_2 folding emplacement. However, these data are far from being conclusive. Petrofabric analysis of the metanorite biotite and orthopyroxene may clarify this problem.

Bibliography

Bucher, W.H., 1934, Geologic problems of the Beartooth-Bighorn region; Geol. Soc. America Bull., v.45.

Bucher, W.H., Chamberlin, R.T., and Thom, W.T., Jr., 1933, Results of structural research in Beartooth-Bighorn region, Montana and Wyoming; Am. Assoc. Petroleum Geologists Bull., v.17.

Carey, S. Warren, 1962, Folding; Jour. Alberta Soc. Petroleum Geologists, v.10, no.3, pp.95-144.

Casella, C., in press, Geologic Evolution of the Beartooth Mountains, Montana-Wyoming, Part 5, The Line Creek Area, 96pp.

Catanzaro, E.J. and Kulp, J.L., 1964, Discordant zircons from the Little Belt (Montana), Beartooth (Montana) and Santa Catalina (Arizona) Mountains; Geochim, et Cosmochim. Acta, vol. 28.

Chamberlin, R.T., 1945, Basement control in Rocky Mountain deformation; Am. Jour. Sci., Daly Volume.

Clifford, P., 1960, The geological structure of the Loch Luichart area, Ross-shire; Geol. Soc. London Quart. Jour., vol. 115.

Cloos, E., 1946, Lineation; Geol. Soc. America Mem. 18.

Cloos, E. and Cloos, H., 1933, Pre-cambrian structure of the Beartooth, the Bighorn and the Black Hills uplift and its coincidence with Tertiary uplifting (abstract); Geol. Soc. America Proc.

den Tex, E., 1953, Stereographic distinction of linear and planar structures from apparent lineations in random exposure planes; Geol. Soc. Australia Jour. vol. 1.

Donath, F.A. and Parker, R.B., 1964, Folds and folding; Geol. Soc. America Bull., v.75.

Duschatko, R., 1955, Mechanical aid for plotting and counting out pole diagrams; Geol. Soc. America Bull., v.66.

Eardley, A.J., 1963, Relation of uplifts to thrusts in Rocky Mountains, Am. Assoc. of Petroleum Geologists, Memoir 2, Backbone of North America.

Eckelmann, F.D. and Poldervaart, Arie, 1957, Geologic evolution of the Beartooth Mountains, Montana and Wyoming. Part I. Archean history of the Quad Creek area; Geol. Soc. America Bull., v.68.

Flinn, D., 1958, On tests of significance of preferred orientation in three-dimensional diagrams; Jour. Geology, vol. 66.

Foose, R.M., Wise, D.U., and Garbarini, G.S., 1961, Structural geology of the Beartooth Mountains, Montana and Wyoming; Geol. Soc. America Bull., v.72.

Fyfe, W.S., Turner, F.J., and Verhoogen, J., 1958, Metamorphic reactions and metamorphic facies; Geol. Soc. America Mem. 73.

Gast, P.W., Kulp, J.L., and Long, L.E., 1958, Absolute ages of early Precambrian rocks in the Bighorn Basin of Montana and Wyoming, and Southeast Manitoba; Am. Geophys. Union Trans., v.39.

Giletti, Bruno, 1960, Rb-Sr and K-A ages of the Precambrian of Western Montana and Wyoming, abstract; Geol. Soc. America Proc.

Goodspeed, G.E., 1948, Xenoliths and skialiths; Am. Jour. Sci., v.246.

Harris, R.L., 1959, Geologic evolution of the Beartooth Mountains, Montana and Wyoming, Part 3, Gardner Lake area, Wyoming; Geol. Soc. America Bull., v.70, pp. 1185-1216.

Hoppin, R.A., 1961, Precambrian rocks and their relationship to Laramide structure along the east flank of Bighorn Mountains near Buffalo, Mountains, Wyoming; Geol. Soc. America Bull., v.72, pp.351-368.

Hughes, R.V., 1933a, The geology of the Beartooth Mountain front in Park county, Wyoming; National Acad. Sci. Proceedings, v.19.

Hughes, R.V., 1933b, Peneplanation of the Beartooth Mountains; Pan-American Geologist, v.59.

James, H.L., 1946, Chromite deposits near Red Lodge, Carbon County, Montana; U.S. Geol. Survey Bull. 945-F.

Kanizay, S.P., 1962, Mohr's theory of strength and Prandtl's compressed cell in relation to vertical tectonics; U.S. Geol. Survey Prof. Paper 414-B.

Knill and Knill, 1958, Some discordant-fold structures from its Dalradian of Craignish, Argyll and Rosguill Co. Donegal; Geol. Mag., v.95, p.697.

Lammers, E.C.H., 1939, Pre-cambrian control of Laramide structures in the Beartooth Range, Montana and Wyoming (abstract); Geol. Soc. America Bull., v.50.

Larsen, Leonard H., Poldervaart, Arie and Kirchmayer, Martin, in preparation, Geologic evolution of the Beartooth Mountains, Montana-Wyoming, Part 4, Geology and fabric of the Lonesome Mountain Area.

Leveson, D.F., 1960, Orbicular rocks of the Lonesome Mountain area, Beartooth Mountains, Montana and Wyoming; Bull. Geol. Soc. America, vol. 74, pp. 1015-1040.

Lovering, T.S., 1929, The New World or Cooke City Mining district, Park County, Montana; U.S. Geol. Survey Bull, 811-A.

Noble, J.A., Harder, J.O. and Alaughter, A.L., 1949, Structure of a part of the northern Black Hills and the Homestake Mine, Lead, South Dakota; Geol. Soc. Amer. Bull., v.60.

Osterwald, F.W., 1959, Structure and petrology of the Northern Bighorn Mountains, Wyoming; Geol. Survey of Wyoming Bull. 48.

Parsons, W.P. and Bryden, E.L., 1952, Precambrian rocks near Gardiner, Montana; Mich. Acad. Science, Arts, and Letters, v. 37, pp. 245-255.

Poldervaart, Arie, in preparation, Ultramafic rocks in Highline Lakes area, Beartooth Mountains, Wyoming, Columbia University.

Poldervaart, A. and Bentley, R.D., 1958, Precambrian and later evolution of the Beartooth Mountains, Montana and Wyoming; Billings Geol. Soc. Guidebook 9th Ann. Field Conf.

Ramsay, J.G., 1958, Superimposed folding at Loch Monar, enverness-Shire and Ross-Shire; Geol. Soc. London Quart. Jour. v.113.

Ramsay, J.G., 1960, The deformation of earlier linear structures in areas of repeated folding; Jour. Geology, v.68.

Reed, J.C., 1963, Structure of Precambrian crystalline rocks in the northern part of the Grand Teton National Park, Wyoming; U.S. Geological Survey Professional Paper 475-C; pp.C1-C6.

Reid, R.R., 1963, Metamorphic rocks of the northern Tobacco Root Mountains, Madison County, Montana; Geol. Soc. America. Bull., v.74, pp.293-306.

Sander, Bruno, 1948, Einführung in die gefügekunde der geologischen Körper; Springer-Verlag, Vienna, Austria.

Schafer, P.A., 1937, Chromite deposits of Montana; Montana Bur. Mines and Geol., Mem. 18.

Scotford, D.M., 1955, Axial-plane folding (Abstract); Geol. Soc. America Bull., v.66, p.1614.

Scotford, D.M., 1956, Metamorphism and axial-plane folding in the Poundridge area; N.Y. Geol. Soc. Am. Bul., v.67, p.1155-1198.

Sederholm, J.J., 1926, On migmatites and associated pre-Cambrian rocks of southwestern Finland. Part 2; Comm. Geol. Finlande Bull., no.77.

Spencer, E.W., 1959, Geologic evolution of the Beartooth Mountains, Montana and Wyoming, Part 2. Fracture patterns; Geol. Soc. America Bull., v.70.

Tansley, Wilfred, Schafer, P.A., and Hart, L.H., 1933, A geological reconnaisance of the Tobacco Root Mountains, Madison County, Montana; Mont. Bur. Mines Geology Mem. 9, 57p.

Thom, W.T., Jr., 1957, Tectonic relationships, evolutionary history and mechanics of origin of the Crazy Mountain Basin, Montana; Billings Geol. Soc., Guidebook 8th Ann. Field Conference, p. 9-21.

Turner and Weiss, 1963, Structural analysis of metamorphic tectonics; McGraw-Hill Book Co., Inc.

Weiss, L.E., 1959, Structural analysis of the basement system at Turoka, Kenya; Overseas Geol. Mineral Resources, v.7, 65pp.

Wilson, G., 1953, Mullions and rodding structures in the Moine Series of Scotland; Geologists' Assoc. Proc., v.64.

Wise, D.U., 1958, The relationship of Precambrian and Laramide structures in the southern Beartooth Mountains, Wyoming; Billings Geol. Soc. Guidebook 9th Ann. Field Conf.

Wise, D.U., 1963, Keystone faulting and gravity sliding driven by basement uplift of Owl Creek Mountains, Wyoming; Am. Assoc. of Petroleum Geologists Bull., v.47, no.4, pp.586-598.

Wynne-Edwards, H.R., 1962, Flow folding, Seminars in Tectonics; McGill University, pp. 26-30.

A P P E N D I X

Introduction

Appendices for penetrative fabric elements, S_0, S_1, S_2, B_1, B_2, and L_1 include detailed discussions of individual diagrams, as well as pertinent data. Summaries are presented for each element also.

Poles to foliations have been plotted on lower hemisphere equal area projections and contoured using a Duschatko device (Duschatko, 1955). All possible π-circles and corresponding β-axes have been constructed and discussed on the facing page for each diagram. All feasible lineation girdles are shown also. S_2 and B_2 data are uncontoured.

Mesoscopic structure stations homogeneous with respect to a particular penetrative fabric element have been combined to form sub-areas. These diagrams are keyed to appropriate areas on Maps 2a, 2b, 3a, 3b (Text). Homogeneity and fabric symmetry are variable, especially in the S_0-subfabric. Emphasis is placed on fold geometries, but fold mechanisms are also implied and considered.

APPENDIX I

S_o-subfabric

Mesoscopic:

The mesoscopic S_o-subfabric is complicated by overprinting of F_1 and F_2 fold sets. The symmetry ranges from monoclinic to triclinic, the lowest order of symmetry being in the major F_2 fold noses. Measurements at the structure stations number from 22 to 92, and the areal extent ranges from about 17,000 to 100,000 square yards. These are unusually large mesoscopic domains, which accounts in part for their complexity. However, attempts to ascertain homogeneity by subdividing these stations has not simplified the S_o-subfabric significantly. Since the S_1-subfabric possesses higher symmetry and is less complex than the S_o-subfabric, emphasis in the geometrical analysis of F_2 folds is placed on the S_1-subfabric and lineation subfabrics. Map 2a shows the S_o-subfabric diagrams.

Macroscopic analysis of the S_o-subfabric does not appear to be justified, since homogeneity has not been obtained on the mesoscopic scale.

and plunging gently south.

4). Superposition of fold sets.

Preferred Interpretation - Alternative number 4 is preferred by the writer for the following reasons:

1). Refolded F_1 folds are suggested by the S_1- and B_1-subfabrics at this station. Superposition of F_2 folds on F_1 folds has produced broad, open warps which generally trend perpendicular to the axial trend of the Quad Creek synform. These may be true F_2 cross-folds or due to superposition only.

2). Small isoclinal folds with appressed limbs and sharp hinges have been observed in the field. The πSob girdle may represent poles to S_o in the hinge zone of larger folds.

3). Measured later fold axes (L_2) plunge gently south.

4). No evidence supporting the existence of recumbent folds has been found in the field at this station.

STRUCTURE STATION 1

General Statement

Location - West flank of Quad Creek synform (Map 2a).

Areal Extent - Approximately 75,000 sq. yds.

Number of Measurements - 44 S_o measurements.

Rock Types - Pink biotite migmatite, quartzite and para-amphibolite.

Geologist - L.C. Rowan.

Geometrical Analysis

Symmetry - Triclinic.

Scale - Mesoscopic.

Homogeneity - Inhomogeneous with respect to S_o.

π S_o-girdles - (a). N10E, 20°W; (b). N78E, 70°W.

β S_o-axes - (a). N80W, 70°E; (b). S12E, 20°SE.

Reliability - (a)-Good ; (b)-Poor.

$\pi S_{oa} \wedge \pi S_{ob}$ - Strike - 90 degrees; Dip - 50 degrees.

Fold Geometry - The S_o-subfabric pattern suggests the following fold geometries may be possible:

1). Open folds plunging steeply east with nearly vertical axial planes.

2). Recumbent folds plunging steeply east (Turner and Weiss, 1963, p.161).

3). Isoclinal, appressed folds overturned to the west

STRUCTURE STATION 1.

44 S_o Measurements
Contour Interval: 1-5-10%

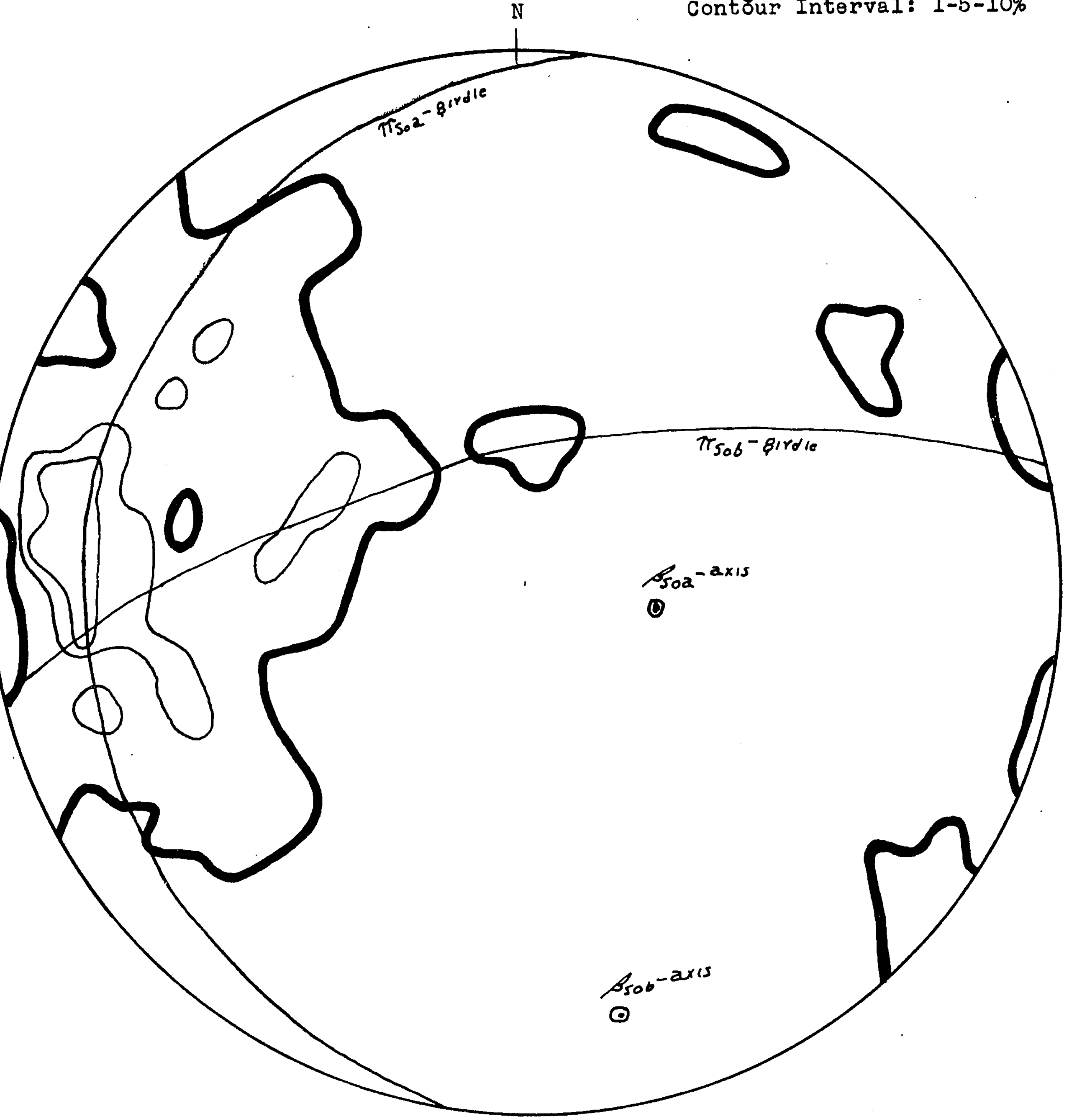

of the above alternatives. The pattern very strongly suggests a β S_o-axis plunging gently S-SW. The π Sob-girdle is too well defined to be considered a part of the π Soa-girdle. B_2 and the β Soa-axis agree closely (Map 2a). Overprinting of the broad, open cross-folds, β Sob-axis, is less pronounced at this station than it is at Station 1.

STRUCTURE STATION 2

General Statement

Location - Northwest portion of Quad Creek synform nose (Map 2a).

Areal Extent - Approximately 20,000 sq. yds.

Number of Measurements - 37 S_0 measurements.

Rock Types - Quartzite, migmatites and para-amphibolite.

Geologist - L.C. Rowan.

Geometrical Analysis

Symmetry - Monoclinic.

Scale - Mesoscopic.

Homogeneity - Nearly homogeneous with respect to S_0.

πS_0-girdles - (a). N67W, vertical ; (b). N35E, 45°NW.

βS_0-axes - (a). S23W, horizontal;(b). S55E, 45°SE.

Reliability - (a)-Good ; (b)-Fair.

$\pi S_{oa} \angle \pi S_{ob}$ - Strike - 78 degrees; Dip - 45 degrees.

Fold Geometry - The S_0-subfabric pattern at Station 2 may represent one of the following fold geometries:

1). Folds plunging gently S-SW and overturned to the west. These folds would be nearly isoclinal.

2). Overprinting of folds sets F_1 and F_2.

Preferred Interpretation - The writer prefers the second

STRUCTURE STATION 2.

37 S_o Measurements
Contour Interval: 1-5-10%

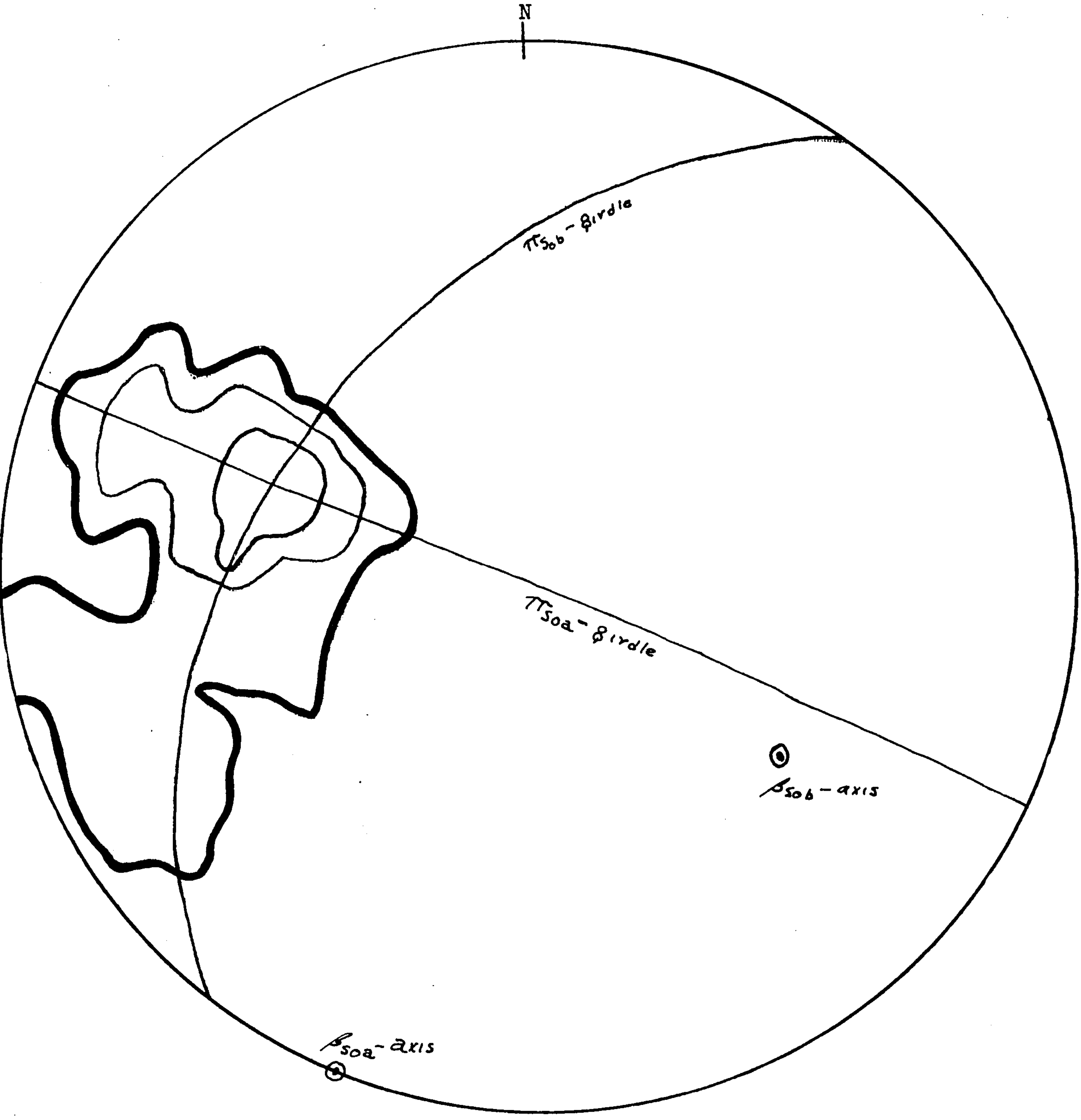

suggests F_2 folds which are slightly open and overturned to the NE. This is in agreement with the S_1-subfabric and field observations here. The orientation of the πS_{ob}-girdle suggests that these few measurements were derived from the south flank of the E-W trending F_1 synform. However, these S_o measurements may have come from small F_1 folds also.

STRUCTURE STATION 3

General Statement

Location - Nose of the Quad Creek synform (Map 2a).

Areal Extent - 3,000 sq. yds.

Number of Measurements - 78 S_o measurements.

Rock Types - Quartzites, migmatites and para-amphibolite.

Geologist - L.C. Rowan.

Geometrical Analysis

Symmetry - Tirlinic.

Scale - Mesoscopic.

Homogeneity - Inhomogeneous with respect to S_o.

πS_o-girdles - (a). N20E, 52°NW; (b). N8e, 55°SE.

βS_o-axes - (a). S70E, 38°SE; (b). N82W, 35°NW.

$\pi S_{oa} \angle \pi S_{ob}$ - Strike - 12°; Dip - 73°

Reliability - (a)-Good ; (b)-Fair.

Fold Geometry - The triclinic symmetry at this station precludes the possibility of explaining this S_o pattern by one fold set. Field observations and other subfabric data indicate that overprinting of F_2 on F_1 is very intense in the Quad Creek synform nose. The βS_{oa}-axis is nearly coincident with the B_2-axes (Map 2b) here, while the βS_{ob}-axis agrees reasonably closely with the B_1-maximum. Additionally, the shape of the πS_{oa}-girdle

STRUCTURE STATION 3.

78 S_0 Measurements.
Contour Interval: 1-5-10-15%.

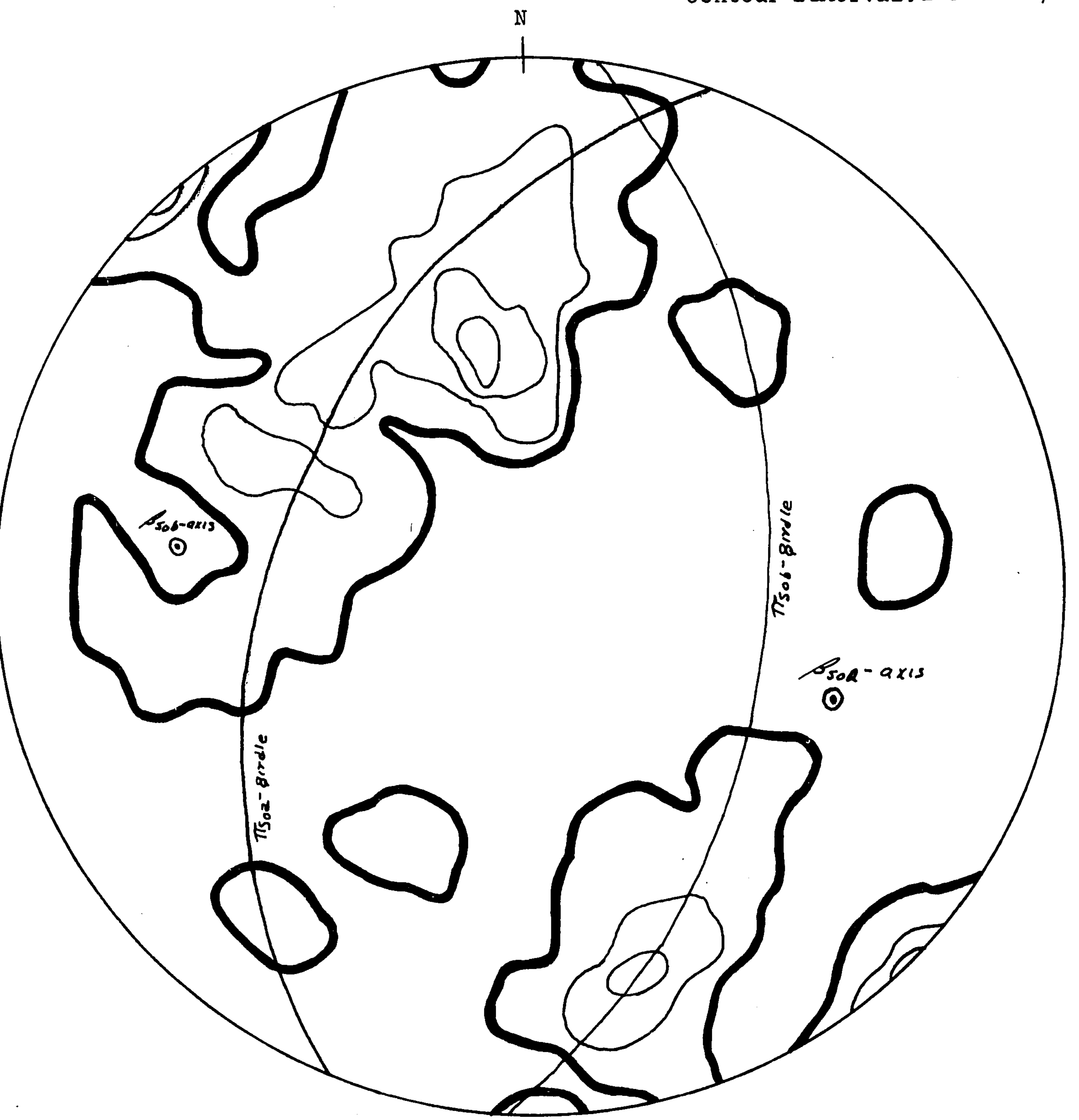

Preferred Interpretation - Alternative number 2 is the preferred interpretation of the S_0-subfabric, because

1). Measurements of F_1 small folds show that they are non-plane and non-cylindrical at this station. A maximum of F_1 fold axes (B_1) occurs at an attitude which agrees closely with the β Soa-axis (Map 2b).

2). The constructed βS_1-axis plunges gently east and is coincident with B_2. Therefore, the axes of the fold sets are only slightly oblique but have discordant plunges. Superposition of these fold sets creates gentle warping of the F_1 fold axial surface, S_1. This can be seen in the quartzite outcrop pattern in the area near this station (Map 1). The writer proposes that the πSob-girdle results from warping of earlier folds on the north limb of the larger E-W trending F_1 synform (Map 1) by F_2 folds with axes B_2 and βS_1.

3). βSob defines the trend of flexures caused by the above described overprinting and are not the result of a separate phase or period of deformation.

STRUCTURE STATION 4

General Statement

Location - Northeast portion of Quad Creek synform nose (Map 2a).

Areal Extent - Approximately 17,000 sq. yds.

Number of Measurements - 32 S_o measurements.

Rock Types - Para-amphibolite and ultramafic bodies.

Geologist - L.C. Rowan.

Geometrical Analysis

Symmetry - Triclinic, nearly monoclinic.

Scale - Mesoscopic.

Homogeneity - Nearly homogeneous with respect to S_o.

πS_o-girdles - (a). N2W, 50°W ; (b). N48W, 30°NE.

βS_o-axes - (a). S88W, 40°W; (b). S43W, 60°SW.

Reliability - (a)-Good ; (b)-Fair.

$\pi Soa \angle \pi Sob$ - Strike - 46 degrees; Dip - 20 degrees.

Fold Geometry - The pattern can be interpreted to represent;

1). Nearly isoclinal folds, overturned to the north and plunging moderately west, or

2). Interference of a fold set with the geometry of number 1 and a set which trends obliquely to number 1.

STRUCTURE STATION 4.

32 S_o Measurements
Contour Interval: 1-5-10%

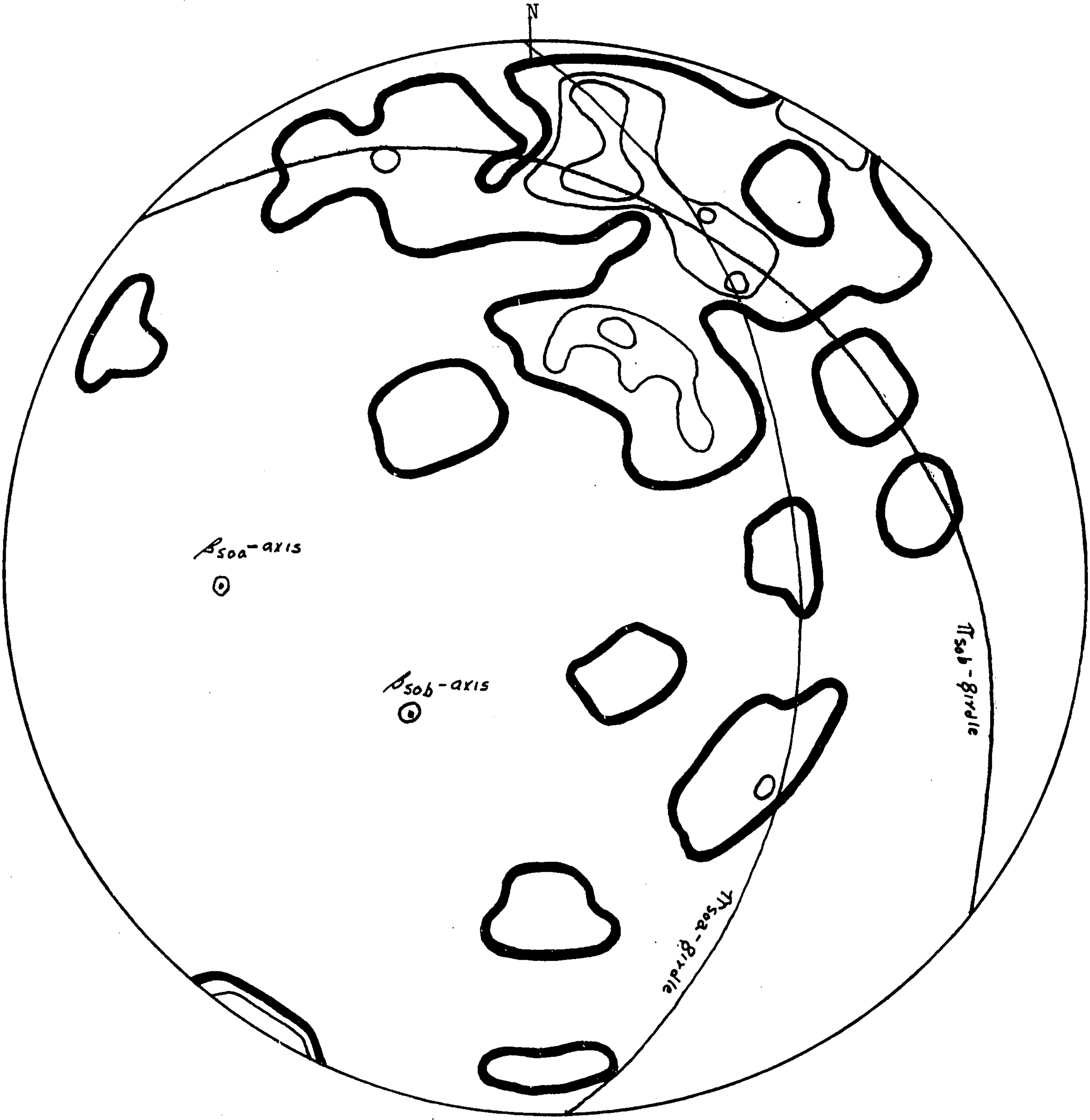

1). Early fold axes, B_1, plunge dominantly west, although they are folded (Map 2b). These folds are isoclinal and non-plane.

2). B_2 plunges gently east. These folds are non-isoclinal and plane on the mesoscopic scale, and the axial surface dips south (Map 2a).

The overall S_0-subfabric pattern is suggestive of alternative number 1, but the β Soa-axis is coincident with B_2. The form of the folds appears to be isoclinal, when it is known from field observations that F_2 folds are non-isoclinal and overturned to the north. Therefore, it appears that F_1 and F_2 are overprinted, giving the form of F_1 and the attitude of F_2, as well as creating dispersion of the maxima into π Sob- and π Soc-girdles.

STRUCTURE STATION 5

General Statement

Location - Northeast portion of Quad Creek synform nose (Map 2a).

Areal Extent - Approximately 16,000 sq. yds.

Number of Measurements - 32 S_o measurements.

Rock Types - Quartzite and para-amphibolite.

Geologist - L.C. Rowan.

Geometrical Analysis

Symmetry - Monoclinic - triclinic in detail.

Scale - Mesoscopic.

Homogeneity - Nearly homogeneous with respect to S_o.

πS_o-girdles - (a). N3W, 70°W ; (b). N84E, 10°S; (c).N6E,15°W.

βS_o-axes - (a). N87E, 20°E; (b). N6W, 80°N ; (c).S84E,75°E.

Reliability - (a)-Good (b)-Good (c). Fair

$\pi Soa \angle \pi Sob$ - Strike - 93 degrees; Dip - 60 degrees.

Fold Geometry - The following interpretations appear to be possible;

1). Nearly isoclinal folds plunging gently east and overturned to the south.

2). Superposition of folds sets F_1 and F_2.

Preferred Interpretation - Consideration of other data at this station makes the second alternative the most feasible:

STRUCTURE STATION 5.

32 S Measurements
Cont8ur Interval: 1-5-10%

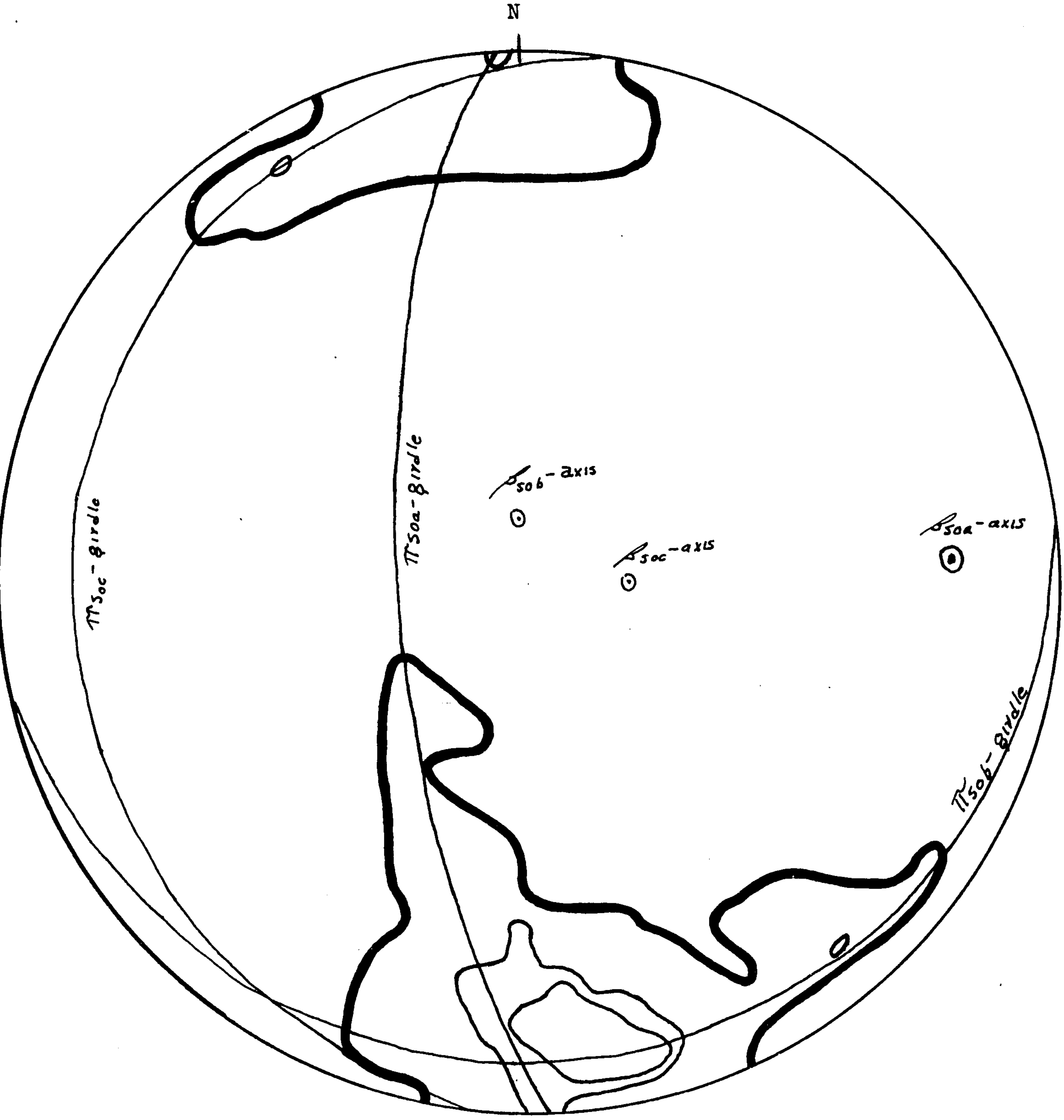

<u>Preferred Interpretation</u> - Field and laboratory observations suggest refolding in this area. Complete homogeneity is therefore untenable. Overprinting of data renders geometric analysis difficult, but two types of folds have been observed:

(1) Appressed, isoclinal folds overturned to the east. β Sob may represent the axis of these F_2 folds.

(2) Open, broad folds which plunge steeply west and appear to be younger than number 1. These later folds (F_3) strike nearly perpendicular to the Quad Creek synform and may be defined by β Soa.

The writer concludes that F_2 folds have gently deformed the earlier S_o-surface. Great accuracy is not attached to the β Sob-axis, since overprinting has probably altered its original position. Broad, open warps trending west may be due to superposition of F_2 on F_1 rather than being a distinct and later F_2 cross-fold set.

STRUCTURE STATION 6

General Statement

Location - North portion of east flank of Quad Creek synform (Map 2a).

Areal Extent - Approximately 35,000 sq. yds.

Number of Measurements - 48 S_o measurements.

Rock Types - Pink biotite migmatite and para-amphibolite.

Geologist - L.C. Rowan.

Geometrical Analysis

Symmetry - Orthorhombic, but monoclinic in detail.

Scale - Mesoscopic.

Homogeneity - Inhomogeneous with respect to S_o when considered in detail.

πS_o-girdles - (a). N17E, 30°SE ; (b). N72W, 80°NE.

βS_o-axes - (a). N73W, 60°NW ; (b). S18W, 10°SW.

Reliability - (a)-Fair ; (b). Fair.

$\pi S_{oa} \wedge \pi S_{ob}$ - Strike - 89 degrees; Dip - 50 degrees.

Fold Geometry - Considering the pattern in general this could be a homogeneous sub-domain. However, the maximum is dispersed sufficiently in the direction of the πS_o-girdles that superposition of fold sets should be considered.

STRUCTURE STATION 6.

48 S_0 Measurements
Contour Interval: 1-5-10%

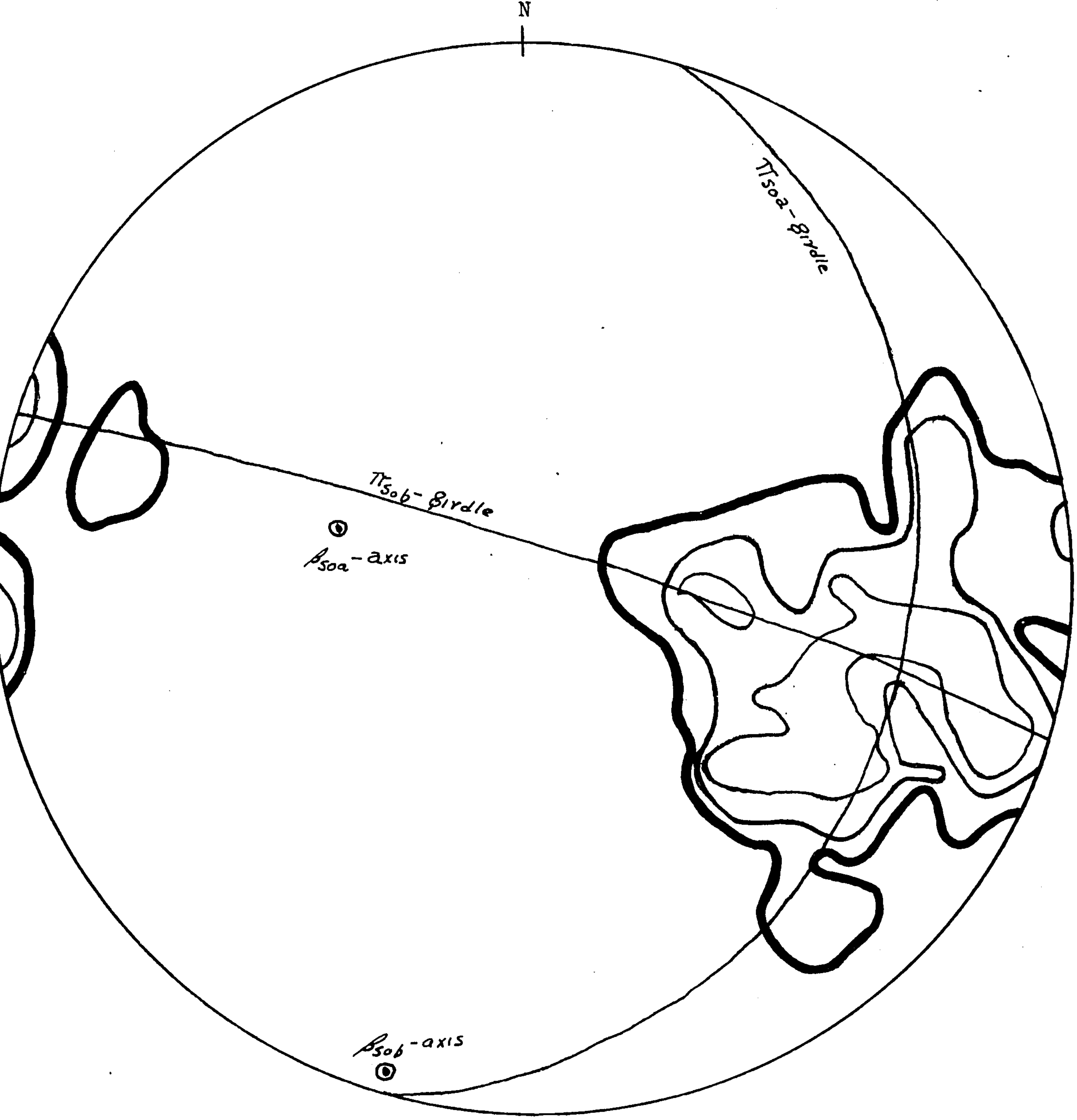

supported by the B_1-subfabric at this station (Map 2b). Overprinting is very slight but may indicate the presence of a few broad, open folds (F_2) plunging steeply east. The writer believes that these gentle F_2 cross-warps are due to superposition of F_2 on F_1, rather than being a distinct F_2 fold set.

STRUCTURE STATION 7

General Statement

Location - East flank of Quad Creek synform (Map 2a).

Areal Extent - Approximately 60,000 sq. yds.

Number of Measurements - 22 S_o measurements.

Rock Types - Pink biotite migmatite and para-amphibolite.

Geologists - L.C. Rowan and Richard Ellis.

Geometrical Analysis

Symmetry - Monoclinic.

Scale - Mesoscopic.

Homogeneity - Inhomogeneous with respect to S_o.

πS_o-girdles - (a). N70W, 84°NE ; (b). N16E, 35°SE.

βS_o-axes - (a). S20W, 6°SW ; (b). N74W, 55°NW.

Reliability - (a)-Good ; (b). Fair.

πSoa∠πSob - Strike - 86 degrees; Dip - 49 degrees.

Fold Geometry - The S_o-subfabric pattern suggests the following alternatives;

1). Isoclinal, appressed folds plunging gently south and overturned to the east.

2). Interference of fold sets F_1 and F_2.

Preferred Interpretation - The well-defined π Soa-girdle suggests the existence of folds described by number 1 and

STRUCTURE STATION 7.

22 S_o Measurements
Contour Interval: 1-5-10%

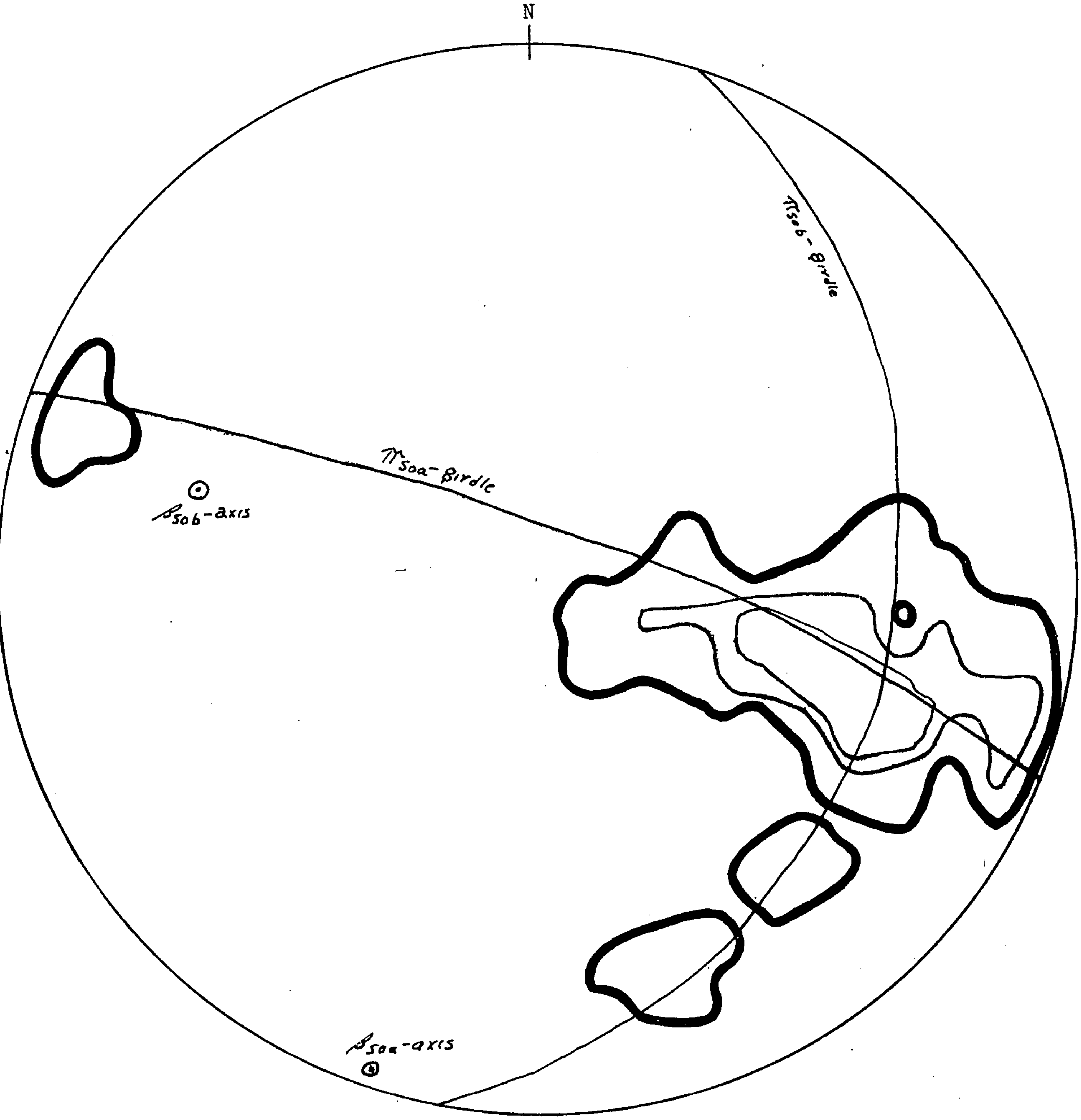

observed in the field. Broad, open folds plunging west have been observed and can be discerned on Map 1. "Hook" patterns (Carey, 1962, p.101) observed in hand specimens indicate refolding of isoclinal folds (F_1) by later, nearly isoclinal folds (F_2) plunging south. These folds may be represented at this station by the slight widening of the maxima in a SW-NE direction. Note that the π S_o-girdle in this diagram is rotated 28° west from the orientation of the π S_o-girdle at Station 7.

STRUCTURE STATION 8

General Statement

Location - West flank of Wyoming Creek antiform (Map 2a).

Areal Extent - Approximately 60,000 sq. yds.

Number of Measurements - 29 S_o measurements.

Rock Types - Pink biotite migmatite, para-amphibolite, quartzite and agmatite.

Geologists - L.C. Rowan and Richard Ellis.

Geometrical Analysis

Symmetry - Monoclinic.

Scale - Mesoscopic.

Homogeneity - Inhomogeneous with respect to S_o.

πS_o-girdle - (a). N12W, 35°NE.

βS_o-axis - (a). S78W, 55°NE.

Reliability - (a)-Good.

Fold Geometry - The overall pattern suggests the presence of folds plunging 55° to S78W. These folds are either open or recumbent (Turner and Weiss, 1963, p.161). The secondary maximum near the center of the diagram may indicate overprinting of folds, but a π Sob-girdle is not justified.

Preferred Interpretation - No recumbent folds have been

STRUCTURE STATION 8.

29 S_o Measurements
Contour Interval: 1-5-10%

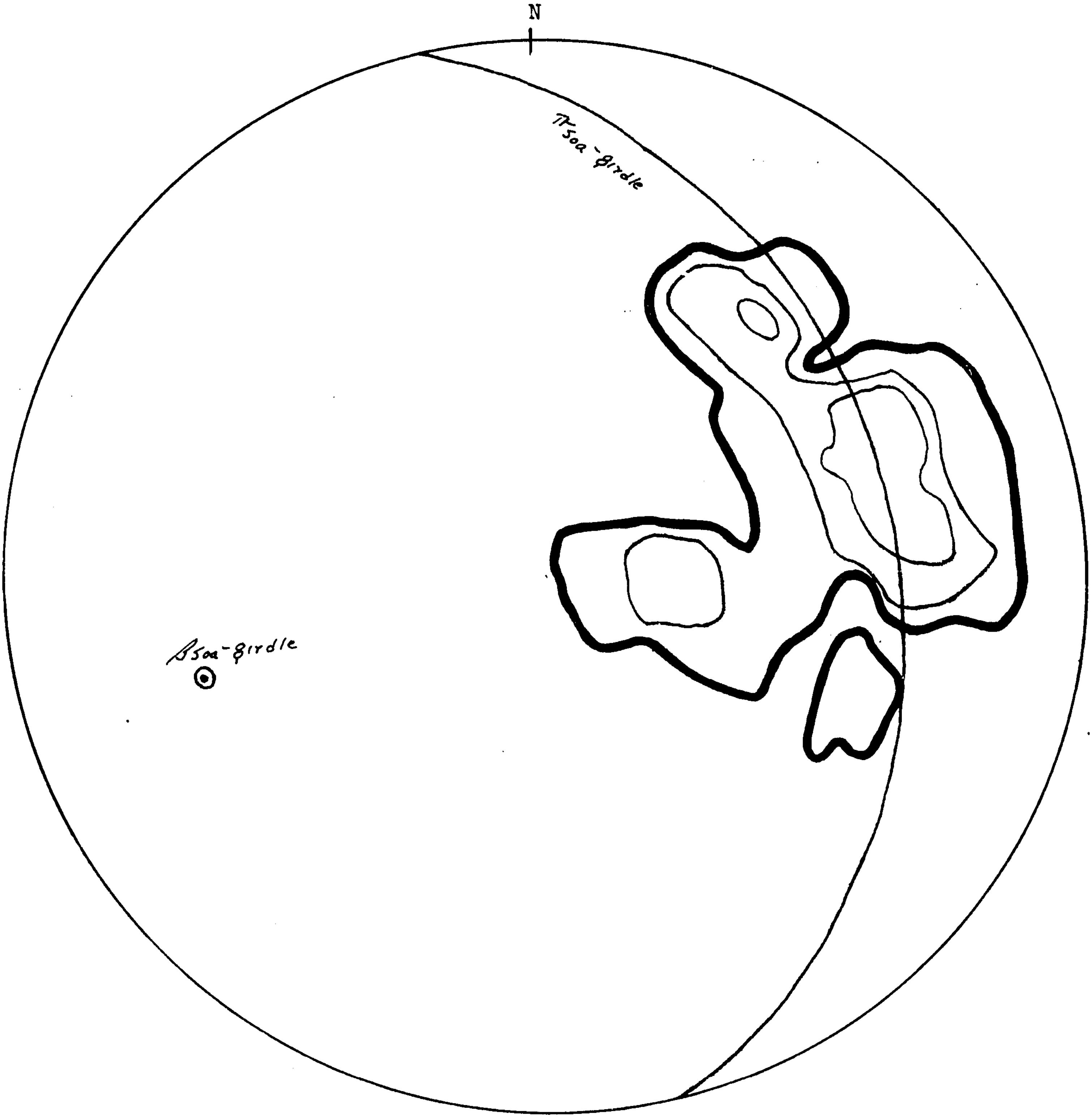

The writer prefers the latter alternative, since nearly isoclinal older F_1 folds have been observed in the field striking N-S and plunging south and north.

STRUCTURE STATION 9

General Statement

Location - Southwest portion of the Wyoming Creek antiform nose (Map 2a).

Areal Extent - Approximately 60,000 sq. yds.

Number of Measurements - 86 S_o measurements.

Rock Types - Pink migmatite, para-amphibolite, quartzite and agmatite.

Geologists - L.C. Rowan and Richard Ellis.

Geometrical Analysis

Symmetry - Triclinic.

Scale - Mesoscopic.

Homogeneity - Inhomogeneous with respect to S_o.

πS_o-girdle - (a). N57W, 40°NE.

βS_o-axis - (a). S33W, 50°SW.

Reliability - (a)-Good.

Fold Geometry - The S_o-subfabric suggests F_2 folds overturned to the SE and plunging 50° to S33W. Note that the πS_o-girdle is rotated 45° W from the πS_o-girdle at Station 8. The point maxima located near the great circle with an E-W strike may be due to the presence of measurements taken from too large an area or to overprinting.

STRUCTURE STATION 9.

86 S_o Measurements
Contour Interval: 1-5-10-15%

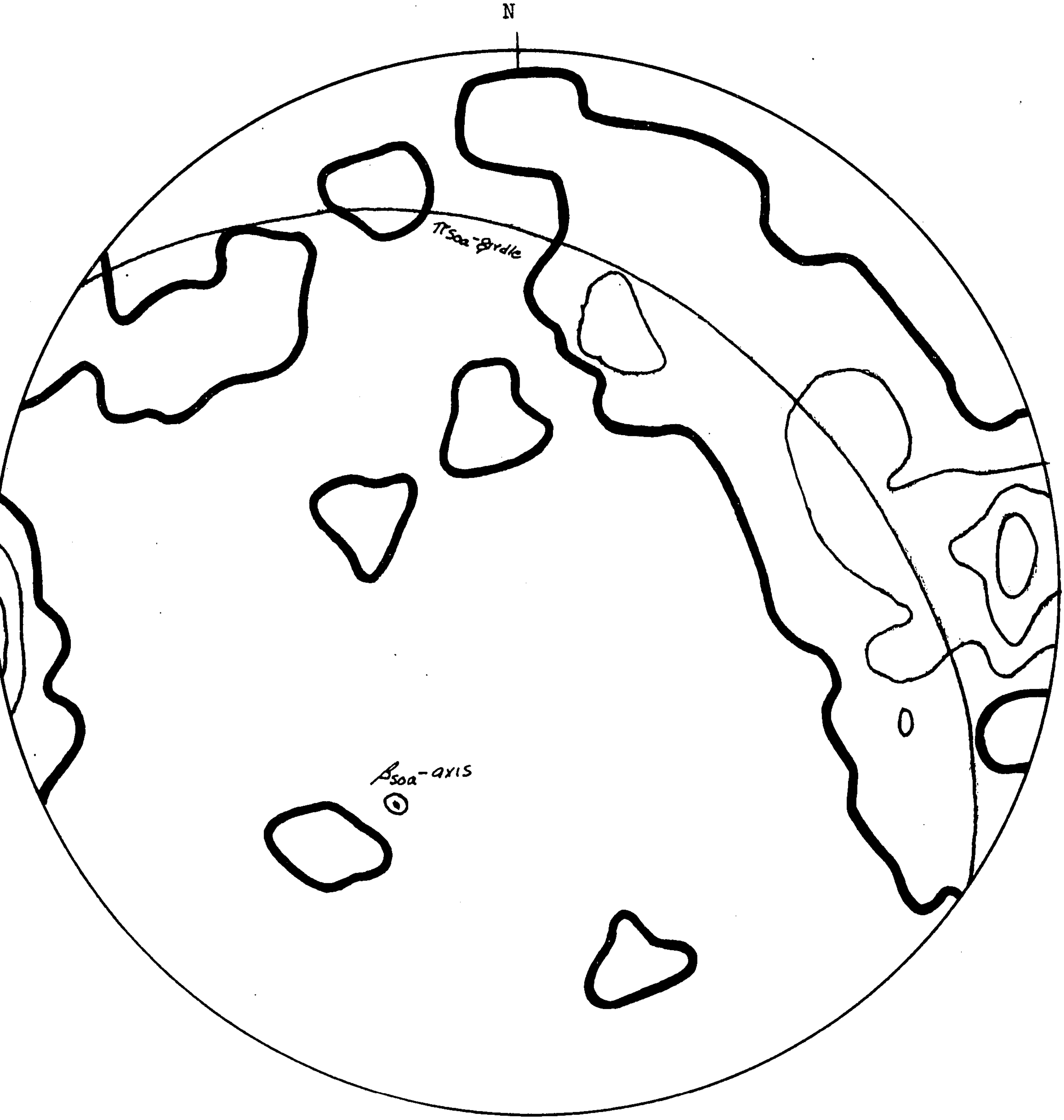

βSoa-axis orientation is questionable. Note that the βS_1-axis and B_2 do not agree with the βSoa-axis at this station but are nearly coincident with the βSob-axis. These facts and the low order of symmetry may be due to interference of fold sets. Note the westward rotation of the π Soa-girdle at this station from the orientation at Station 9. The E-W point maxima on the great circle may be indicative of overprinting also.

STRUCTURE STATION 10

General Statement

Location - Southeast portion of Wyoming Creek antiform nose (Map 2a).

Areal Extent - Approximately 40,000 sq. yds.

Number of Measurements - 38 S_0 measurements.

Rock Types - Agmatite, quartzite and para-amphibolite.

Geologists - L.C. Rowan and Richard Ellis.

Geometrical Analysis

Symmetry - Tirclinic.

Scale - Mesoscopic.

Homogeneity - Inhomogeneous with respect to S_0.

πS_0-girdles - (a).N28E,40°NW; (b).N87W,30°N; (c).N87W,75°N.

βS_0-axes - (a).S62E,50°SE; (b).S3W,60°SW; (c).S3W,15°S.

Reliability - (a)-Good ; (b)-Fair ; (c)-Poor.

πSoa$\angle\pi$Sob - Strike - 115 degrees; Dip - 10 degrees.

Fold Geometry - The S_0-subfabric at this station strongly indicates the existence of;

1). Folds plunging moderately SE and overturned NE, and

2). Overprinting of data creating lower symmetry and inhomogeneity with respect to S_0.

Preferred Interpretation - The writer accepts the fold form suggested by the S_0-subfabric pattern (1), but the

STRUCTURE STATION 10.

38 S_0 Measurements
Contour Interval: 1-5-10-15%

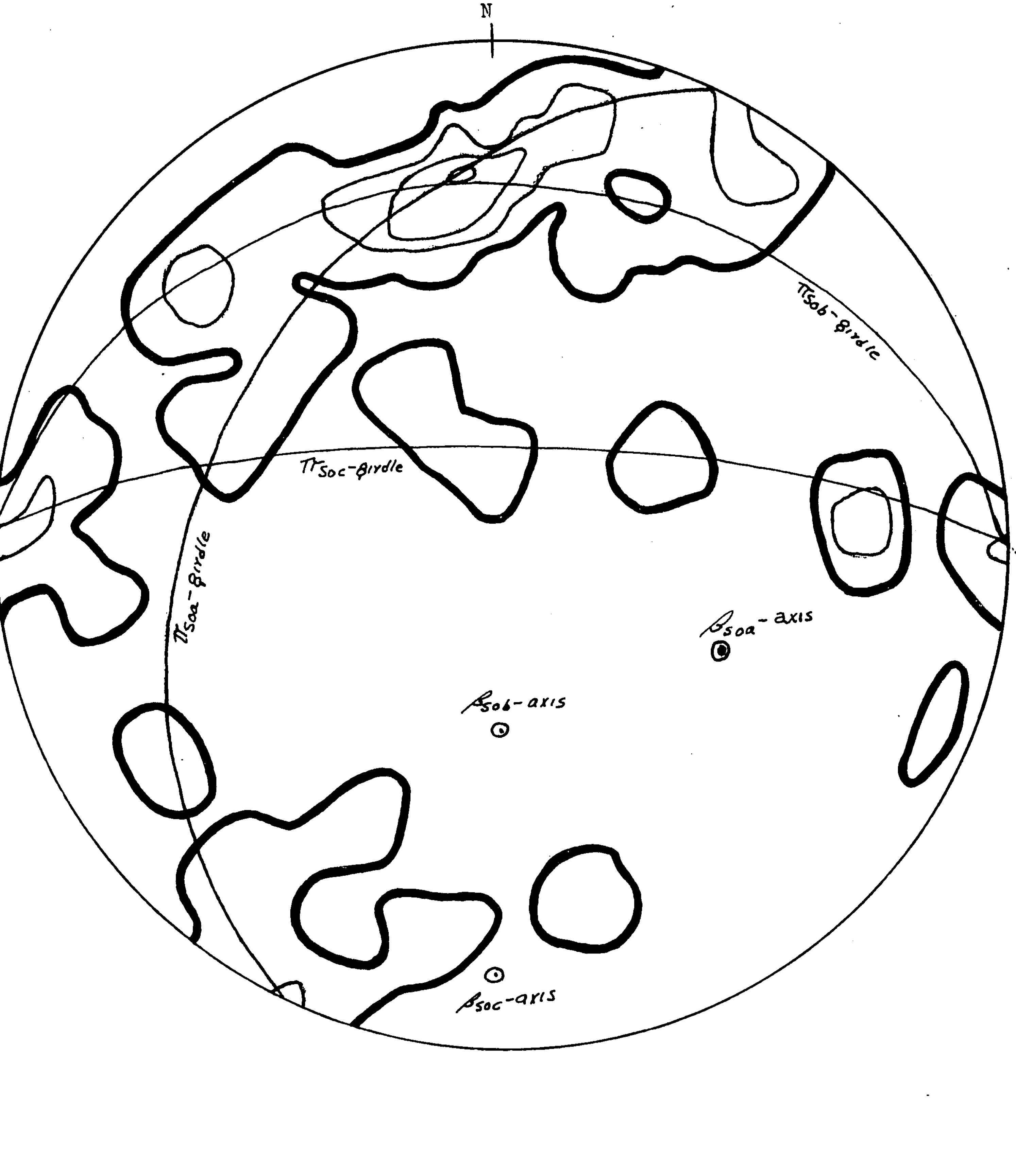

Preferred Interpretation - Dispersion of the S_0-poles along the π S_0-girdle appears too pronounced to make alternative 3 acceptable, and no field evidence supports alternative 2. Note that the β Soa-axis from this station and Station 10 are nearly coincident and that overturning NE is indicated in both sub-domains. No overprinting of fold sets is indicated at this station.

STRUCTURE STATION 11

General Statement

Location - South flank of the Wyoming Creek antiform (Map 2a).

Areal Extent - Approximately 40,000 sq. yds.

Number of Measurements - 32 S_0 measurements.

Rock Types - Pink biotite migmatite, agmatite, quartzite and para-amphibolite.

Geologists - L.C. Rowan and Richard Ellis.

Geometrical Analysis

Symmetry - Orthorhombic.

Scale - Mesoscopic.

Homogeneity - Homogeneous with respect to S_0.

πS_0-girdle - (a). N41E, 30°NW.

βS_0-axes - (a). S49E, 60°SE.

Reliability - (a)-Good.

Fold Geometry - The following interpretations are feasible explanations for this S_0 pattern.

1). Open folds plunging moderately (60°) SE and overturned NE.

2). Recumbent folds plunging 60° SE.

3). S_0 is sub-planar and no folds are represented.

STRUCTURE STATION 11.

32 S_0 Measurements
Contour Interval: 1-5-10-15%

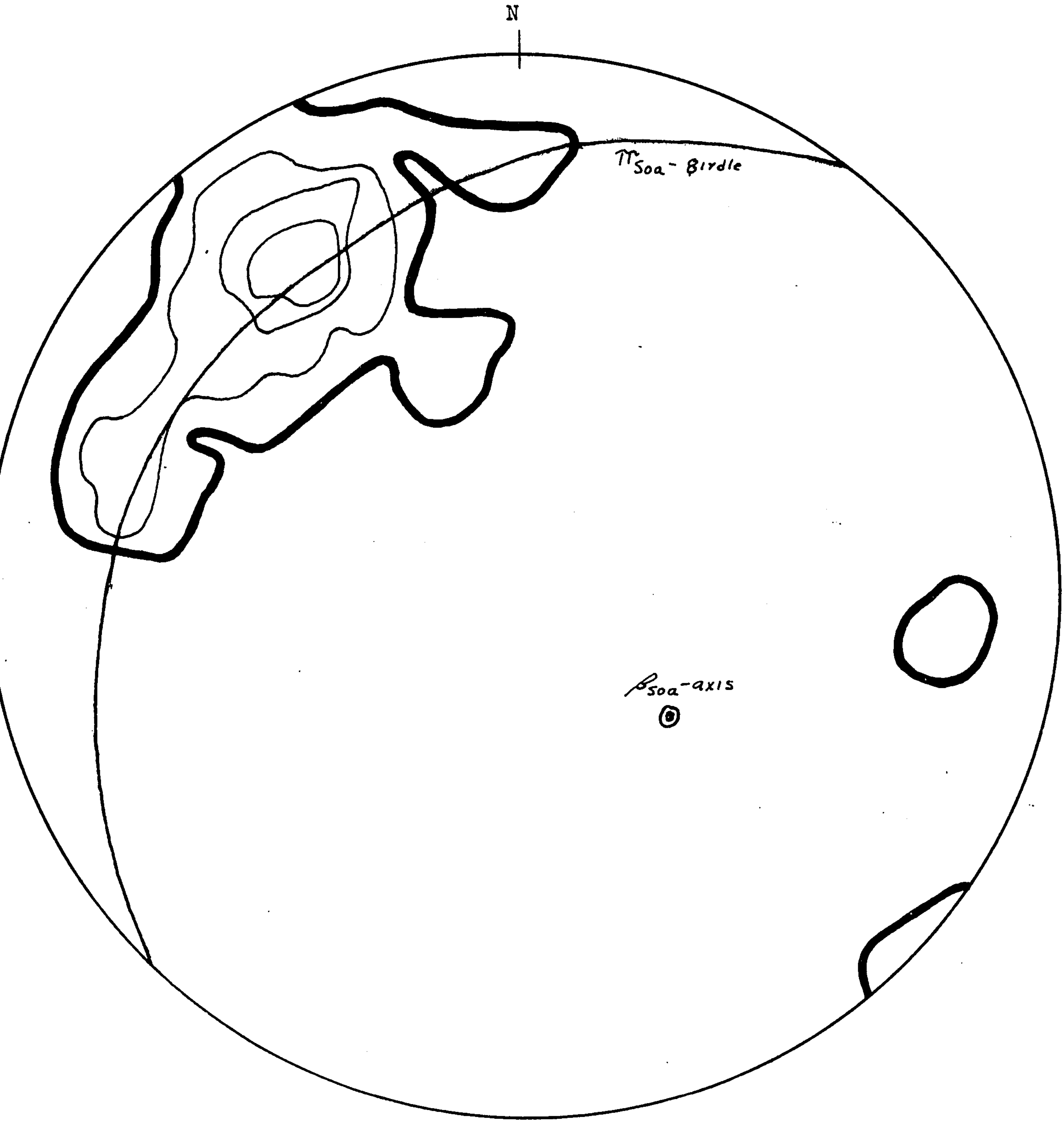

alternative 2 and many folds described by alternative 1 have been observed and mapped in the field, the writer selects alternative 1 with confidence. The βS_0-axis agrees relatively closely with the β S_1- and B_2 axes here.

STRUCTURE STATION 12

General Statement

Location - Eastern portion of the Wyoming Creek antiform south flank (Map 2a).

Areal Extent - Approximately 100,000 sq. yds.

Number of Measurements - 92 S_o measurements.

Rock Types - Quartzites, para-amphibolite, migmatites and micaceous schists.

Geologists - L.C. Rowan.

Geometrical Analysis

Symmetry - Monoclinic.

Scale - Mesoscopic.

Homogeneity - Homogeneous with respect to S_o.

πS_o-girdle - (a). N85E, 25°N.

βS_o-axis - (a). S5E, 65°S.

Reliability - (a)-Good.

Fold Geometry - The well-defined girdle and the single dispersed girdle suggest either;

1). Open folds plunging steeply south with vertical axial planes, or

2). Recumbent folds plunging steeply south (Turner and Weiss, 1963, p.161).

Preferred Interpretation - Since no evidence supports

STRUCTURE STATION 12.

92 S_o Measurements
Contour Interval: 1-5-10-15%

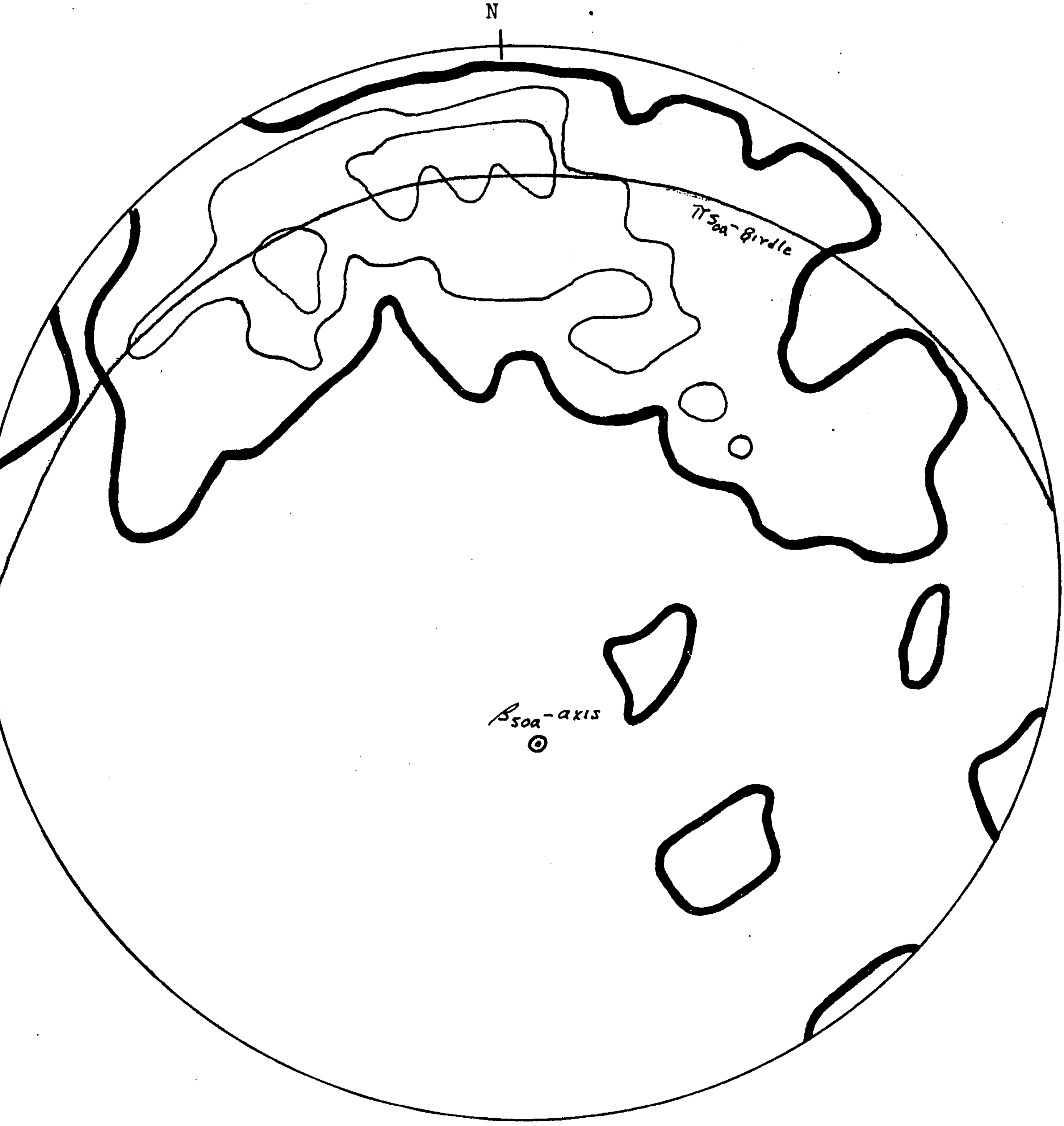

SUMMARY

<u>S_o-subfabric</u> - The S_o-subfabric is complicated by overprinting of F_2 on F_1 and generally has triclinic symmetry. It defines βS_o-axes which correspond roughly to B_2 and βS_1-axes at Stations 11 and 12, where F_1 has been observed on the scale of small folds only. Constructed βS_o-axes in the flanks of the Quad Creek synform generally define steeply plunging cross-folds related to the major synform. However, the writer believes that these cross-warps are not a distinct fold set but are manifestations of F_2-F_1 superposition. Warping of this type has been observed in the E-W trending F_1 synform in Quad Creek (Map 1). βS_o-axes which plunge in the direction of B_2 only approximate the actual B_2 attitude. Most of the S_o measurements at Stations 1, 6 and 7 are from migmatites in which refolding is intense and S_2 axial plane foliation is evident. The S_o-subfabric patterns at these stations reflect these relations.

F_1 and F_2 folds exist on the small and large scales in the Quad Creek synform nose, so that the S_o-subfabric is very complex here. βS_o-axes generally agree roughly with B_2- and βS_1-axes. The patterns at Stations 4 and 5 substantiate the existence of the F_1 synform in this area. The S_o-subfabric has not been treated on the macroscopic scale, except in the Wyoming Creek antiform. Figure 29 shows the βS_o-axis and πS_o-girdle for this major fold. βS_o-, B_2-, and βS_1-axes agree rather closely. Therefore, the S_o-subfabric is homogeneous on the macroscopic scale but not on the mesoscopic scale.

APPENDIX II

S_1-subfabric

<u>Mesoscopic:</u>

Axial planes, S_1, of small, isoclinal F_1 folds have been measured at all 12 structure stations. Measurements number from 13 to 43. The S_1-subfabric is particularly significant in the geometric analysis, because it is not affected by overprinting of F_1 and F_2 on the mesoscopic scale. These measurements are believed to be accurate, since S_1 is easily ascertained in isoclinal F_1 folds.

folds. S_1 data are dispersed rather widely along the πS_1-girdles. This may be due to broad, open F_2 cross-folds which plunge steeply east or to the apparent non-cylindrical nature of small and large F_2 folds.

STRUCTURE STATION 1

General Statement

Location - West flank of the Quad Creek synform (Map 2a).

Areal Extent - Approximately 16,000 sq. yds.

Number of Measurements - 30 S_1 measurements.

Rock Types - Pink biotite migmatite, quartzite and para-amphibolite.

Geologists - L.C. Rowan and C.E. Larsen.

Geometrical Analysis

Symmetry - Monoclinic.

Scale - Mesoscopic.

Homogeneity - Homogeneous with respect to S_1.

πS_1-girdles - (a). N45E, 20°E ; (b). N32E, 20°NW.

βS_1-axes - (a). N45W, 70°NW; (b). S58E, 70°E.

Reliability - (a)-Good ; (b)-Good.

$\pi S_{1a} \wedge \pi S_{1b}$ - Strike - 13 degrees; Dip - 140 degrees (from the horizontal plane).

Fold Geometry - The S_1-subfabric pattern indicates that S_1 has been folded by tightly appressed similar folds (F_2) which are slightly overturned to the west. B_2 strikes S-SW, but the plunge cannot be defined. Therefore, the πS_1-girdles define the limbs of these F_2

STRUCTURE STATION 1
30 S_1 Measurements
Contour Interval 1-5-10%

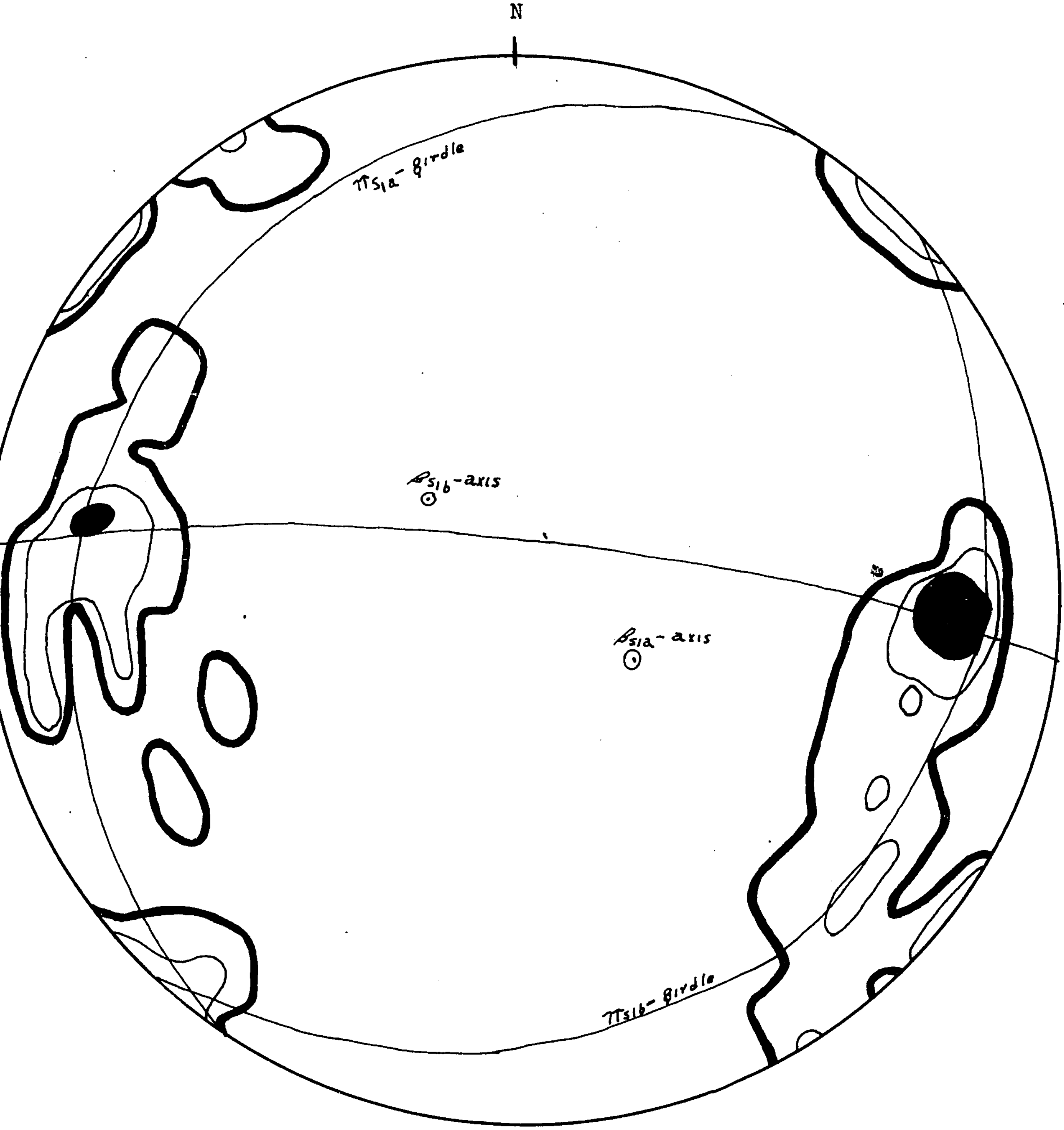

alternative. Refolded F_1 folds at this station have B_2 plunging gently south. The β S_{1b}-axis agrees closely with B_2 and the β Sob-axis. However, the π S_{1a}-girdle does not show a simple, homogeneous geometrical relationship with the π S_{1a}-girdle. This relationship may be due to insufficient S_1 data or slightly disharmonic F_2 folding here.

STRUCTURE STATION 2

General Statement

Location - $N_o$rthwest portion of the Quad Creek synform nose (Map 2a).

Areal Extent - Approximately 2,000 sq. yds.

Number of Measurements - 18 S_1 measurements.

Rock Types - Quartzites, migmatites and para-amphibolites.

Geologists - L.C. Rowan and C.E. Larsen.

Geometrical Analysis

Symmetry - Triclinic, nearly monoclinic.

Scale - Mesoscopic.

Homogeneity - Inhomogeneous with respect to S_1.

πS_1-girdles - (a). N-S, 30°W ; (b). N84E, 70°N.

βS_1-axes - (a). E-W, 60°E ; (b). S6E, 20°S.

Reliability - (a)-Good ; (b)-Good.

$\pi S_{1a} \angle \pi S_{1b}$ - Strike - 84 degrees; Dip - 40 degrees.

Fold Geometry - The S_1-subfabric pattern suggests the following interpretations:

1). Isoclinal, appressed F_2 folds, plunging gently south and overturned west.

2). Interference of fold sets F_1 and F_2.

Preferred Interpretation - The writer prefers the second

STRUCTURE STATION 2.

18 S_1 Measurements
Contour Interval: 1-5-10%

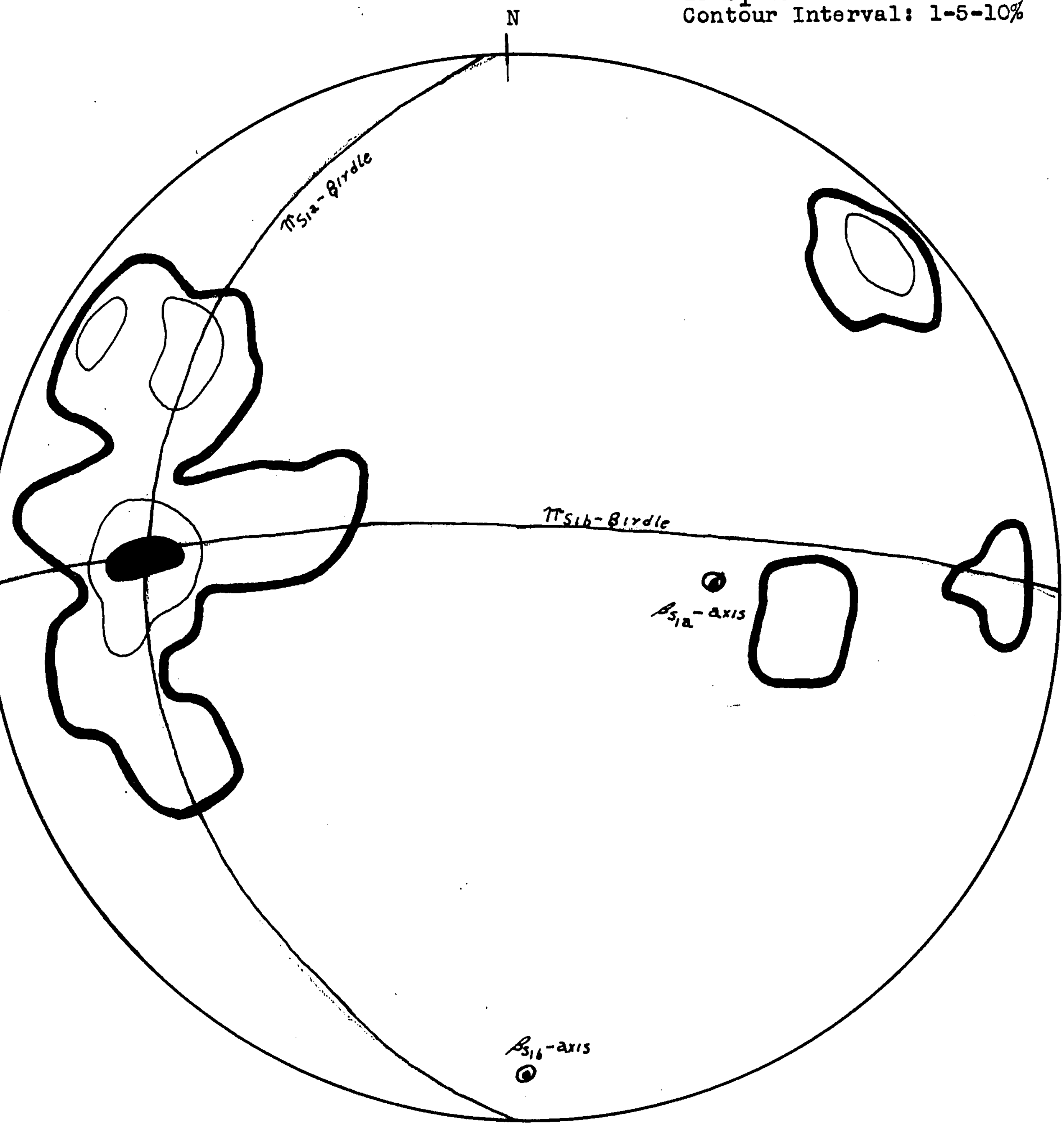

3). F_2 folds are non-cylindrical and non-plane.

4). F_2 fold style and orientation are strongly influenced by rock type.

Preferred Interpretation: The writer prefers the fourth alternative, because a systematic variation has been detected in measurements taken in migmatites and quartzites. The proximity of the metanorite body may also be a significant factor. The βS_{1b}-axis agrees closely with B_2 (Fig. 2b) and the βS_{0a}-axis (Fig. 2a). Note that the βS_1-axes at this station have rotated approximately 90 degrees from the orientation of the βS_1-axes at Stations 1 and 2. B_2 and S_2 data are sparse, but they do not suggest that F_2 folds are non-cylindrical or non-plane.

STRUCTURE STATION 3

General Statement

Location - Central portion of Quad Creek synform nose (Map 2a).

Areal Extent - Approximately 5,000 sq. yds.

Number of Measurements - 26 S_1 measurements.

Rock Types - Quartzites, para-amphibolite and granitic gneisses.

Geologists - L.C. Rowan and C.E. Larsen.

Geometrical Analysis

Symmetry - Tirclinic.

Scale - Mesoscopic.

Homogeneity - Inhomogeneous with respect to S_1.

πS_1-girdles - (a). N67E, 25°NW ; (b). N4W, 75°W.

βS_1-axes - (a). S23E, 65°SE ; (b). N76E, 15°E.

Reliability - (a)-Good ; (b)-Good.

$\pi S_{1a} \wedge \pi S_{1b}$ - Strike - 71 degrees; Dip - 50 degrees.

Fold Geometry - The S_1-subfabric at this station suggests relatively open F_2 folds plunging SE and overturned to the NE. The definition of two πS_1-girdles may be due to:

1). Superposition of fold sets F_1 and F_2.

2). Areal extent of the structure station is too large.

STRUCTURE STATION 3.

26 S_1 Measurements
Contour Interval: 1-5-10%

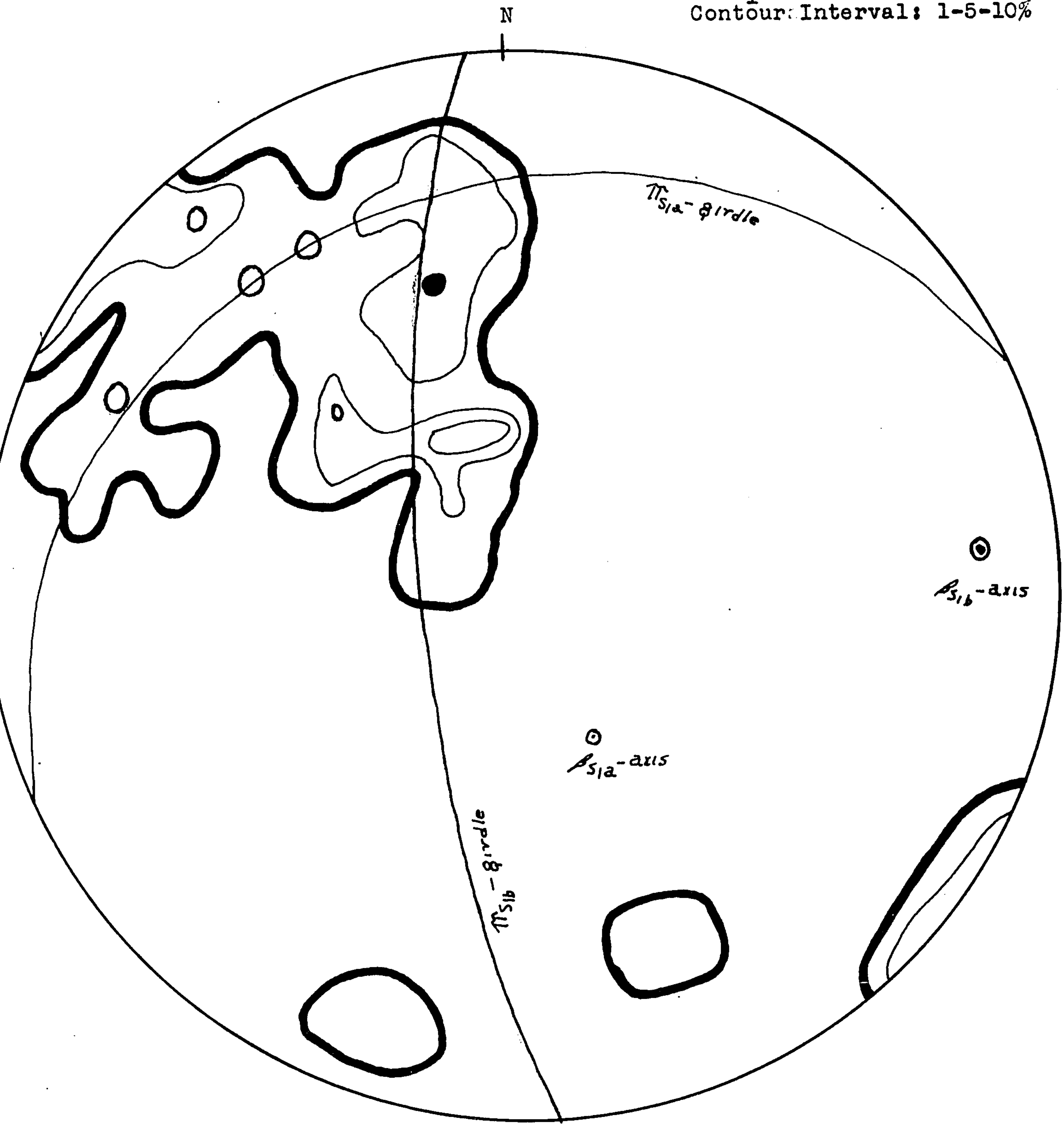

STRUCTURE STATION 4

General Statement

Location - Northeast portion of Quad Creek synform nose (Map 2a).

Areal Extent - Approximately 1,000 sq. yds.

Number of Measurements - 22 poles to S_1.

Rock Types - Para-amphibolite and ultramafic bodies.

Geologists - L.C. Rowan and C.E. Larsen.

Geometrical Analysis

Symmetry - Monoclinic.

Scale - Mesoscopic.

Homogeneity - Homogeneous with respect to S_1.

πS_1-girdle - (a). N22E, 50°NW.

βS_1-axis - (a). S68E, 40°SE.

Reliability - (a)-Good.

Fold Geometry - The S_1-subfabric suggests reasonably open folds (F_2) overturned to the NE and plunging moderately S-SE (Turner and Weiss, 1963, p.161). Note that there is no indication of overprinting, and no alternative geometry is suggested.

STRUCTURE STATION 4.

22 S_1 Measurements
Contour Interval: 1-5-10-15%

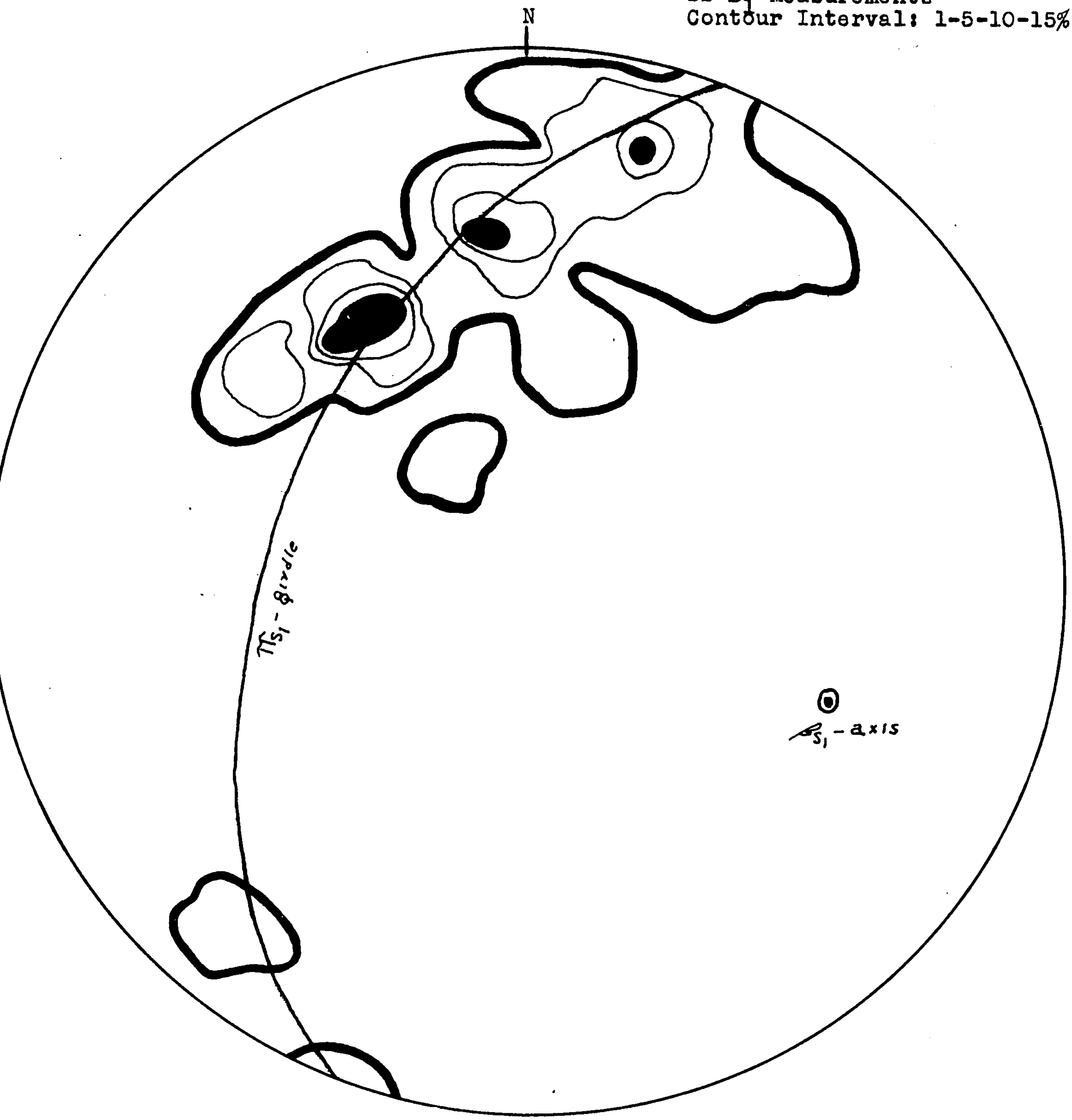

STRUCTURE STATION 5

General Statement

Location - Northeast portion of Quad Creek synform nose (Map 2a).

Areal Extent - Approximately 250 sq. yds.

Number of Measurements - 21 S_1 measurements.

Rock Types - Quartzites.

Geologists - L.C. Rowan and C.E. Larsen.

Geometrical Analysis

Symmetry - Monoclinic.

Scale - Mesoscopic.

Homogeneity - Homogeneous with respect to S_1.

πS_1-girdle - (a). N14W, vertical.

βS_1-axis - (a). S76E, horizontal.

Reliability - (a)-Good.

Fold Geometry - S_1 appears to be folded by F_2 flexures which have;

1). A nearly horizontal axis, B_2

2). and are overturned to the NE (See Map 2a, S_2). This geometry is in agreement with the orientation of F_2 folds observed in the field. Note that βS_1- and B_2-axes are nearly coincident at this station (Map 2b).

STRUCTURE STATION 5.

21 S_1 Measurements
Contour Interval: 1-5-10%

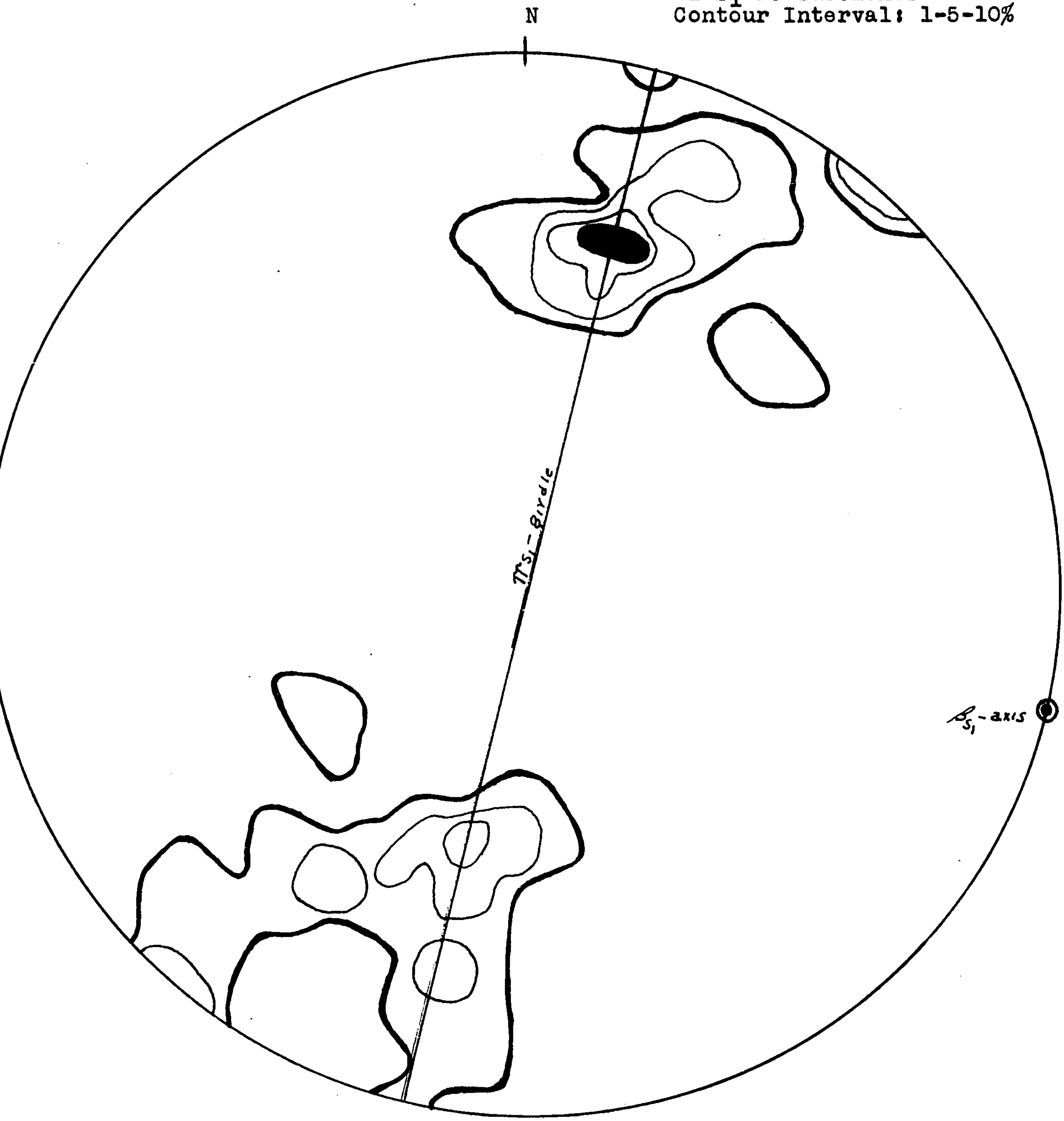

2). Same geometry as (1) above but the F_2 folds are slightly non-cylindrical and non-plane.

Preferred Interpretation: The second alternative is preferred by the writer, since broad, open folds (F_2) have been observed in the field. However, these appear to be very gentle cross-folds, and the slight dispersion of the maxima may be the only effect of this later fold set. The dominance of the folds (F_2) described in number 1 above is apparent to the writer. However, it is difficult to determine the F_2 plunge, since the appressed style of folding does not develop the π S_{1c}-girdle fully. The cross-warps may be due only to F_2 folds being slightly non-cylindrical and non-plane as a manifestation of triaxial strain.

STRUCTURE STATION 6

General Statement

Location - North portion of Quad Creek synform east flank (Map 2a).

Areal Extent - Approximately 23,000 sq. yds.

Number of Measurements - 35 S_1 and S_2 measurements.

Rock Types - Pink biotite migmatite and para-amphibolite.

Geologists - L.C. Rowan and C.E. Larsen.

Geometrical Analysis

Symmetry - Monoclinic.

Scale - Mesoscopic.

Homogeneity - Homogeneous with respect to S_1.

πS_1-girdles - (a). N8E, 25°E ; (b). N8E, horizontal.

βS_1-axes - (a). N82W, 65°W; (b). S82E, vertical.

Reliability - (a)-Good ; (b)-Good.

$\pi S_{1a} \measuredangle \pi S_{1b}$ - Strike - 0 degrees; Dip - 25 degrees.

Fold Geometry - This pattern is very similar to the S_1-subfabric pattern at Station 1. The following interpretations are feasible;

1). Appressed, isoclinal F_2 folds plunge moderately S and are slightly overturned to the E.

STRUCTURE STATION 6

35 S1 and S2 Measurements
Contour Interval: 1-5-10-15%

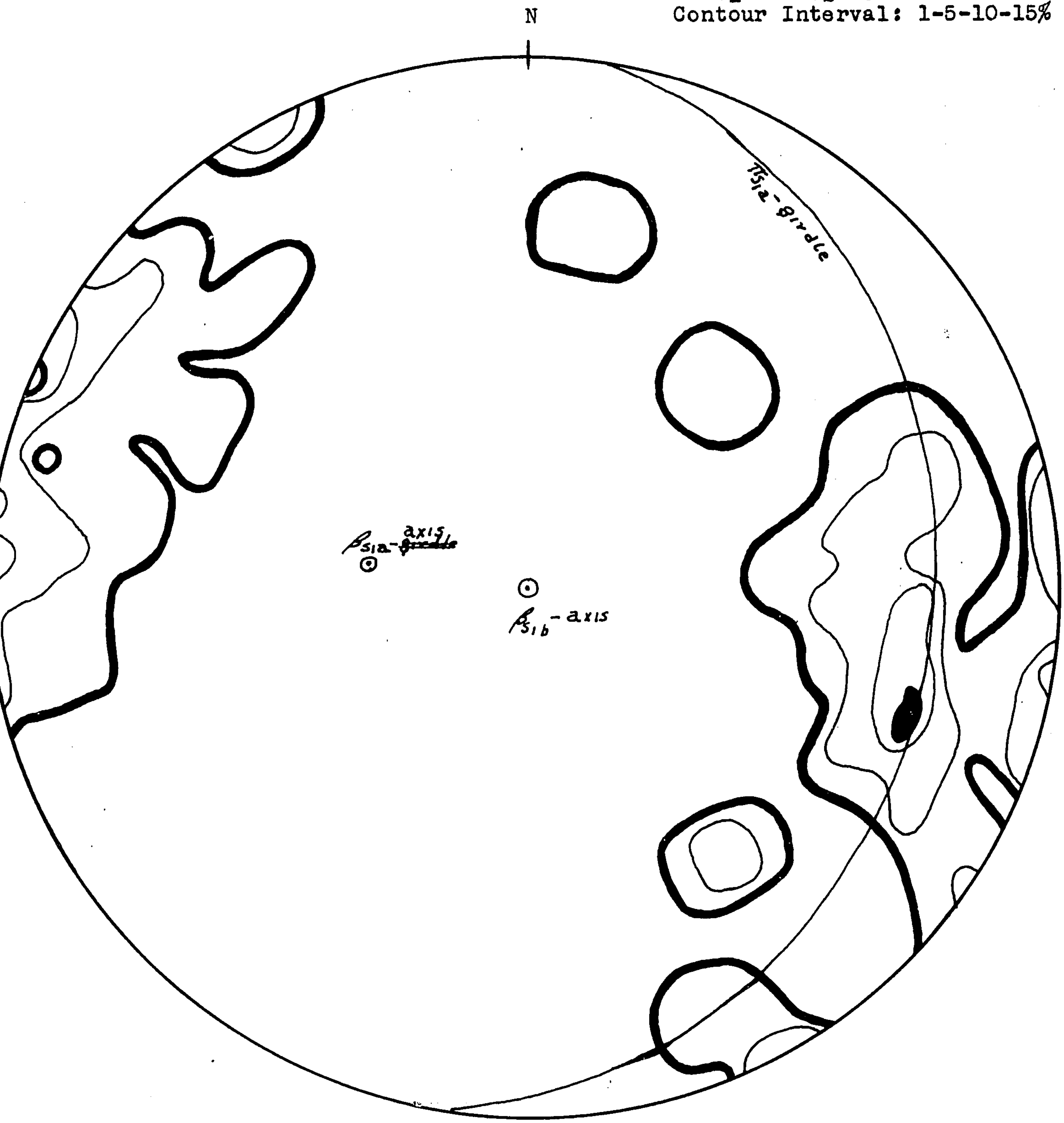

Preferred Interpretation : The writer accepts the third alternative because F_2 folds with this geometry have been observed by the writer in the field. Additionally, "hook" (Carey, 1962, p.101) outcrop patterns are common in these migmatites. Although very open, broad cross-warps are suggested by mapping here (Map 1), these may be due to the slightly non-cylindrical nature of small and large F_2 folds. The S_o-subfabric suggests folds described by (3) above.

STRUCTURE STATION 7

General Statement

Location - East flank of Quad Creek synform (Map 2a).

Areal Extent - Approximately 6,000 sq. yds.

Number of Measurements - 26 S_1 and S_2 measurements.

Rock Types - Pink biotite migmatite and para-amphibolite.

Geologists - L.C. Rowan and C.E. Larsen.

Geometrical Analysis

Symmetry - Monoclinic.

Scale - Mesoscopic.

Homogeneity - Homogeneous with respect to S_1.

πS_1-girdle - (a). N22E, 25°SE.

βS_1-axis - (a). N68W, 70°SE.

Reliability - (a)-Good.

Fold Geometry - This S_1-subfabric pattern indicates the F_2 fold geometry is characteristic of;

1). Open folds plunging steeply NW with vertical axial planes, or

2). Recumbent folds plunging steeply NW (Turner and Weiss, 1963, p.161).

3). F_2 folds are highly appressed and overturned to the east in the S_0-plane.

STRUCTURE STATION 7.

26 S_1 and S_2 Measurements
Contour Interval: 1-5-10-15%

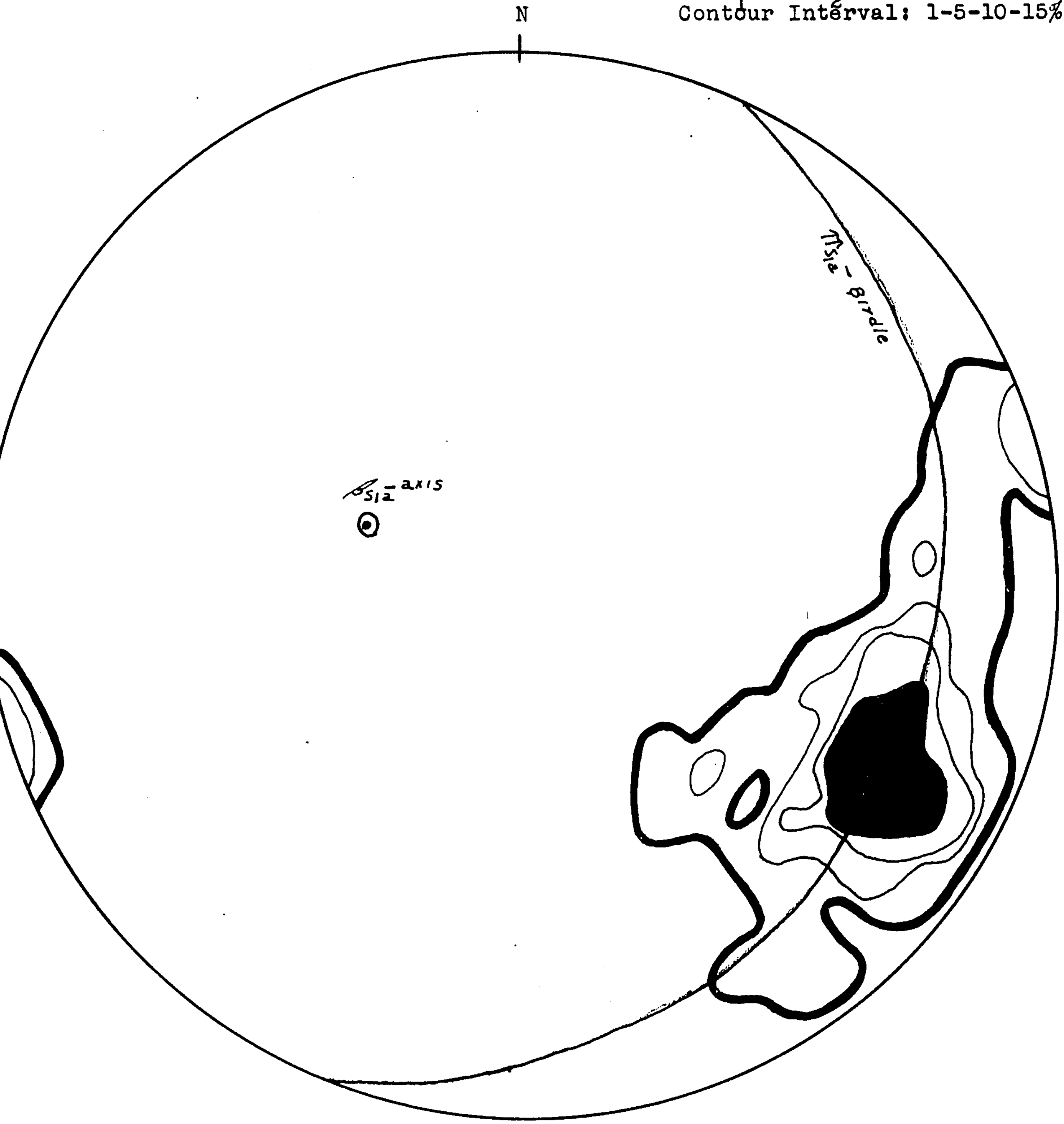

STRUCTURE STATION 8

General Statement

Location - West flank of Wyoming Creek antiform (Map 2a).

Areal Extent - Approximately 6,000 sq. yds.

Number of Measurements - 13 S_1 and S_2 measurements.

Rock Types - Pink biotite migmatite, para-amphibolite, quartzite and agmatite.

Geologists - L.C. Rowan and C.E. Larsen.

Geometrical Analysis

Symmetry - Monoclinic.

Scale - Mesoscopic.

Homogeneity - Homogeneous with respect to S_1.

π-girdles and βS_1-axes - No π S_1-girdles or β S_1-axes have been constructed due to the sparseness of the data. The pattern is similar to the S_0-subfabric pattern at this station, and similar interpretations seem plausible. Note that the S_1-maximum has rotated west at this station from the position at Station 7.

STRUCTURE STATION 8.

13 S_1 and S_2 Measurements
Uncontoured

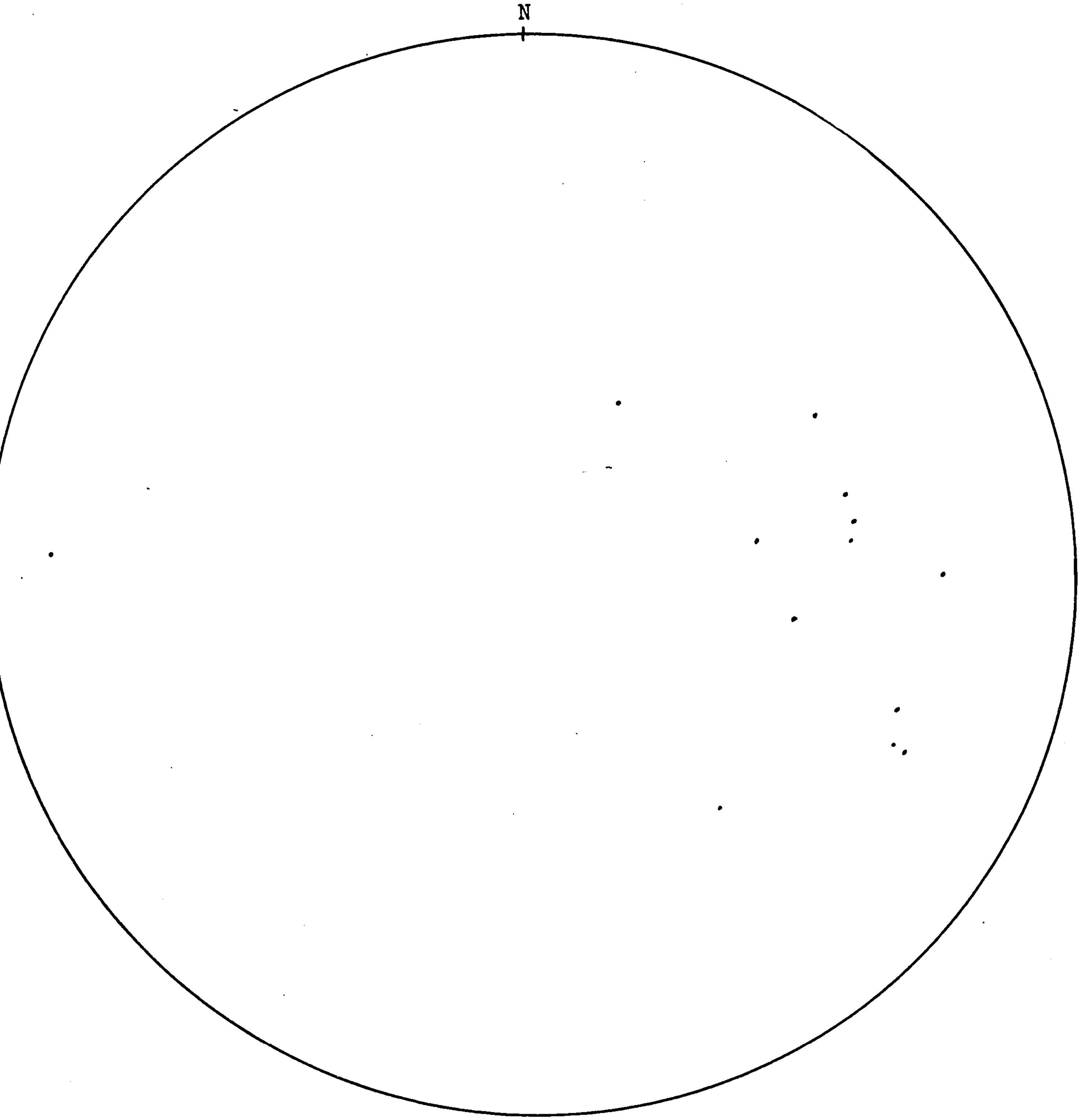

1). Open folds plunging steeply W and slightly overturned to the N.

2). Appressed, isoclinal folds plunging gently S and overturned to the E.

3). Superposition of fold sets F_1, F_2 and F_2 cross-folds.

Preferred Interpretation - Alternative 3 is preferred by the writer. B_1 and B_2 (Map 2b) appear to be nearly parallel at this station, and no fold axes form a maximum which would agree with the βS_{1a}-axis. The most acceptable interpretation is folding of S_1 by later folds (F_2) possessing the characteristics described in number 2 above. βS_{1b}- and B_2-axes are not coincident at this station. It is difficult to construct the βS_{1b}-axis with confidence due to the folding style of F_2. As previously mentioned, the F_2 cross-folds are probably due to superposition of F_2 on F_1 folds. Additionally, F_2 appears to be non-cylindrical and non-plane at Stations 10 and 12.

STRUCTURE STATION 9

General Statement

Location - Southwest portion of the Wyoming Creek anti-form nose (Map 2a).

Areal Extent - Approximately 14,000 sq. yds.

Number of Measurements - 43 S_1 and S_2 measurements.

Rock Types - Pink migmatite, para-amphibolite, quartzites and agmatite.

Geologists - L.C. Rowan and C.E. Larsen.

Geometrical Analysis

Symmetry - Tirclinic, nearly monoclinic.

Scale - Mesoscopic.

Homogeneity - Nearly homogeneous with respect to S_1.

πS_1-girdles - (a). N5E, 20°E ; (b). N85W, 70°N.

βS_1-axes - (a). N85W, 70°W; (b). S5W, 20°S.

Reliability - (a)-Good ; (b)-Poor.

$\pi S_{1a} \angle \pi S_{1b}$ - Strike - 90 degrees; Dip - 50 degrees.

Fold Geometry - The overall S_1-subfabric pattern suggests open folds (Turner and Weiss, 1963, p.161) plunging steeply W and overturned slightly to the N. However, the πS_{1b}-girdle is significant when other data are considered. The following geometrical interpretations are available;

STRUCTURE STATION 9.

43 S_1 and S_2 Measurements
Contour Interval: 1-5-10-15%

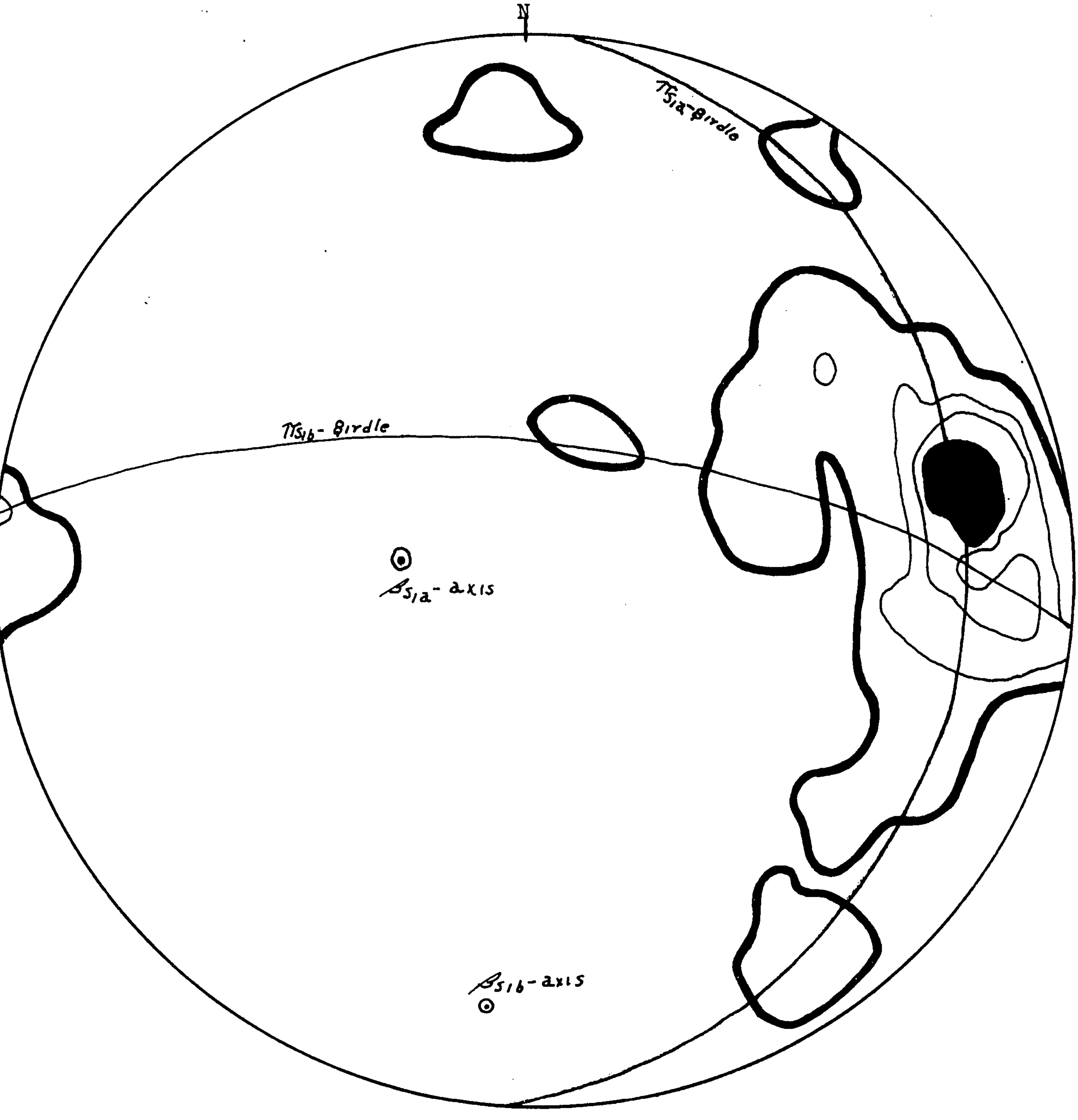

Preferred Interpretation: The writer concludes that S_1 is folded about axes (B_2) which plunge moderately SW, because the βS_{1a}-axis agrees closely with B_2 (Map 2b) at this station. Field observations indicate that these folds are relatively open. Note that βS_0-axes do not coincide with the βS_1-axes. F_2 cross-folds may be indicated by the S_2-subfabric (Map 2a). However, these cross-warps may be a manifestation of triaxial strain in F_2 folding rather than superposition of later or synchronous cross-folds. Therefore, the subscript (2) is used.

STRUCTURE STATION 10

General Statement

Location - Southeast portion of Wyoming Creek antiform nose (Map 2a).

Areal Extent - Approximately 16,000 sq. yds.

Number of Measurements - 23 S_1 measurements.

Rock Types - Agmatite, quartzites and para-amphibolite.

Geologists - L.C. Rowan and C.E. Larsen.

Geometrical Analysis

Symmetry - Tirclinic.

Scale - Mesoscopic.

Homogeneity - Nearly homogeneous with respect to S_1.

πS_1-girdles - (a). N41W, 40°NE ; (b). N88W, 70°N.

βS_1-axes - (a). S49W, 50°SW ; (b). S2W, 20°S.

Reliability - (a)-Good ; (b)-Fair.

$\pi S_{1a} \angle \pi S_{1b}$ - Strike - 47 degrees; Dip - 30 degrees.

Fold Geometry - The following geometrical interpretations deserve consideration;

1). Open fold plunging moderately SW and overturned slightly to the NW.

2). Superposition of fold sets; F_1, F_2, and F_2 cross-folds.

STRUCTURE STATION 10.

23 S_1 Measurements
Contour Interval: 1-5-10-15%

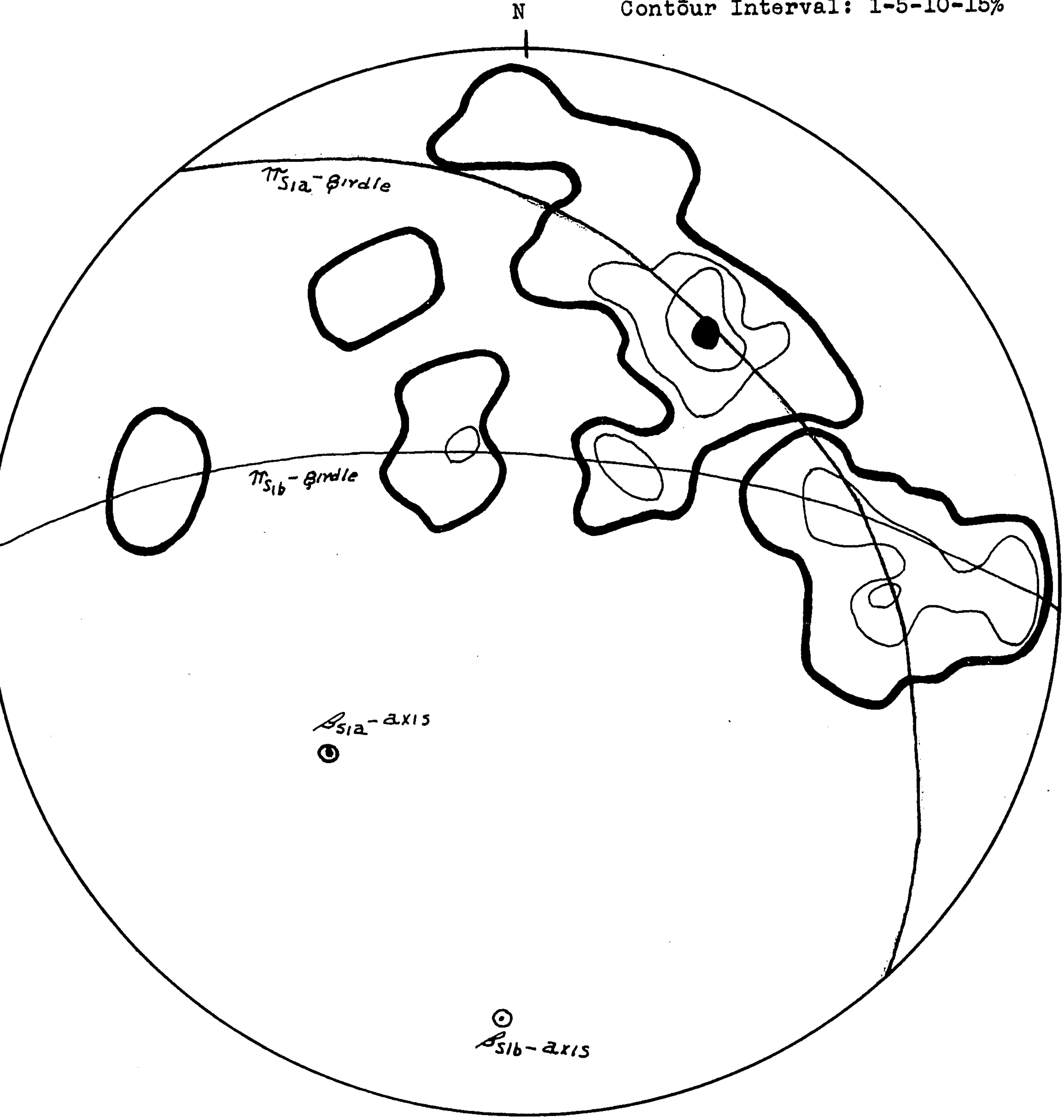

that there is approximately 50 degrees divergence in strike between βS_0- and βS_1-axes at this station. The two β-axes plunge at about the same angle.

STRUCTURE STATION 11

General Statement

Location - South flank of the Wyoming Creek antiform (Map 2a).

Areal Extent - Approximately 66,000 sq. yds.

Number of Measurements - 16 S_1 measurements.

Rock Types - Pink biotite migmatite, agmatite, quartzite and para-amphibolite.

Geologists - L.C. Rowan and C.E. Larsen.

Geometrical Analysis

Symmetry - Monoclinic.

Scale - Mesoscopic.

Homogeneity - Homogeneous with respect to S_1.

π S_1-girdle - (a). N84W, 30°N.

β S_1-axis - (a). S6W, 60°S.

Reliability - (a)-Good.

Fold Geometry - The S_1-subfabric pattern indicates folding of S_1 by open F_2 folds or recumbent F_2 folds which plunge steeply S. The open folds would be slightly overturned to the SE.

Preferred Interpretation: The writer believes that these later folds are open, since there is no evidence supporting the existence of recumbent folds at this station.

STRUCTURE STATION 11.

16 S_1 Measurements
Contour Interval: 1-10-18%

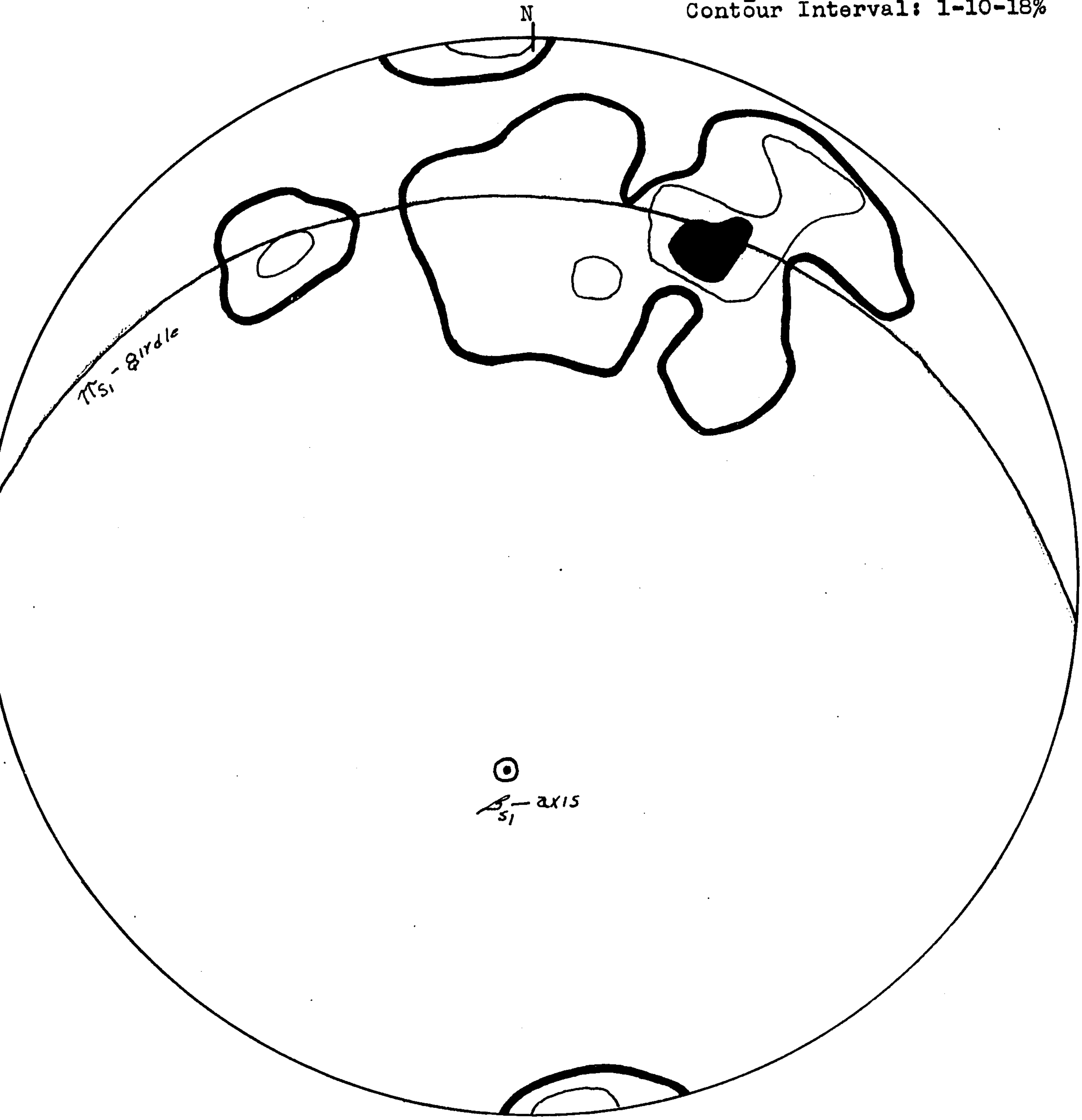

no other evidence is indicative of recumbent folds. These later folds (F_2) appear to be slightly overturned to the NW. Map 2a with respect to S_2, and the symmetry of the S_1-subfabric suggest that these later folds are non-cylindrical in this sub-domain. This may be due to very gentle warping later than S_2. Note that the β S_1-axis agrees closely with B_2 (Map 2b) and reasonably well with the β So-axis.

STRUCTURE STATION 12

General Statement

Location - Eastern portion of the Wyoming Creek antiform south flank (Map 2a).

Areal Extent - Approximately 100,000 sq. yds.

Number of Measurements - 33 S_1 measurements.

Rock Types - Quartzite, para-amphibolite, migmatites and micaceous schists.

Geologists - L.C. Rowan and C.E. Larsen.

Geometrical Analysis

Symmetry - Nearly monoclinic.

Scale - Mesoscopic.

Homogeneity - Nearly homogeneous with respect to S_1.

π S_1-girdle - (a). N60W, 35°NE.

β S_1-axis - (a). S30W, 55°SW.

Reliability - (a)-Good.

Fold Geometry - The S_1-pattern suggests refolding of S_1 by F_2 folds which plunge steeply SW and are either

1). open, or

2). recumbent (Turner and Weiss, 1963, p.161).

Preferred Interpretation; The writer has observed relatively open folds (F_2) folding S_1 at this station, and

STRUCTURE STATION 12.

33 S_1 Measurements
Contour Interval: 1-5-10-15%

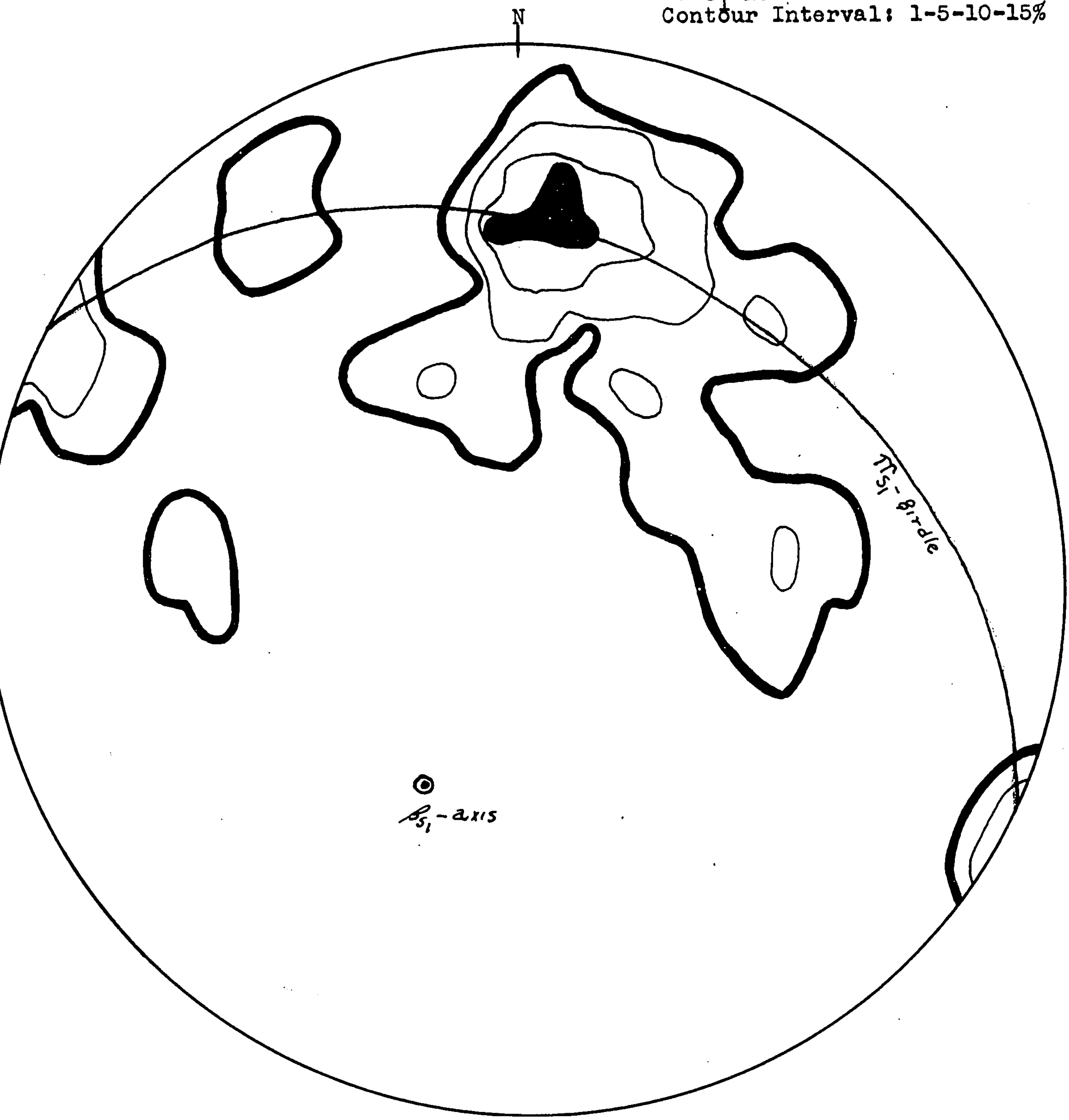

Macroscopic Scale:

Treatment of the S_1-subfabric on the macroscopic scale has been conducted by combining structure stations homogeneous with respect to S_1 into subareas. Six subareas have been constructed in this manner and are keyed to the appropriate subareas on Map 3a. Measurements number from 18 to 117. The symmetry for the individual subareas is generally monoclinic. Homogeneity is slightly greater in the Wyoming Creek antiform than in the Quad Creek synform. In general, S_1 is not a penetrative fabric element for the two major folds, because it rotates around the major noses (Turner and Weiss, 1963, pp.144-151).

cross-folds. These folds are suggested by the S_0- and S_1-subfabrics on the mesoscopic scale here. However, they may be the non-cylindrical nature of small and large F_2 folds due to triaxial strain.

SUBAREA 1

General Statement

Location - West flank of Quad Creek synform, including Structure Stations 1 and 2 (Map 3a).

Areal Extent - 0.1 square miles.

Number of Measurements - 51 S_1 measurements.

Rock Types - Migmatites.

Geologists - L.C. Rowan and C.E. Larsen.

Geometrical Analysis

Symmetry - Nearly Monoclinic.

Scale - Macroscopic.

Homogeneity - Nearly homogeneous with respect to S_1.

πS_1-girdles - (a).N-S,30°W; (b).N10E,20°E; (c).N87W,80°N.

βS_1-axes - (a).E-W,60°E; (b).N80W,70°W; (c).S3W,10°S.

Reliability - (a)-Good ; (b)-Fair ; (c)-Fair.

Fold Geometry - This subfabric pattern is characteristic of appressed, isoclinal folds (F_2) which are slightly overturned to the W. The πS_{1a}- and πS_{1b}-girdles define the limbs of the F_2 folds which contain S_1. Although it is difficult to construct a βS_1-axis from a diagram with these features, the βS_{1c}-axis agrees quite well with B_2. The dispersion of the πS_{1a}-girdle is believed by the writer to be due to slight warping by the broad, open F_2

SUBAREA 1

51 S_1 Measurements
Contour Interval: 1-4-8%

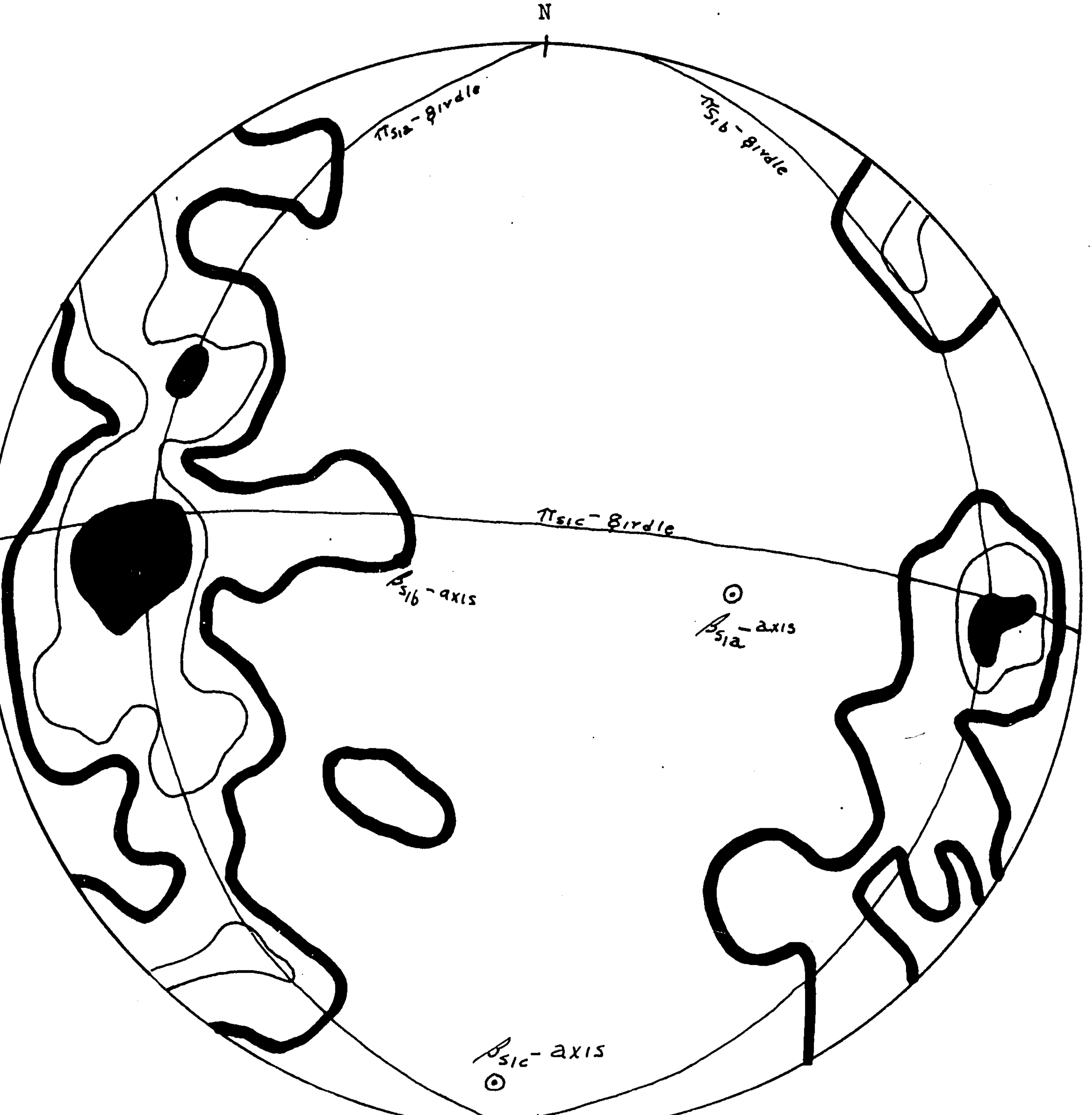

SUBAREA 2

General Statement

Location - Nose of Quad Creek synform, including Structure Stations 3, 4, and 5 (Map 3a).

Areal Extent - 0.08 square miles.

Number of Measurements - 75 S_1 measurements.

Rock Types - Quartzites, para-amphibolite and migmatites.

Geologists - L.C. Rowan and C.E. Larsen.

Geometrical Analysis

Symmetry - Monoclinic.

Scale - Macroscopic.

Homogeneity - Homogeneous with respect to S_1.

πS_1-girdle - (a). N45E, 40°NW.

βS_1-axis - (a). S45E, 50°SE.

Reliability - (a)-Good.

Fold Geometry - This S_1-subfabric indicates that S_1 is deformed by non-isoclinal, relatively open F_2 folds which are overturned to the NE (Turner and Weiss, 1963, p.161) and plunge 50° to S45E. Note that βS_1- agrees reasonably well with the B_2-axes.

SUBAREA 2.

75 S_1 Measurements
Contour Interval: 1-4-8%

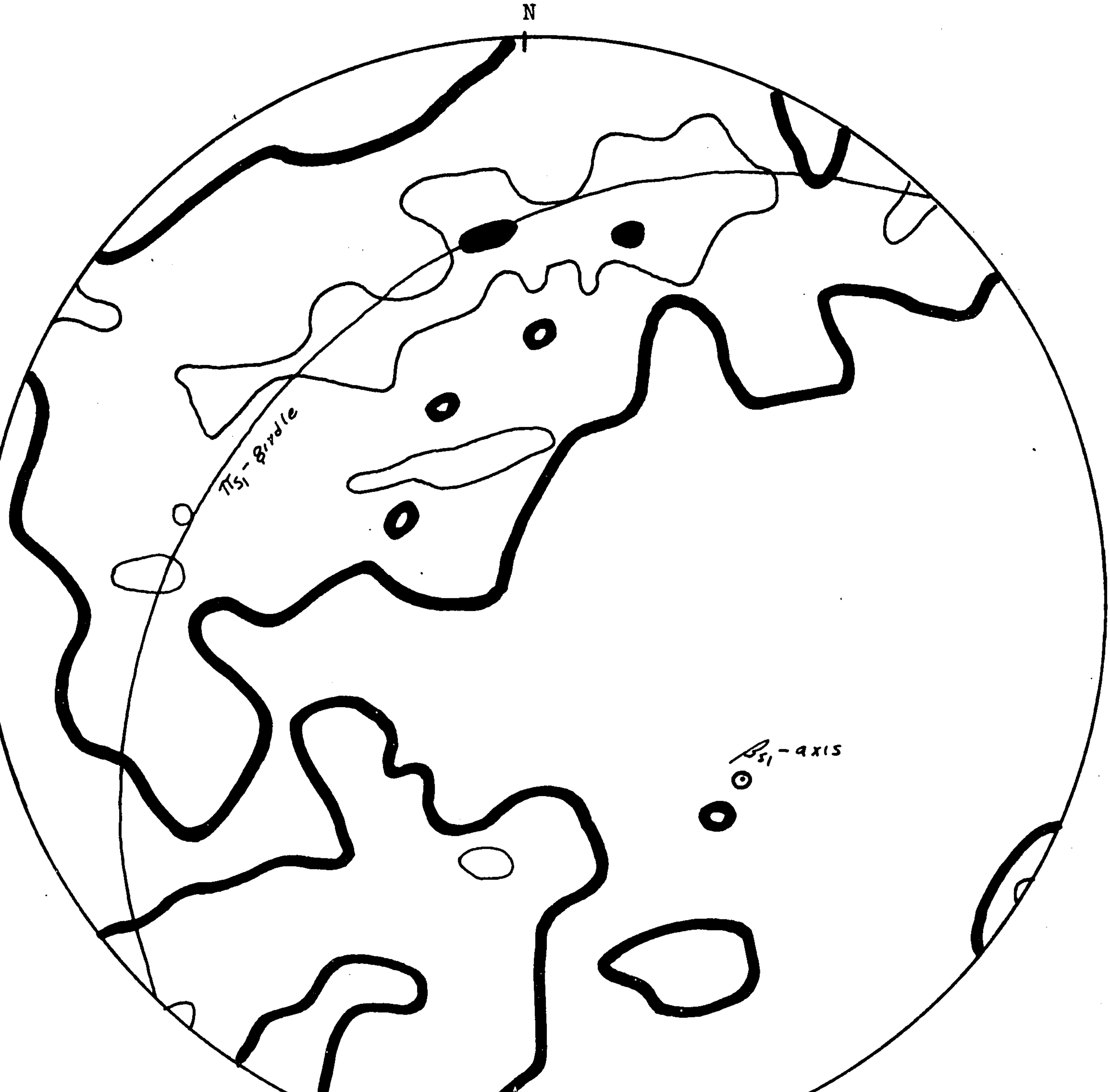

SUBAREA 3

General Statement

Location - West flank of the Quad Creek synform, including Structure Stations 6, 7 and 8 (Map 3a).

Areal Extent - 0.60 square miles.

Number of Measurements - 89 S_1 and S_2 measurements.

Rock Types - Pink biotite migmatite.

Geologists - L.C. Rowan and C.E. Larsen.

Geometrical Analysis

Symmetry - Generally monoclinic.

Scale - Macroscopic.

Homogeneity - Homogeneous with respect to S_1.

πS_1-girdles - (a). N01E, 28°E ; (b). N58W, 55°NE.

βS_1-axes - (a). N89W, 62°W ; (b). S32W, 35°SW.

Reliability - (a)-Good. ; (b)-Good.

Fold Geometry - This S_1-subfabric suggests that S_1 is folded by appressed nearly isoclinal folds (F_2) which are slightly overturned to the E-SE (Turner and Weiss, 1963, p.161). S_1 and S_2 are not separable at this station. Therefore, the maximum may be a reflection of S_2 poles. The writer believes that the πS_{1a}-girdle is a result of very open, broad F_2 cross-folds which may be due to superposition of F_2 on F_1 or the non-cylindrical character of F_2 folds.

SUBAREA 3.

89 S_1 and S_2 Measurement
Contour Interval:
1-4-8-12%

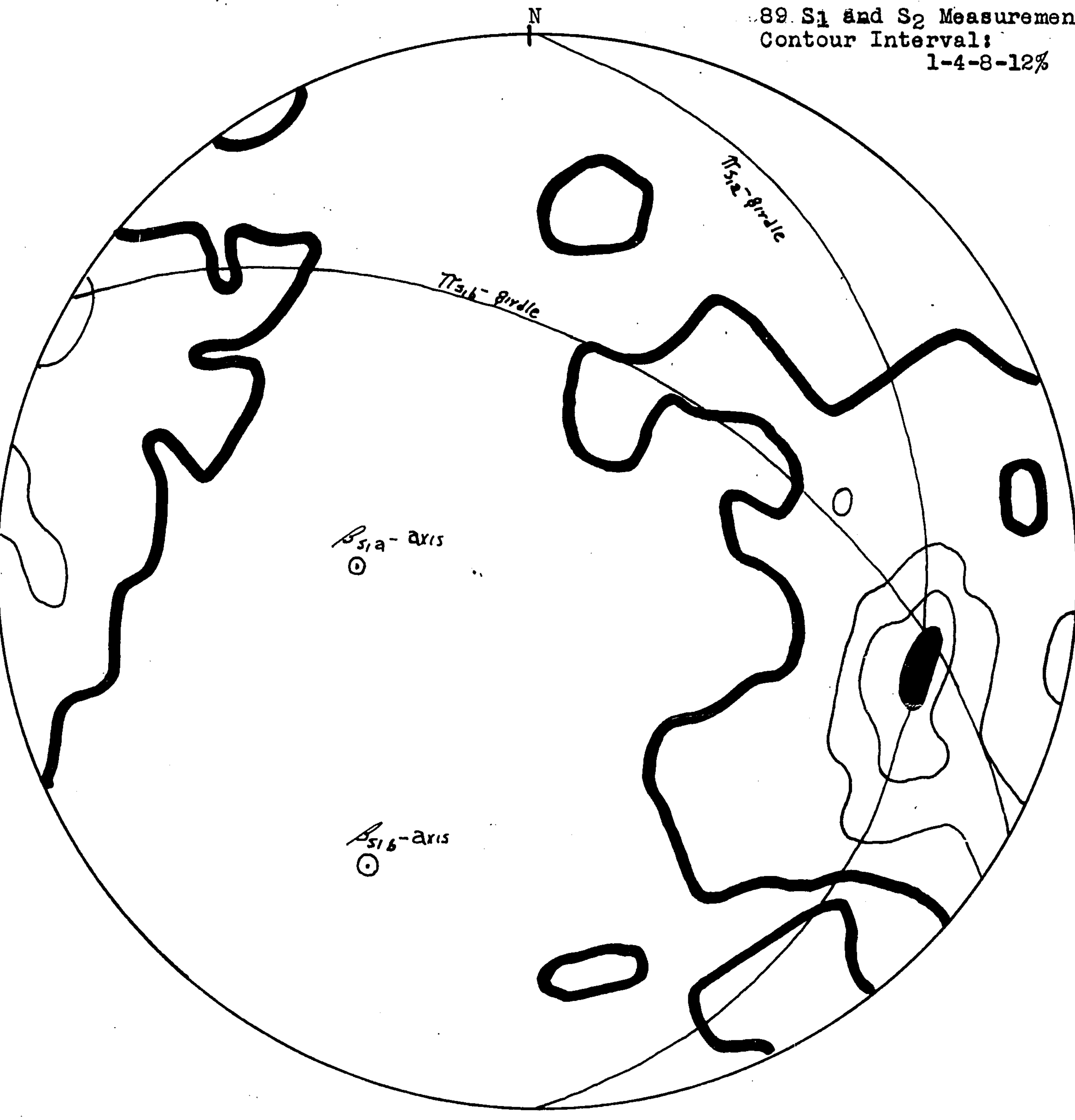

Station 9. S_2 (Map 2a) suggests slight warping which is later than F_2 or non-cylindrical F_2 folds due to triaxial strain. This folding may be defined by the βS_{1b}-axis in this subarea.

SUBAREA 4

General Statement

Location - Nose of Wyoming Creek antiform, including Structure Stations 9 and 10 (Map 3a).

Areal Extent - 0.2 square miles.

Number of Measurements - 67 S_1 and S_2 (Station 9) measurements.

Rock Types - Pink biotite migmatite, quartzites and para-amphibolite.

Geologists - L.C. Rowan and C.E. Larsen.

Geometrical Analysis

Symmetry - Generally monoclinic.

Scale - Macroscopic.

Homogeneity - Nearly homogeneous with respect to S_1.

πS_1-girdles - (a). N80W, 44°NE ; (b). N2E, 18°E.

βS_1-axes - (a). S10W, 46°SW ; (b). N88W, 72°W.

Reliability - (a)-Good ; (b)-Fair.

Fold Geometry - This S_1-subfabric suggests deformation of S_1 by F_2 folds which are non-isoclinal and overturned to the E. (Turner and Weiss, 1963, p.161). The constructed βS_{1a}-axis agrees with B_2. The very intense maximum may be due to the fact that some S_2 measurements are included in this diagram. F_1 and F_2 are not separable at Structure

SUBAREA 4.

67 S_1 and S_2 Measurements
Contour Interval:
1-4-8-12-16%

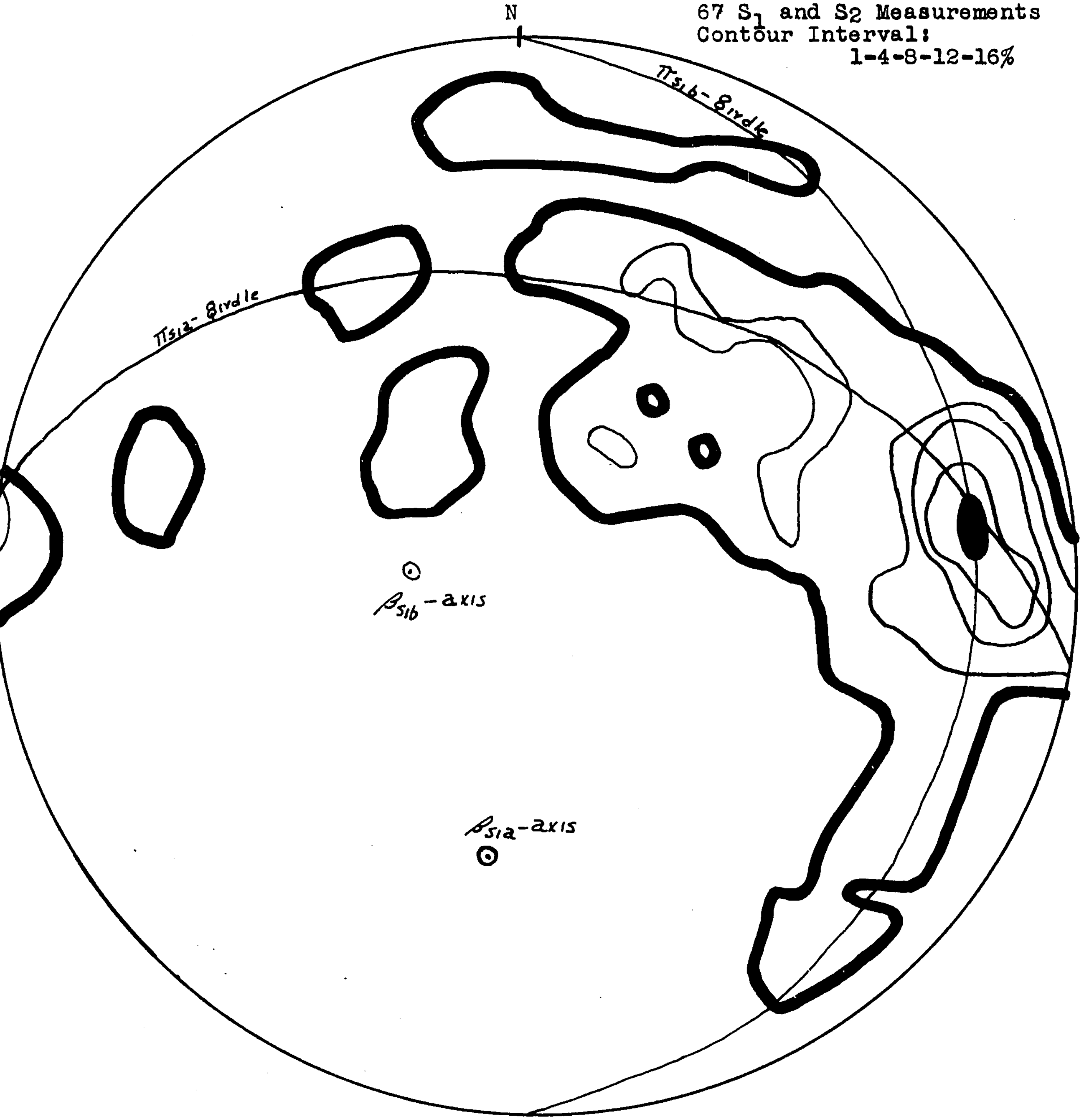

(1) S_2 forms an ill-defined girdle, (2) this is also defined at Subarea 4 (Map 3a) and (3) is characteristic of the major folds in the area (Text Figure 4).

SUBAREA 5

General Statement

Location - South flank of the Wyoming Creek antiform, including Structure Stations 11 and 12 (Map 3a).

Areal Extent - 0.3 square miles.

Number of Measurements - 57 S_1 measurements.

Rock Types - Migmatites, quartzites, mica schists.

Geologists - L.C. Rowan and C.E. Larsen.

Geometrical Analysis

Symmetry - Generally monoclinic.

Scale - Macroscopic.

Homogeneity - Nearly homogeneous with respect to S_1.

πS_1-girdles - (a). N82W, 35°N ; (b). N8W, 60°E.

βS_1-axes - (a). S8W, 55°S ; (b). S82W, 30°W.

Reliability - (a)-Good ; (b)-Fair.

Fold Geometry - This S_1-subfabric suggests F_2 are open folds with nearly vertical axial planes (S_2). Overturning very gently to the E is suggested by direct S_2 measurements (Map 2a). Note that B_2- and βS_{1a}-axes are nearly coincident (Map 3b). The π S_{1b}-girdle may be due to (1) F_3 warping which is gentle, or (a) inhomogeneous F_2 deformation. The writer prefers the second alternative, because

SUBAREA 5.

57 S_1 Measurements
Contour Interval: 1-4-8-12%

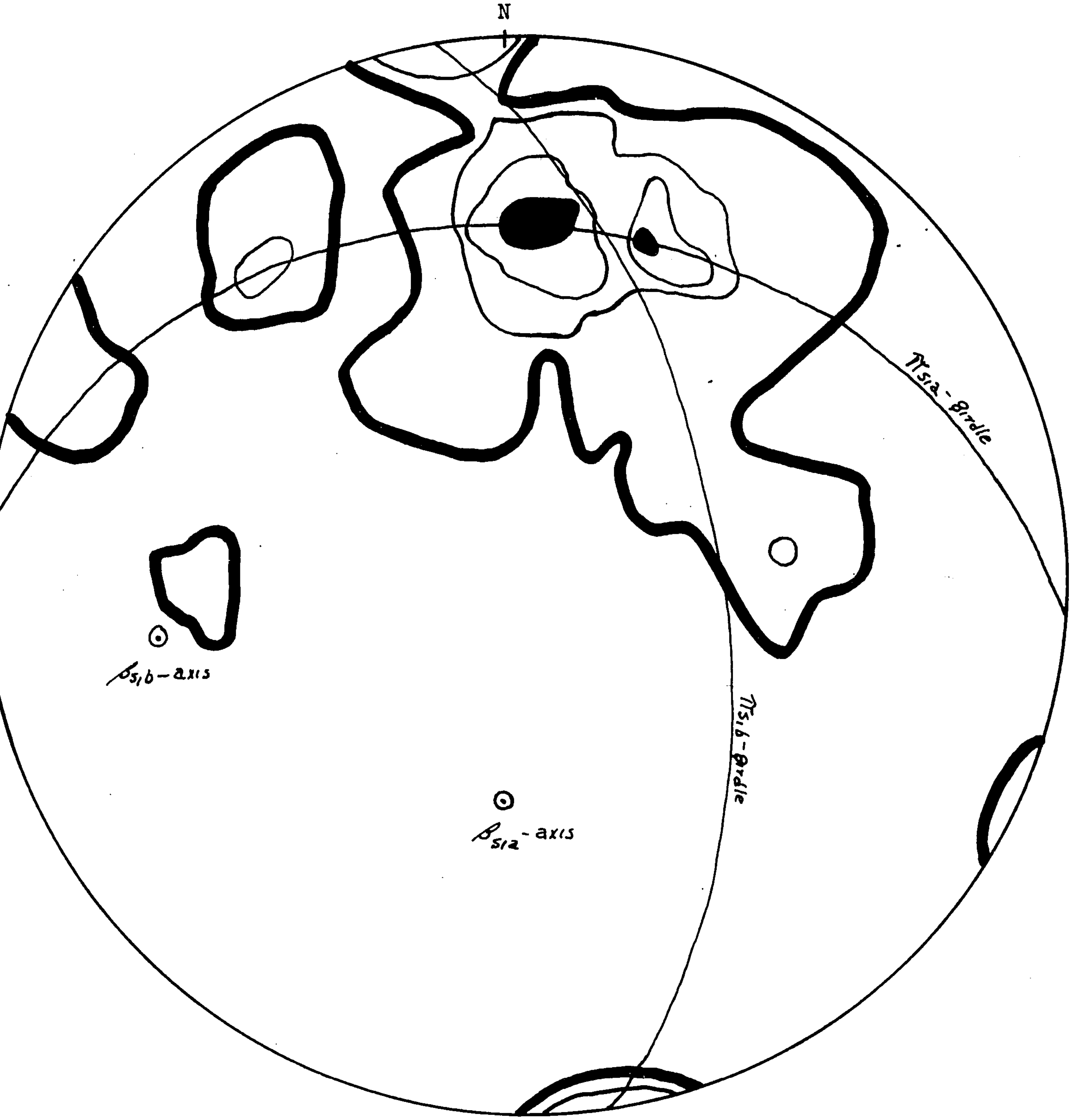

SUMMARY

S_1-subfabric - The S_1-subfabric has been especially useful in determining the F_2 fold geometry. Open F_2 folds are demonstrated by the S_1-subfabric in the southeast flank of the Wyoming Creek antiform, where non-ductile quartzites and para-amphibolite dominate. SW plunging, asymmetrical F_2 folds are defined in the nose of the major antiform. S_1 and S_2 are not separated in the east flank of the Quad Creek synform. However, south plunging, isoclinal, nearly symmetrical F_2 folds are defined at Station 6. This pattern is poorly developed at Stations 7, 8 and 9. The dominant rock types at these stations are migmatites. The writer believes that F_2 folds fold S_1 at these stations, but that they are appressed and overturned in the plane of S_0. The macroscopic S_1-subfabric demonstrates the interpreted F_2 fold geometry in this area. Additionally, the presence of highly ductile migmatites appears to be an influential factor in F_2 fold style. In general, F_2 folds are slightly appressed and "similar" in migmatites and granitic gneisses, while they are generally open and partially flexural in non-ductile quartzites (Figure 21) and para-amphibolite. Although cross-flexures related to the major synform are suggested at Stations 1, 2, 6, 7, 8 and 9, the writer believes that these broad, open warps are manifestations of refolding. β S_1-axes at Stations

6, 10, 11 and 12, as well as in Subareas 3, 4 and 5, are closely coincident with B_2-axes. Figure 30 shows the βS_1-axis for the entire Wyoming Creek antiform. The S_1-subfabric is homogeneous on the macroscopic scale, and the mesoscopic subfabric is significantly more homogeneous than the S_0-subfabric.

The S_1-subfabric at Station 1 is similar to the Station 6 pattern. F_2 folds which are relatively open and are overturned to the N-NE dominate in the Quad Creek synform nose. The constructed βS_1-axes agree closely with measured B_2-axes. βS_1-axes rotate around the Quad Creek synform nose, while little rotation is noted in the Wyoming Creek antiform.

APPENDIX III

S_2-subfabric

Mesoscopic:

S_2 measurements are not numerous at any of the 12 structure stations, because F_1 and F_2 small folds are frequently very similar in style. As previously mentioned, F_1 and F_2 are not distinguishable at Structure Stations 6, 7, 8, 9 and 11. Nearly all of the S_2 measurements were taken from F_2 folds showing refolding at Stations 2, 3 and 5. S_2-subfabric symmetry ranges from axial to monoclinic.

STRUCTURE STATION 2

General Statement

Location - Northwest portion of Quad Creek synform nose (Map 3a).

Areal Extent - Approximately 2,000 square yards.

Number of Measurements - 6 S_2 measurements from samples showing refolding.

Rock Types - Migmatites and quartzites.

Geologists - L.C. Rowan and C.E. Larsen.

Geometrical Analysis

Symmetry - Monoclinic.

Scale - Mesoscopic.

Homogeneity - Homogeneous with respect to S_2.

πS_2-girdle - (a). N8E, 25°W.

βS_2-axis - (a). S82E, 65°E.

Reliability - (a)-Good considering the number of points.

Fold Geometry - All S_2 measurements have been made on oriented samples showing folding of F_1 about B_2 with S_2 as later (F_2) axial planes. Although the data are sparse, the π S_2-girdle seems to be well justified. Open folds plunging steeply E are defined by the π S_2-girdle. Note that the S_o- and S_1-subfabrics suggest the existence of these gentle, open F_2 cross-folds also. These folds may be due to triaxial strain during F_2 folding.

STRUCTURE STATION 2.

6 S_2 Measurements

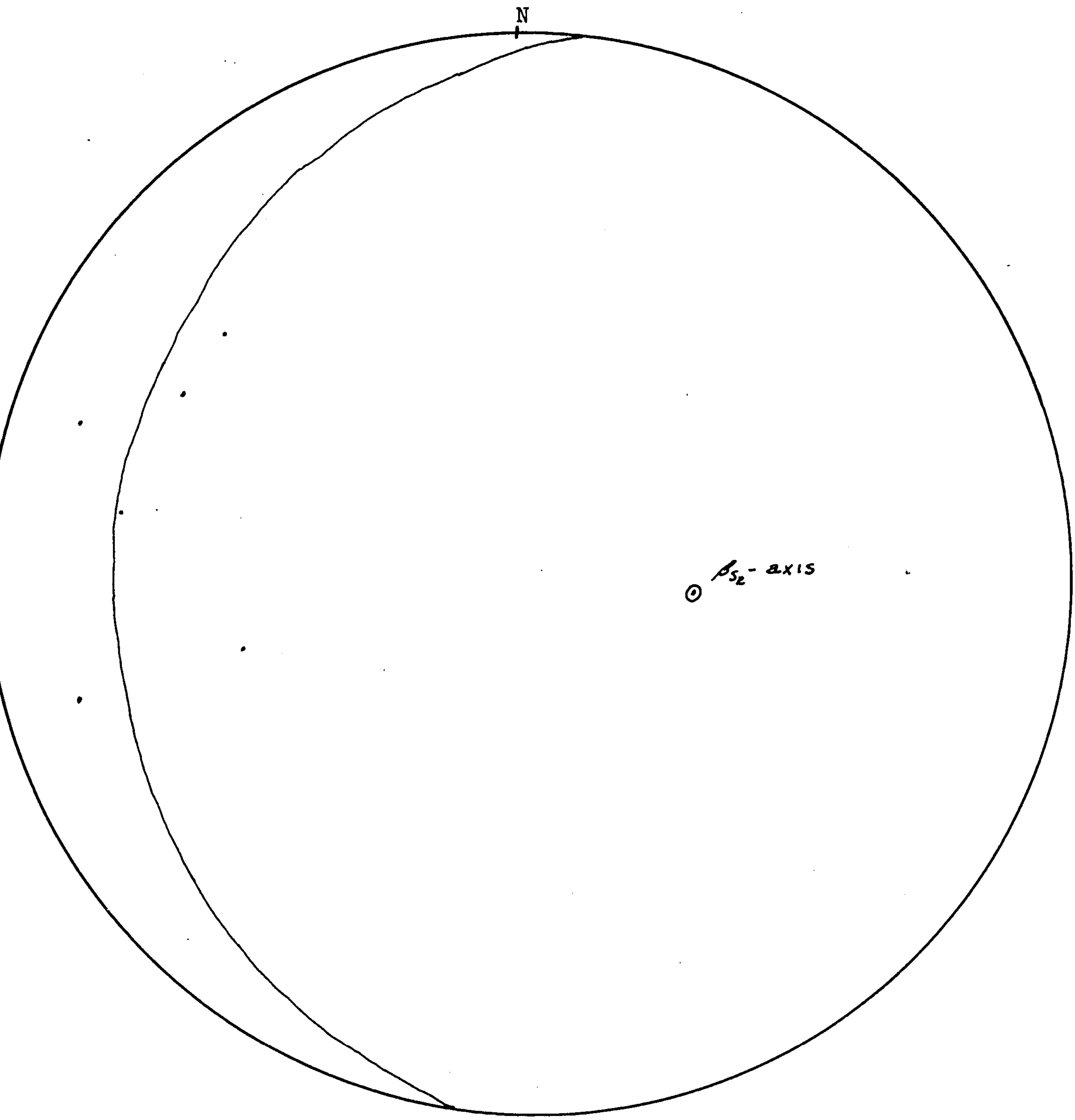

STRUCTURE STATION 3

General Statement

Location - Nose of the Quad Creek synform (Map 3a).

Areal Extent - Approximately 3,000 square yards.

Number of Measurements - 3 S_2 measurements.

Rock Types - Migmatites and quartzites.

Geologists - L.C. Rowan and C.E. Larsen.

Geometrical Analysis

Symmetry - Axial.

Scale - Mesoscopic.

Homogeneity - Homogeneous with respect to S_2.

Maximum - (a). N8W, 57°N.

Remarks - S_2 is homogeneous on this scale, and F_2 is overturned to the north.

STRUCTURE STATION 3.

3 S_2 Measurements

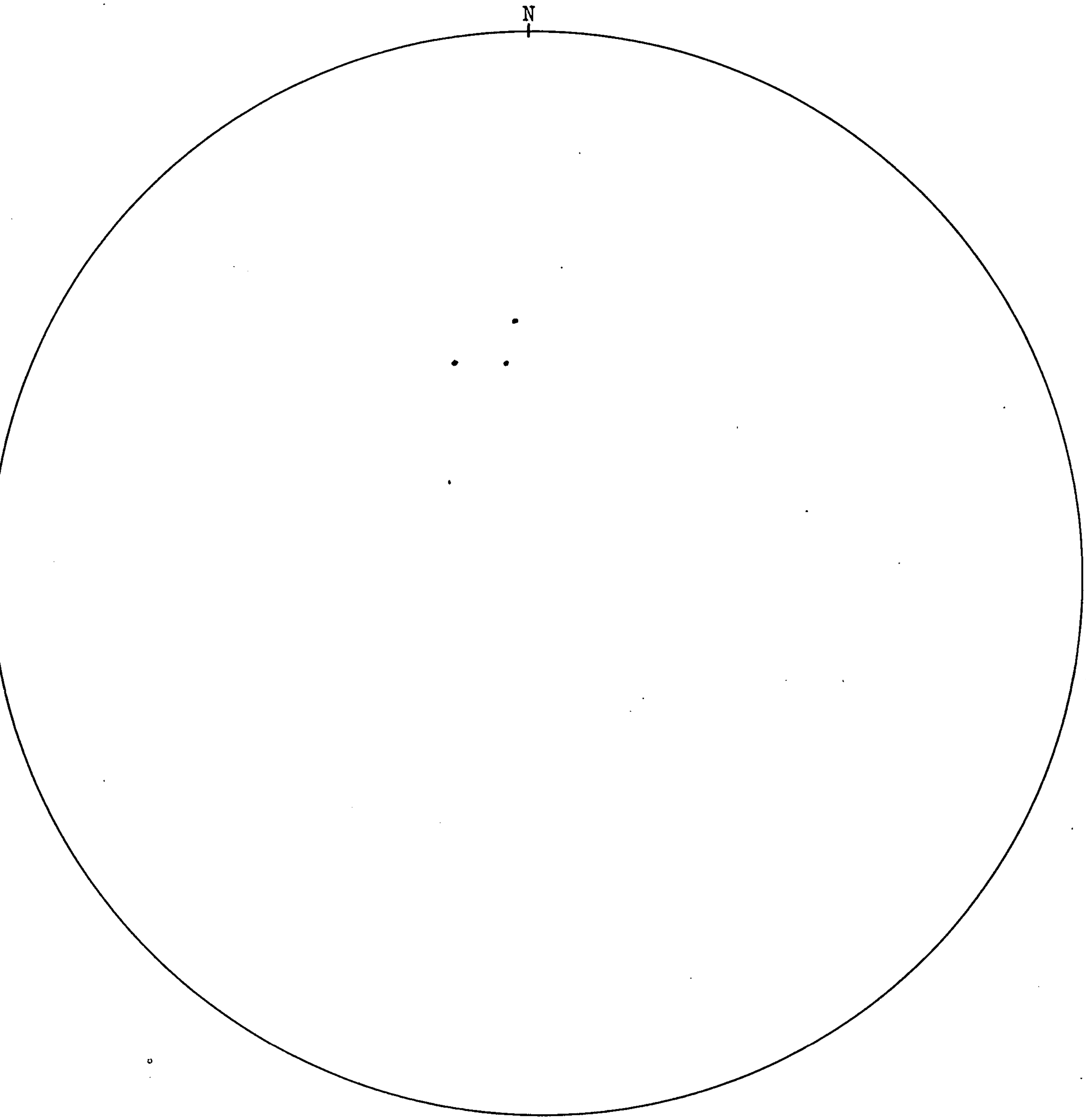

STRUCTURE STATION 5

General Statement

Location - Northeast portion of the Quad Creek synform nose (Map 3a).

Areal Extent - Approximately 250 square yards.

Number of Measurements - 6 S_2 measurements, 3 of which are from oriented samples showing refolding.

Rock Type - Quartzites.

Geologists - L.C. Rowan and C.E. Larsen.

Geometrical Analysis

Symmetry - Axial.

Scale - Mesoscopic.

Homogeneity - Homogeneous with respect to S_2

Maximum - (a). N-S, 20°N.

Remarks - S_2 is homogeneous on this scale. F_2 folds are nearly recumbent to the north.

STRUCTURE STATION 5.

6 S_2 Measurements

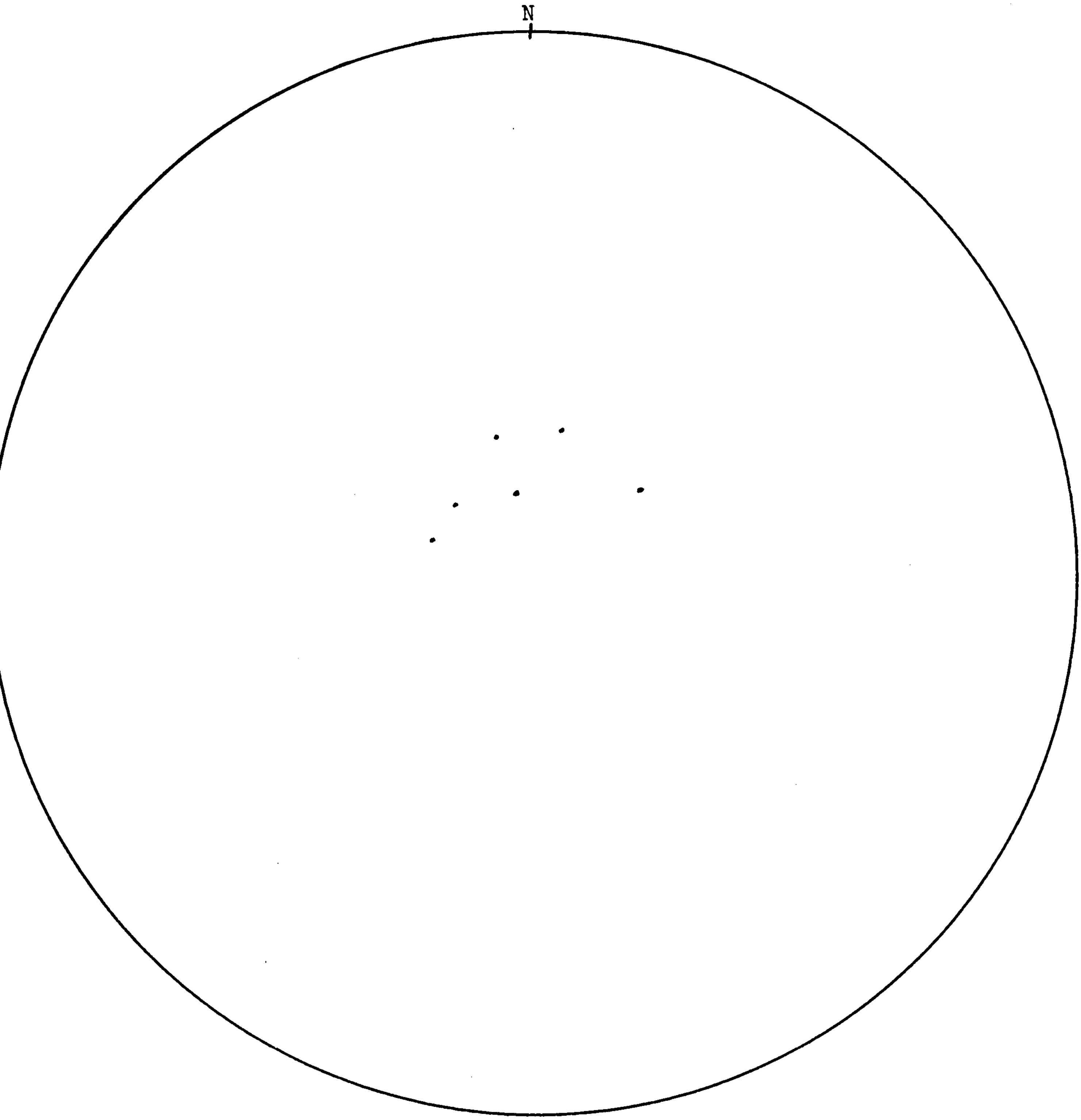

STRUCTURE STATION 10

General Statement

Location - Southeast portion of Wyoming Creek antiform (Map 2a).

Areal Extent - Approximately 16,000 square yards.

Number of Measurements - 8 S_2 measurements.

Rock Types - Migmatites, quartzites and agmatite.

Geologists - L.C. Rowan and C.E. Larsen.

Geometrical Analysis

Symmetry - Monoclinic.

Scale - Mesoscopic.

Homogeneity - Homogeneous with respect to S_2.

πS_2-girdle - (a). N22W, 30°NE.

βS_2-axis - (a). S68W, 60°SW.

Reliability - (a)-Good, considering the small number of S_2 measurements.

Fold Geometry - The warping of S_2 is very gentle. S_2 may be deformed by folds later than F_2 or may be characteristic of the larger F_2 folds. Text figure 4 shows the variable trend of major folds. Since no folds later than F_2 have been identified in the field at this station, the writer believes the variable S_2 trend is a reflection of the non-cylindrical major flexures.

STRUCTURE STATION 10.

B: S_2 Measurements

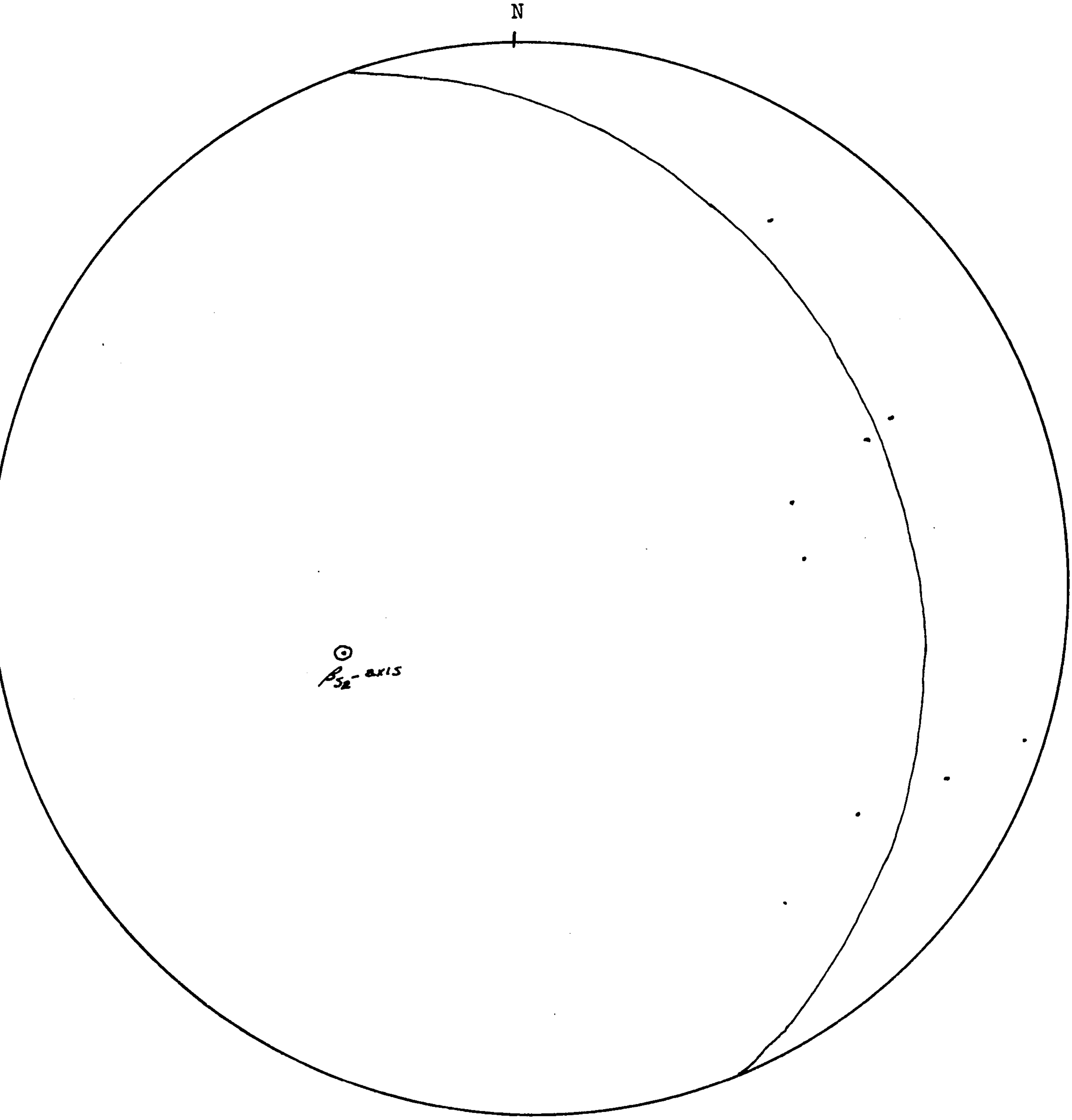

STRUCTURE STATION 12

General Statement

Location - South flank of the Wyoming Creek antiform (Map 2a).

Areal Extent - Approximately 100,000 square yards.

Number of Measurements - 17 S_2 measurements.

Rock Types - Quartzites, para-amphibolite and micaceous schists.

Geologists - L.C. Rowan and C.E. Larsen.

Geometrical Analysis

Symmetry - Monoclinic.

Scale - Mesoscopic.

Homogeneity - Homogeneous with respect to S_2.

πS_2-girdle - (a). N43W, 50°NE.

βS_2-axis - (a). S47W, 40°SW.

Reliability - (a). Good.

Remarks - The pattern at this station is similar to the S_2-subfabric at number 10, and the writer applies remarks concerning that sub-domain to this structure station.

STRUCTURE STATION 12.

17 S_2 Measurements

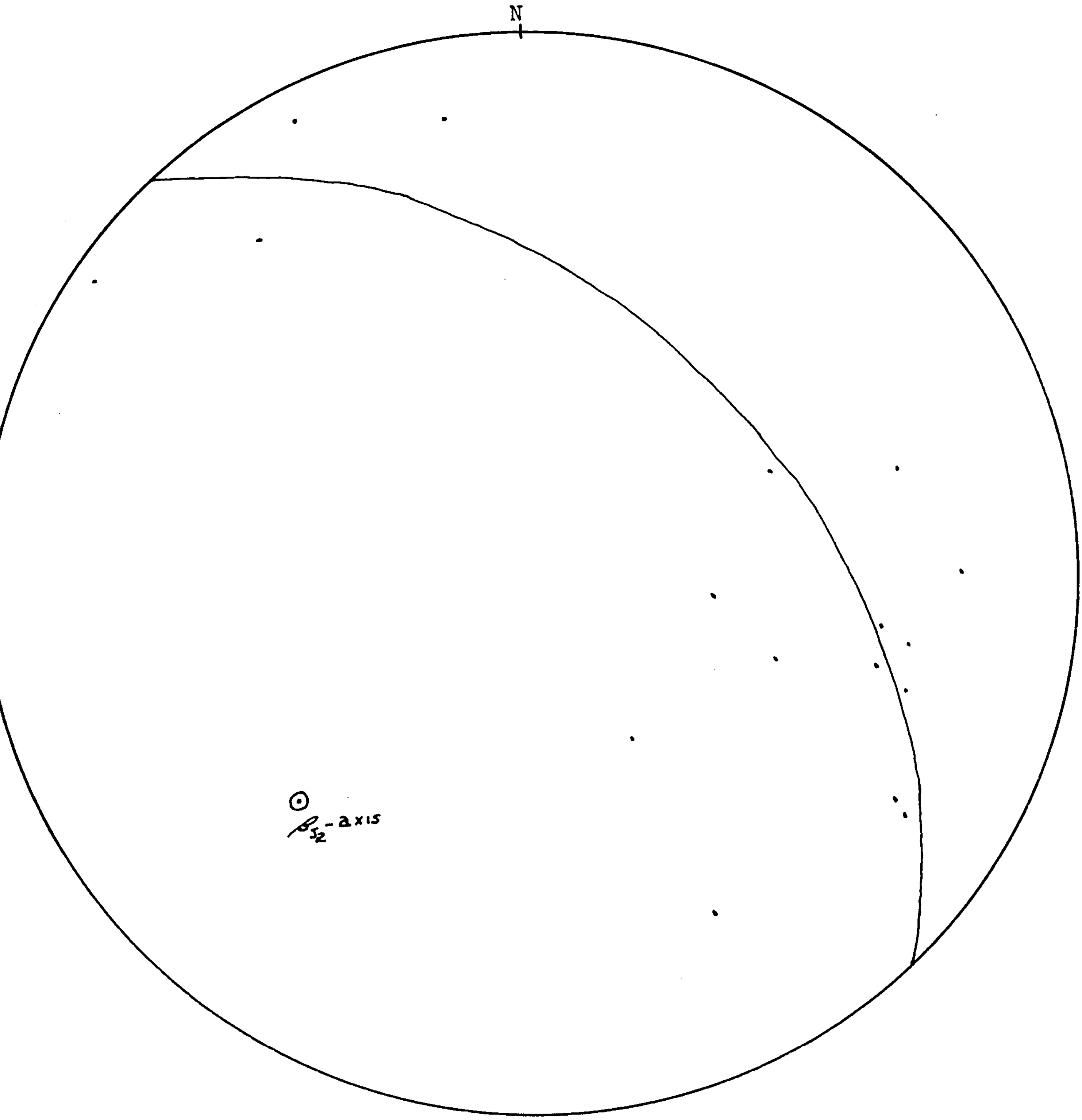

Macroscopic:

Three macroscopic subareas have been constructed by combining stations homogeneous with respect to S_2. Although S_1 and S_2 are not separated at Structure Stations 6, 7, 8 and 9, these stations are included in Subarea 3. The pattern at these stations suggests S_2 orientations similar to the attitude at Stations 10 and 12. Map 3a shows the subareas and corresponding uncontoured diagrams.

SUBAREA 1

General Statement

This subarea is equivalent to Structure Station 2.

SUBAREA 1.

6 S_2 Measurements

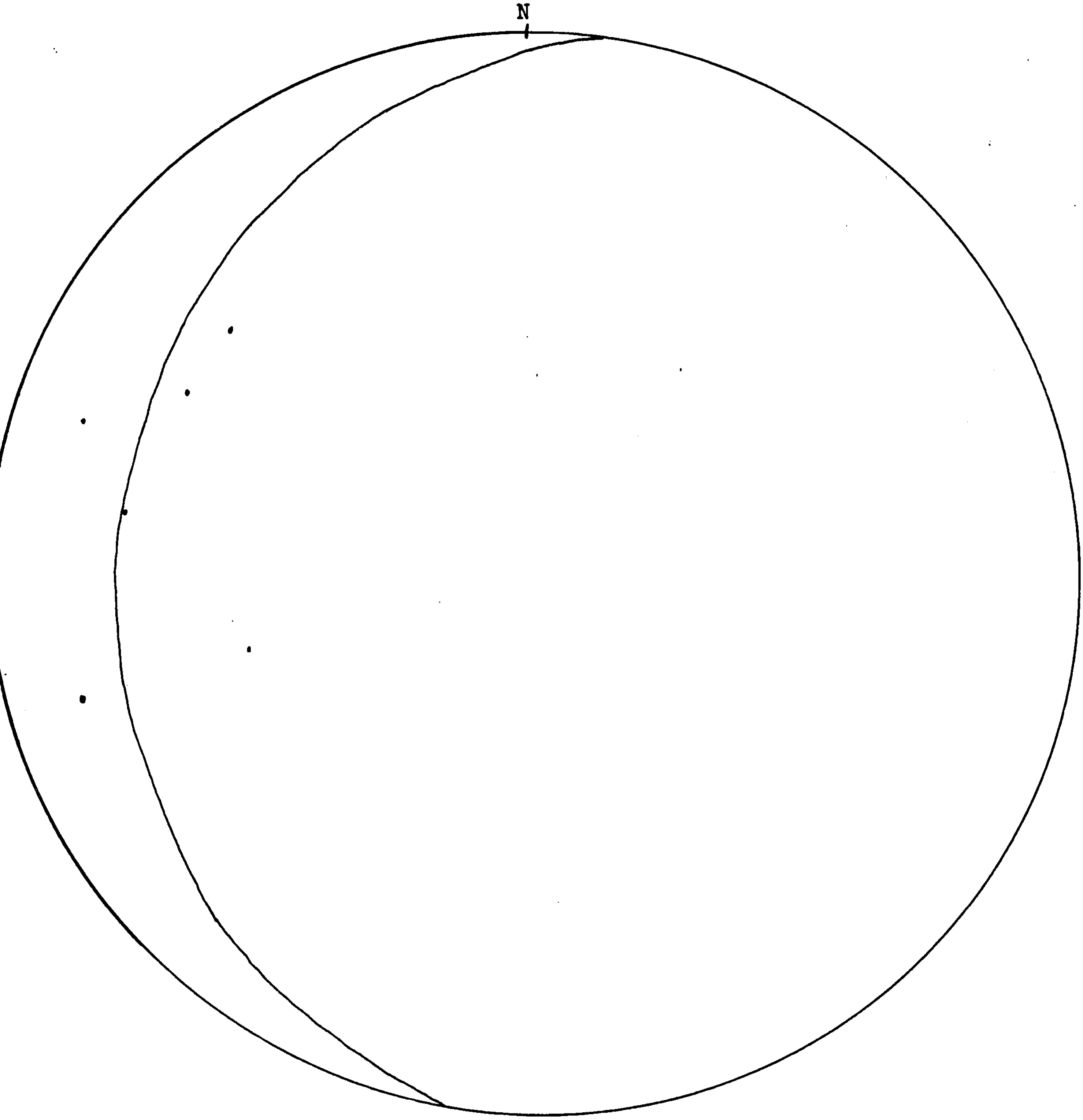

SUBAREA 2

General Statement

Location - Nose of Quad Creek synform (Map 3a).

Areal Extent - Approximately 0.08 square miles.

Number of Measurements - 9 S_2 measurements, 3 of which were taken from specimens showing refolding of F_1 by F_2.

Rock Types - Quartzite, migmatites and para-amphibolite.

Geologists - L.C. Rowan and C.E. Larsen.

Geometrical Analysis

Symmetry - Axial.

Scale - Macroscopic.

Homogeneity - Homogeneous with respect to S_2.

Maximum - (a). N10W, 60°NW.

Fold Geometry - In general, a point maximum is formed by the S_2 poles. The greatest dispersion is in the dip of the planes. This may be due to the prxomity of the meta-norite body.

SUBAREA 2.

9 S_2 Measurements

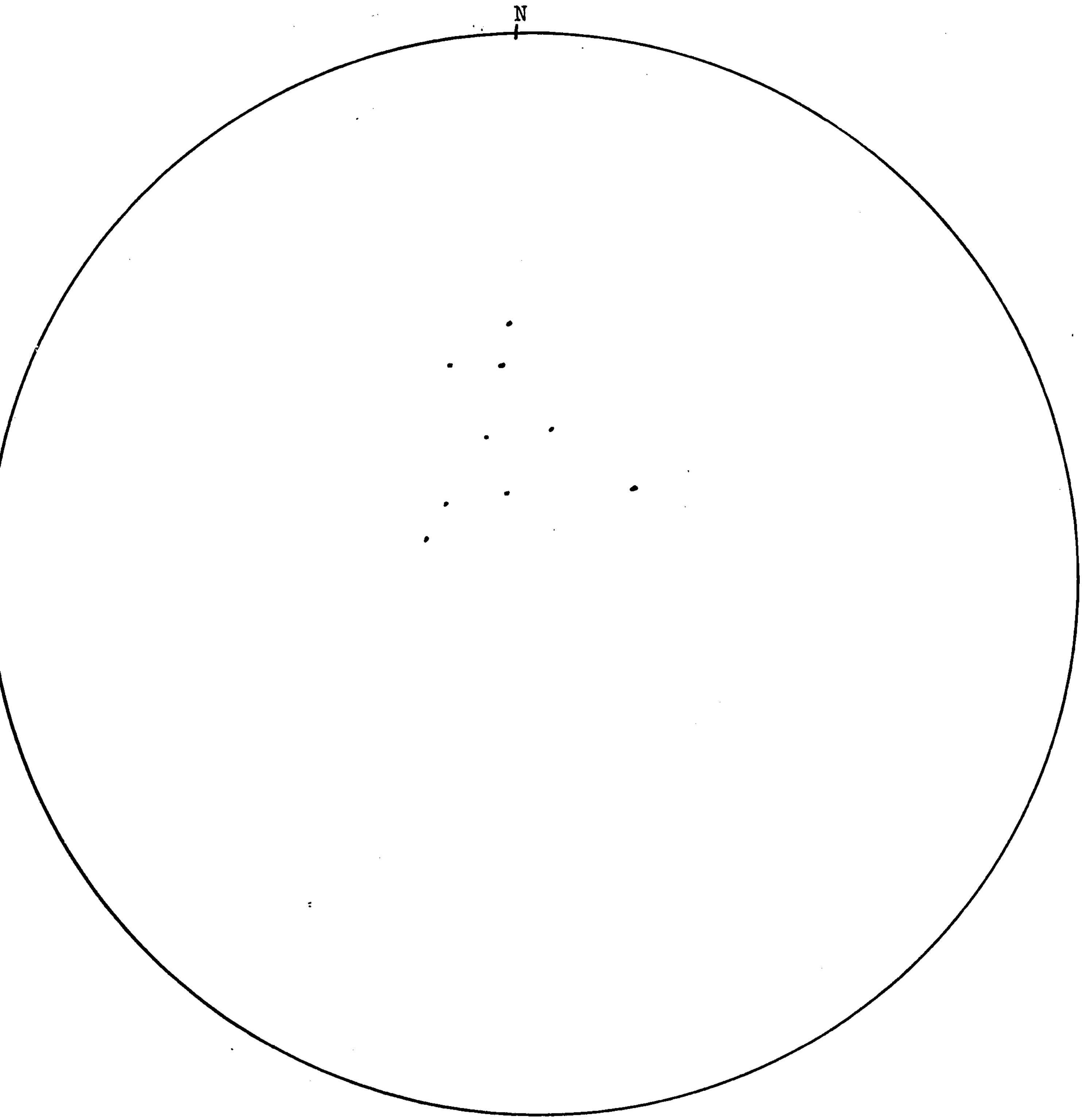

SUBAREA 3

General Statement

Location - Wyoming Creek antiform (Map 3a).

Areal Extent - Approximately 1.1 square miles.

Number of Measurements - 25 S_2 measurements.

Rock Types - Pink migmatite, quartzites and para-amphibolite.

Geologists - L.C. Rowan and C.E. Larsen.

Geometrical Analysis

Symmetry - Monoclinic.

Scale - Macroscopic.

Homogeneity - Homogeneous with respect to S_2.

πS_2-girdle - Does not seem justified, but would agree with the Station 12 πS_2-girdle.

βS_2-axis - See above.

Reliability - Poor.

Fold Geometry - S_2, as well as B_2, show that F_2 folds are slightly non-cylindrical and non-plane. However, πS_2-girdles are poorly defined. This F_2 geometry may be due to slight triaxial strain during F_2 folding in the Wyoming Creek antiform or to a deformation later than F_2.

SUBAREA 3.

25 S_2 Measurements

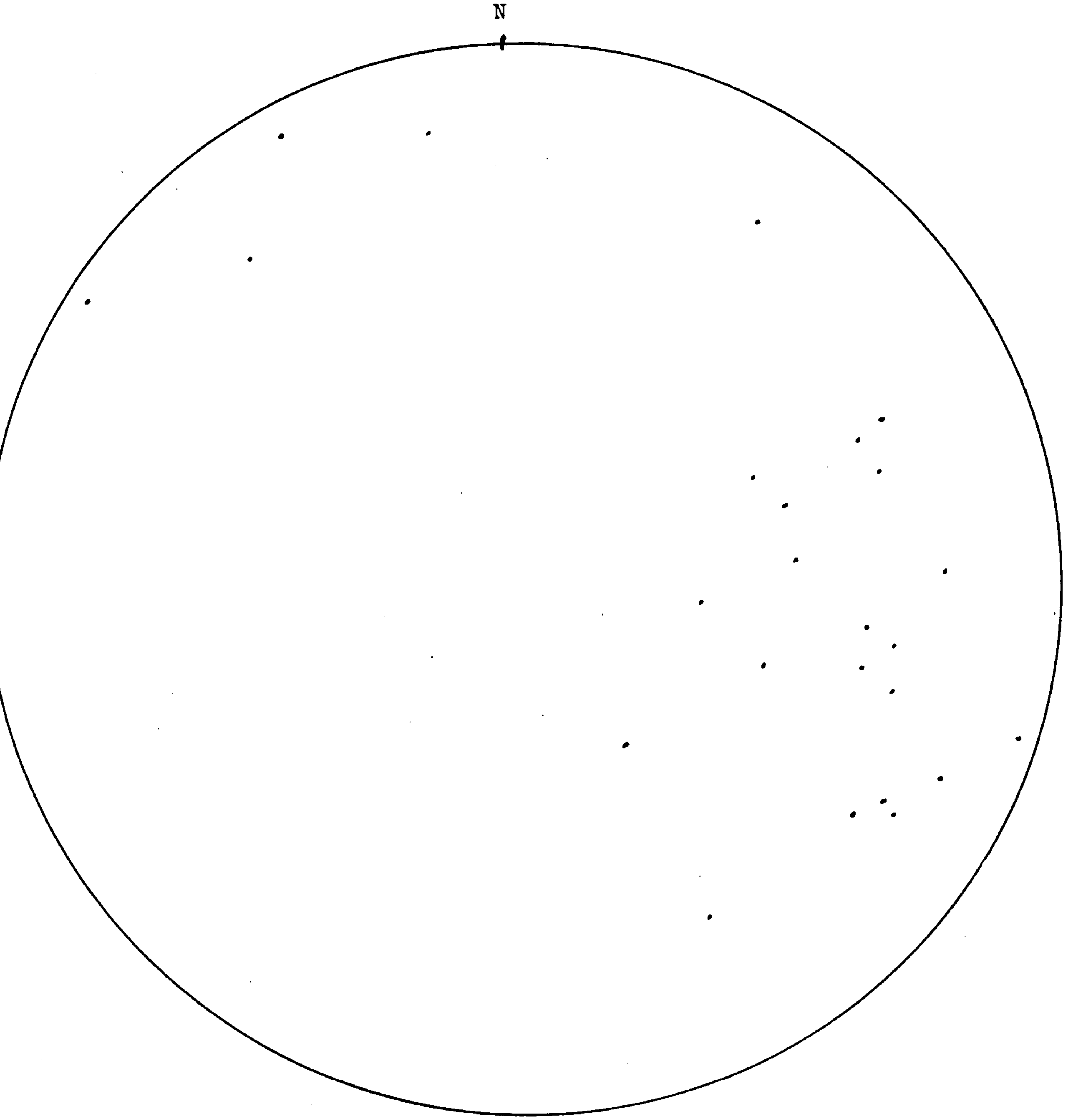

SUMMARY

<u>S_2-subfabric</u> - S_2 measurements are sparse at most stations and are absent in areas where F_1 and F_2 have not been separated. Although S_2 is somewhat dispersed in Subarea 3, the subfabric does not suggest rotation around the Wyoming Creek antiform nose. The writer believes that these F_2 folds are parasitically related to the large SW plunging antiform. The dispersion of S_2 data is attributed to triaxial strain, rather than to a later deformation.

S_2 rotates around the Quad Creek synform nose, suggesting that this major fold is younger than F_2 folds. However, the buttressing effect of the metanorite body is believed to have produced sufficient north directed stress to cause this local change in orientation of small F_2 folds. S_2 is nearly recumbent to the north at Station 5. This is believed to be due to buttressing of the metanorite and not to intrusion of the body. However, the βS_1-axis probably approximates the true Quad Creek synform axial attitude (Fig. 32).

Axial plane foliation (S_2) has developed locally, especially in migmatites of the Quad Creek synform flanks. It has not been detected in the quartzites here, but is well illustrated in quartzites from the Quad Creek synform nose (Fig. 19). The $S_2 \wedge S_0$ angle does not appear to exceed 10°-15°.

APPENDIX IV

B_1-subfabric

<u>Mesoscopic</u>:

B_1 measurements are fold axes and hinge lines of small, isoclinal F_1 folds, numbering from 13 at Station 8 to 36 at Station 12. Contoured diagrams are keyed to the corresponding structure stations on Map 2b. It must be emphasized that both B_1 and B_2 measurements are included at Structure Stations 6, 7, 8 and 9, since F_1 and F_2 are not separated in these sub-domains.

(1). folding of B_1 by later "concentric" folds (F_3),

(2). B_1 being non-rectilinear prior to F_2, or

(3). F_2 folds are dominantly "similar" but some are relatively "concentric".

Preferred Interpretation - Although alternative 2 is difficult to discount, the following points appear to indicate a small deviation from rectilinearity;

(a). L_1 and B_1 show nearly parallel orientations at most of the other structure stations (4, 5, 6, 7, 8, 9 and 12).

(b). The B_1-subfabric pattern is very consistent with respect to girdle types and does not suggest a random orientation of B_1 prior to F_2 folding.

The most acceptable interpretation is one which combines alternatives 1 and 3, since

(a). although F_2 is dominantly "similar" at this station, a few folds (F_2) have been observed in the field which were somewhat "concentric", and

(b). open folds (F_2) plunging steeply east are suggested by the S_0-subfabric (Map 2a). However, these cross-warps may be due to superposition of F_2 on F_1, rather than being a distinct fold set. S_2 data are dispersed at this station, suggesting that F_2 folds are non-cylindrical and non-plane. This may be a manifestation of triaxial strain or an F_3 deformation.

STRUCTURE STATION 1

General Statement

Location - West flank of Quad Creek synform (Map 2b).

Areal Extent - Approximately 50,000 sq. yds.

Number of Measurements - 30 B_1 measurements.

Rock Types - Pink biotite migmatite and biotite schist.

Geologists - L.C. Rowan and C.E. Larsen.

Geometrical Analysis

Symmetry - Generally monoclinic - triclinic in detail.

Scale - Mesoscopic.

Homogeneity - Nearly homogeneous with respect to B_1.

B_1-girdle - (a): N18W, 80°NE.

Reliability-(a)-Fair.

Maximum -(a).N5E, 70°N.

Fold Geometry - Ramsay (1960, pp.75-93) has shown that earlier, rectilinear lineations are deformed into partial small circles on equal area projections by "concentric" folds. "Similar" folding disperses these lineations into partial great circles. The great circle B_1-girdle is prominent, suggesting folding (F_2) of B_1 by nearly "similar" folds. Deviation from the constructed B_1-girdle may be explained by

STRUCTURE STATION 1.

30 B_1 Measurements
Contour Interval: 1-5-10%

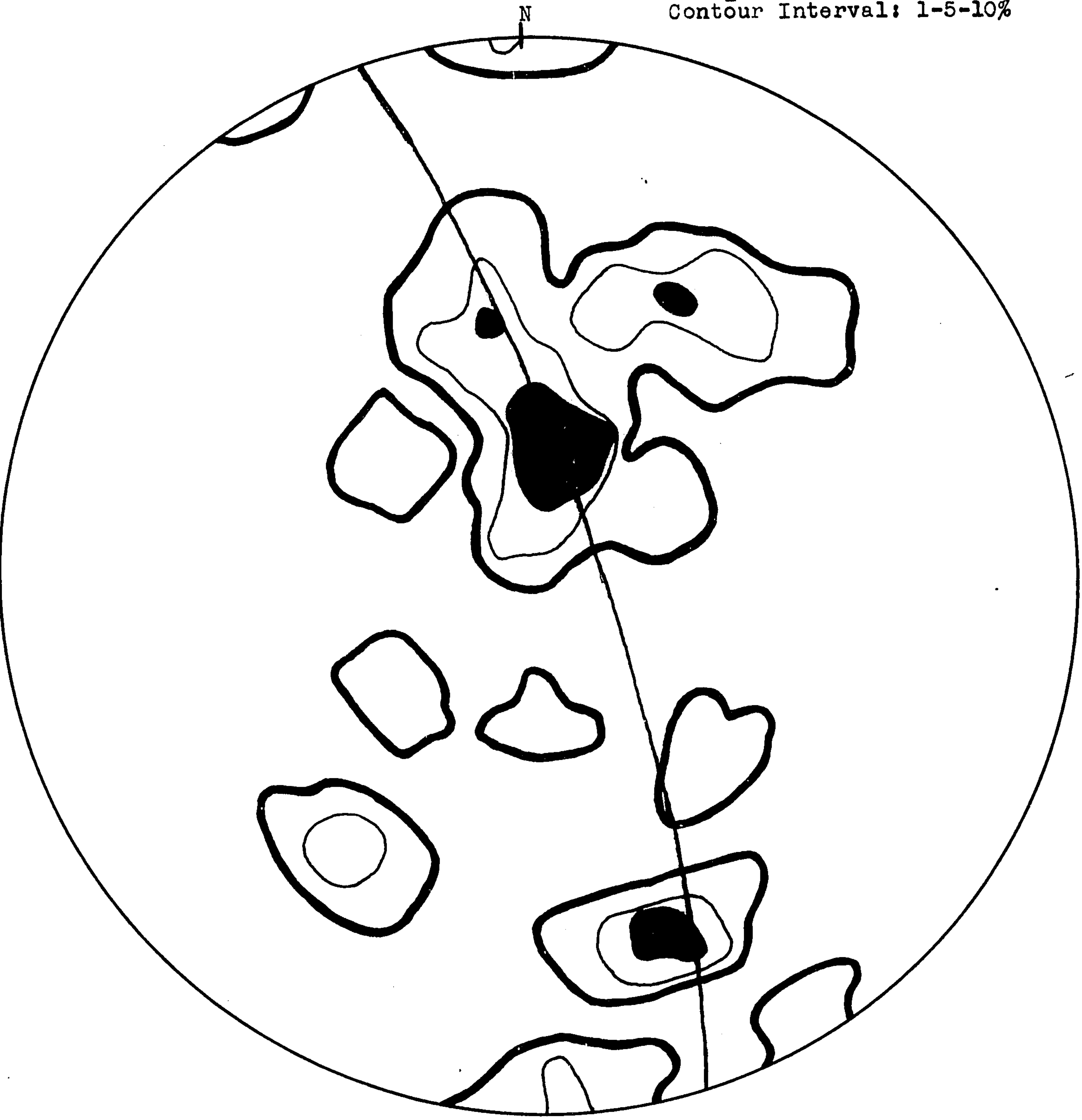

1). Folding of B_1 by both nearly "concentric" and "similar" folds (F_2) which plunge gently south or north (Map 2b, B_2). B_1 are rectilinear prior to F_2.

2). Gentle warping of B_1 and B_2 by nearly "concentric" F_2 folds plunging steeply east (See Map 2a, π S_1-girdle). S_2 (Map 2a) suggests the existence of very open F_2 folds also. The origin of these folds is somewhat problematical. They may be due to triaxial strain during F_2 folding or to a later deformation. The writer prefers the former alternative.

STRUCTURE STATION 2

General Statement

Location - Northeast portion of Quad Creek nose (Map 2b).

Areal Extent - Approximately 1000 sq yds.

Number of Measurements - 20 B_1 measurements.

Rock Types - Pink migmatites and para-amphibolite.

Geologists - L.C. Rowan and C.E. Larsen.

Geometrical Analysis

Symmetry - Monoclinic.

Scale - Mesoscopic.

Homogeneity - Homogeneous with respect to B_1.

B_1-girdle - (a). N6E, 70°E.

Reliability- (a). Fair.

Maxima - (a). N25E, 48°NE ; (b). S6E, 58°S.

Fold Geometry - The B_1-girdle is not well-defined, and there is a suggestion of dispersion of B_1 into a curviplanar surface which approaches a small circle. For this reason, F_2 appears to be transitional between "concentric" and "similar" folds (Ramsay, 1960, p.92), or folds of both types exist. Later (F_2) "concentric" folds may explain the suggested small circle girdles also.

Preferred Interpretation - The writer prefers the following interpretation;

STRUCTURE STATION 2.

20 B_1 Measurements
Contour Interval: 1-5-10%

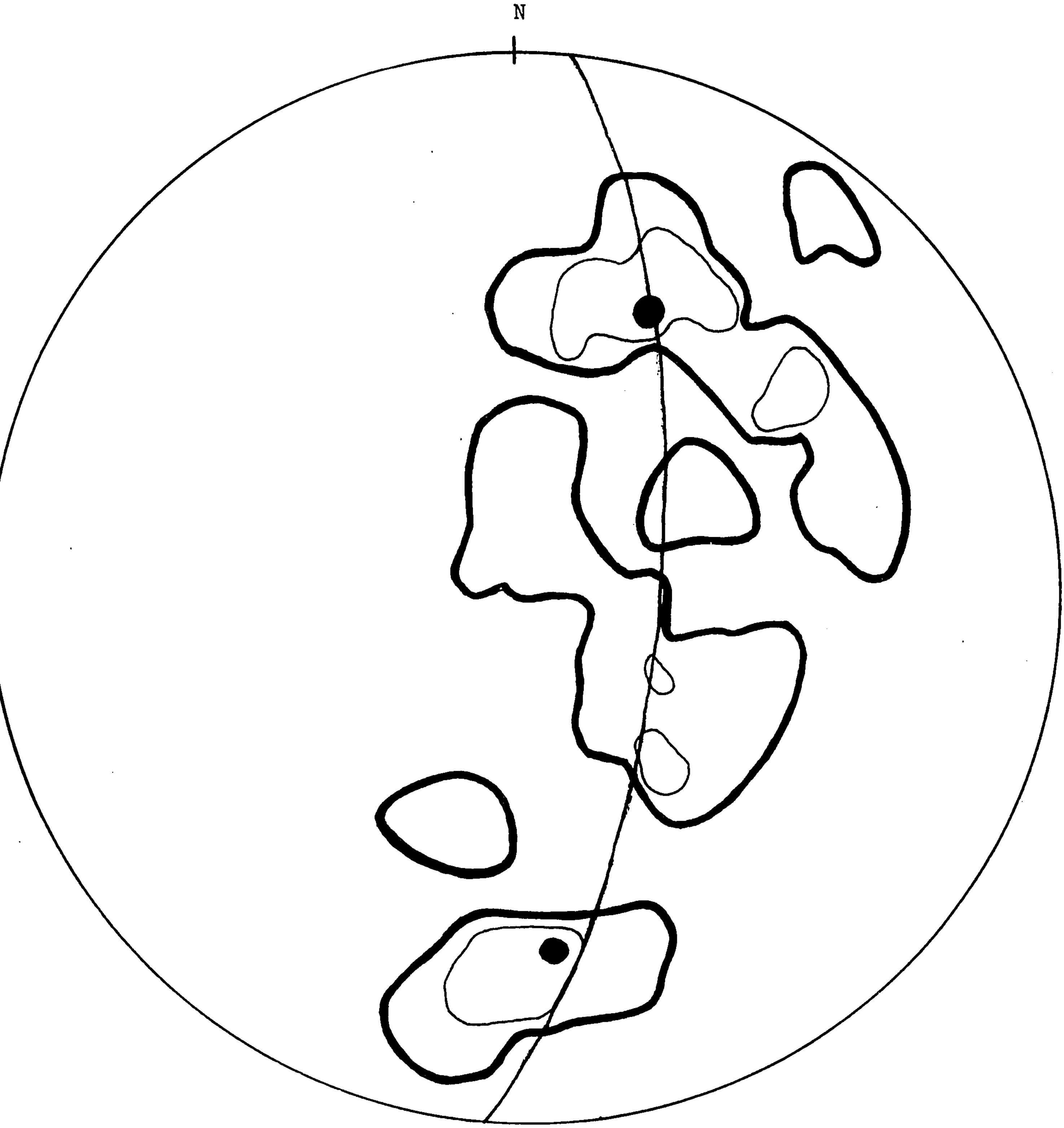

<u>Preferred Interpretation</u> - The writer prefers the F_2 geometry outlined above in alternative 2 because,

1). Although F_2 is generally "concentric" in the less ductile quartzites, it is "similar" in the migmatites.

2). Alternative 1 is discounted, since B_1 and L_1 are nearly coincident at most of the other structure stations (4, 5, 6, 7, 8, 9 and 12).

STRUCTURE STATION 3

General Statement

Location - Nose of Quad Creek synform (Map 2b).

Areal Extent - Approximately 1000 sq. yds.

Number of Measurements - 27 B_1 measurements.

Rock Types - Quartzites and migmatites.

Geologists - L.C. Rowan and C.E. Larsen.

Geometrical Analysis

Symmetry - Nearly monoclinic; tirclinic in detail.

Scale - Mesoscopic.

Homogeneity - Nearly homogeneous with respect to B_1.

B_1-girdle - (a). N30W, 20°SW; small circle suggested also.

Reliability- (a). Good.

Maxima - (a). S84W, 20°W; (b). S38W, 30°SW.

Fold Geometry - The partial small circle suggests folding of B_1 by nearly "concentric" folds (Ramsay, 1960, p.76-77). The angle B_2 (Map 2b) B_1 is not constant; therefore, F_2 cannot be truly "concentric" (Ramsay, 1960, p.77). Deviation from the partial small circle may be due to;

1). B_1 was not rectilinear prior to F_2, or

2). F_2 is both "similar" and "concentric" (Ramsay, 1960, p.92).

STRUCTURE STATION 3.

27 B_1 Measurements
Contour Interval: 1-5-10%

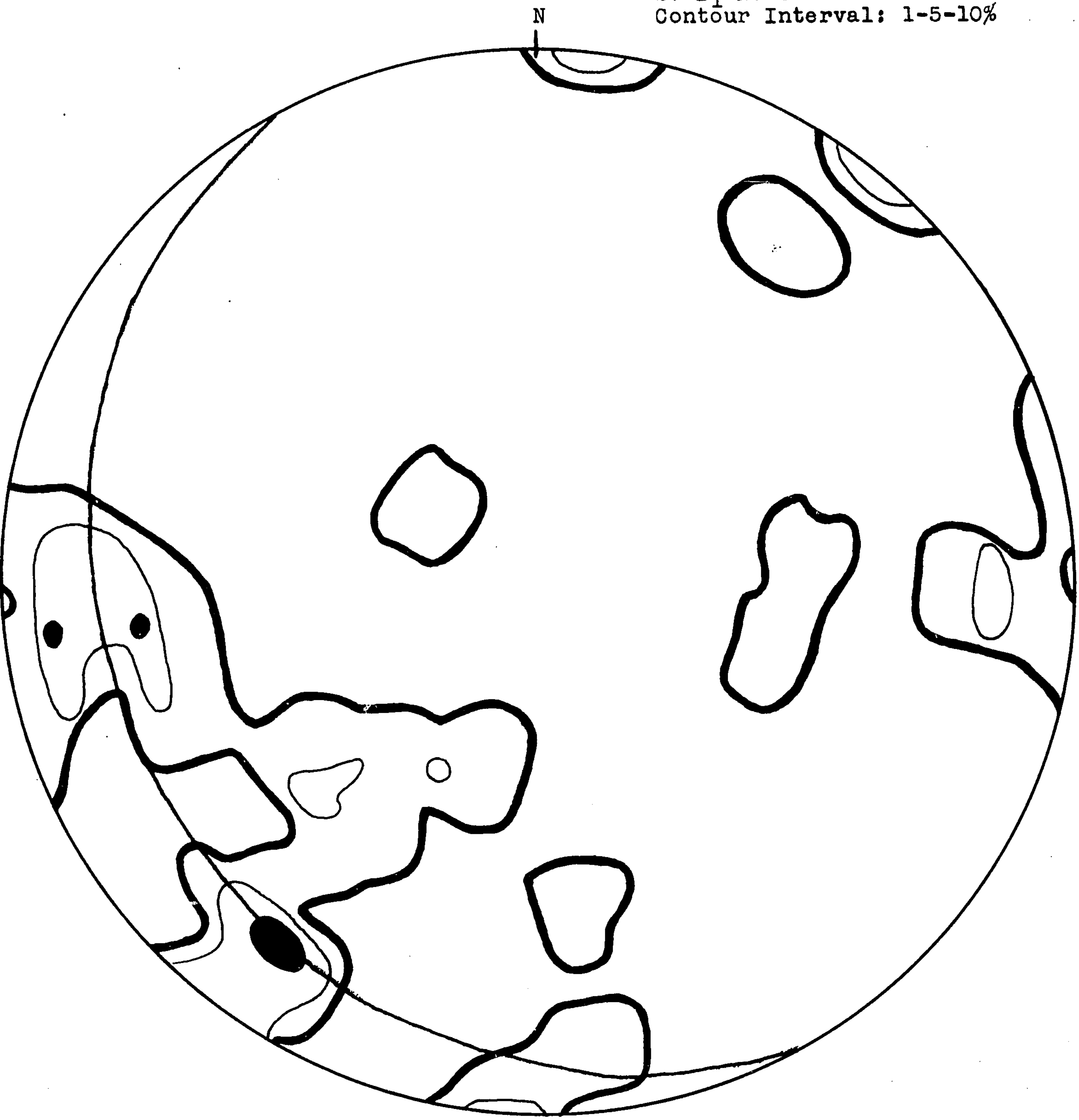

4). Maxima plunge moderately west, whereas they plunge dominantly N-NE at Stations 1 and 2.

These geometric features suggest that B_1 has been deformed by nearly "concentric" folds (F_2). However, number 2 precludes the possibility that these F_2 folds are truly "concentric" (Ramsay, 1960, pp.76-77). Deviations of B_1 from a partial small circle or a great circle may be explained by

(1). F_2 being both "similar" and "concentric" in this sub-domain (Ramsay, 1960, p.92, Table no.5), or

(2). B_1 being non-rectilinear prior to F_2 folding.

<u>Preferred Interpretation</u> - The writer prefers alternative 1, because F_2 folds are frequently "concentric" and "similar" in these rock types. Although the rocks are dominantly para-amphibolite, some layers appear to be more ductile than others. The writer believes that is due to mineralogical differences.

STRUCTURE STATION 4

General Statement

Location - Northeast portion of Quad Creek synform nose (Map 2b).

Areal Extent - Approximately 1000 sq. yds.

Number of Measurements - 20 B_1 measurements.

Rock Type - Para-amphibolite.

Geologists - L.C. Rowan and C.E. Larsen.

Geometrical Analysis

Symmetry - Monoclinic.

Scale - Mesoscopic.

Homogeneity - Homogeneous with respect to B_1.

B_1-girdle - (a). N20W, 45°SW - small circle B_1-girdle suggested also

Reliability- (a). Good.

Maximum - (a). N80W, 40°NW.

Fold Geometry - Several features are important regarding F_2 fold geometry at this station and numbers 3 and 5;

1). B_1 is not rectilinear on the mesoscopic scale,

2). $B_1 \wedge B_2$ is not constant,

3). A partial small circle girdle is strongly suggested, and

STRUCTURE STATION 4.

20 B1 Measurements
Contour Interval: 1-5-9-13-17%

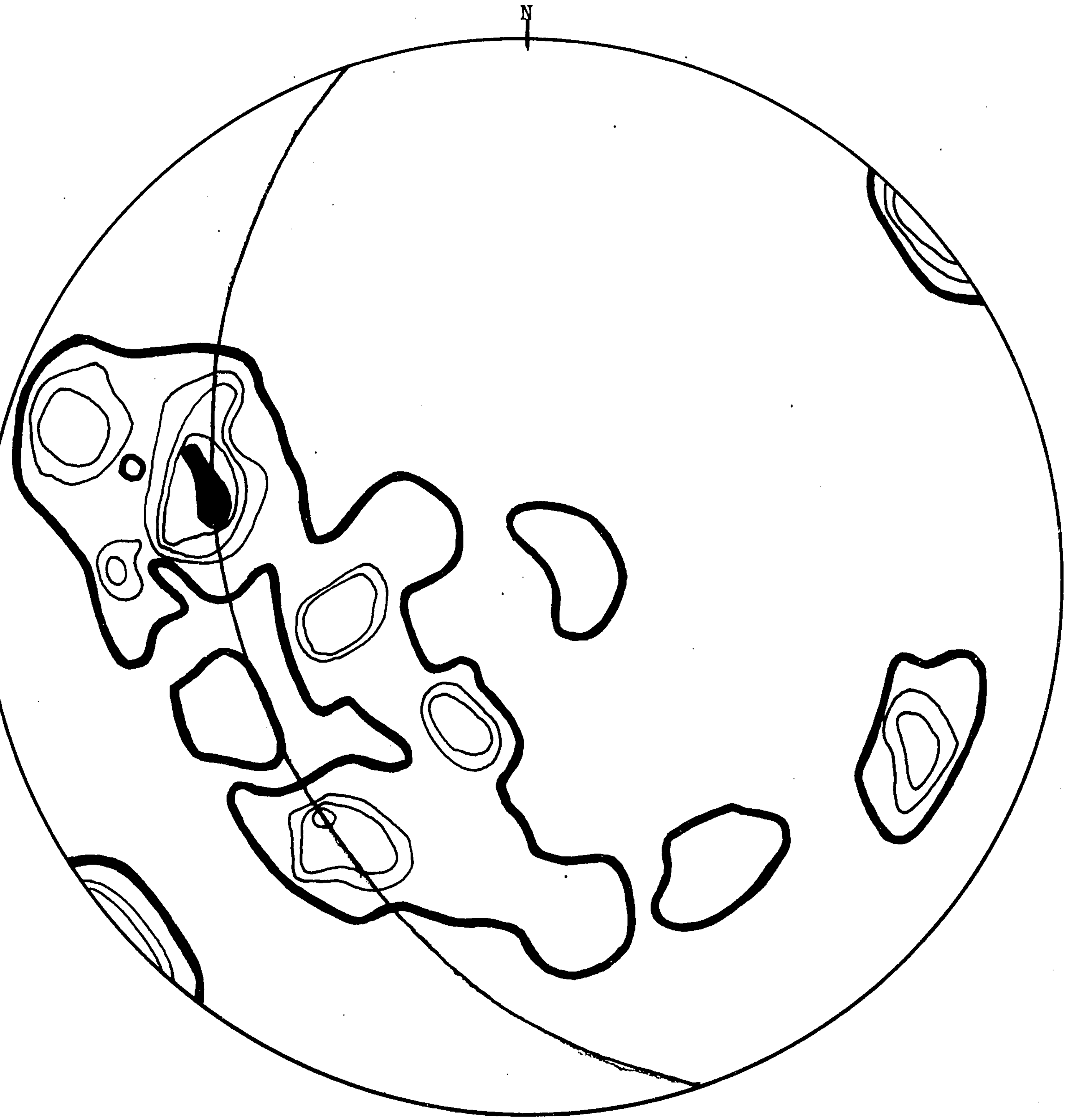

linear in this relatively small sub-domain. Since F_2 is known by field observations to be more nearly "concentric" than "similar" in style, the writer concludes that B_1 is folded in a few instances (Text Figure 23) by folds (F_2) possessing a slightly "concentric" shape.

STRUCTURE STATION 5

General Statement

Location - Northeast portion of the Quad Creek synform nose (Map 2b).

Areal Extent - Approximately 100 sq. yds.

Number of Measurements - 22 B_1 measurements.

Rock Types - Quartzites.

Geologists - L.C. Rowan and C.E. Larsen.

Geometrical Analysis

Symmetry - Monoclinic.

Scale - Mesoscopic.

Homogeneity - Homogeneous with respect to B_1.

B_1-girdle - (a). N18E, 40°NW.

Reliability- (a)-Good.

Maximum - (a). N75W, 42°NW.

Fold Geometry - Although a great circle B_1-girdle has been constructed, the pattern approaches a partial cone (partial small circle in projection). Ramsay (1960, p.77) has shown that this is characteristic of flexural folding. However, the maximum is quite intense, and the girdle is relatively incomplete.

Preferred Interpretation - B_1 appears to be nearly recti-

STRUCTURE STATION 5.

22 B_1 Measurements
Contour Interval: 1-5-10%

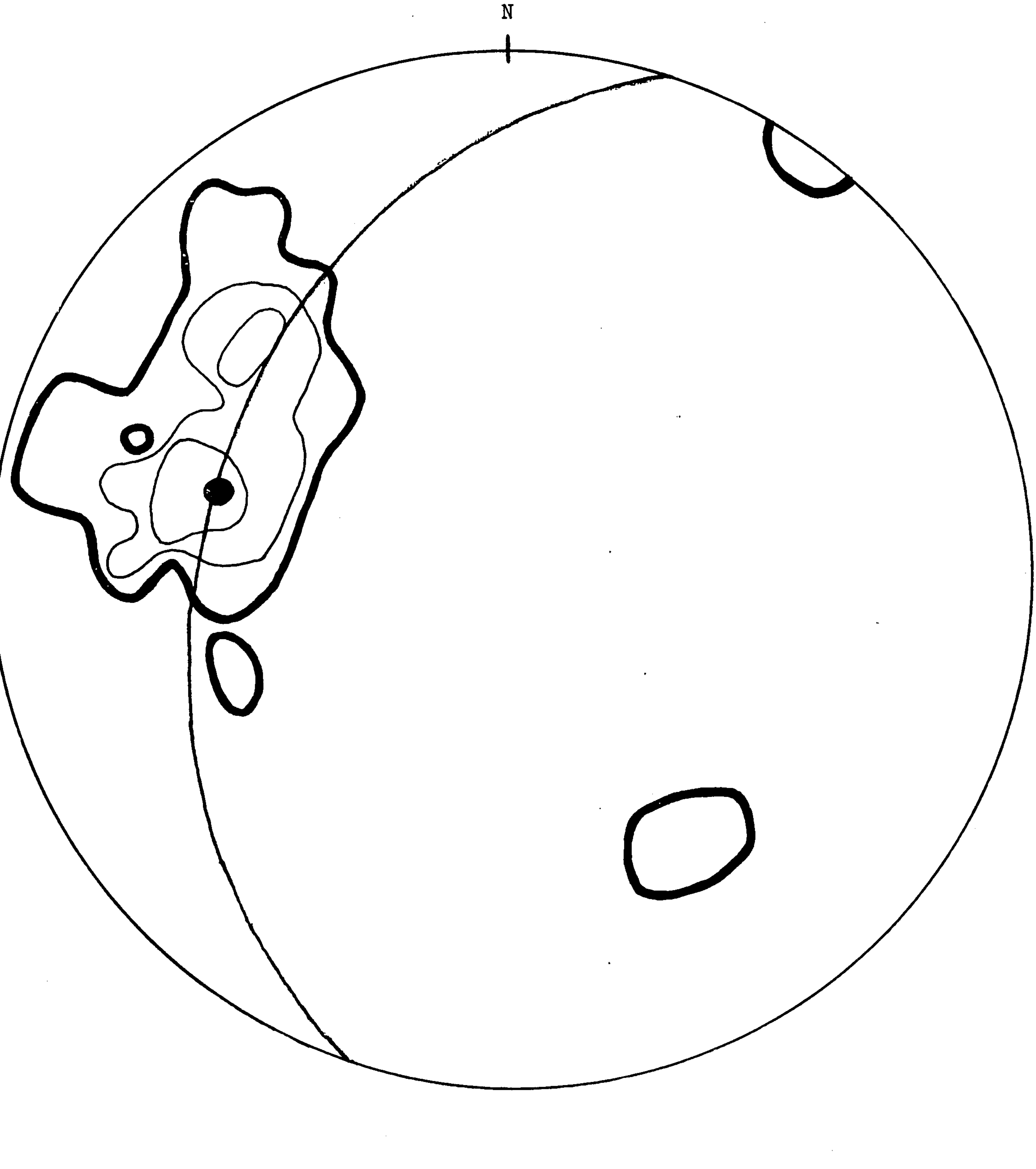

2). B_1 and B_2 are nearly parallel at these stations, although B_2 apparently plunges more steeply south than B_1.

3). F_1 and F_2 are highly appressed at these stations. F_1 is nearly destroyed in many cases, being expressed only as "hook" and "crescent" patterns (Carey, 1962, p.101).

The pattern suggests the following possible fold geometries;

1). B_1 is folded by nearly "concentric" folds (F_2).

2). B_1 is folded by "similar" folds (F_2) developing a B_1-girdle trending N-S and dipping nearly vertically. The dispersion of B_1 into the partial small circles may be due to;

a). B_1 was not rectilinear prior to F_2, or

b). later "concentric" cross-folds (F_2).

Preferred Interpretation - Since no F_2 "concentric" folds have been observed in the field, and there is a suggestion of a N-S partial great circle, the first alternative is not accepted by the writer. The existence of F_2 "similar" folds at this station is supported by the S_1- and S_o-sub-fabric. Later "concentric" cross-folds (F_2) probably correspond to the β S_{oa}-axis at this station, dispersing B_1 into partial small circles (b). These gentle, open cross-warps are probably due to triaxial strain during F_2 folding.

Note that B_1 and B_2 show about 90 degrees rotation from Stations 3, 4 and 5 to this station and that B_1 dips dominantly S, probably at a low angle.

STRUCTURE STATION 6

General Statement

Location - North portion of east flank of Quad Creek synform (Map 2b).

Areal Extent - Approximately 1500 sq. yds.

Number of Measurements - 42 B_1 and B_2 measurements.

Rock Types - Pink biotite migmatite.

Geologists - L.C. Rowan and C.E. Larsen.

Geometrical Analysis

Symmetry - Generally monoclinic; triclinic in detail.

Scale - Mesoscopic.

Homogeneity - Inhomogeneous with respect to B_1 and B_2.

B_1-girdle - (a). N38W, 40°W.

Reliability -(a)-Fair.

Maximum - (a). S21W, 34°SW.

Fold Geometry - The B_1-subfabric is complex at this station and resembles the patterns at other stations located in the Quad Creek synform flanks. It must be emphasized that B_1 and B_2 are not separable at Stations 6, 7, 8 and 9 because;

1). F_1 and F_2 are "similar" folds at these stations, so that no distinction based on fold style is applicable.

STRUCTURE STATION 6.

42 B_1 and B_2 Measurements
Contour Interval: 1-5-10-15%

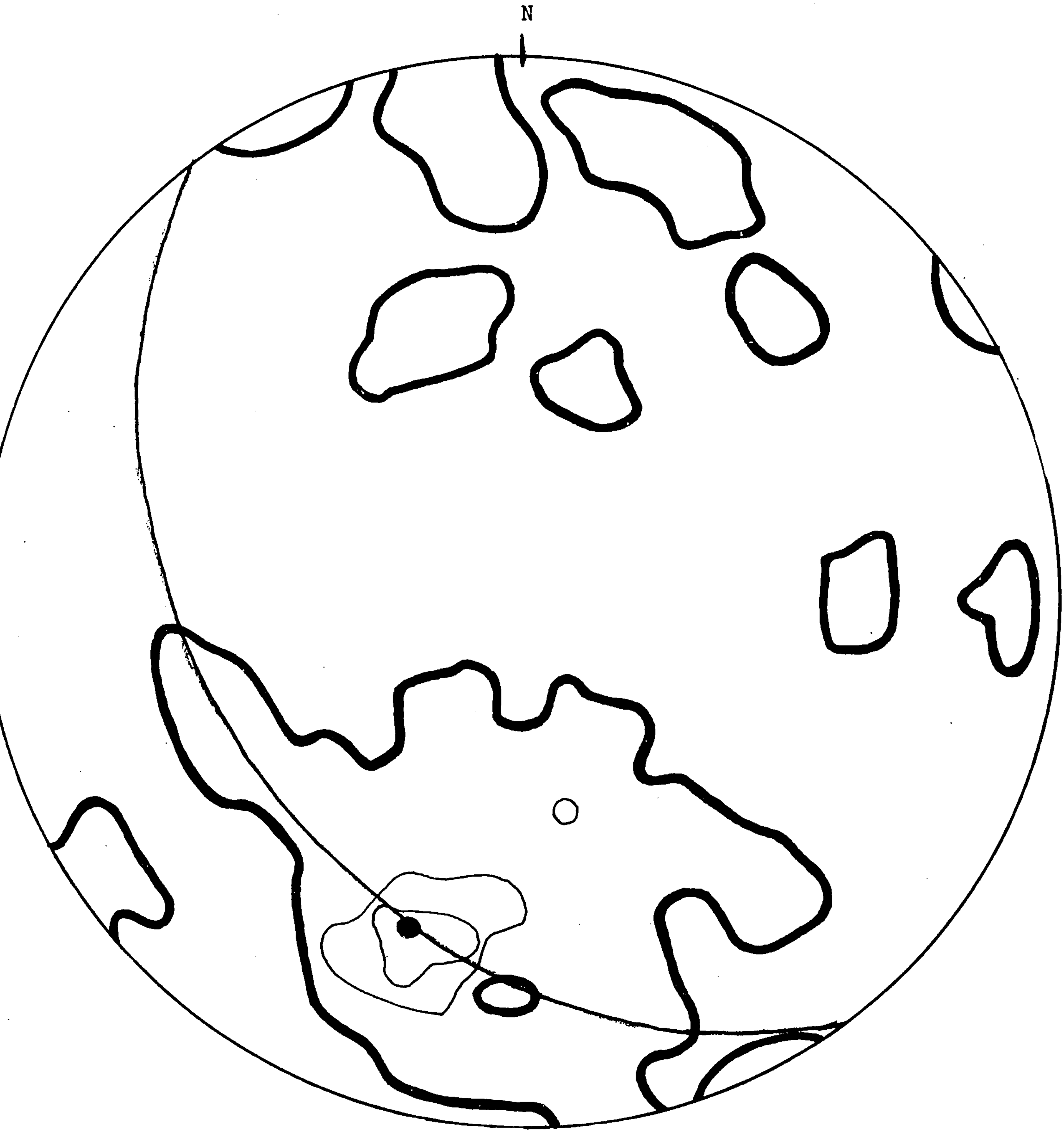

<u>Preferred Interpretation</u> - Alternative (b) is preferred by the writer, because open (F_2) folds are suggested by the S_o- and S_1-subfabrics at this station. Field observations do not suggest that F_2 folds are "concentric" at this station.

STRUCTURE STATION 7

General Statement

Location - East Quad Creek synform (Map 2b).

Areal Extent - Approximately 6,000 sq. yds.

Number of Measurements - 25 B_1 and B_2 measurements.

Rock Types - Pink biotite migmatite.

Geologists - L.C. Rowan and C.E. Larsen.

Geometrical Analysis

Symmetry - Monoclinic.

Scale - Mesoscopic.

Homogeneity - Homogeneous with respect to B_1 and B_2.

B_1-girdle - (a). N12E, 75°W.

Reliability- (a). Good.

Maximum - (a). S20W, 15°SW.

Fold Geometry - This B_1-subfabric pattern suggests folding of B_1 by "similar" folds (F_2) dispersing B_1 into a relatively complete great circle. The slight dispersion of B_1 into partial small circle girdles may be attributed to either;

(a). B_1 being non-rectilinear prior to F_2, or

(b). deformation of B_1 by late (F_2) "concentric" cross-folds.

STRUCTURE STATION 7.

25 B_1 and B_2 Measurements
Contour Interval: 1-5-10-15%

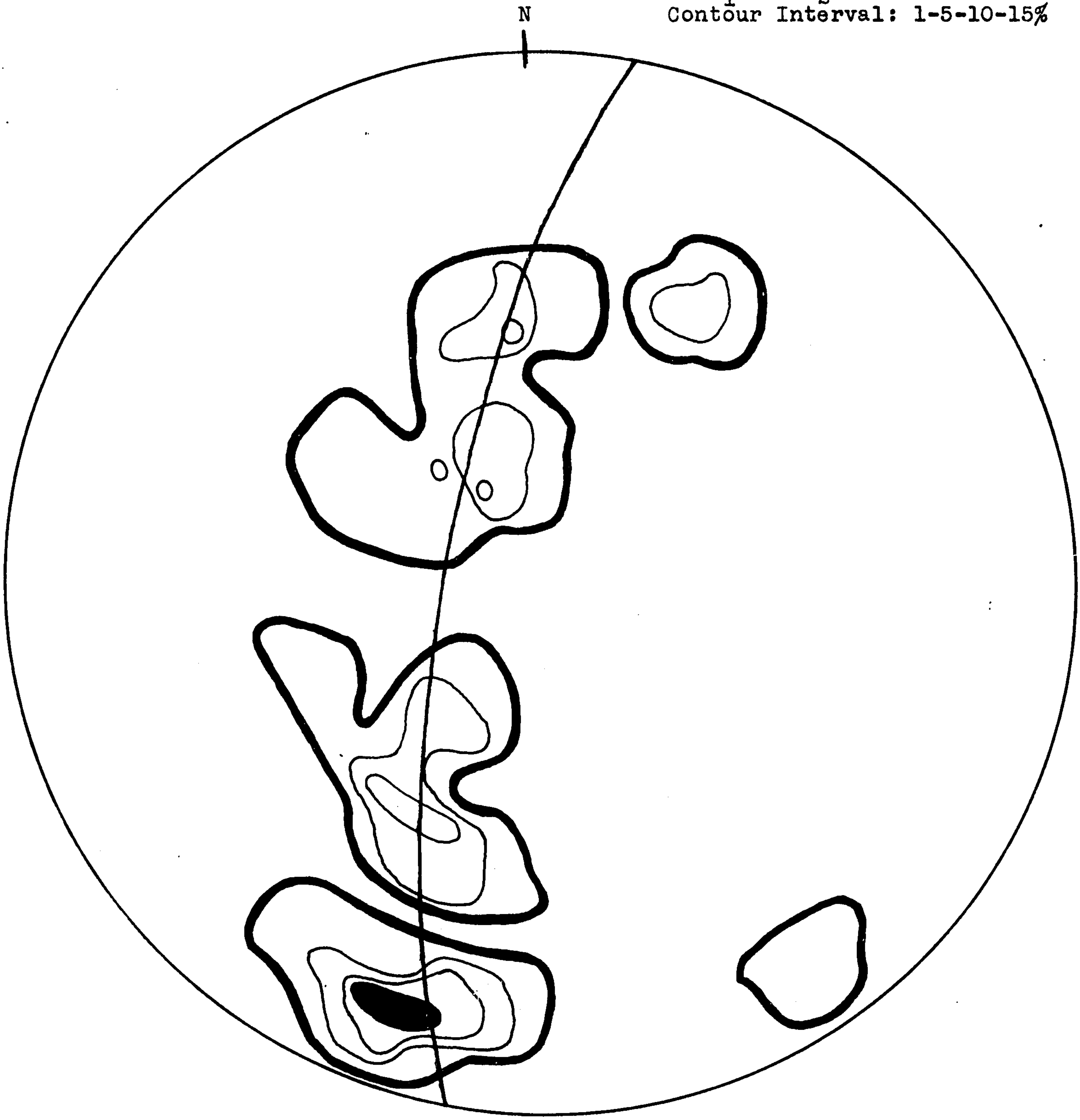

STRUCTURE STATION 8

Location - West flank of the Wyoming Creek antiform (Map 2b).

Areal Extent - Approximately 6,000 sq. yds.

Number of Measurements - 13 B_1 and B_2 measurements.

Rock Types - Pink biotite migmatite.

Geologists - L.C. Rowan and C.E. Larsen.

Geometrical Analysis

Symmetry - Monoclinic.

Scale - Mesoscopic.

Homogeneity - Homogeneous with respect to B_1 and B_2.

B_1-girdle - (a). N-S, 75°W.

Reliability- (a)-Fair.

Maximum - (a). Moderately to S-SW.

Fold Geometry - The sparse data suggest a N-S girdle dipping steeply west. The overall pattern is similar to the B_1-patterns at Stations 6, 7 and 9 and a similar interpretation appears to be justified.

STRUCTURE STATION 8.

13 B_1 and B_2 Measurements

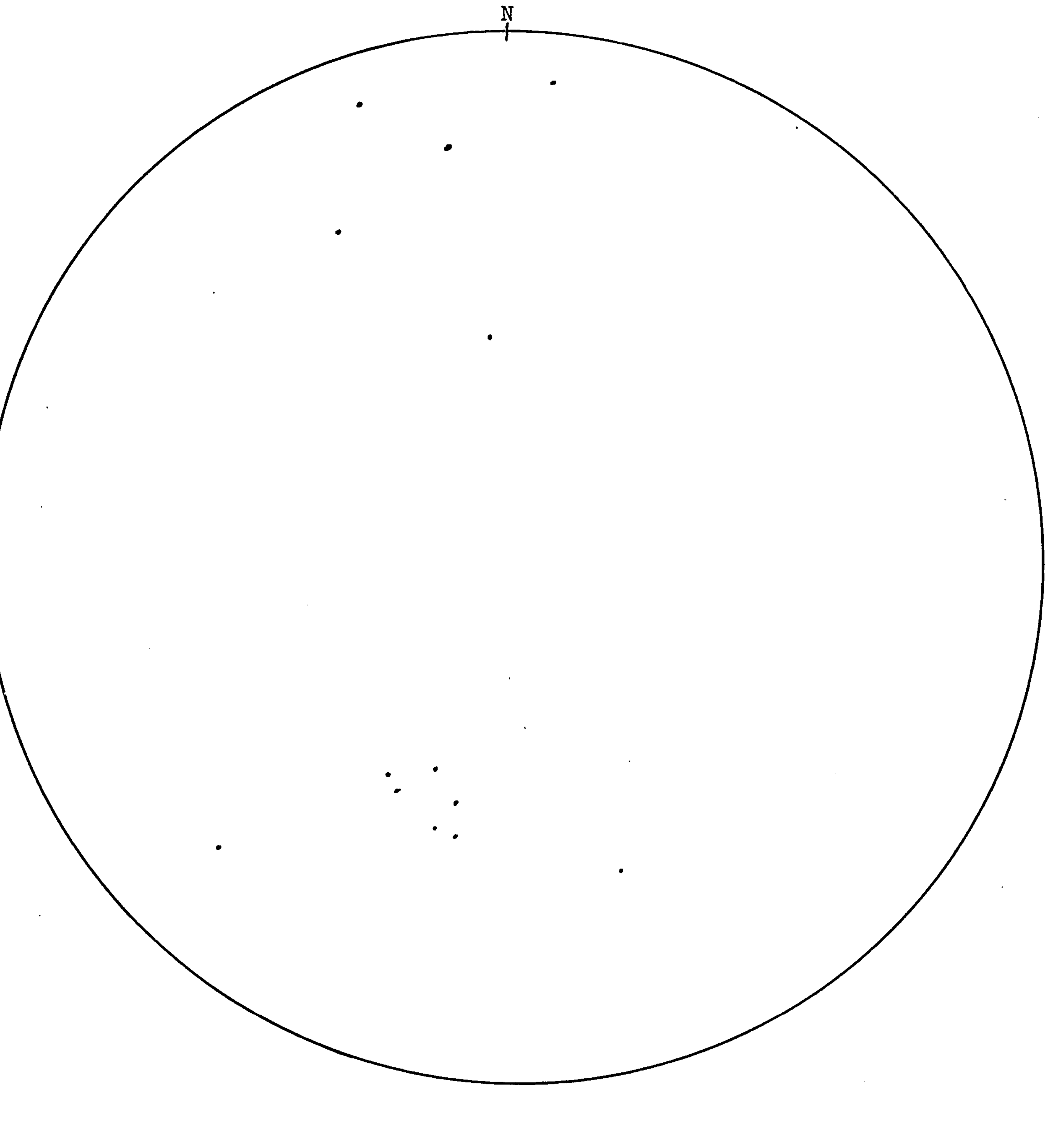

These folds (F_1) do not appear to be small folds related to the Wyoming Creek antiform because,

1). The corresponding axial planes, S_1, have been folded (Map 2a),

2). B_1 is dispersed into a great circle girdle, and

3). The trend of the Wyoming Creek antiform is N25°E, which does not correspond to the B_1 maximum at this station.

The dispersion of B_1 into a partial small circle girdle appears to be due to either;

(1). F_2 cross-folding of B_1 in a "concentric" manner, or

(2). coaxial folding of B_1 by F_2(about B_2) (Clifford, 1960, p.377, Fig. 9-D9).

<u>Preferred Interpretation</u> - No F_2 cross-folds have been definitely identified at this station. Coaxial folding of F_1 by F_2 folds is an adequate explanation. B_2 and βS_1-axes coincide reasonably well at this station. F_2 folds are not ideally "concentric" and are nearly "similar" frequently. Therefore, development of a well-defined partial great circle B_1-girdle is to be anticipated. For the same reason, the partial small circle will be poorly defined. Some of the dispersion may be due to the non-cylindrical nature of F_2 folds.

STRUCTURE STATION 9

General Statement

Location - Southwest portion of Wyoming Creek antiform nose (Map 2b).

Areal Extent - Approximately 14,000 sq. yds.

Number of Measurements - 44 B_1 and B_2 measurements.

Rock Types - Pink biotite migmatite, para-amphibolite and quartzites.

Geologists - L.C. Rowan and C.E. Larsen.

Geometrical Analysis

Symmetry - Monoclinic.

Scale - Mesoscopic.

Homogeneity - Homogeneous with respect to B_1 and B_2.

B_1-girdle - (a). N5W, 80°W.

Reliability - (a). Good.

Maximum - (a). S6W, 65°S.

Fold Geometry - The prominent maximum probably defines F_2 folds axes (B_2) which have not been separated from B_1 at this station. The B_1-girdle is well-defined and indicates folding of B_1 by "similar" folds (F_2). B_1 and B_2 appear to be nearly coaxial. The B_1-girdle shows about 5 degrees rotation from Station 8 to this station.

STRUCTURE STATION 9.

44 B_1 and B_2 Measurements
Contour Interval: 1-5-10-15-20%

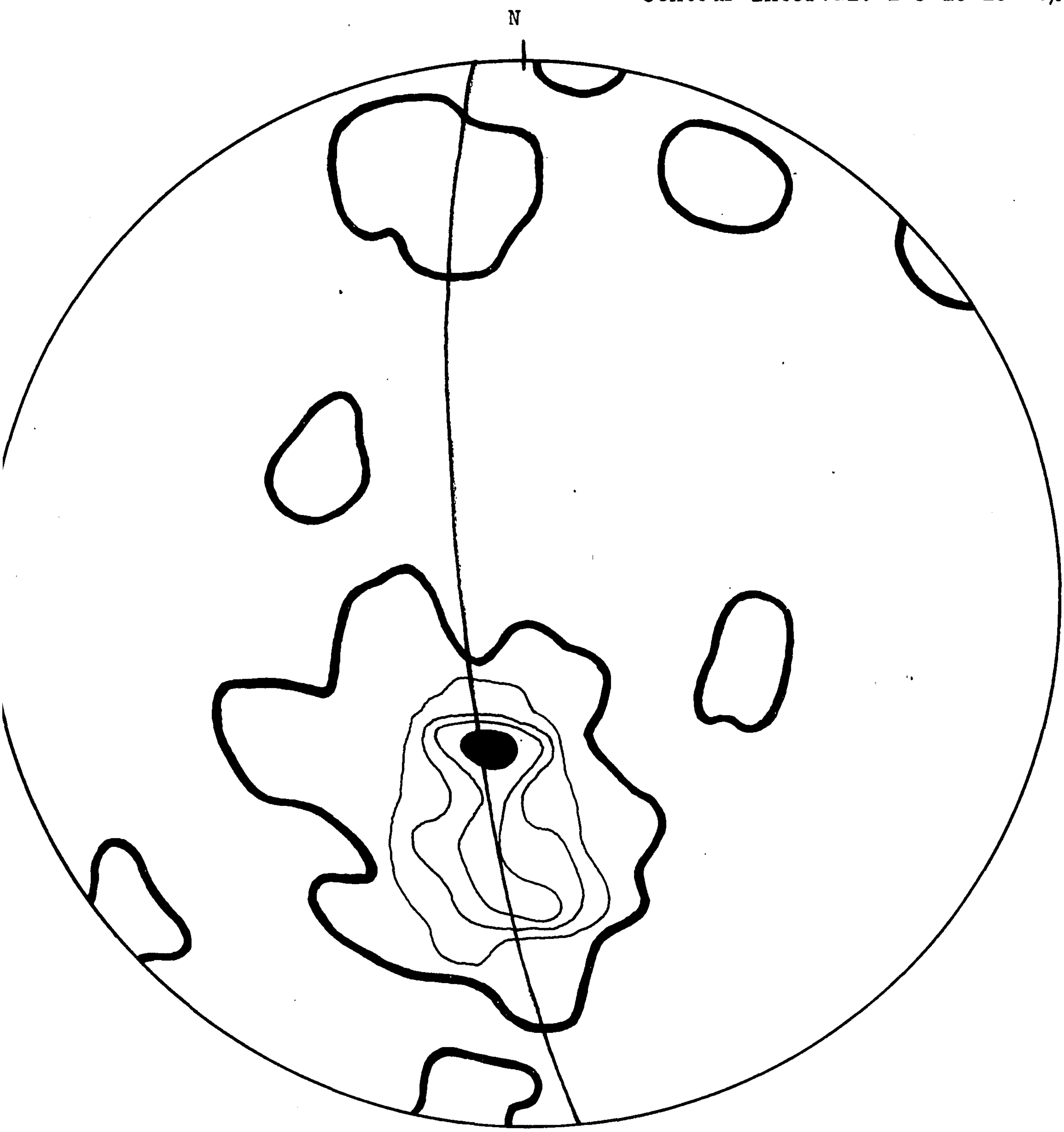

nearly coaxial at Station 10 (Clifford, 1960, p.377, Fig. 9-D9).

The pattern at this station suggests dispersion of B_1 into a plane approaching a partial small circle. This indicates that F_2 is somewhat "concentric" (Ramsay, 1960, pp.75-93), but "similar" F_2 folds have been observed here also. No folds later than F_2 have been identified in the field at this structure station.

STRUCTURE STATION 10

General Statement

Location - Southeast portion of Wyoming Creek antiform nose (Map 2b).

Areal Extent - Approximately 16,000 sq. yds.

Number of Measurements - 23 B_1 measurements.

Rock Types - Quartzites and pink biotite migmatite.

Geologists - L.C. Rowan and C.E. Larsen.

Geometrical Analysis

Symmetry - Triclinic.

Scale - Mesoscopic.

Homogeneity - Inhomogeneous with respect to B_1.

B_1-girdle - (a). N10W, 70°W.

Reliability-(a). Fair.

Maxima - (a). S35E, 54°SE; (b). S2W, 34°S.

Fold Geometry - This B_1-subfabric pattern resembles the patterns at Stations 6, 7, 8 and 9. Although the ill-defined B_1-girdle has rotated about 10° from Station 8 to this station, B_1 does not show the complete rotation around the nose of the major antiform as it does in the Quad Creek synform. B_1 does not diverge from this major axial zone as anticipated from the pattern at Stations 1, 2, 3, 4 and 5. Map 2a suggests that B_1 and B_2 are

STRUCTURE STATION 10.

23 B_1 Measurements
Contour Interval: 1-5-10%

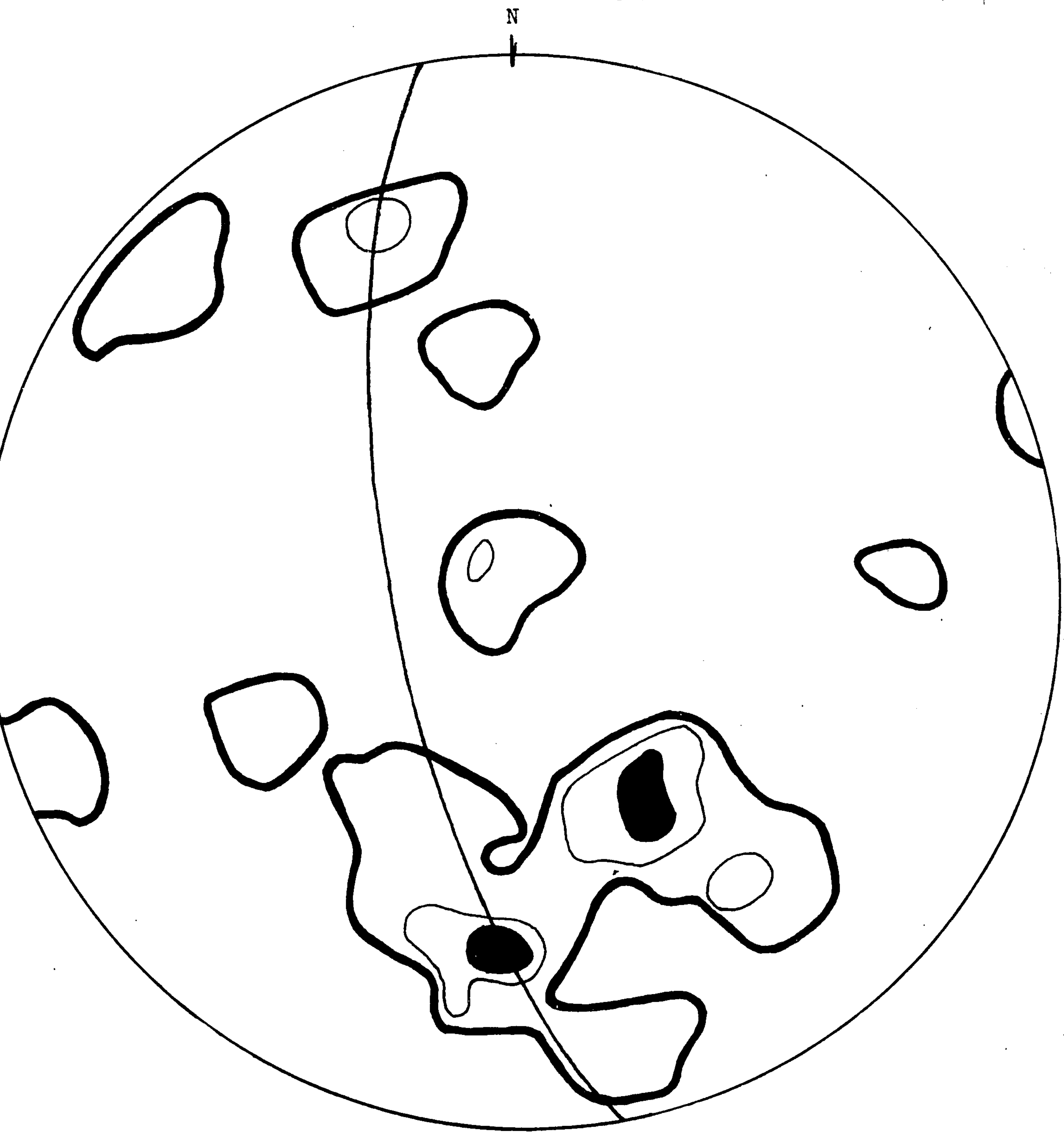

3). B_1 was not similarly oriented at these stations, prior to F_2. Note that B_1 and B_2 are nearly parallel at Stations 9, 10 and 12.

4). B_1 attained its orientation at Station 10 by internal rotation of F_1 due to transport of plastic material into the antiform nose during F_2 folding.

<u>Preferred Interpretation</u> - No evidence supports the existence of faults between these stations. On the other hand, agmatization is extensive in these sub-domains but does not seem adequate to explain 90° rotation. This relationship may be explained by passive flow F_1 folding in ductile layers between rigid quartzite and para-amphibolite plates if the area is assumed to be a B-tectonite. However, L_1 rotates around this major F_2 antiform nose and appears to be genetically and temporally related to B_1. Therefore, the writer concludes that F_1 folds have been internally rotated in the antiform nose during F_2 flexural flow folding.

STRUCTURE STATION 11

General Statement

Location - South flank of Wyoming Creek antiform (Map 2b).

Areal Extent - Approximately 66,000 sq. yds.

Number of Measurements - 21 B_1 and B_2 measurements.

Rock Types - Pink biotite migmatite, micaceous schists and para-amphibolite.

Geologists - L.C. Rowan and C.E. Larsen.

Geometrical Analysis

Symmetry - Triclinic, nearly monoclinic.

Scale - Mesoscopic.

Homogeneity - Inhomogeneous with respect to B_1 and B_2.

B_1-girdle - (a). N88W, vertical.

Reliability- (a). Fair.

Maximum - (a). N88W, 58°W.

Fold Geometry - B_1 has rotated approximately 90 degrees from Station 10 to this station. The pattern suggests folding of B_1 by nearly "similar" folds (Ramsay, 1960, pp.76-78), producing a girdle trending N88W. The rotation of this data relative to the adjacent station may be explained in several ways;

1). Faulting between the stations,

2). Block rotation during agmatization, or

STRUCTURE STATION 11.

21 B_1 Measurements
Contour Interval: 1-5-10%

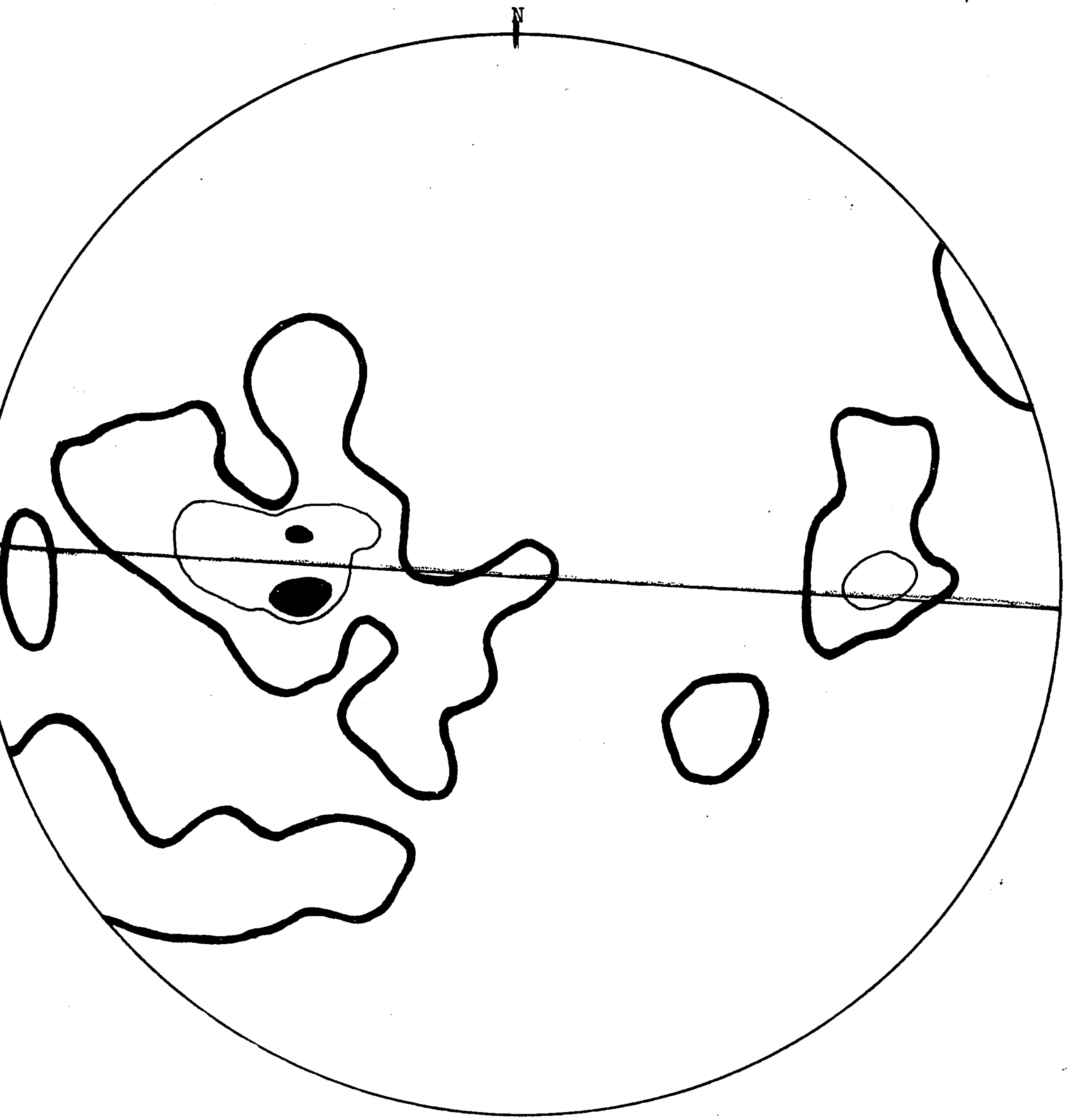

STRUCTURE STATION 12

General Statement

Location - South flank of Wyoming Creek antiform (Map 2b).

Areal Extent - Approximately 100,000 sq. yds.

Number of Measurements - 36 B_1 measurements.

Rock Types - Quartzites and mica schists.

Geologists - L.C. Rowan and C.E. Larsen.

Geometrical Analysis

Symmetry - Generally monoclinic.

Scale - Mesoscopic.

Homogeneity - Nearly homogeneous with respect to B_1.

B_1-girdle - (a). N73E, 60°S.

Reliability- (a)-Good.

Maxima - (a). N73E, horizontal.

Fold Geometry - B_1 is dispersed so that it does not form a partial small circle nor a partial great circle. Map 2b indicates that B1 and B_2 are nearly coaxial at this station. F_2 folds are nearly "concentric" in most cases. The suggested partial small circle B_1-girdle and the coaxial orientation of B_2 (Map 2b) suggests that F_2 folds have deformed B_1 and that the mechanism of folding was at least partially flexural (Clifford, 1960, p.377, Fig. 9-D9).

STRUCTURE STATION 12.

36 B_1 Measurements
Contour Interval: 1-5-10-15%

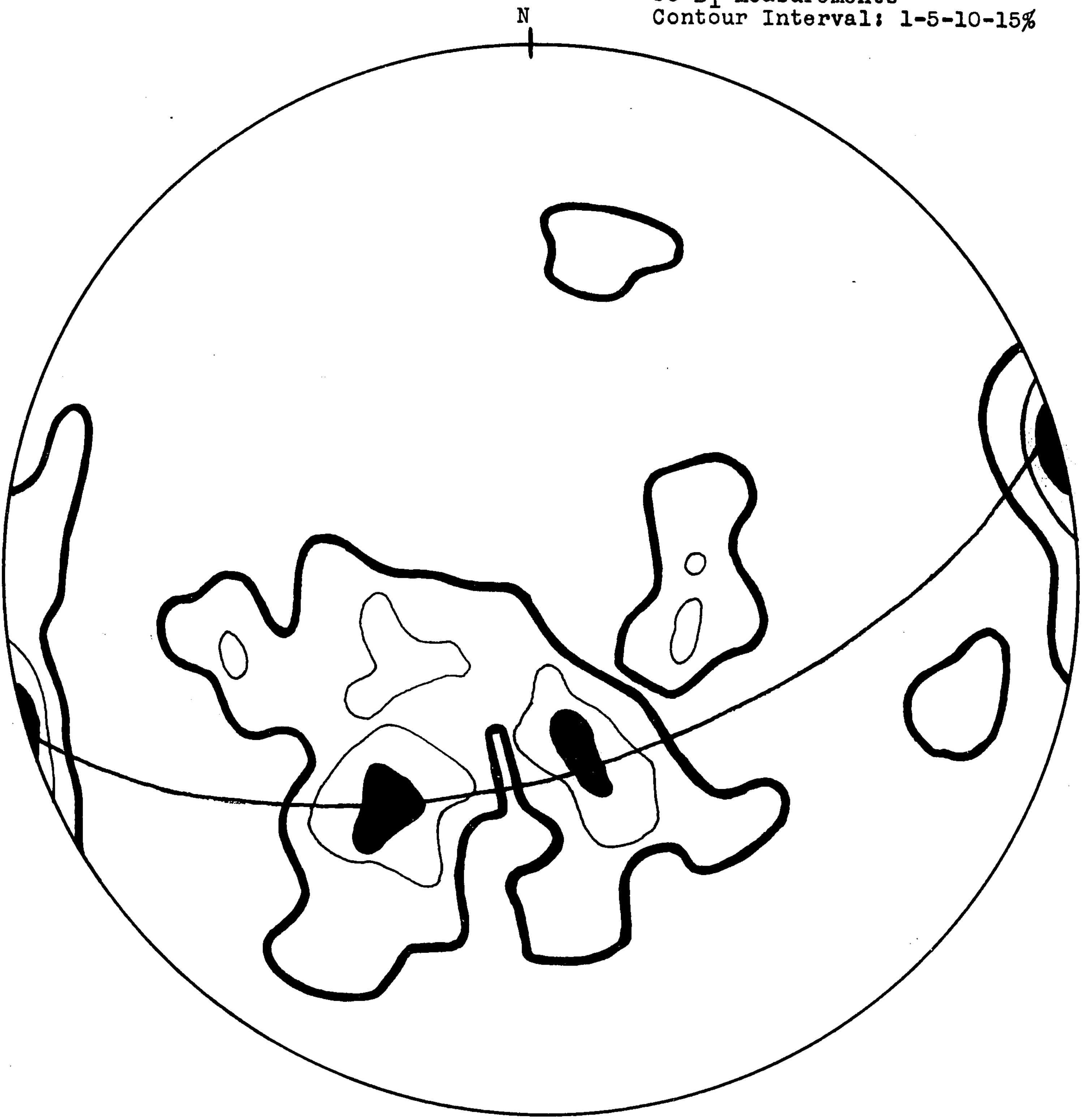

Macroscopic Scale:

Stations homogeneous with respect to B_1 have been combined to form macroscopic subareas (Turner and Weiss, 1963, pp.144-151). Five subareas are shown on Map 3b with the corresponding subfabric diagrams. Measurements number from 50 to 89. Although B_1 is nearly homogeneous for the Wyoming Creek antiform, sufficient variation exists to necessitate construction of 3 subareas here. The subfabric symmetry is generally monoclinic. Homogeneity is significantly greater for the B_1-subfabric than for the S_1-subfabric, especially in the Wyoming Creek antiform.

(S_2) (Map 3a and Subarea 1) is closely coincident with the B_1-girdle.

2). S_2 shows sufficient dispersion to suggest very open, gentle cross-flexures (F_2) plunging steeply east.

Preferred Interpretation - These geometric elements suggest deformation of B_1 by appressed, south-plunging F_2 folds which are overturned to the west. Since the B_1-girdle approximates S_2 (Map 3a), these F_2 folds must be nearly isoclinal and "similar". The separation of the maxima is due to the spread of B_1 at Stations 1 and 2 (Map 2b). The complex dispersion of B_1 is at least partially explained by superposed warping by broad, open F_2 cross-folds (see Structure Stations 1 and 2, S_o and S_1). These cross-warps may be due to triaxial strain during F_2 folding or a later deformation.

SUBAREA 1

General Statement

Location - West flank of Quad Creek synform, including Structure Stations 1 and 2 (Map 3b).

Areal Extent - 0.1 square miles.

Number of Measurements - 52 B_1 measurements.

Rock Types - Pink biotite migmatite.

Geologists - L.C. Rowan and C.E. Larsen.

Geometrical Analysis

Symmetry - Nearly monoclinic.

Scale - Macroscopic.

Homogeneity - Nearly homogeneous with respect to B_1.

B_1-girdles - (a). N-S, 65°E.

Reliability- (a). Good.

Maxima - (a). N27E, 42°NE; (b). N-S, 23°N.

Fold Geometry - B_1 is dispersed into a N-S trending great circle girdle. This B_1-subfabric pattern is characterized by a large amount of scatter and possible subsidiary girdles. Very little can be said about the F_2 geometry without considering other subfabric elements:

1). The constructed β S_{1c}-axis in Subarea 1 suggests F_2 folds plunging gently south. Note that these folds are overturned to the west, and that the axial plane

SUBAREA 1.

51 B1 Measurements
Contour Interval: 1-4-8-12%

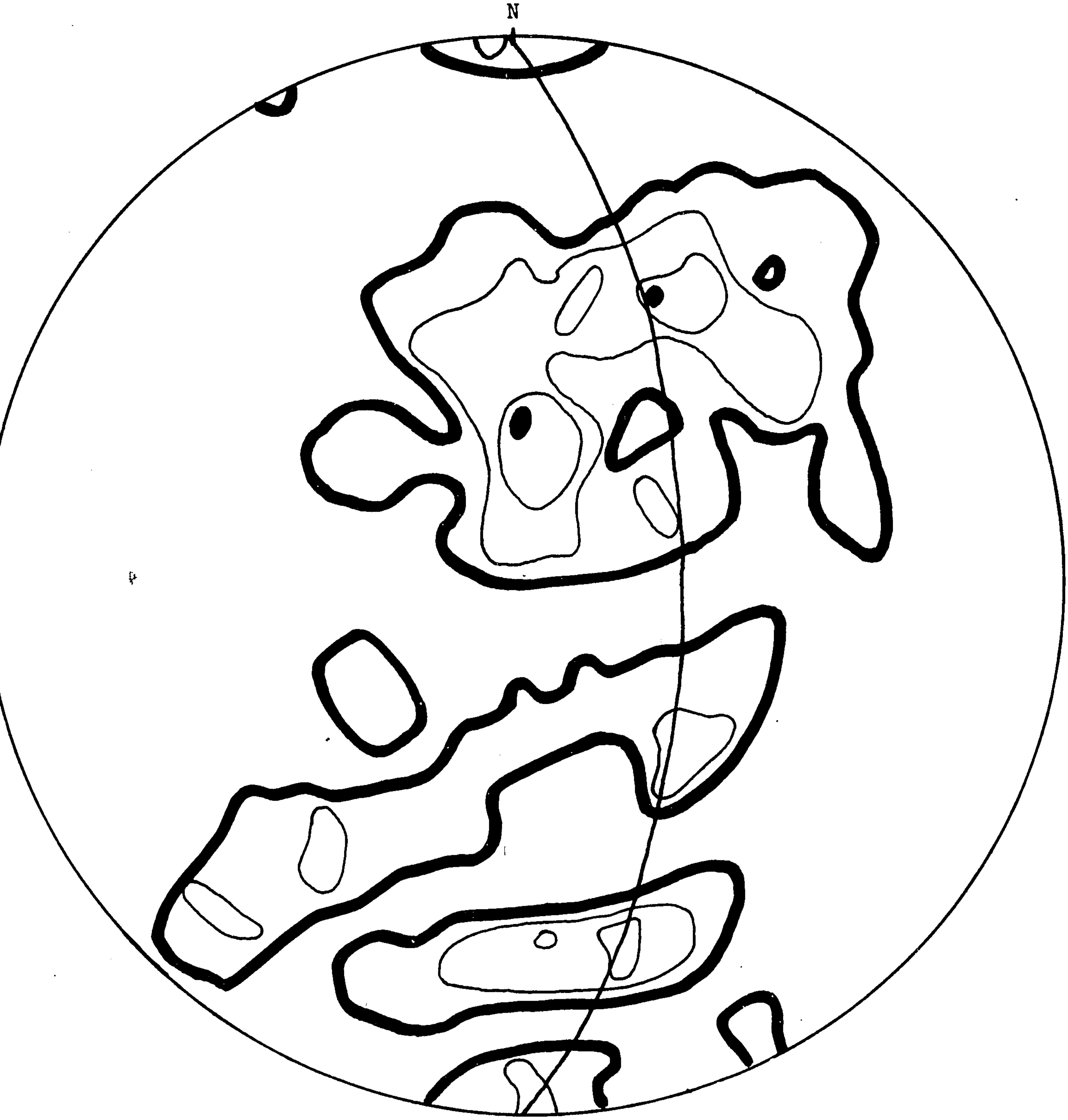

3). F_1 is folded by F_2 (oriented refolded specimens) dispersing B_1 into a girdle which is intermediate between a small and a great circle. S_1 defines S_1-girdles (Maps 3a and 2a) characteristic of overturned, non-isoclinal folds (F_2) (Turner and Weiss, 1963, p.161).

Preferred Interpretation - B_1 appears to be deformed by F_2 folds which are not "similar", appressed or isoclinal. They plunge gently SE and are overturned to the north. Note that S_2 (Map 3a) trends obliquely to the B_1-girdle in this subarea, whereas these two planes are nearly parallel at Subarea 1. The writer does not interpret this relationship as being indicative of a 90 degree change in the $B_2 \wedge B_1$-girdle from Subarea 1 to Subarea 2. On the contrary, a significant change in F_2 fold styles is indicated. F_2 appears to be appressed, isoclinal and "similar" at Subarea 1 and non-isoclinal, relatively open and somewhat "concentric" at Station 2. The writer believes that this difference in fold style is a function of mean ductility (Donath and Parker, 1964, pp.45-63). The migmatites of Subarea 1 are ductile and contain generally "similar" F_2 folds, whereas less "similar" F_2 folds characterize the less ductile quartzites and para-amphibolite of Subarea 2.

SUBAREA 2

General Statement

Location - Nose of the Quad Creek synform, including Structure Stations 3, 4 and 5 (Map 3b).

Areal Extent - Approximately 0.08 square miles.

Number of Measurements - 75 B_1 measurements.

Rock Types - Quartzites, para-amphibolite and migmatites.

Geologists - L.C. Rowan and C.E. Larsen.

Geometrical Analysis

Symmetry - Monoclinic.

Scale - Macroscopic.

Homogeneity - Homogeneous with respect to B_1.

B_1-girdle - (a). N5E, 40°W.

Reliability - (a)-Good.

Maximum - (a). N81W, 40°W.

Fold Geometry - The geometric relations of F_1 and F_2 are well-defined in this subarea.

1). B_2 generally plunges E-SE at a low angle and is in close agreement with the constructed βS_1- and βS_o-axes.

2). S_2 dips moderately S-SW, indicating overturning of F_2 to the north.

SUBAREA 2.

75 B_1 Measurements
Contour Interval: 1-4-8-12%

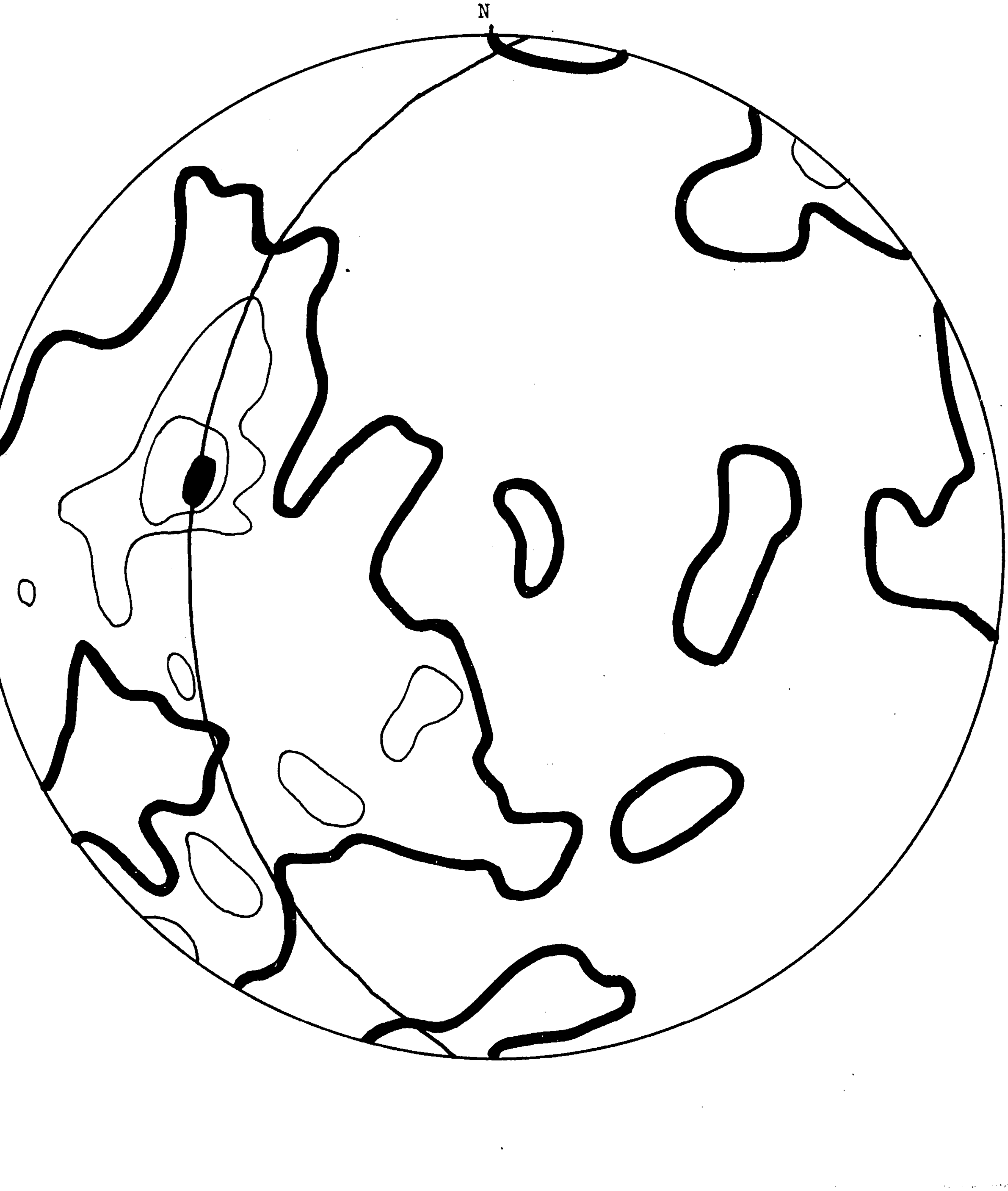

prefers the third alternative. A few non-isoclinal, nearly "concentric" F_2 folds have been identified in the field but were not measurable. Therefore, alternative 2 may partially explain this B_1-subfabric pattern.

1). B_1 is nearly parallel to B_2 and is deformed by F_2 folds which are appressed, nearly "similar" and plunge moderately S-SW. These folds are overturned to the east.

2). B_1 is nearly parallel to B_2 and is deformed by "similar" and appressed F_2 folds plunging moderately south and overturned to the east. These folds have dispersed B_1 into the B_{1a}-girdle. The B_{1b}-girdle is formed during very gentle warping by F_2 cross-folds.

3). The $B_1 \wedge B_2$ is small. B_1 is deformed by both "similar" and somewhat "concentric" folds which plunge moderately S-SW and are overturned to the east.

Preferred Interpretation - The S_1-subfabric at this subarea indicates that F_2 folds are nearly "similar", S-SW plunging, and overturned to the east. Subarea 2 data indicate that B_1 and B_2 have nearly parallel strikes and are separated in plunge by about 40-50°. Therefore, both axes have rotated approximately 90° east from their Subarea 2 orientation, and B_2 now plunges about 40° SW. B_1 plunges more gently SW to SE and is dispersed into a steeply inclined N-S girdle. The B_{1a}-girdle corresponds closely to the anticipated S_2-plane. The writer does not believe that alternative 1 is an entirely adequate explanation for this pattern. Since gentle, open F_2 folds are suggested by the S_0-subfabric (Maps 2a and 3a), the writer

SUBAREA 3

General Statement

Location - East flank of the Quad Creek synform, including Structure Stations 6, 7 and 8 (Map 3b).

Areal Extent - Approximately 0.6 square miles.

Number of Measurements - 89 B_1 and B_2 measurements.

Rock Types - Pink biotite migmatite.

Geologists - L.C. Rowan and C.E. Larsen.

Geometrical Analysis

Symmetry - Monoclinic.

Scale - Macroscopic.

Homogeneity - Homogeneous with respect to B_1 and B_2.

B_1-girdles - (a). N10E, 80°W; (b). N50W, 50°SW.

Reliability- (a)-Good ; (b)-Good.

Maximum - (a). S17W, 50°SW.

Fold Geometry - This B_1-subfabric pattern is characterized by two girdles which are nearly perpendicularly oriented. F_1 and F_2 are not separable in the subarea, but the writer believes that the maximum indicates the principal orientation of B_2. This pattern may be explained by one or a combination of the following geometries;

SUBAREA 3.

89 B_1 and B_2 Measurements
Contour Interval: 1-4-8-12%

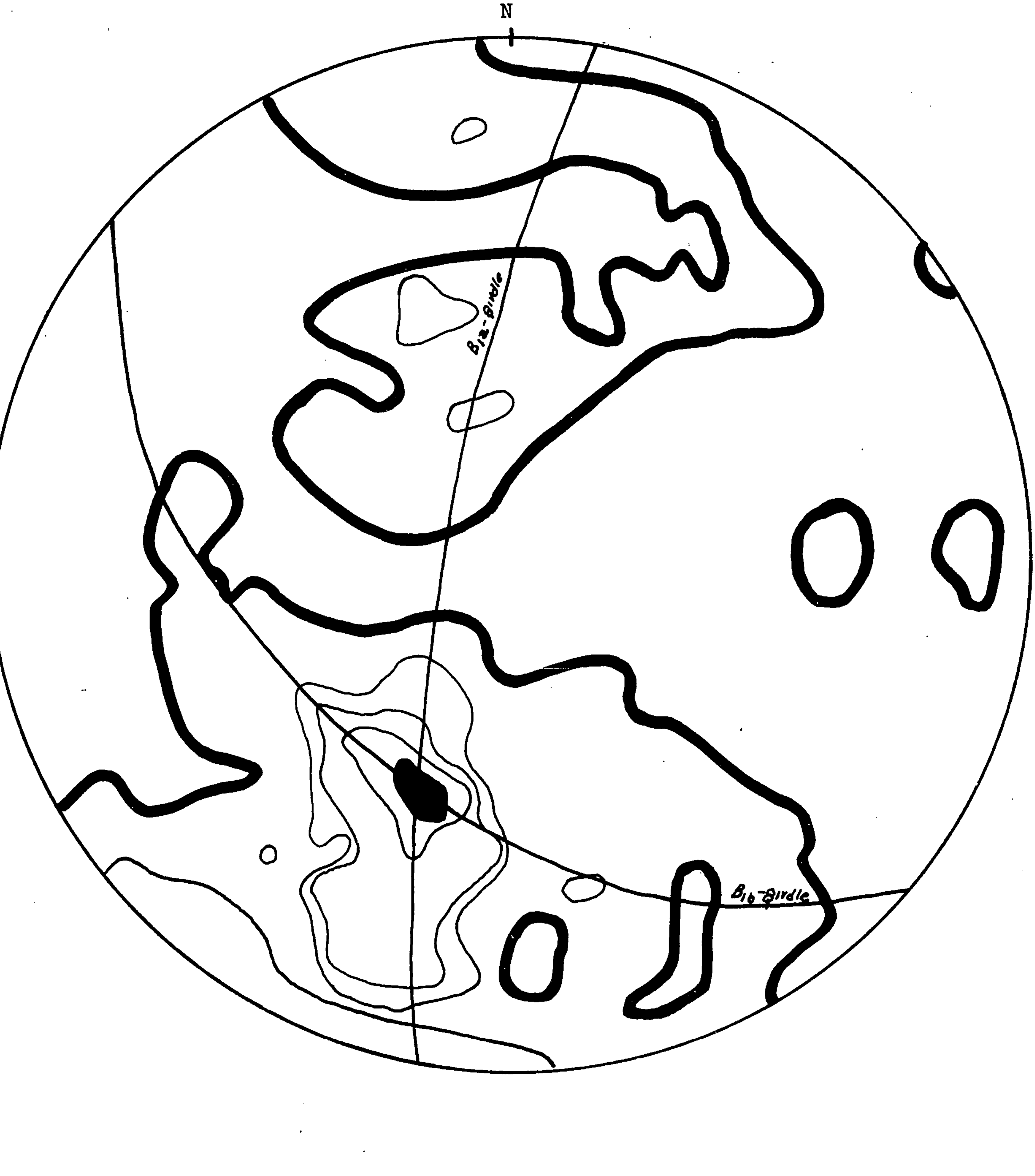

Preferred Interpretation - The writer prefers alternative 2 at this subarea, because field evidence supports the existence of both "similar" and nearly open "concentric" F_2 folds in this subarea. The F_2 folds at Station 9 are not "concentric" but nearly "similar" in most cases. These relations are very similar to those demonstrated by Clifford in coaxial folding (1960, p.377, Fig. 9-D9). S_2 (Map 3a) suggests that alternative 3 may also partially explain this B_1-subfabric pattern.

SUBAREA 4

General Statement

Location - Nose of Wyoming Creek antiform, including Structure Stations 9 and 10 (Map 3b).

Areal Extent - Approximately 0.2 square miles.

Number of Measurements - 67 B_1 and B_2 measurements.

Rock Types - Pink biotite migmatites, quartzites.

Geologists - L.C. Rowan and C.E. Larsen.

Geometrical Analysis

Symmetry - Monoclinic.

Scale - Macroscopic.

Homogeneity - Homogeneous with respect to B_1 and B_2.

B_1-girdles - (a). N-S, 90° ; (b). N79W, 60°S.

Reliability - (a)-Good ; (b)-Fair.

Maxima - (a). S2W, 60°S; (b). S4E, 40°S.

Fold Geometry - This B_1-subfabric is striking similar to the pattern in Subarea 3, although the 1 percent area is less widespread here. The B_{1a}-girdle is rotated 10° to a N-S trend in this subarea. It should be emphasized that B_1 and B_2 are separated at Station 10 but not at Station 9. The alternatives presented for Subarea 3 are applicable at this subarea and will not be restated here.

SUBAREA 4.

67 B_1 and B_2 Measurements
Contour Interval: 1-4-8-12%

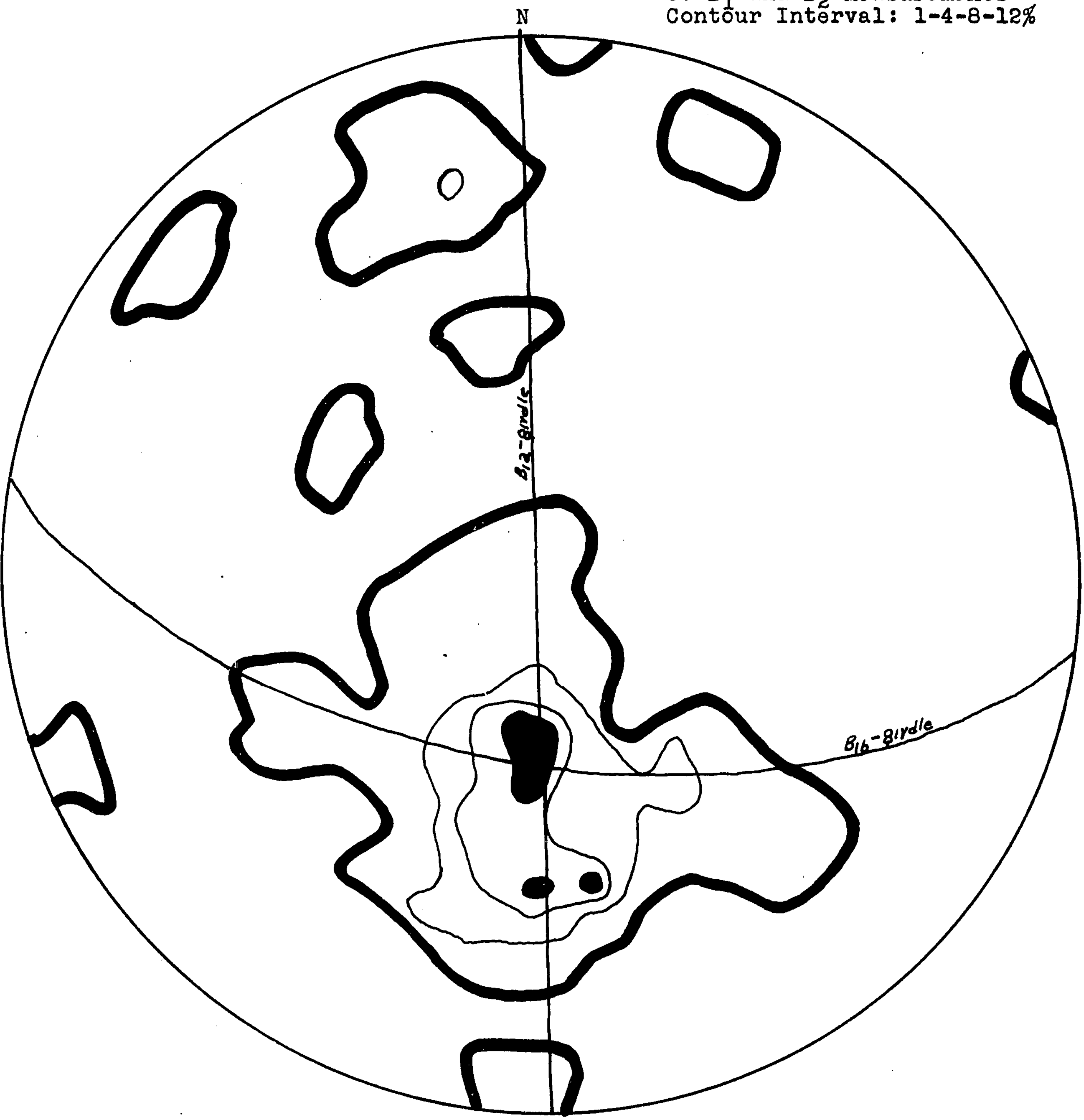

maximum is excluded. B_2 (Map 3b) is scattered along the B_{1b}-girdle, and S_2-poles do not form a simple point maximum. These features suggest gentle warping later than F_2 or due to triaxial strain during F_2 folding. F_2 folds are generally open, non-isoclinal and overturned to the east. S_2 strikes about perpendicular to the π S_{1a}-girdle (Map 3a).

SUBAREA 5

General Statement

Location - South flank of Wyoming Creek antiform, including Structure Stations 11 and 12 (Map 3b).

Areal Extent - Approximately 0.3 square miles.

Number of Measurements - 57 B_1 measurements.

Rock Types - Quartzites, migmatites, micaceous schists.

Geologists - L.C. Rowan and C.E. Larsen.

Geometrical Analysis

Symmetry - Generally monoclinic.

Scale - Macroscopic.

Homogeneity - Nearly homogeneous with respect to B_1.

B_1-girdles - (a). N72E, 65°S ; (b). N10W, 60°W.

Reliability - (a). Good ; (b). Good.

Maximum - (a). N73E, 0°.

Fold Geometry - This B_1-subfabric pattern is different from the patterns in Subareas 3 and 4 by virtue of the better definition of the B_{1b}-girdle in this subarea. Part of this completeness results from the B_1 measurements at Structure Station 11 (Map 2b). Although two great circle girdles have been constructed, note that a small circle girdle fits the pattern quite well if the

SUBAREA 5.

57 B_1 Measurements
Contour Interval: 1-4-8%

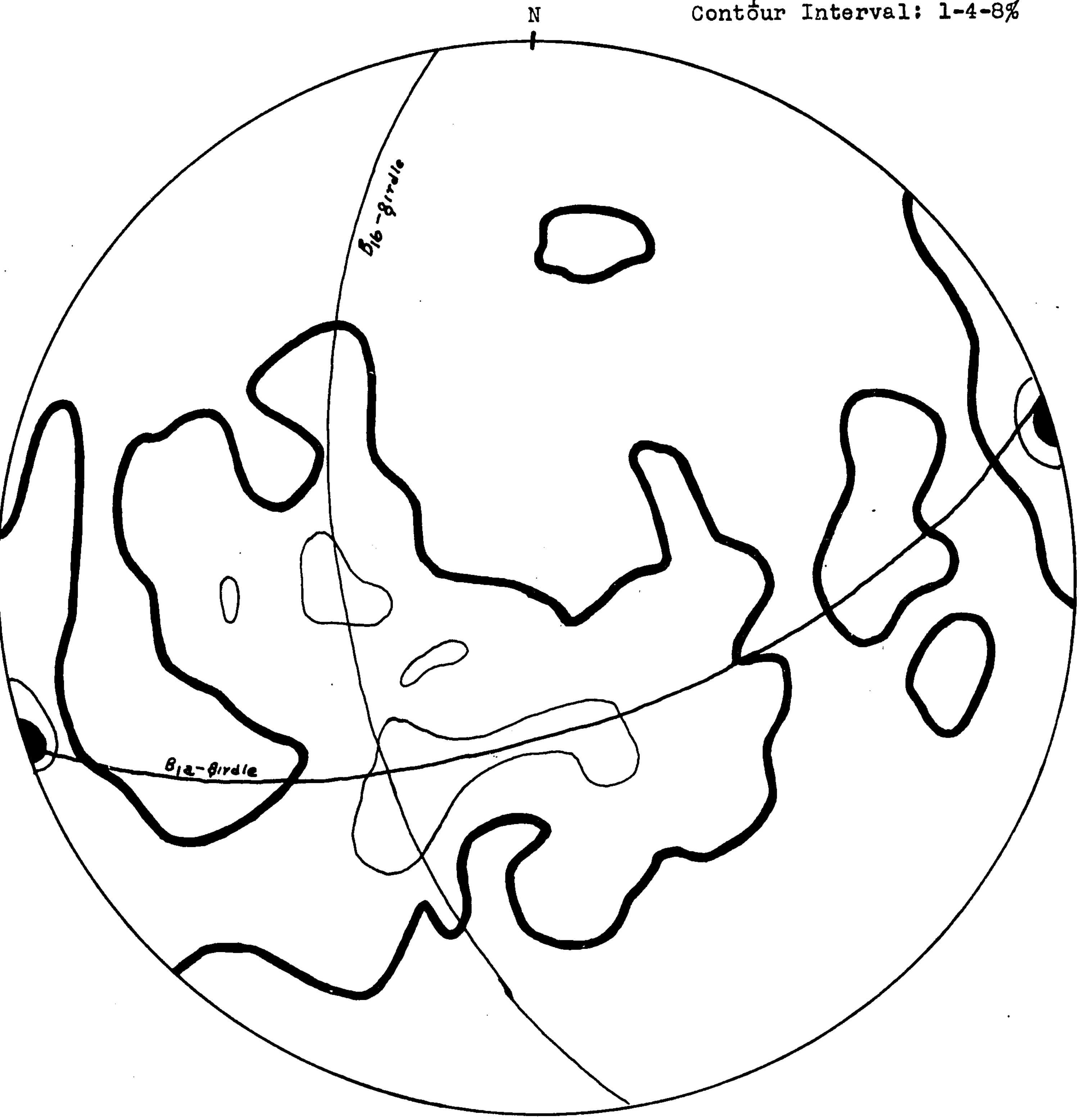

SUMMARY

<u>B_1-subfabric</u> - The axes of isoclinal flow folds, B_1, have been folded by "similar" F_2 folds in migmatites and granitic gneisses throughout the Quad-Wyoming-Line Creeks area. Therefore, B_1 is dispersed into a partial great circle which generally trends perpendicular to the S_0-plane. Slightly "concentric" F_2 folds have deformed B_1 at Stations 3, 4, 5, 9, 10 and 12, where the rocks are relatively non-ductile quartzites. The B_1-girdle is a curvi-planar surface intermediate between a partial small circle girdle and a partial great circle girdle, suggesting that F_2 folds are intermediate between "similar" and "concentric" styles (Ramsay, 1960, pp.75-93) in these non-ductile rocks. B_1 and B_2 are generally parallel, the greatest divergence being at Stations 11 and 12. B_1 converges on the major Quad Creek synform axis and rotates around the nose. In contrast, B_1 does not converge on the Wyoming Creek antiform axis, nor does it show any significant rotation in strike in the nose. The B_1-girdle for the entire Wyoming Creek antiform is shown in Figure 40.

APPENDIX V

L_1-Subfabric

Mesoscopic:

Seventy-five (75) hornblende lineations (L_1) have been taken from para-amphibolite at all twelve structure stations. L_1-subfabric diagrams are keyed to the appropriate areas on Map 2b.

(a). statistically biased measurements,

(b). B_1 is not parallel to L_1 at this structure station, or

(c). F_2 is more nearly "concentric" in para-amphibolite due to lower mean ductility (Donath and Parker, 1964, pp.45-63). F_2 is nearly "similar" in the ductile migmatites at this station.

<u>Preferred Interpretation</u> - Reasons have been given previously (Text, pp. 74-75) which appear to eliminate bias in the L_1 measurements. B_1 appears to be nearly parallel to L_1 at Stations 4 and 5. Deviations from parallelism at other stations do not appear large; therefore, number 2 above does not explain the differences in the L_1- and B_1-subfabrics. The writer concludes that differences in fold styles due to differential mean ductilities adequately explain the two different patterns. Note that the β S_{ob}-axis (Map 2a) strikes about N-S and is nearly horizontal at this station. In general, deformation of L_1 by nearly "concentric" folds with this orientation would give two partial small circle girdles located in the NE and SW (Donath and Parker, 1964, p.54). Highly appressed, nearly "similar" folds (F_2) would deform L_1 into a plane defined by a great circle girdle (Ramsay, 1960, pp.77-78). This pattern is shown by B_1 at this station (Map 2b). F_2 is not truly "concentric", since the $B_2 \wedge L_1$ is not constant (Ramsay, p.77).

STRUCTURE STATION 1

General Statement

Location - West flank of Quad Creek synform (Map 2b).

Areal Extent - Approximately 500 sq. yds.

Number of Measurements - 75 hornblende (L_1) measurements.

Rock Type - Para-amphibolite.

Geologists - L.C. Rowan and C.E. Larsen.

Geometrical Analysis

Symmetry - Generally Monoclinic.

Scale - Mesoscopic.

Homogeneity - Homogeneous with respect to L_1.

L_1-girdle - (a). N35W, 20°NE.

Reliability - (a)-Good.

Maximum - (a). N38E, 18°NE.

Fold Geometry - The L_1-girdle approaches a partial small circle, and the maximum plunges more gently NE than the B_1-maximum (Map 2b). These features imply differences with respect to the F_2 fold geometry:

1). The partial small circle suggests that more "concentric" F_2 folds deform L_1 than the folds (F_2) deforming B_1 at this station (Ramsay, 1960, pp.76-77).

2). The location of the L_1-maximum at a gentle NE plunge relative to the B_1-maximum may be due to:

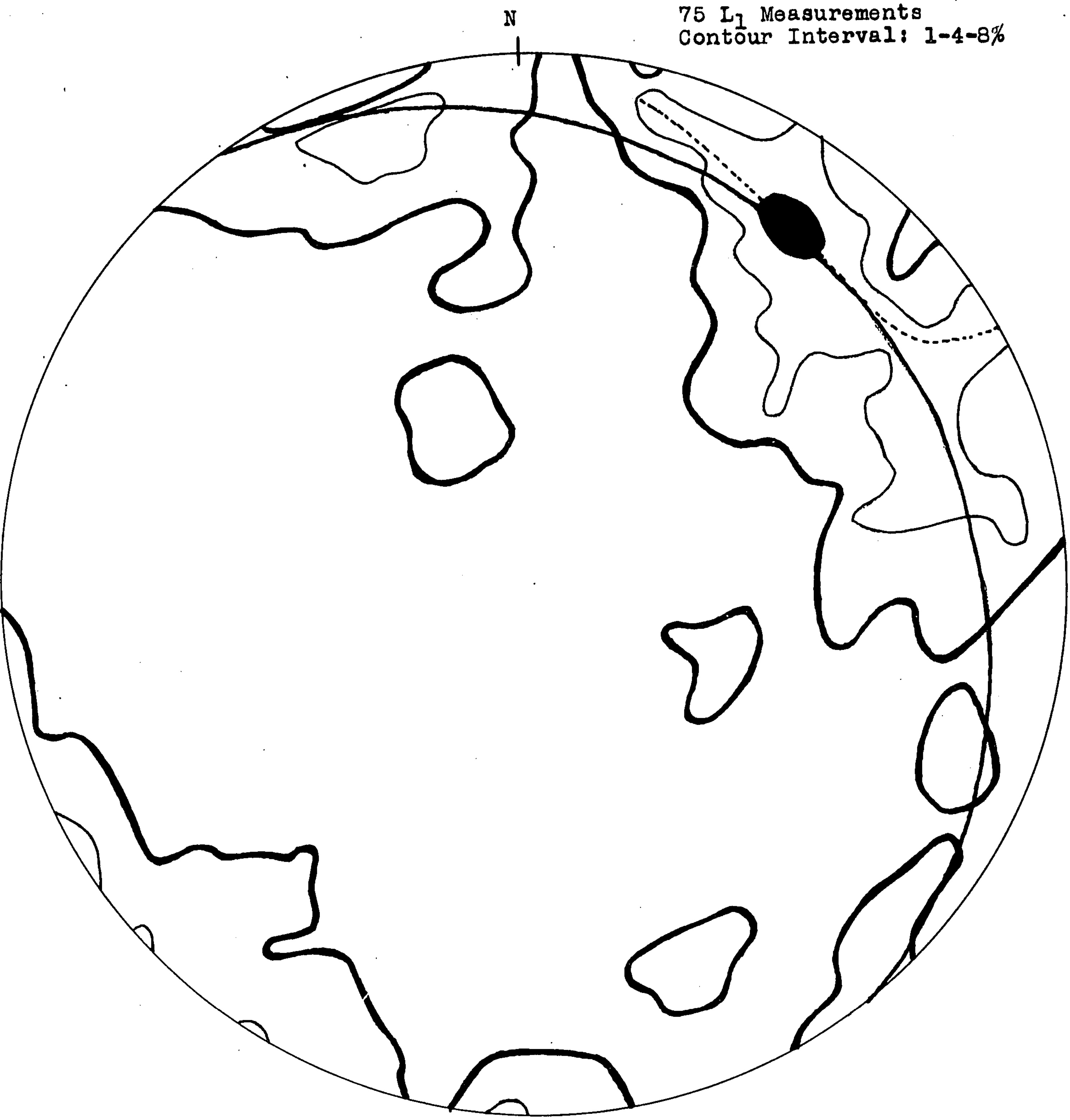

STRUCTURE STATION 1.

75 L_1 Measurements
Contour Interval: 1-4-8%

constructed at this station, suggestion of a partial small circle is evident. Field observations indicate that the para-amphibolite has responded to deformation in a less ductile manner than the migmatites. B_1 measurements were obtained from the latter ductile rocks, and the containing plane is an ill-defined great circle girdle. There is a tendency towards a small circle girdle also. Note that all of the L_1 measurements were derived from less ductile para-amphibolite.

Preferred Interpretation - The writer interprets this L_1-subfabric pattern as being a product of folding of earlier lineations (L_1) by folds which more nearly approached a "concentric" than "similar" style. It is further concluded that "concentric" folds have developed primarily in para-amphibolite due to its lower mean ductility. In contrast, migmatites have reacted to deformation in a "similar" manner by virtue of its high mean ductility. It cannot be concluded that B_1 and L_1 were parallel prior to deformation on the basis of this diagram. However, B_1 and L_1 diagrams suggest parallelism of these elements at Stations 3, 4 and 5. The rocks at these stations are dominantly quartzite and para-amphibolite, which possess nearly equivalent mean ductilities.

STRUCTURE STATION 2

General Statement

Location - Northwest portion of Quad Creek synform nose (Map 2b).

Areal Extent - Approximately 100 sq. yds.

Number of Measurements - 75 hornblende measurements.

Rock Type - Para-amphibolite.

Geologists - L.C. Rowan and C.E. Larsen.

Geometrical Analysis

Symmetry - Triclinic in detail, monoclinic in general.

Scale - Mesoscopic.

Homogeneity - Nearly homogeneous with respect to L_1.

L_1-girdle - (a). N77W, 35°NE.

Reliability- (a)-Good.

Maximum - (a). N20E, 33°NE.

Fold Geometry - The NE maximum is more intense at this station than at the preceding.(1) station. The L_1-girdle attitude is nearly perpendicular to the B_1-girdle at this station. However, Ramsay (1960, pp.76-78) and others have shown that "concentric" folds deform earlier rectilinear lineations into partial small circles on equal area nets. "Similar" folding disperses earlier lineations into partial great circles. Although a great circle L_1-girdle has been

STRUCTURE STATION 2.

75 L_1 Measurements
Contour Interval: 1-4-8-12%

1). L_1 has been deformed by slightly "concentric" F_2 folds dispersing this element into a curviplanar surface which is intermediate between a great circle and a small circle girdle. These later F_2 folds are not truly "concentric", since the $L_1 \measuredangle B_2$ is not constant (Ramsay, 1960, pp.76-77). Note that S_2 is overturned to the north (Map 2a).

2). Deviations of L_1- and B_1-girdles and maxima by about 128° can be explained by one or a combination of the following factors;

(a). $B_1 \measuredangle L_1$ may have been 128° prior to F_2, or

(b). Non-ductile para-amphibolite may have been agmatized and rotated in this area. No relationship to the proximity of the metanorite body is necessarily suggested.

(c). Measurements are biased at this station.

The writer believes that L_1 measurements were biased at this station. Limited suitable outcrops limited L_1 measurements to a small area which the writer believes was the south flank of a mesoscopic F_2 fold overturned to the north.

STRUCTURE STATION 3

General Statement

Location - Nose of Quad Creek synform (Map 2b).

Areal Extent - Approximately 600 sq. yds.

Number of Measurements - 75 hornblende (L_1) measurements.

Rock Type - Para-amphibolite.

Geologists - L.C. Rowan and C.E. Larsen.

Geometrical Analysis

Symmetry - Monoclinic.

Scale - Mesoscopic.

Homogeneity - Homogeneous with respect to L_1.

L_1-girdle - (a). N85W, 35°S.

Reliability- (a)-Good.

Maximum - (a). S34E, 35°SE.

Fold Geometry - Although a great circle L_1-girdle has been constructed, the 1-4 percent area suggests a tendency towards a partial small circle L_1-girdle. Note that this girdle is generally similar in shape to the B_1-girdle. However, the L_1-girdle and maximum are rotated about 128 degrees to the SE relative to B_1.

Preferred Interpretation - The writer interprets this L_1-subfabric pattern in the following manner;

STRUCTURE STATION 3.

75 L_1 Measurements
Contour Interval: 1-4-8-12%

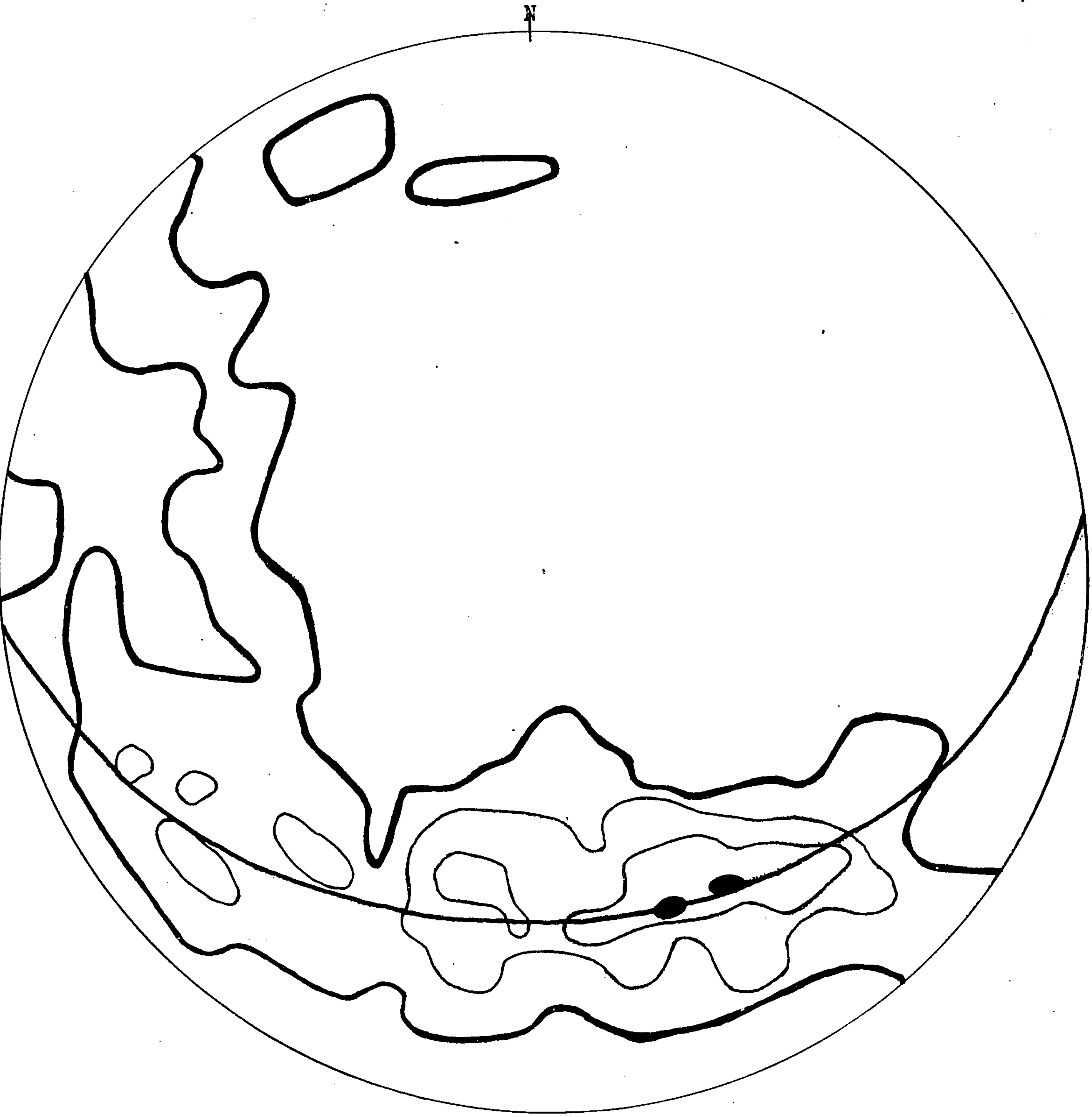

deformed by slightly "concentric" F_2 folds (Ramsay, 1960, pp.75-93). Since the $L_1 \measuredangle B_2$ is not constant, these folds can not be truly "concentric". It is important to realize that F_2 is overturned to the north at this station (Map 2a, S_1-diagram). The folding mechanism is probably flexural flow (Donath and Parker, 1963, p.51).

STRUCTURE STATION 4

General Statement

Location - Northeast portion of Quad Creek synform nose (Map 2b).

Areal Extent - Approximately 300 sq. yds.

Number of Measurements - 75 hornblende (L_1) measurements.

Rock Type - Para-amphibolite.

Geologists - L.C. Rowan and C.E. Larsen.

Geometrical Analysis

Symmetry - Monoclinic.

Scale - Mesoscopic.

Homogeneity - Homogeneous with respect to L_1.

L_1-girdle - (a). N26W, 40°SE.

Reliability - (a)-Good.

Maximum - (a). N66W, 30°NW.

Fold Geometry - B_1 and L_1 are strongly concordant at this station. The 1-4 percent area closely approaches a partial small circle, although a great circle L_1-girdle has been constructed. Note that the L_1-maximum plunges west at this station, whereas it plunges NE at Stations 1 and 2.

Preferred Interpretation - The writer concludes that L_1 and B_1 are generally parallel at this station and have been

STRUCTURE STATION 4.

75 L_1 Measurements
Contour Interval: 1-4-8%

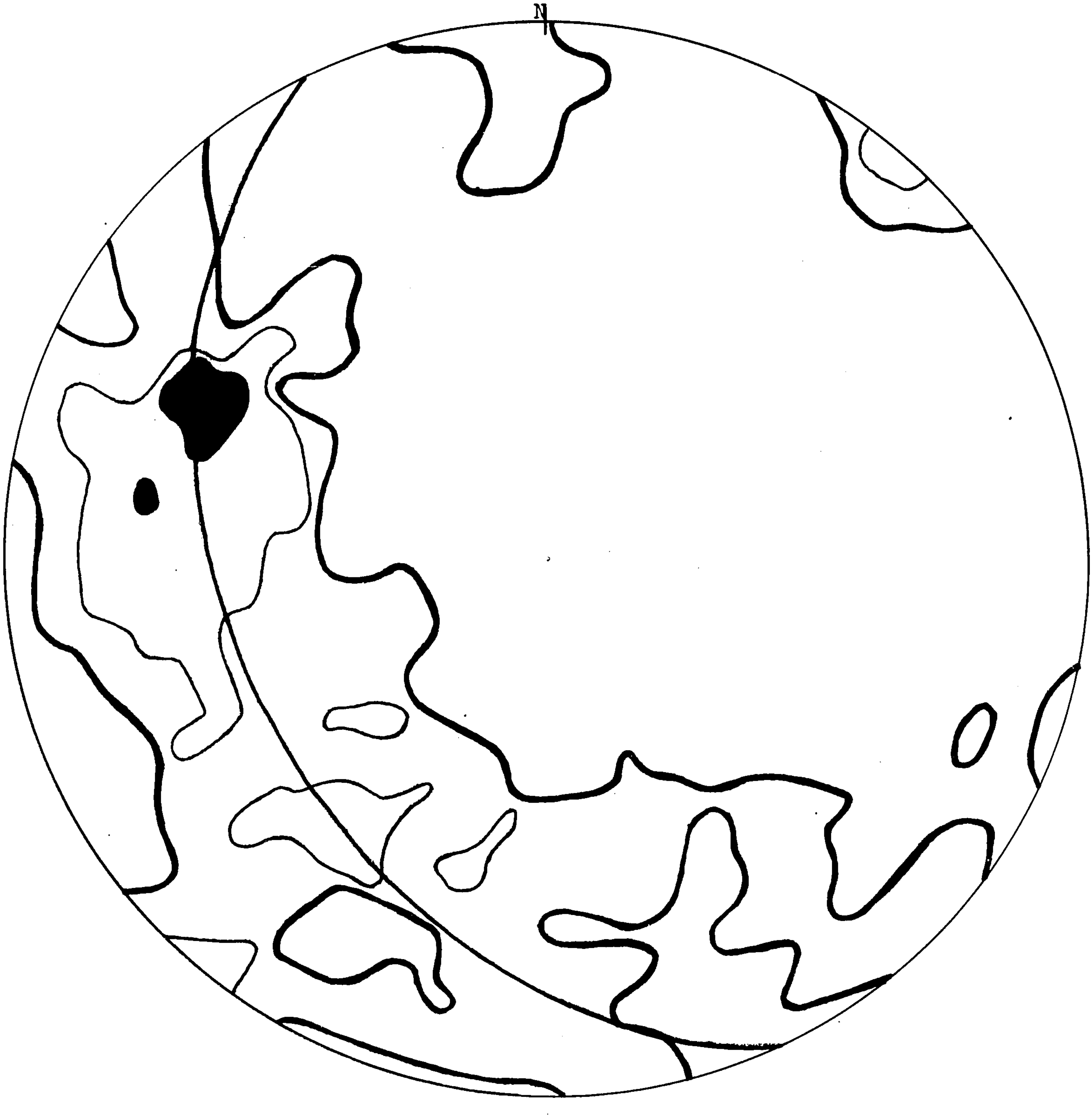

Preferred Interpretation - The writer concludes that L_1 and B_1 are generally parallel at this station and have been deformed by slightly "concentric" folds (F_2). The $L_1 \measuredangle B_2$ is not constant. Therefore, these folds cannot be truly "concentric" (Ramsay, 1960, p.76). Note that F_2 is overturned to the north at this station (Map 2a, S_2 diagram). F_2 appears to have developed through flexural flow in these para-amphibolites.

STRUCTURE STATION 5

General Statement

Location - Northeast portion of Quad Creek synform nose (Map 2b).

Areal Extent - Approximately 100 sq. yds.

Number of Measurements - 75 hornblende (L_1) measurements.

Rock Type - Quartzites and para-amphibolite.

Geologists - L.C. Rowan and C.E. Larsen.

Geometrical Analysis

Symmetry - Generally monoclinic.

Scale - Mesoscopic.

Homogeneity - Nearly homogeneous with respect to L_1.

L_1-girdle - (a). N20W, 35°SW.

Reliability - (a)-Good.

Maximum - (a). S86W, 35°W.

Fold Geometry - Deformation of L_1 by slightly "concentric" folds (F_2) is suggested by the tendency of a small circle girdle to form at this station. The 1-4 per cent area outlines the projected and distorted partial cone (Ramsay, 1960, pp.75-93). The B_1- and L_1-girdles and maxima are generally coincident, suggesting parallelism of these elements.

STRUCTURE STATION 5.

75 L_1 Measurements
Contour Interval: 1-4-8-12-16%

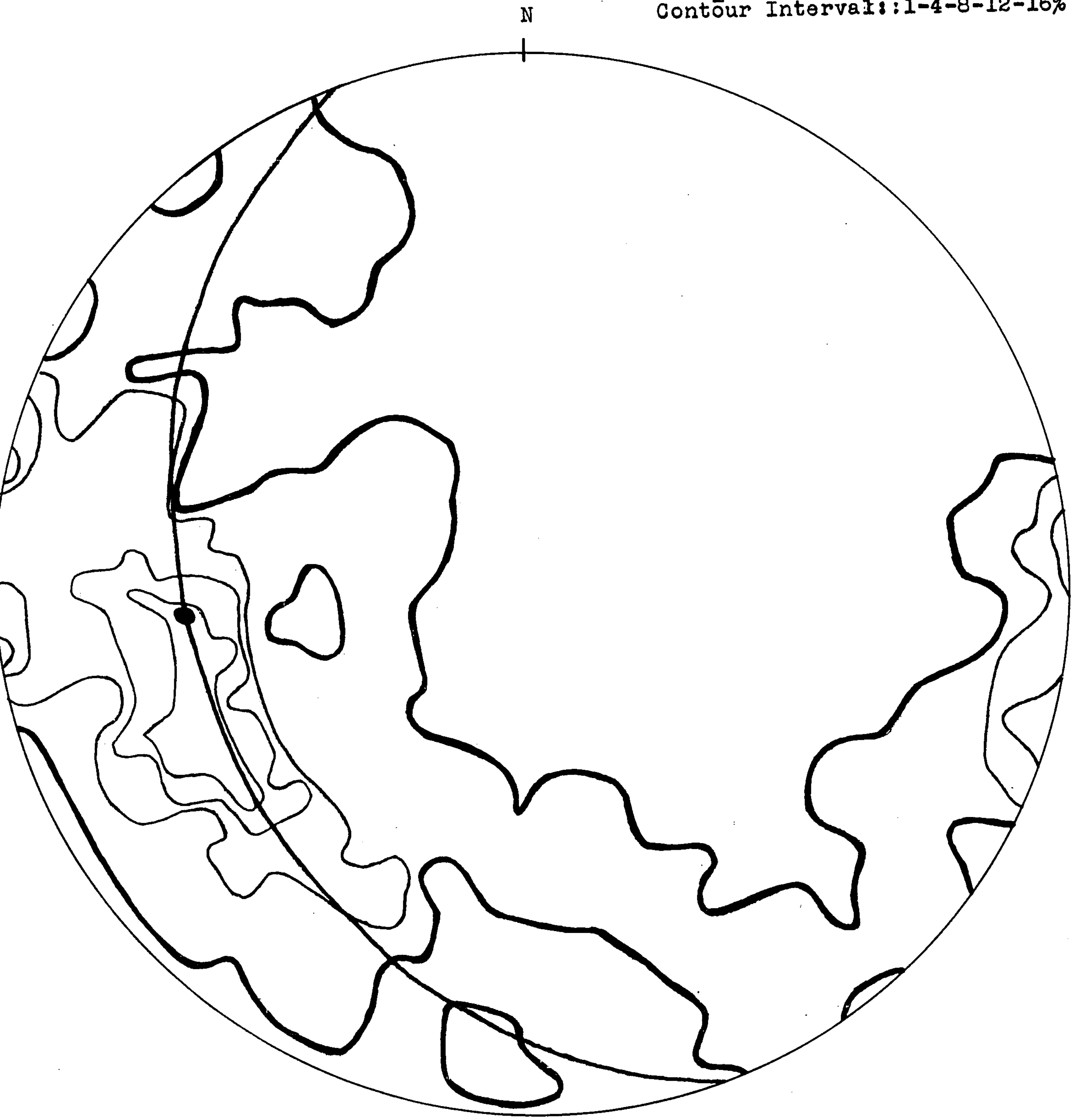

(b). Later cross-folds (F_2) which are suggested by the

S_o-subfabric to be "concentric".

The writer believes that these factors account for the L_1-subfabric at this station. Note that if the subfabric diagram from Station 5 is rotated 90 degrees east, and if the entire pattern is then rotated about 40° south, the resultant L_1-subfabric corresponds closely to number 6. Greater dispersion at Station 6 is probably due to (a) and (b) above. The rotations from Stations 5 to 6 is the approximate rotation involved in going from the Quad Creek synform nose (Station 5) to the east flank (Station 6).

1). The general plunge of L_1 is more gentle than B_1.

2). L_1 forms a less intense maximum than B_1 shows.

3). The L_1-small circle girdle is more complete than the B_1-small circle girdle.

These differences may be explained in one or a combination of the following ways:

1). L_1 measurements are biased.

2). L_1 and B_1 were not parallel prior to F_2.

3). Para-amphibolite has responded to stress in a less ductile manner than the migmatites. Therefore, L_1 is deformed by development of the L_1-girdle. Later (F_2) cross-folds suggested by the S_0-subfabric probably also explain some of the B_1 dispersion.

Preferred Interpretation - The subject of bias has been discussed (Text, pp.74-75) and is not regarded as significant. B_1 and L_1 have been shown to be nearly parallel and coincident at Stations 4 and 5. The writer interprets this L_1-subfabric pattern as a product of folding of L_1 by folds (F_2) which are somewhat "concentric". Since the S_1- and S_0-subfabrics (Map 2a) indicate that F_2 is primarily "similar", the L_1-subfabric cannot be attributed entirely to slightly "concentric" folding. Two other factors appear to be significant:

(a). Rotation during agmatization and

STRUCTURE STATION 6

General Statement

Location - North portion of east flank of Quad Creek synform (Map 2b).

Areal Extent - Approximately 1000 sq. yds.

Number of Measurements - 75 hornblende measurements.

Rock Type - Para-amphibolite.

Geologists - L.C. Rowan and C.E. Larsen.

Geometrical Analysis

Symmetry - Generally monoclinic.

Scale - Mesoscopic.

Homogeneity - Generally homogeneous with respect to L_1.

L_1-girdles - (a). N52E, 25°SE ; (b). N34W, 10°NE.

Reliability - (a)-Good ; (b)-Fair.

Maximum - (a). S33E, 25°SE.

Fold Geometry - Dispersion of L_1 at this station is in a plane which approximates the great circle. Although B_1 and B_2 (Map 2b) are not separated at this station, geometric relations of these two elements defined at other stations (3, 4 and 5) suggest that B_1 plunges gently south. Dispersion of B_1 into a partial small circle gives a pattern somewhat similar to the L1-subfabric pattern. However, the following differences exist:

STRUCTURE STATION 6.

75 L_1 Measurements
Contour Interval: 1-4-8%

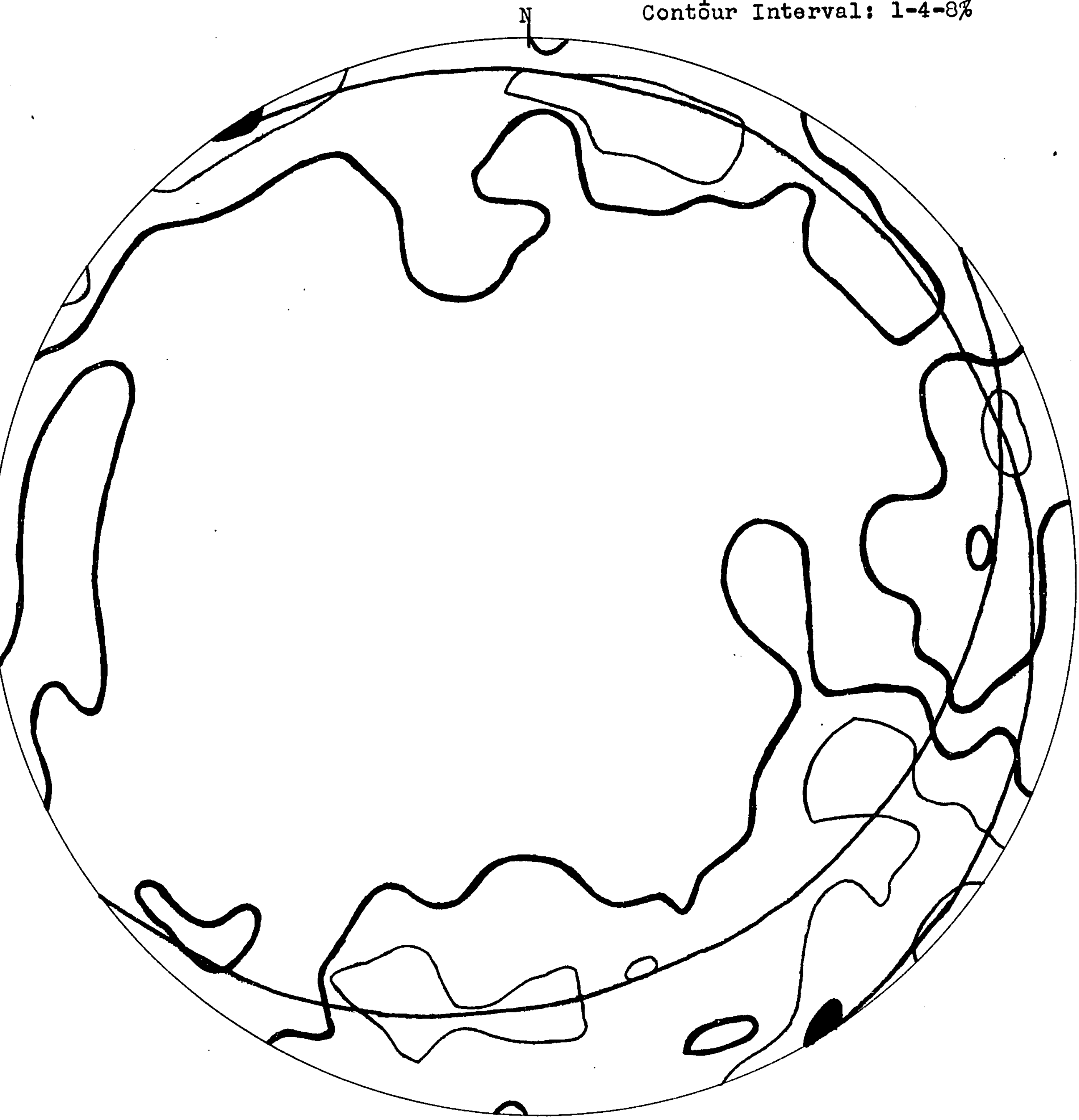

1). Bias in the L_1 measurements.

2). Rotation of para-amphibolite blocks during agmatization.

3). Formation of less "similar" and more "concentric" folds (F_2) in less ductile para-amphibolite (Ramsay, 1960, pp.75-93).

Preferred Interpretation - The writer believes that a combination of alternatives 2 and 3 adequately explains this pattern. Bias has been discussed previously (Text, pp.74-75) and is not believed to be significant. Agmatization appears to be in the incipient stages of development at this station. Ramsay (1960, p.92, Table 5) has shown that folded lineations which do not fit on partial great circle or small circle girdles have been folded by both "similar" and "concentric" flexures.

STRUCTURE STATION 7

General Statement

Location - East flank of Quad Creek synform (Map 2b).

Areal Extent - Approximately 600 sq. yds.

Number of Measurements - 75 hornblende (L_1) measurements.

Rock Types - Para-amphibolite.

Geologists - L.C. Rowan and C.E. Larsen.

Geometrical Analysis

Symmetry - Generally monoclinic.

Scale - Mesoscopic.

Homogeneity - Nearly homogeneous with respect to L_1.

L_1- girdles - (a). N76W, 10°S ; (b). N18E, 75°W.

Reliability - (a)-Good ; (b)-Good.

Maxima - (a). S15W, 10°SW.

Fold Geometry - This diagram shows the same features as the preceding L_1-subfabric pattern, except that there is a reasonably well-defined N-S trending great circle girdle at this station. The pattern suggests deformation of L_1 by both "concentric" and "similar" folds (Ramsay, 1960, p.92, table 5). L_1 mimics B_1, except that the former lineation plunges more gently south and is slightly more dispersed. These differences may be explained by one or a combination of these factors;

STRUCTURE STATION 7.

75 L_1 Measurements
Contour Interval: 1-4-8%

(1). Formation of less "similar" and more "concentric" folds (F_2) in less ductile amphibolite.

(2). Rotation of para-amphibolite blocks during agmatization.

Preferred Interpretation - The writer prefers a combination of these two factors. Agmatization is extensive here. Although B_1 data are sparse at this station, note that the B_1 measurements plunging gently S-SW closely coincide with an L_1-maximum. No L_1-great circle girdle is developed which corresponds to the nearly N-S B_1-girdle. Field observation indicates that para-amphibolite has reacted to deformation in a less ductile manner than the migmatites. Therefore, less "similar" and more "concentric" folds might develop in para-amphibolite, developing a partial small circle girdle near the great circle in L_1. East plunging F_2 cross-folds and agmatization adequately explain the wide dispersion of L_1.

STRUCTURE STATION 8

General Statement

Location - West flank of Wyoming Creek antiform (Map 2b).

Areal Extent - Approximately 800 sq. yds.

Number of Measurements - 75 hornblende (L_1) measurements.

Rock Type - Para-amphibolite.

Geologists - L.C. Rowan and C.E. Larsen.

Geometrical Analysis

Symmetry - Monoclinic.

Scale - Mesoscopic.

Homogeneity - Generally homogeneous with respect to L_1.

L_1-girdle - (a). N85W, 20°S.

Reliability- (a)-Good.

Maxima - (a). S27W, 18°SW; (b). S15E, 20°E.

Fold Geometry - This L_1-subfabric displays features common to Stations 6, 7, and 9:

1). Dispersion of L_1 into a girdle which approaches a small circle,

2). Principal maxima plunge gently south, and

3). Wide dispersion of L_1

These features form a characteristic pattern which may be explained by one or a combination of the following processes;

STRUCTURE STATION 8.

75 L_1 Measurements
Contour Interval: 1-4-8%

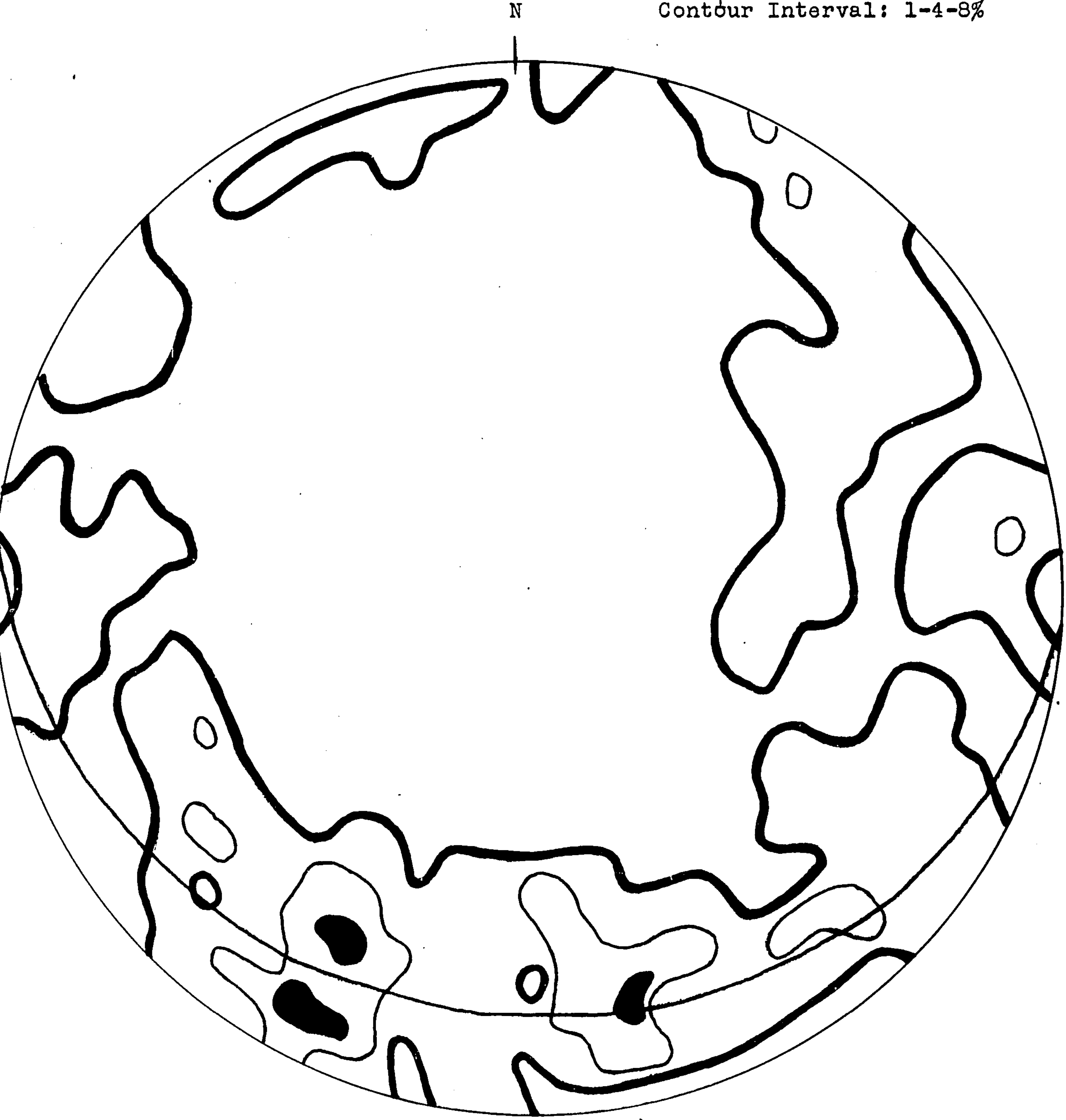

3). F_2 folds are more "concentric" in para-amphibolite than in the migmatites. Therefore, the L_1-girdle approaches a small circle more completely than the B_1-girdle (Ramsay, 1960, pp.76-78).

Preferred Interpretation - A combination of these factors is believed by the writer to explain the L_1-subfabric pattern here. The B_1- and B_2-subfabrics suggest that these elements are nearly parallel. L_1 plunges more gently than B_1. This may be due to the formation of more "concentric" folds in para-amphibolite than in the more ductile migmatites.

STRUCTURE STATION 9

General Statement

Location - Southwest nose of Wyoming Creek antiform (Map 2b).

Areal Extent - Approximately 400 sq. yds.

Number of Measurements - 75 hornblende measurements (L_1).

Rock Types - Para-amphibolite.

Geologist - L.C. Rowan.

Geometrical Analysis

Symmetry - Monoclinic.

Scale - Mesoscopic.

Homogeneity - Homogeneous with respect to L_1.

L_1-girdle - (a). N75E, 20°S.

Reliability - (a)-Good.

Maximum - (a). S10E, 20°S.

Fold Geometry - The L_1-subfabric pattern at this station differs from the preceding pattern in that the maximum is more intense here. The nearly E-W girdles approach small circles. The following factors may explain the L_1-subfabric:

1). L_1 is nearly parallel to B_1 and B_2 (Map 2b).

2). Para-amphibolite blocks have been rotated during agmatization.

STRUCTURE STATION 9.

75 L_1 Measurements
Contour Interval: 1-4-8%

combination of the following fold geometries and related processes;

1). L_1 is deformed into partial small circle girdles by slightly "concentric" folds (F_2) and dispersed around the great circle by rotation of para-amphibolite blocks during agmatization, or

2). L_1 measurements have been derived from the hinge portion of SW plunging folds (F_2).

Preferred Interpretation - F_2 folds plunge SW and are overturned about 25°SE at this station. L_1 lies in the So-plane and rotates around the Wyoming Creek antiform. F_2 folds are relatively "concentric". The partial L_1 small circle girdles are dispersed somewhat by agmatization and the non-cylindrical nature of the F_2 folds.

STRUCTURE STATION 10

General Statement

Location - Southeast portion of the Wyoming Creek antiform nose (Map 2b).

Areal Extent - Approximately 50 sq. yds.

Number of Measurements - 75 hornblende (L_1) measurements.

Rock Types - Para-amphibolite.

Geologists - L.C. Rowan and C.E. Larsen.

Geometrical Analysis

Symmetry - Monoclinic.

Scale - Mesoscopic.

Homogeneity - Homogeneous with respect to L_1.

L_1-girdle - (a). N12E, 30°E.

Reliability- (a)-Good.

Maximum - (a). N87E, 30°E.

Fold Geometry - This L_1-subfabric displays one feature which is striking different from the B_1-subfabric - L_1 rotates around the nose of the Wyoming Creek antiform as it does in the nose of the Quad Creek synform. B_1 rotates around the latter major fold but not around the former fold (Map 2b). Note that the L_1-girdle is approximately perpendicular to the S_1- and S_o-planes, and the L_1 maximum plunges gently east. The pattern suggests one or a

STRUCTURE STATION 10.

75 L_1 Measurements
Contour Interval: 1-4-8%

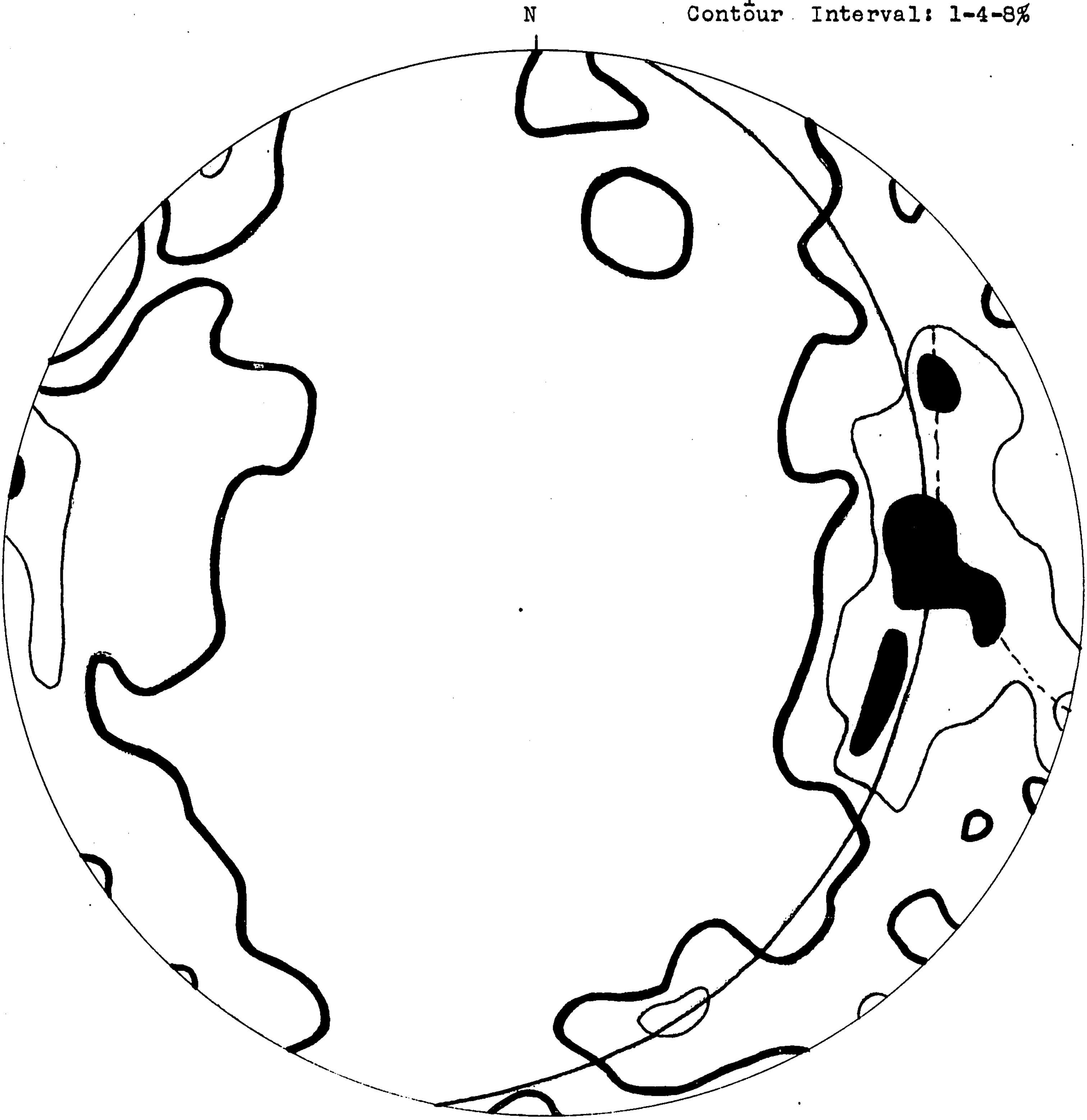

1). Rotation of para-amphibolite blocks during the process of agmatization.

2). Development of less "similar" F_2 folds in non-ductile para-amphibolite compared to "similar" F_2 folds in migmatites. A small circle L_1-girdle would be approached in the less "similar" folds (Ramsay, 1960, pp.76-77). Since the mechanism of folding (F_2) is not purely flexural, the small circle girdle will only be approximated.

3). L_1 is nearly parallel with B_1 and B_2 at this station (Map 2b).

Preferred Interpretation - Agmatization is extensive at this station and doubtlessly plays a significant role in developing the L_1-subfabric. "Similar" folds (F_2) characteristically deform earlier lineation into a great circle girdle, whereas more "concentric" folds (F_2) disperse L_1 into a partial small circle (Ramsay, 1960, pp.75-93). Therefore, the writer interprets the L_1-subfabric at this station to be indicative of deformation of L_1 by folds which are intermediate in style between "similar" and "concentric". Agmatization is probably associated with formation of these later folds (F_2) and may account for dispersion of the small circle L_1-girdles.

STRUCTURE STATION 11

General Statement

Location - South flank of Wyoming Creek antiform (Map 2b).

Areal Extent - Approximately 400 sq. yds.

Number of Measurements - 75 hornblende measurements (L_1).

Rock Type - Para-amphibolite.

Geologists - L.C. Rowan, C.E. Larsen and T. Rowekamp.

Geometrical Analysis

Symmetry - Monoclinic.

Scale - Mesoscopic.

Homogeneity - Homogeneous with respect to L_1.

L_1-girdle - (a). N21W, 30°SW.

Reliability- (a)-Good.

Maximum - (a). S47W, 25°W.

Fold Geometry - The L_1-subfabric pattern here is almost identical to the patterns at Stations 6, 7, 8, and 9, except that approximately 45° rotation to the west is evident. B_1 and L_1 are relatively coincident and display similar patterns. Note that the L_1-girdle is nearly perpendicular to the S_0-plane at this and most other stations. The B_1-axes are highly dispersed. This L_1-pattern is explicable by considering the following factors:

STRUCTURE STATION 11.

75 L_1 Measurements
Contour Interval: 1-4-8%

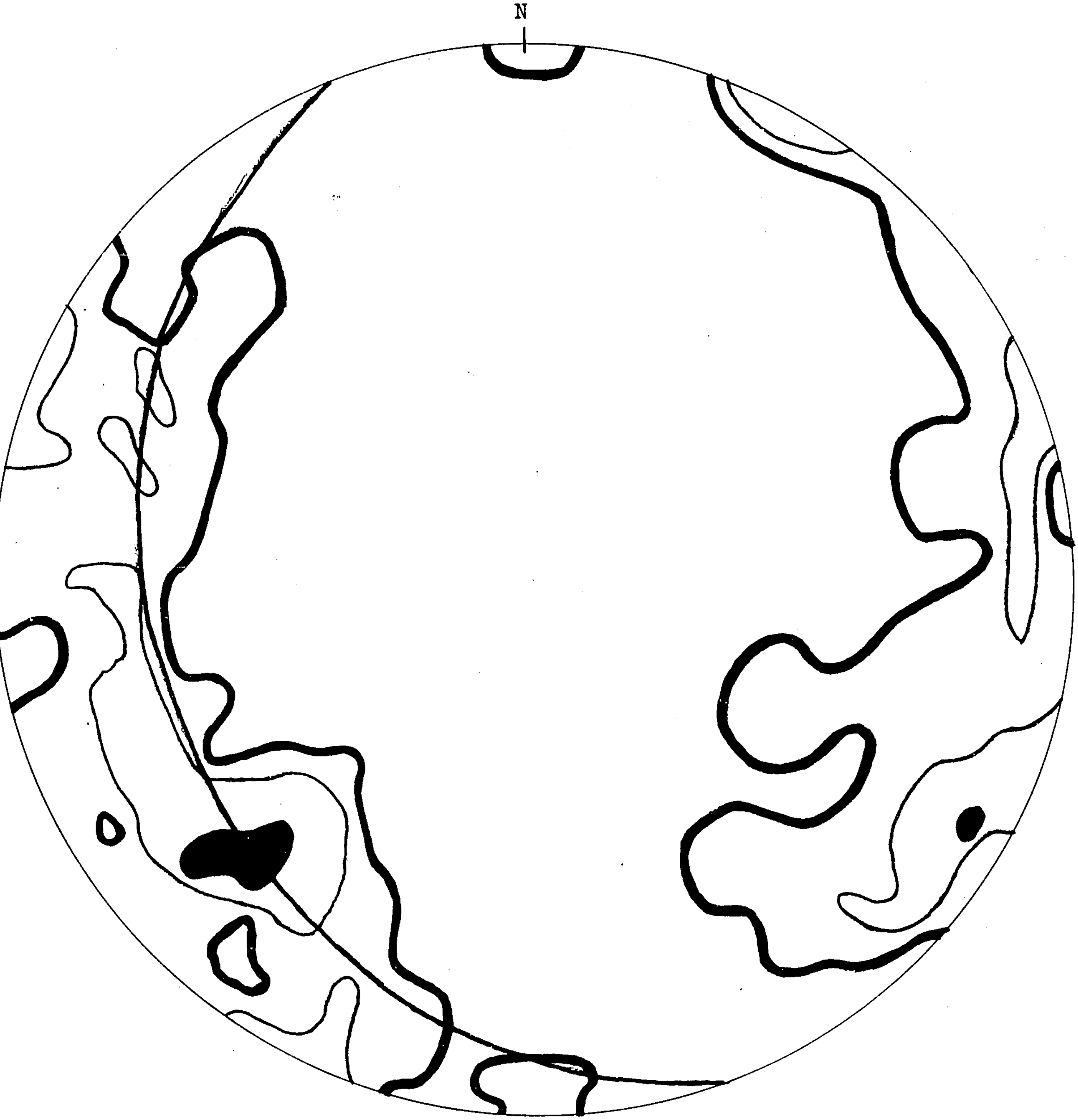

Agmatization is not a prominent process in the area from which these measurements were derived. The girdles are not as dispersed here as they are at stations where agmatite is prevalent.

However, L_1 does not coincide as closely with B_1 here as it does at Station 11. The features suggest the following alternate hypotheses regarding F_2 fold geometry;

(a). L_1 and B_1 were not parallel prior to F_2.

(b). L_1 measurements are biased, or

(c). The fold geometry differs significantly in non-ductile para-amphibolite compared to folds developed in ductile micaceous schists and migmatites.

Preferred Interpretation - Bias in L_1 measurements has been discussed previously (Text, pp. 74-75) and is not believed by the writer to be significant. L_1 appears to be nearly coincident with B_1 at most stations (3, 4, 5, 6, 7, 8, 9 and 11). No other data supports non-parallelism of L_1 and B_1 here. Note that B_1- and L_1- maxima are nearly coincident. The writer believes that less "similar" (F_2) folds have formed in the non-ductile para-amphibolite, and "similar" (F_2) folds have developed in migmatites and micaceous schists. Ramsay (1960, pp.75-93) has shown that earlier rectilinear lineations are dispersed into partial small circle girdles by "concentric" folding and great circle girdles by "similar" folds. Additionally, the L_1 B_2 should remain nearly constant in "concentric" folding by a flexural mechanism (Ramsay, 1960, p.77). This angle is nearly constant here, implying "concentric" folding by a mechanism which is partly flexural.

STRUCTURE STATION 12

General Statement

Location - South flank of Wyoming Creek antiform (Map 2b).

Areal Extent - Approximately 100 sq. yds.

Number of Measurements - 75 hornblende (L_1) measurements.

Rock Type - Para-amphibolite.

Geologists - L.C. Rowan and C.E. Larsen.

Geometrical Analysis

Symmetry - Monoclinic.

Scale - Mesoscopic.

Homogeneity - Homogeneous with respect to L_1.

L_1-girdles - (a). N-S, 8°W ; (b). N37W, 30°NE.

Reliability - (a). Good ; (b). Fair.

Maxima - (a). S70W, 10°SW ; (b). N75E, 32°NE.

Fold Geometry - This L_1-subfabric appears to be identical to the pattern at Station 11;

1). A small circle L_1-girdle is approached by virtue of dispersion of L_1 into planes approaching the attitude of the great circle,

2). SW and E trending maxima are developed, and

3). The L_1-girdles trend nearly perpendicularly to the S_o-plane.

STRUCTURE STATION 12.

75 L_1 Measurements
Contour Interval: 1-4-8%

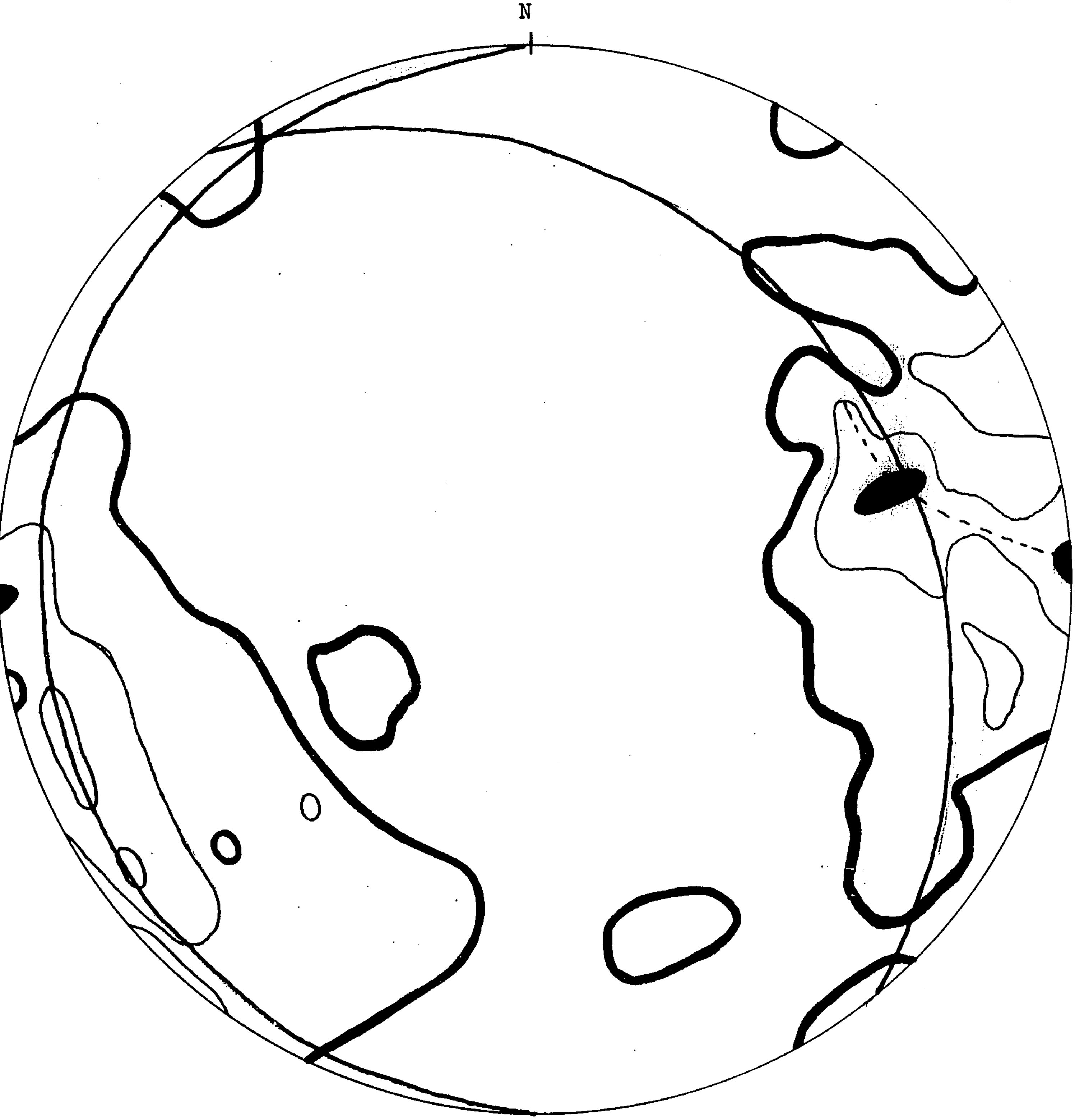

Macroscopic:

Mesoscopic stations homogeneous with respect to L_1 have been combined to form homogeneous macroscopic subareas. Measurements number from 75 to 300 in the 6 subareas which are keyed to the appropriate areas on Map 3b. The symmetry is generally monoclinic, with the highest degree of tirclinity being in Subarea 4.

constant, so these folds (F_2) are not truly "concentric" (Ramsay, 1960, p.77). Overturning and gentle F_2 cross-folding influence this L_1-subfabric pattern also but may be due to triaxial strain only. Overturning slightly to the west produces more gentle L_1 plunges to the NE and open, gentle F_2 folds which are nearly perpendicular to F_2 disperses the L_1-girdle about the great circle.

1). L_1 measurements are biased in this subarea.

2). L_1 and B_1 are not parallel at this subarea.

3). F_2 folds are less appressed and less "similar" in para-amphibolite than in migmatites. This difference in F_2 fold style may be related to the apparent differences in mean ductilities (Donath and Parker, 1964, pp.45-63).

Preferred Interpretation - Bias in L_1 measurements has been previously discussed (Text, pp. 74-75) and is not considered by the writer to be significant. As previously mentioned, the $L_1 \measuredangle B_1$ appears to be small in Subareas 3 and 4. Ramsay (1960, pp.75-93) has shown that "similar" folding deforms earlier rectilinear lineations into a great circle girdle, and that "concentric" folding disperses these lineations along partial small circle girdles. Field observations suggest that para-amphibolite has responded to deforming stresses in a less ductile manner than migmatites. Therefore, less appressed and more "concentric" F_2 folding might be anticipated in para-amphibolite. The L_1-girdle shows some tendency towards a partial small circle girdle. Note that the S_1-subfabric here suggests F_2 folds plunging gently south and overturned to the west. This orientation and folding intermediate between "similar" and "concentric" styles should produce a pattern nearly equivalent to the L_1-subfabric here (Donath and Parker, 1964, p.54). The $L_1 \measuredangle B_2$ is not

SUBAREA 1

General Statement

Location - West flank of Quad Creek synform, including Structure Stations 1 and 2 (Map 3b).

Areal Extent - Approximately 0.1 square miles.

Number of Measurements - 150 L_1 measurements.

Rock Type - Para-amphibolite.

Geologists - L.C. Rowan and C.E. Larsen.

Geometrical Analysis

Symmetry - Monoclinic.

Scale - Macroscopic.

Homogeneity - Homogeneous with respect to L_1.

L_1-girdle - (a). N72W, 30°NE.

Reliability- (a)-Good.

Maximum - (a). N15E, 32°NE.

Fold Geometry - L_1 is dispersed into a NW trending great circle girdle, which is very differently oriented than the B_1-girdle. The L_1-maximum plunges more gently NE than the B_1-maximum. The B_1- and L_1-subfabrics at Subareas 3 and 4 suggest that these linear elements are nearly parallel. Therefore, the following appear to be plausible reasons for the different geometric relations of B_1 and L_1:

SUBAREA 1.

150 L_1 Measurements
Contour Interval:
0.66-2.0-4.0-6.0%

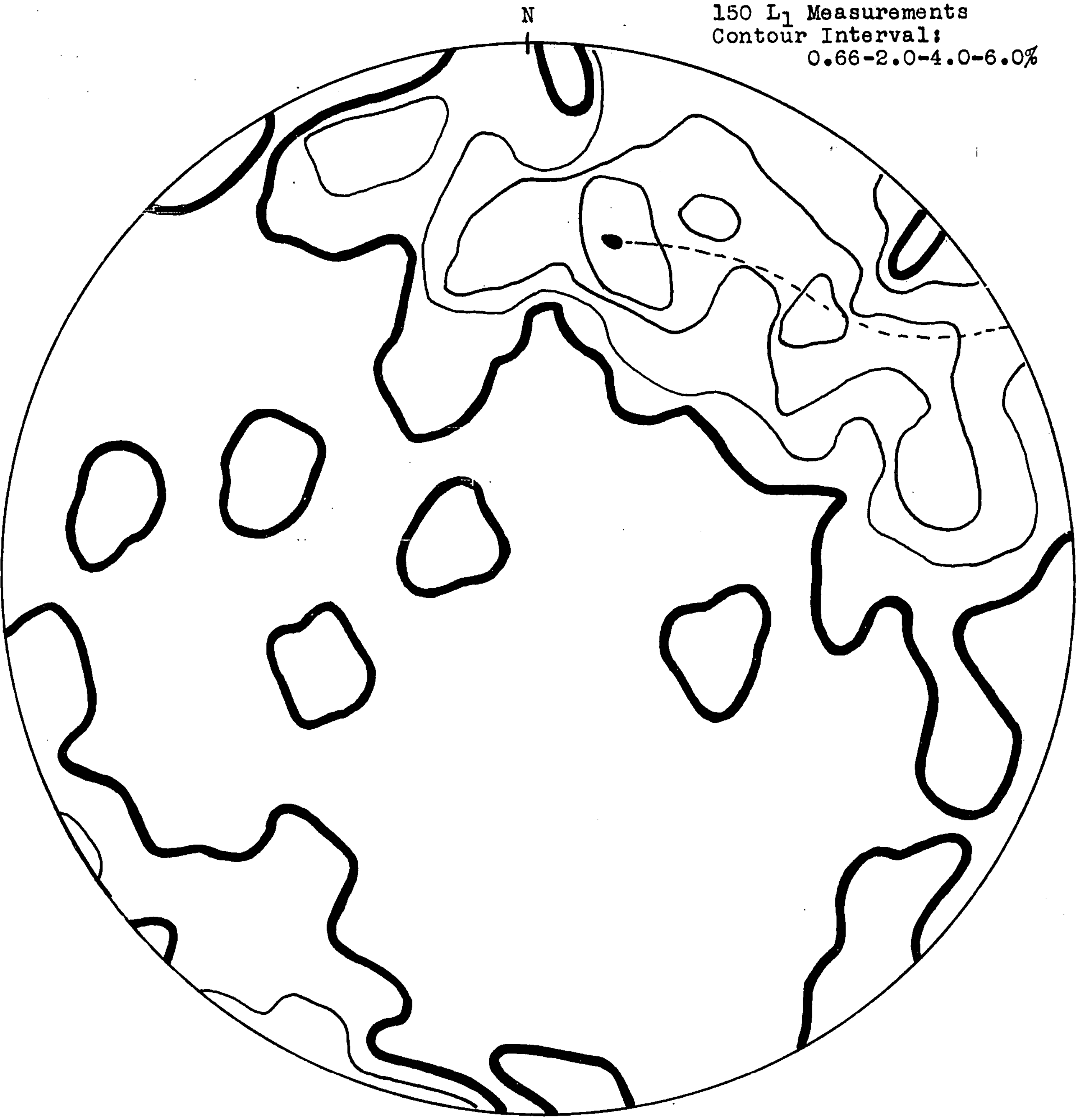

SUBAREA 2

General Statement

Location - Central portion of Quad Creek synform nose.

This subarea is equivalent to Structure Station 3 (Map 2b).

derived primarily from relatively non-ductile quartzites and para-amphibolites.

Preferred Interpretation - L_1 has been dispersed into a pattern which does not fit a great circle or small circle girdle. Ramsay (1960, pp.75-93) has shown that "concentric" folding of earlier lineations produces partial small cirele girdles, whereas "similar" folding disperses these lineations along great circle girdles. F_2 is not truly "concentric," since the $L_1 \measuredangle B_2$ is not constant (Ramsay, 1960, p.77). F_2 is overturned to the north here (S_2, Map 3a), which produces an almost complete small circle girdle in the southern half of the diagram in nearly "concentric" F_2 folds.

SUBAREA 3

General Statement

Location - Northeast portion of Quad Creek synform nose, including Stations 4 and 5 (Map 3b).

Areal Extent - Approximately 0.04 square miles.

Number of Measurements - 150 L_1 measurements.

Rock Type - Para-amphibolite.

Geologists - L.C. Rowan and C.E. Larsen.

Geometrical Analysis

Symmetry - Monoclinic.

Scale - Macroscopic.

Homogeneity - Homogeneous with respect to L_1.

L_1-girdle - (a). N20W, 40°SW.

Reliability-(a)-Good.

Maximum -(a). E-W, 30°W.

Fold Geometry - Approximately 90° rotation eastward from Subarea 1 to Subarea 3, then about 60 degrees rotation west in a vertical plane approximates the L_1-subfabric pattern in the subarea. The scatter is somewhat greater, and a small circle girdle is more strongly suggested in Subarea 3 than in number 1. Note that L_1 and B_1 patterns are very similar here, where the B_1 measurements were

SUBAREA 3.

150 L_1 Measurements
Contour Interval:
0.66-2.0-4.0-6.0%

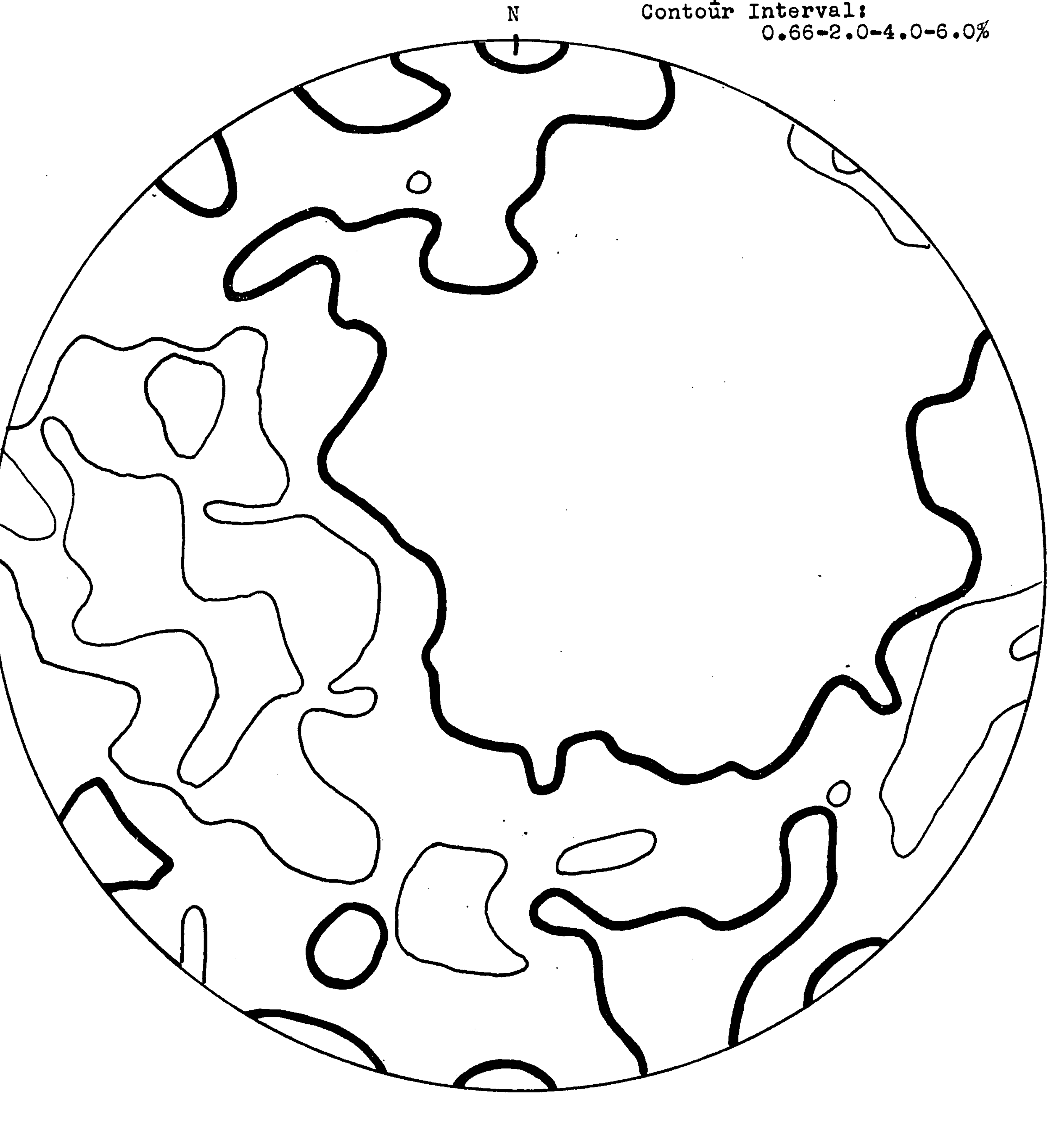

approximates a partial small circle girdle rather than a great circle girdle (Ramsay, 1960, pp.76-78). Note that B_2 plunges moderately S-SW, and S_2 dips steeply west (Map 3a). Open, gentle, east-plunging F_2 cross-folds are suggested by the S_o-subfabric (Map 3a). The writer believes that the large degree of L_1 scatter is due to the F_2 cross-folding. These folds are probably due to triaxial strain during F_2 folding.

1). L_1, B_1 and B_2 have rotated around the nose of the Quad Creek synform, and

2). These elements have been influenced by the plunge of this major F_2 fold.

L_1 plunges more gently south than B_1 (Map 3b) and is more widely dispersed about the great circle. B_1 is dispersed into a nearly vertical N-S partial great circle. This pattern is not evident in the L_1-subfabric here. These differences may be explained by one or a combination of the following factors;

1). L_1 measurements here are biased,

2). The $L_1 \measuredangle B_1$ is large,

3). Para-amphibolite blocks have been rotated during agmatization more than the ductile migmatites. Therefore, partial small circle L_1-girdles are developed by less "similar" and more "concentric" F_2 folds (Ramsay, 1960, pp.75-93).

Preferred Interpretation - Bias has been discussed previously (Text, pp. 74-75) and is not believed to be significant. B_1 and L_1 are believed to be nearly parallel at Subarea 3 where the mean ductilities are similar in para-amphibolite and quartzites. The writer prefers a combination of factors 3 and 4. "Concentricity" in F_2 folds produces dispersion of L_1 into a pattern which

SUBAREA 4

General Statement

Location - East flank of the Quad Creek synform, including Structure Stations 6, 7, 8 and 9 (Map 3b).

Areal Extent - Approximately 1.0 square miles.

Number of Measurements - 300 L_1 measurements.

Rock Type - Para-amphibolite.

Geologists - L.C. Rowan and C.E. Larsen.

Geometrical Analysis

Symmetry - Generally monoclinic.

Scale - Macroscopic.

Homogeneity - Homogeneous with respect to L_1.

L_1-girdle - (a). N76E, 20°S.

Reliability- (a)-Good.

Maximum - (a). S13E, 20°S.

Fold Geometry - The geometrical relations of L_1 and F_2 are more clearly defined on the macroscopic than the mesoscopic scale in this subarea. Note that rotation of the Subarea 3 L_1-subfabric 80° N in a horizontal plane and about 40° S in a vertical plane approximates the L_1-subfabric pattern at this subarea. Two important implications are made by this rotation:

SUBAREA 4.

300 L₁ Measurements
Contour Interval: 1-3-5-7%

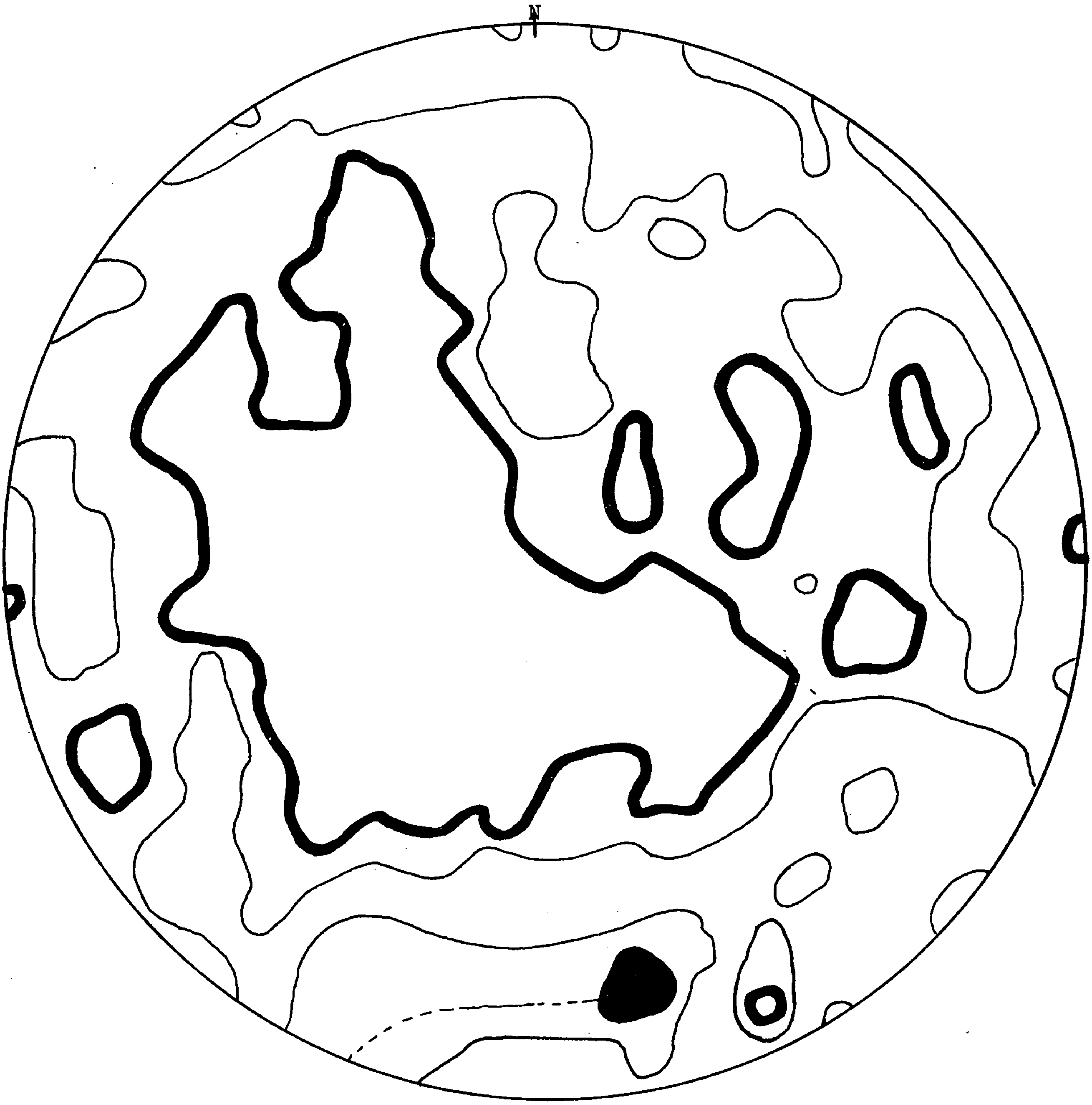

SUBAREA 5

General Statement

Location - Southeast portion of the Wyoming Creek antiform nose. This subarea is equivalent to Structure Station 10 (Map 2b).

SUBAREA 6

General Statement

Location - South flank of the Wyoming Creek antiform, including Structure Stations 11 and 12 (Map 3b).

Areal Extent - Approximately 0.3 square miles.

Number of Measurements - 150 L_1 measurements.

Rock Types - Para-amphibolite.

Geologists - L.C. Rowan, C.E. Larsen and T. Rowekamp.

Geometrical Analysis

Symmetry - Monoclinic.

Scale - Macroscopic.

Homogeneity - Homogeneous with respect to L_1.

L_1-girdle - (a). N43W, 30°NE ; (b). N70W, 30°SW.

Reliability- (a)-Good ; (b)-Good.

Maximum - (a). N64E, 10°NE.

Fold Geometry - L_1 has rotated about 45° NE from Subarea 5 to 6 in the plane of S_0. Although two great circle girdles are constructed, partial small circle girdles are suggested. The L_1 pattern differs from the B_1-subfabric in that few NE plunging B_1-axes were measured. Text Figure 41 shows the orientation of slightly "concentric" F_2 folds here. Very significantly, L_1 rotates around both major F_2 folds.

SUBAREA 6.

150 L_1 Measurements
Contour Interval:
0.66-2.0-4.0-6.0%

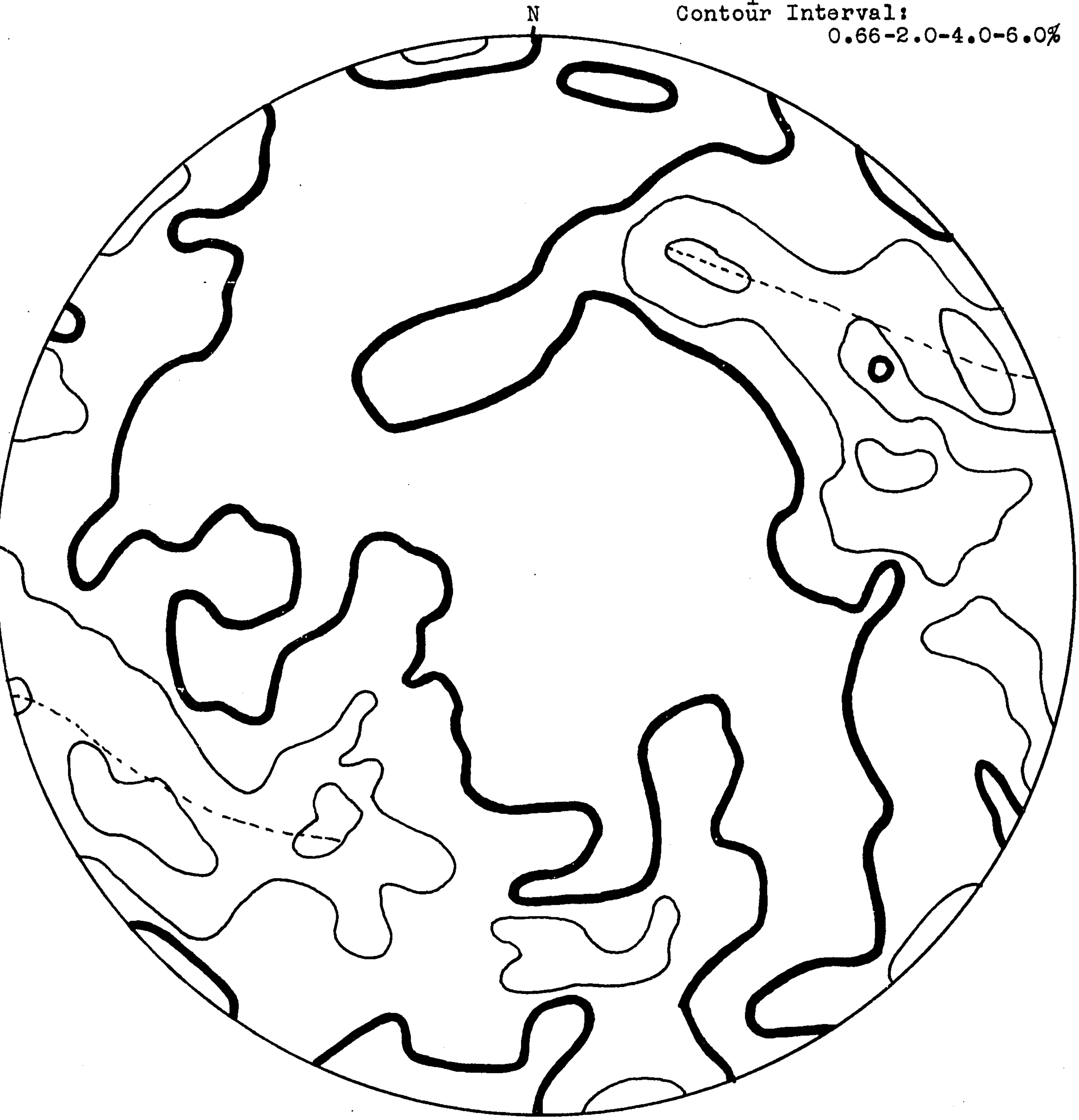

SUMMARY

<u>L_1-subfabric</u> - L_1 is generally parallel to B_1, but nearly "concentric" F_2 folds have formed in the relatively non-ductile para-amphibolite. L_1-girdles generally trend perpendicular to the S_o-plane and the B_1-girdle, because the nearly "concentric" F_2 folds have dispersed L_1 into partial girdles which more nearly approach small circles than great circles. The L_1-subfabric is dispersed by agmatization, especially in the east flank of the Quad Creek synform. L_1 rotates around the Quad Creek synform nose and converges on the major axial zone, while it only rotates around the Wyoming Creek antiform nose. Therefore, the L_1-subfabric mimics the B_1-subfabric when contrasting mean ductilities and F_2 fold styles in para-amphibolite and migmatites are considered except at Station 10. The two subfabrics are nearly identical at Stations 3, 4 and 5, where B_1 was measured in non-ductile quartzites and para-amphibolite. The writer concludes that the subfabrics are similar here because B_1 and L_1 measurements have been derived from rocks with similar mean ductilities. The F_2 folds appear to have formed through flexural flow at these stations. The parallelism of L_1 and B_1 suggests synchronous development of these lineations.

Although measurements of skialith elongations are sparse, the data suggest parallelism of these lineations with B_1 and hornblende elongations. It is, therefore, concluded that skialiths assumed their orientation during F_1 folding.

L_2 measurements are from drawn-out green mica and biotite aggregates. Although they are sparse, they are nearly coincident with B_2.

APPENDIX VI

B_2-Subfabric

Mesoscopic:

B_2 measurements number from 3 to 17 at stations where F_1 and F_2 are separable. No B_2 measurements are given for Stations 1, 4, 6, 7, 8, 9 and 11, because F_1 and F_2 are not easily distinguished in these sub-domains. Most of the B_2-axes at Stations 2, 3 and 5 have been derived from samples showing refolding of F_1. Uncontoured data are keyed to the appropriate areas on Map 2b. B_2-subfabric symmetry ranges from axial at Structure Station 3 to monoclinic at Station 10.

<u>Preferred Interpretation</u> - Although both of these alternatives may explain the B_2-girdle, the writer prefers number 2. Gentle, open F_2 folds are suggested by the S_o- and S_1-subfabric at this station but may be due to superposition of F_2 on F_1. Alternately, the spread of S_2 poles and Text Figure 4 suggest that both large and small F_2 folds are slightly non-cylindrical and non-plane. The writer believes this to be due to triaxial strain.

STRUCTURE STATION 2

General Statement

<u>Location</u> - Northwest portion of Quad Creek synform nose (Map 2b).

<u>Areal Extent</u> - Approximately 2,000 square yards.

<u>Number of Measurements</u> - 6 B_2 measurements from samples showing refolding of F_1.

<u>Rock Types</u> - Migmatites and quartzites.

<u>Geologists</u> - L.C. Rowan and C.E. Larsen.

Geometrical Analysis

<u>Symmetry</u> - Monoclinic.

<u>Scale</u> - Mesoscopic.

<u>Homogeneity</u> - Homogeneous with respect to B_2.

<u>B_2-girdle</u> - (a). E-W, nearly horizontal.

<u>Reliability</u> - (a)-Good.

<u>Maximum</u> - (a). South, nearly horizontal.

<u>Fold Geometry</u> - B_2 is closely coincident with the βS_{1c}- and βS_{0b}-axes at this station. However, B_2 does exhibit some dispersion into an ill-defined girdle which may be explained by

(1). F_2 folds plunging steeply east have deformed B_2, or

(2). The B_2 divergence is due to superposition of F_1 and F_2 (Turner and Weiss, 1963, p.132).

STRUCTURE STATION 2.

6 B_2 Measurements

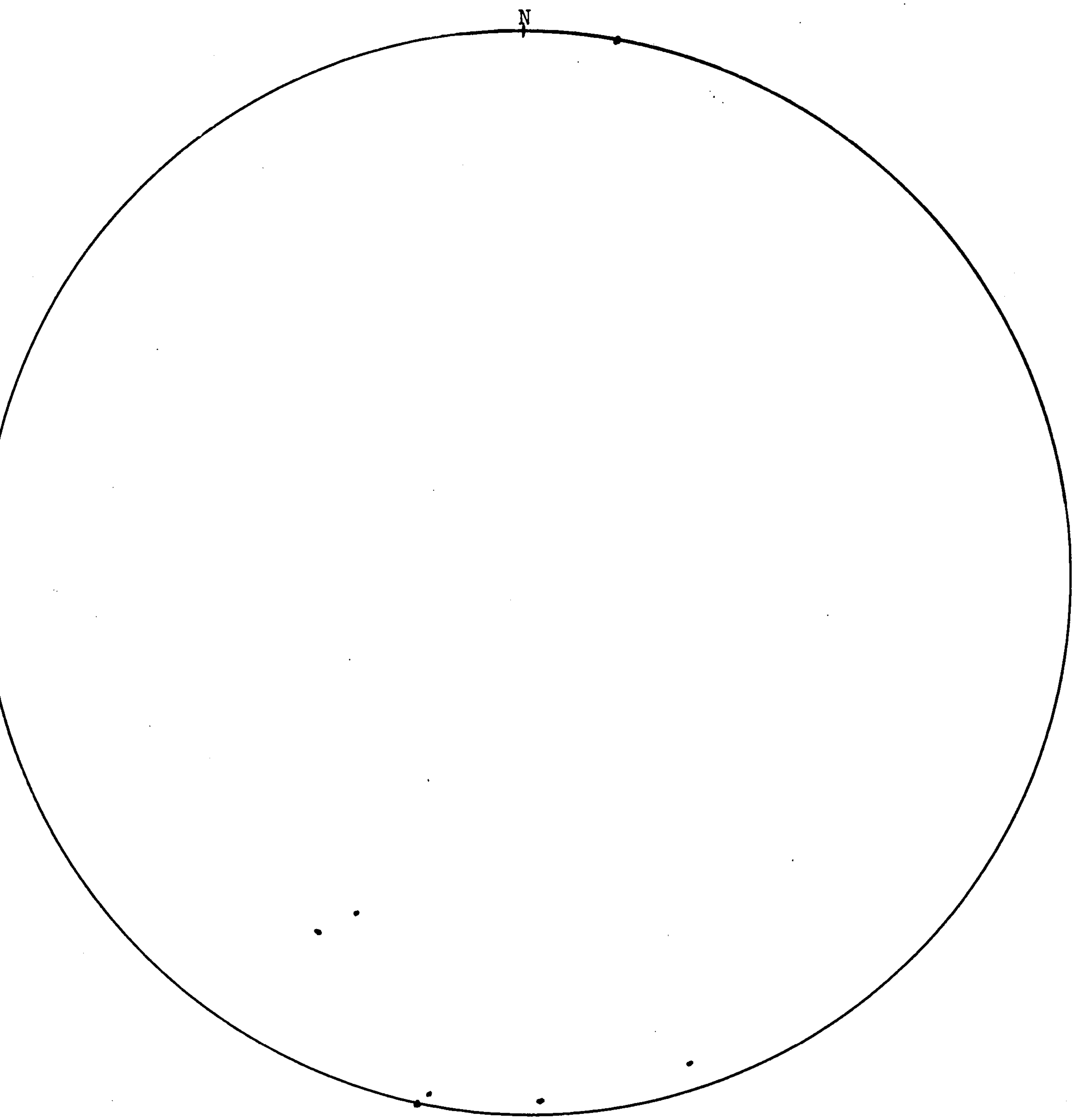

STRUCTURE STATION 3

General Statement

Location - Nose of Quad Creek synform (Map 2b).

Areal Extent - Approximately 3,000 square yards.

Number of Measurements - 3 B_2 measurements from oriented samples showing refolding.

Rock Type - Migmatites and quartzites.

Geologists - L.C. Rowan and C.E. Larsen.

Geometrical Analysis

Symmetry - Axial.

Scale - Mesoscopic.

Homogeneity - Homogeneous with respect to B_2.

Maximum - (a). S80E, 12°SE.

Remarks - Note that B_2 agrees closely with βS_{0a}- and βS_1-axes, and all of these elements rotate around the Quad Creek synform nose.

STRUCTURE STATION 3.

3 B_2 Measurements

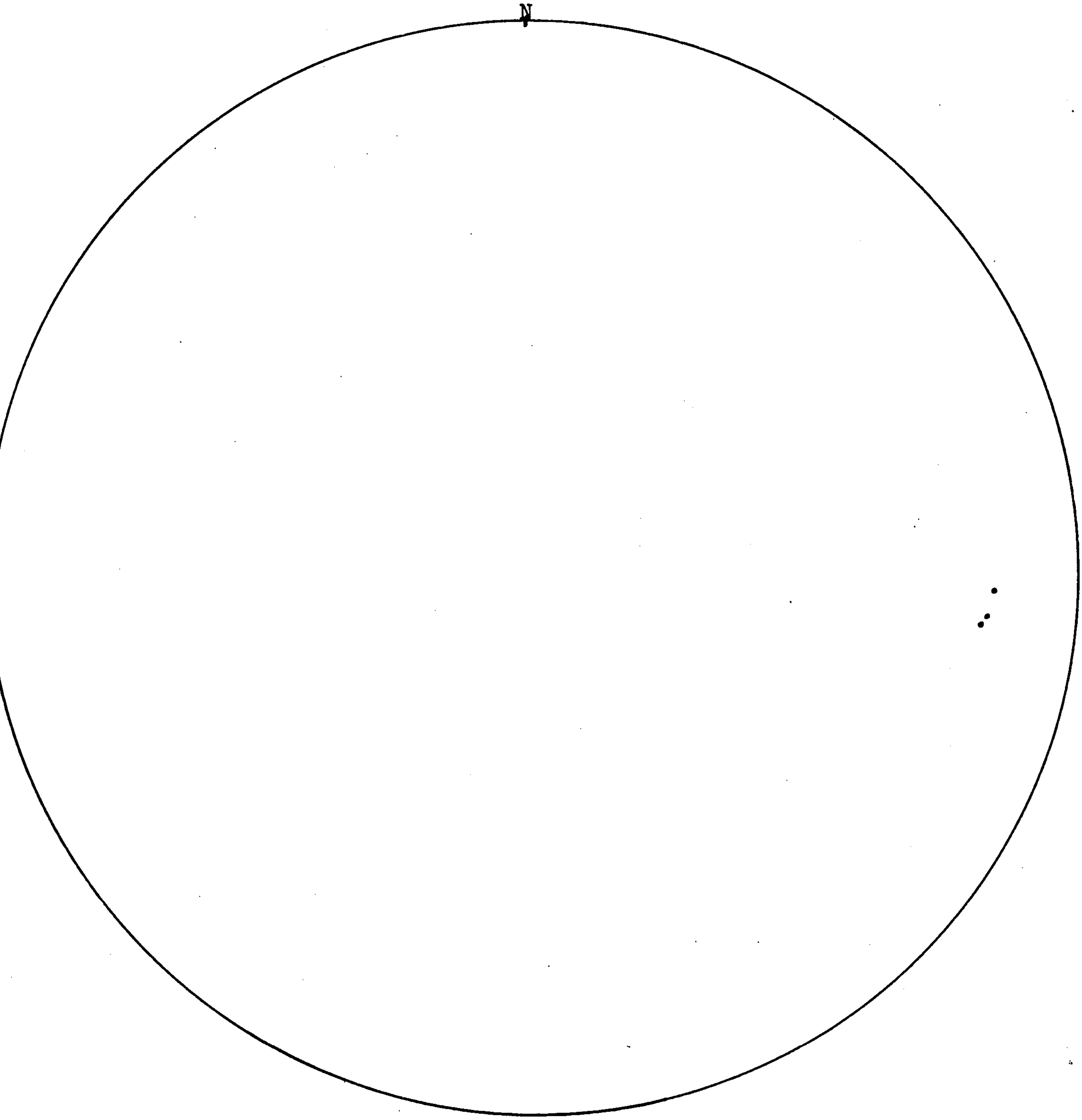

STRUCTURE STATION 5

General Statement

Location - Northeast portion of Quad Creek synform nose (Map 2b).

Areal Extent - Approximately 250 square yards.

Number of Measurements - 6 B_2 measurements, 3 of which are from oriented samples showing refolding.

Rock Types - Quartzites.

Geologists - L.C. Rowan and C.E. Larsen.

Geometrical Analysis

Symmetry - Axial.

Scale - Mesoscopic.

Homogeneity - Homogeneous with respect to B_2.

Maximum - (a). S83E, 8°SE.

Remarks - These B_2 measurements agree closely with the βS_1-axis here and show farther rotation around the Quad Creek synform nose.

STRUCTURE STATION 5.

6 B_2 Measurements

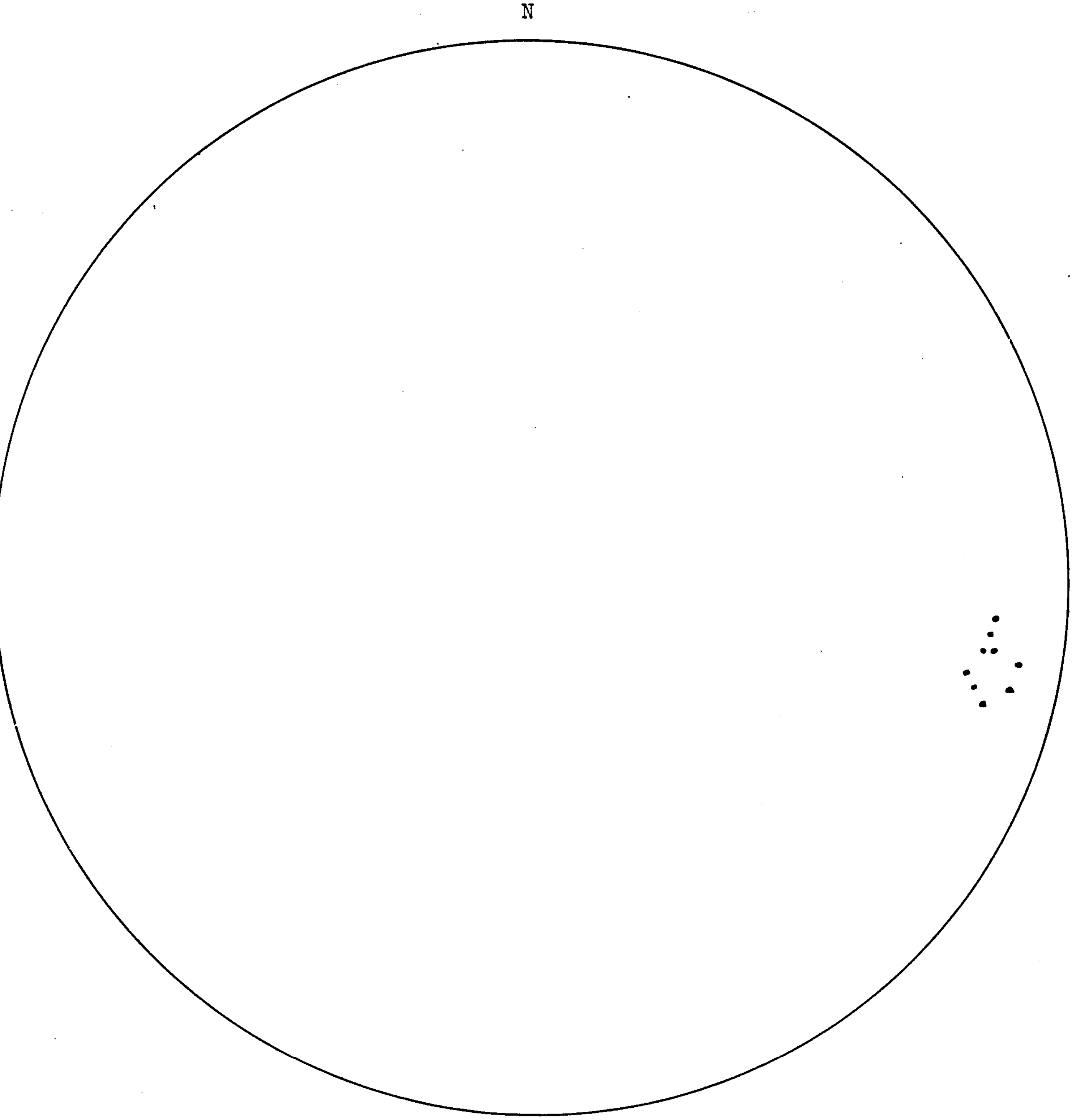

STRUCTURE STATION 10

General Statement

Location - Southeast portion of Wyoming Creek antiform (Map 2b).

Areal Extent - Approximately 16,000 square yards.

Number of Measurements - 16 B_2 measurements.

Rock Types - Migmatites, quartzites and agmatites.

Geologists - L.C. Rowan and C.E. Larsen.

Geometrical Analysis

Symmetry - Nearly axial.

Scale - Mesoscopic.

Homogeneity - Homogeneous with respect to B_2.

Maximum - (a). S23W, 45°SW.

Remarks - The scatter of B_2 may be due to slight warping which is younger than F_2 or to superposition of F_2 on F_1 (Turner and Weiss, 1963, p.132). S_2 (Map 2a) suggests very gentle warping. However, this warping may have been nearly synchronous with F_2 folding.

STRUCTURE STATION 10.

16 B_2 Measurements

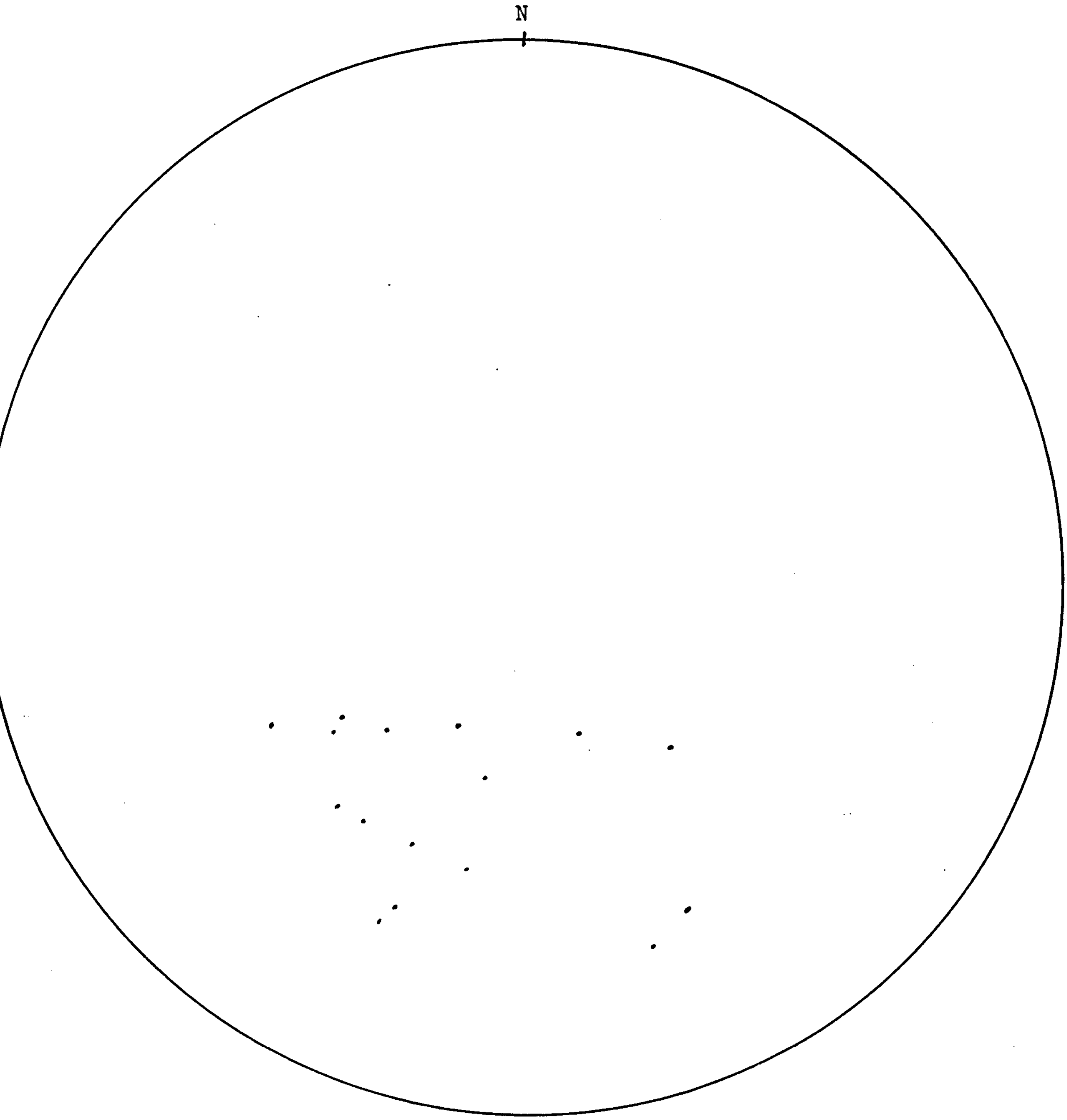

STRUCTURE STATION 12

General Statement

Location - South flank of Wyoming Creek antiform (Map 2b).

Areal Extent - Approximately 100,000 square yards.

Number of Measurements - 17 B_2 measurements.

Rock Types - Quartzites, para-amphibolite and micaceous schists.

Geologists - L.C. Rowan and C.E. Larsen.

Geometrical Analysis

Symmetry - Nearly axial.

Scale - Mesoscopic.

Homogeneity - Homogeneous with respect to B_2.

Maximum - (a). S35W, 55°SW.

Remarks - Comments made regarding the B_2-subfabric at Station 10 are applicable here.

STRUCTURE STATION 12.

17 B_2 Measurements

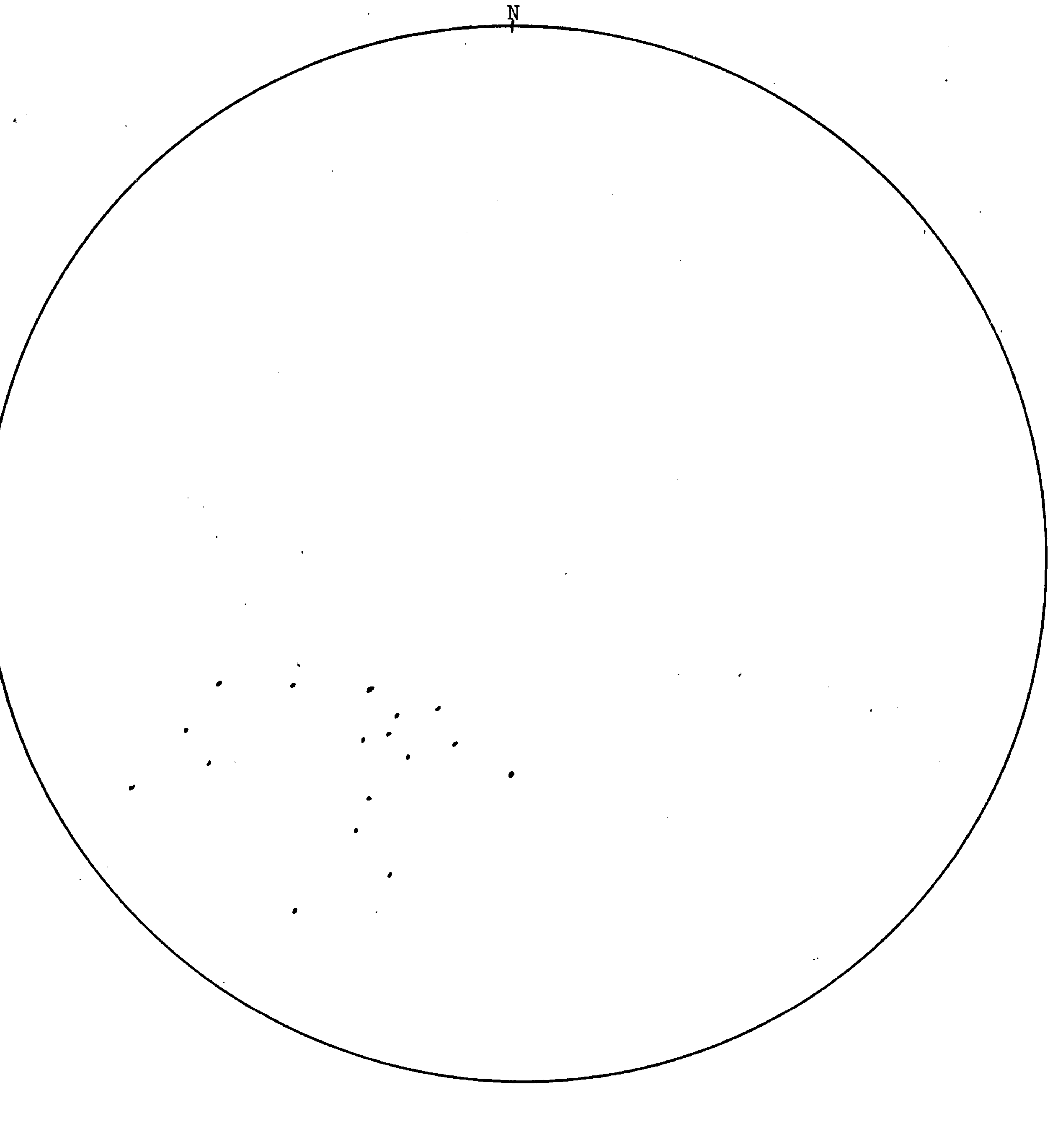

Macroscopic:

Three subareas have been constructed by combining stations homogeneous with respect to B_2. Map 3b shows the uncontoured data keyed to the appropriate areas. The macroscopic B_2-subfabric symmetry is axial in Subarea 2 and monoclinic in Subareas 1 and 3.

SUBAREA 1

General Statement

Location - West flank of Quad Creek synform, including Structure Station 2 (Map 3b).

Areal Extent - Approximately 0.1 square miles.

Number of Measurements - 6 B_2 measurements.

Rock Types - Pink biotite migmatite and quartzites.

Geologists - L.C. Rowan and C.E. Larsen.

Geometrical Analysis

This subarea is equivalent to Structure Station 2.

SUBAREA 1.

6 B_2 Measurements

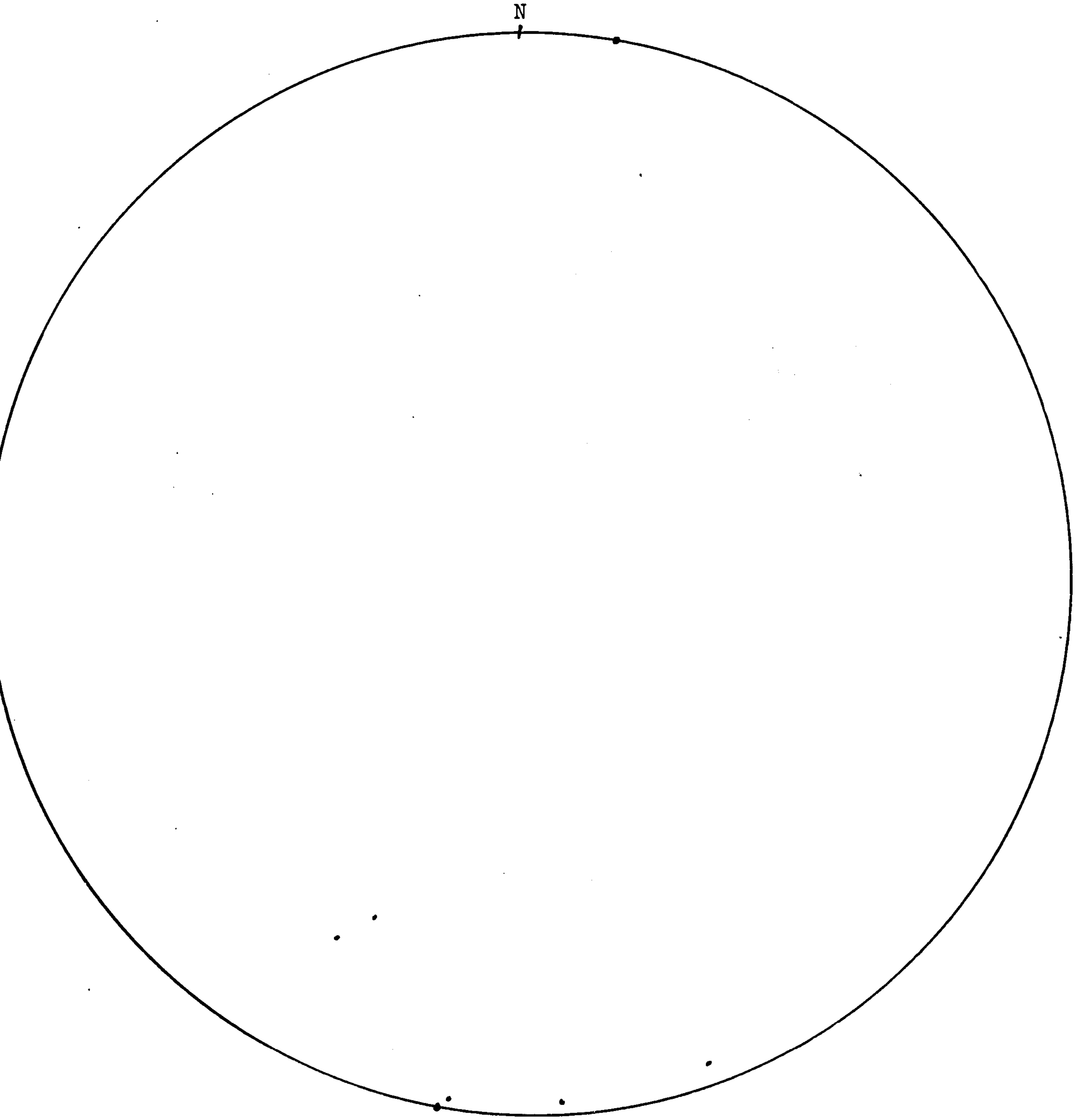

SUBAREA 2

General Statement

Location - Nose of Quad Creek synform, including Structure Stations 3 and 5 (Map 3b).

Areal Extent - Approximately o.1 square miles.

Number of Measurements - 9 B_2 measurements, 3 of which are from oriented samples showing refolding of F_1.

Rock Types - Quartzites and migmatites.

Geologists - L.C. Rowan and C.E. Larsen.

Geometrical Analysis

Symmetry - Axial.

Scale - Macroscopic.

Homogeneity - Homogeneous with respect to B_2.

Maximum - (a). S80E, 10°SE.

Remarks - Although B_2 is homogeneous here, it rotates in strike around the Quad Creek F_2 synform nose.

SUBAREA 2.

9 B2 Measurements

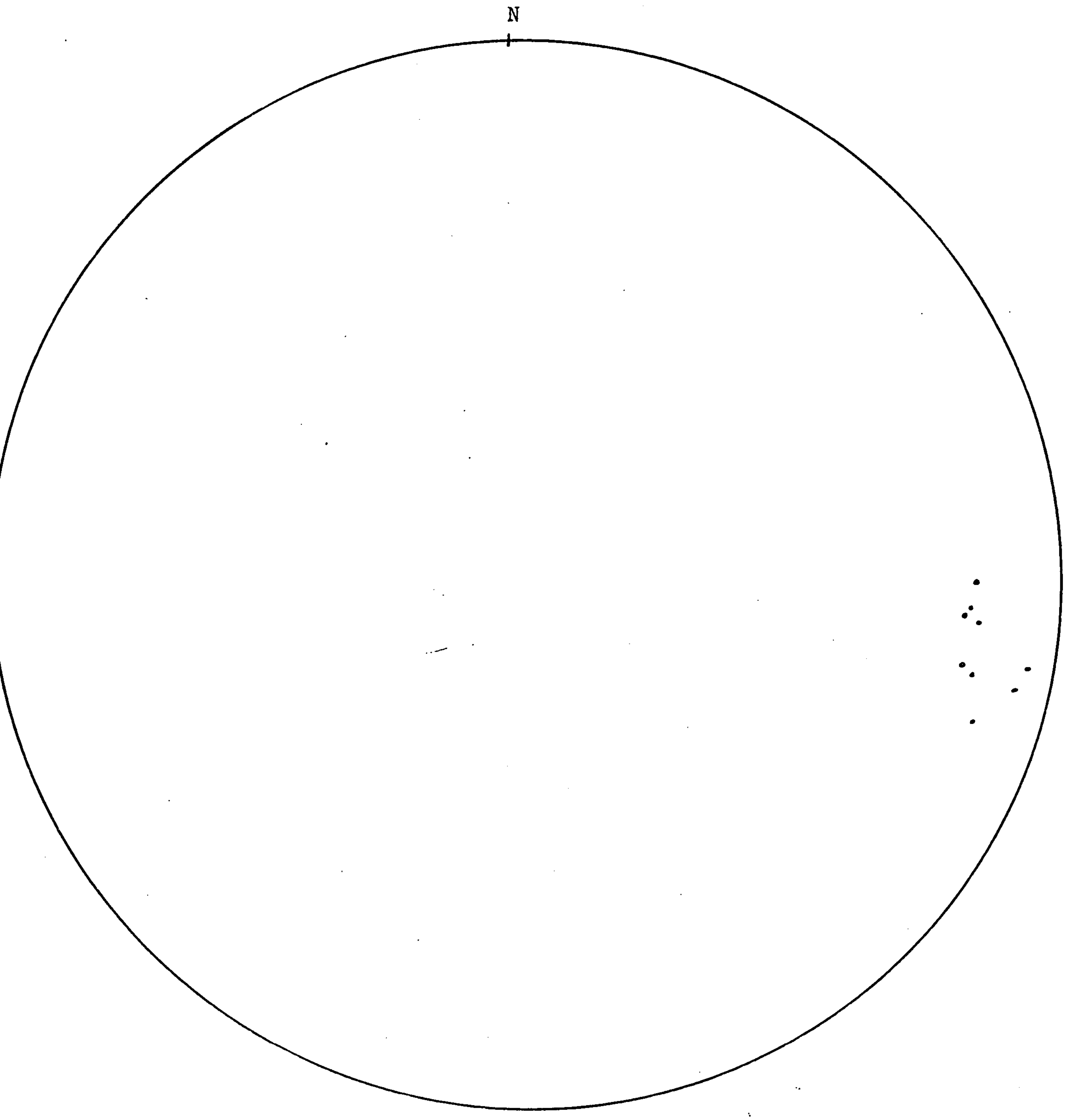

SUBAREA 3

General Statement

Location - Nose and flanks of Wyoming Creek antiform, including Structure Stations 8, 10 and 12 (Map 3b).

Areal Extent - Approximately 1.1 square miles.

Number of Measurements - 25 B_2 measurements.

Rock Types - Pink biotite migmatites, quartzites and para-amphibolite.

Geologists - L.C. Rowan and C.E. Larsen.

Geometrical Analysis

Symmetry - Nearly axial.

Scale - Macroscopic.

Homogeneity - Homogeneous with respect to B_2.

Maximum - (a). S35W, 57°SW.

Remarks - The dispersion of B_2 may be due to superposition. However, S_2 is also dispersed, suggesting that these F_2 folds are non-cylindrical and non-plane. The writer believes that this is due to triaxial strain during F_2 folding, but it may be due to a later (F_3) deformation.

SUBAREA 3.

37 B_2 Measurements

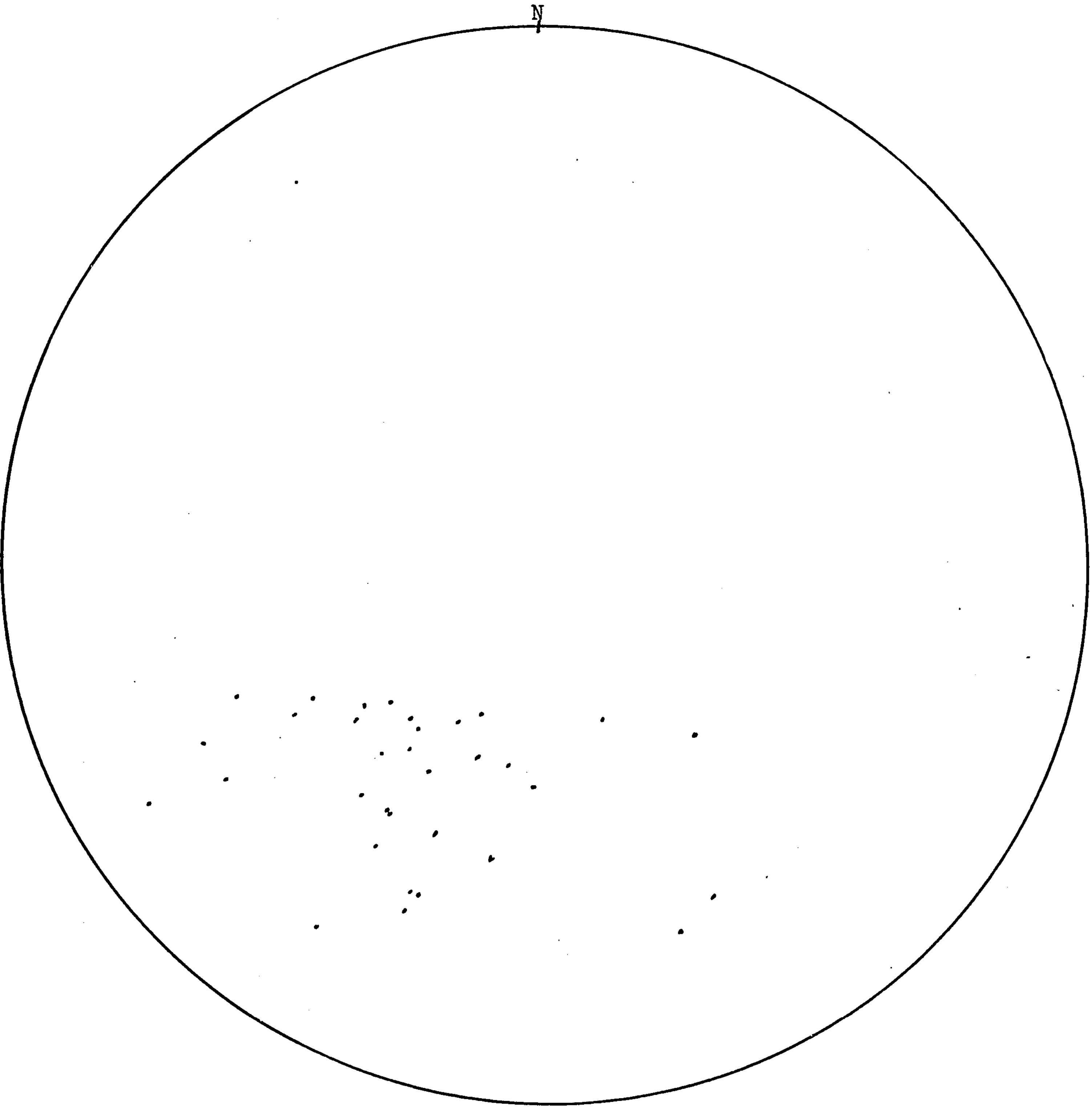

SUMMARY

$\underline{B_2\text{-subfabric}}$ - B_2 measurements are not available at stations where F_1 and F_2 are not separable and are scarce at the other stations. However, the data are sufficient to demonstrate rotation of 90° around the Quad Creek synform nose. In contrast, B_2 strike parallel to the Wyoming Creek antiform axis, and F_2 folds appear to be parasitically related to the major antiform. As previously stated, B_1 and L_1 are generally parallel with B_2, but the largest divergence in strike is approximately 37 degrees at Station 12. The difference in B_1 and B_2 dips may be about 30° here. F_1 and F_2 appear to be nearly coaxial at Stations 6, 7, 8, 9 and 10. Strikes are approximately parallel at Stations 1, 2, 3, 4 and 5, but the B_1-B_2 dip separation is about 35° when measured from the horizontal.

MAP 1 GEOLOGIC MAP OF

LEGEND

CRETACEOUS

L FELSIC PORPHYRY

PRECAMBRIAN

PM PINK BANDED MIGMATITE
GM GRAY BANDED MIGMATITE
PG PINK GRANITIC GNEISS
GG GRAY GRANITIC GNEISS
Q QUARTZITE
A PARA-AMPHIBOLITE
O ORTHO-AMPHIBOLITE
AG AGMATITE
I IRON-SILICATE ROCK
BS BIOTITE SCHIST AND GNEISS
P GRANITIC PEGMATITE
U ULTRAMAFIC ROCKS
DO MAFIC DIKES
M METANORITE
FM FINE-GRAINED METANORITE

SYMBOLS

STRIKE AND DIP OF FOLIATION BANDING, S_0
STRIKE AND DIP OF VERTICAL FOLIATION AND BANDING, S_0
OBSERVED CONTACT
INTERPRETED CONTACT
TRANSITIONAL CONTACT
F_1 SYNFORM AXIS
F_2 SYNFORM AXIS
F_2 ANTIFORM AXIS
FAULT, ARROW INDICATES RELATIVE HORIZONTAL MOVEMENT
200' CONTOUR INTERVAL

SCALE 1:2400

MAP OF THE QUAD-WYOM

ANDING, S_0

LIATION AND BANDING, S_0

HORIZONTAL MOVEMENT

QUAD-WYOMING-LINE CREE

AD-WYOMING-LINE CREEKS A

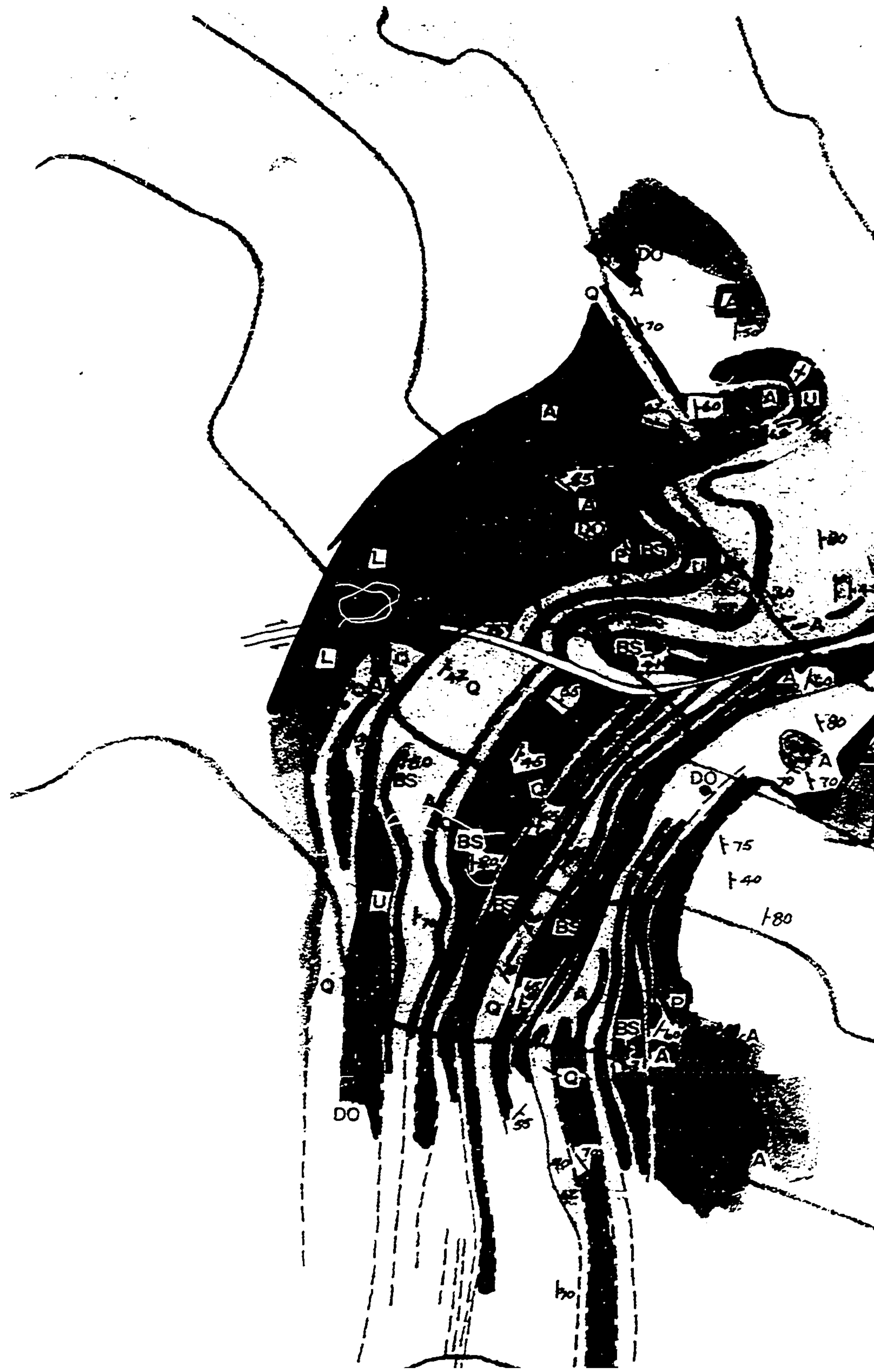

CREEKS AREA


9,200
9,600
LINE
LAKE

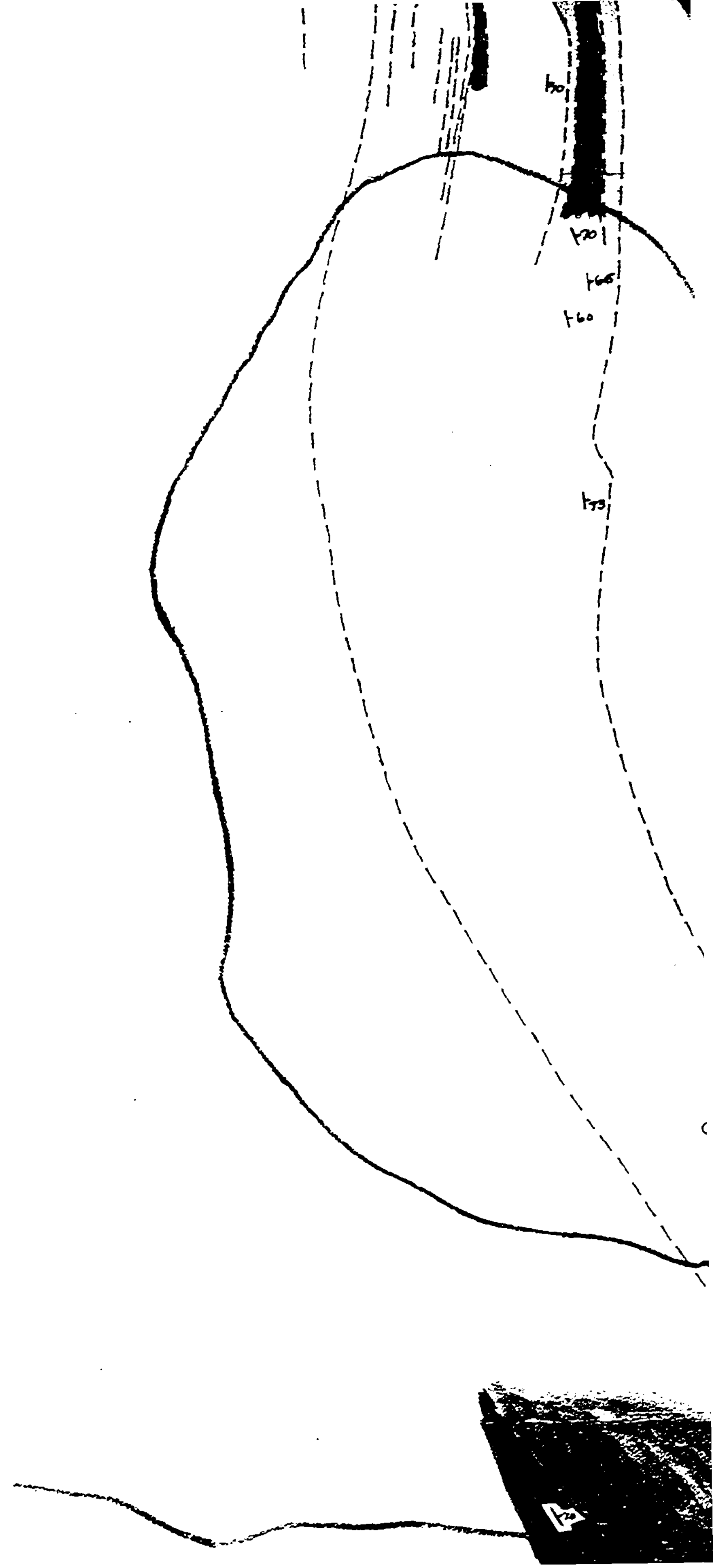


10,000
Q
A'
A
DO
QT
DO
A
A
DO

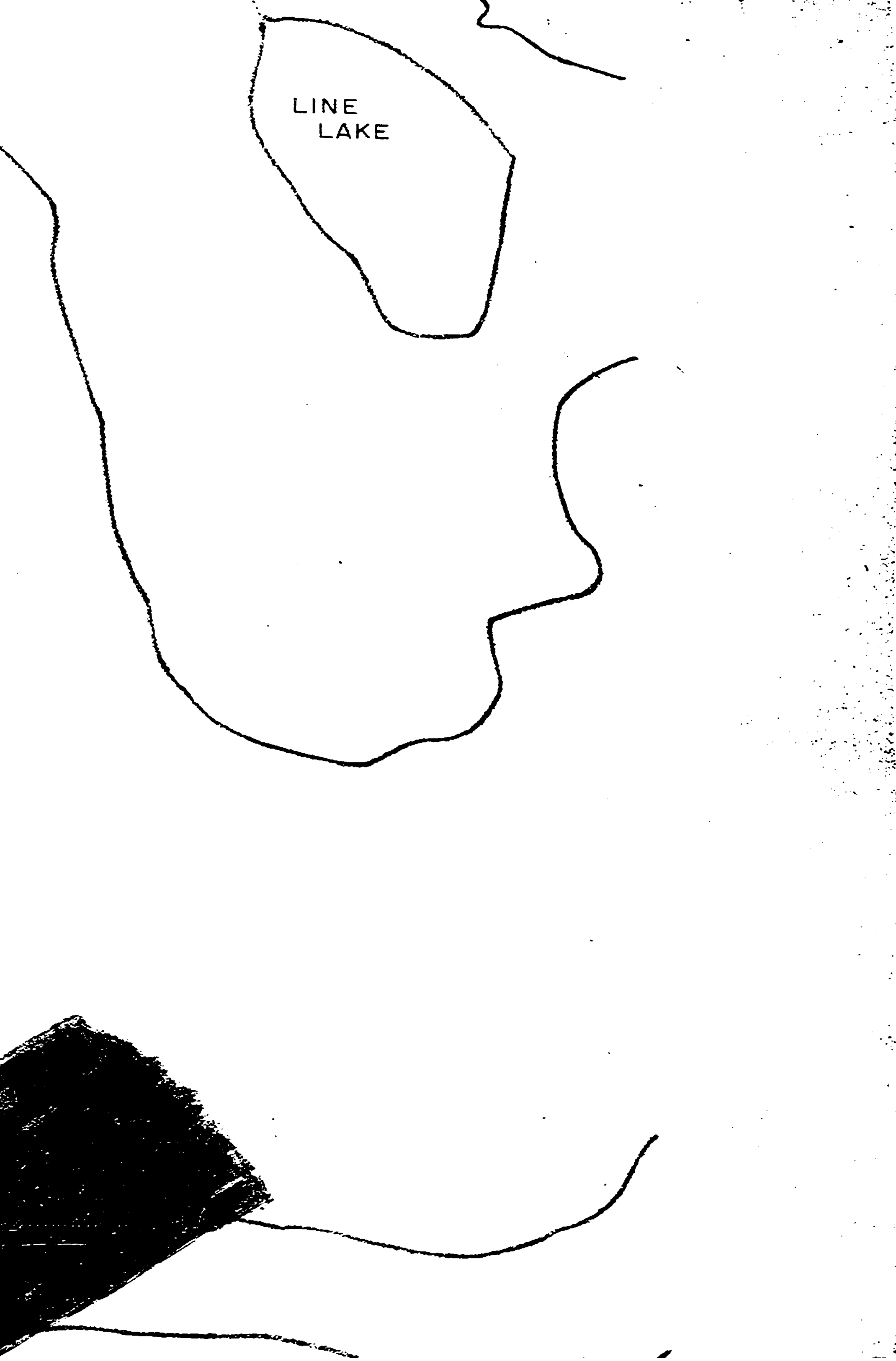
LINE
LAKE

9,600
9,600
A
Q
A


A
Q
DO
L
P
AG


A
Q
P
DO


A
10,000'
9,800'
9,600'
9,400'
9,200'

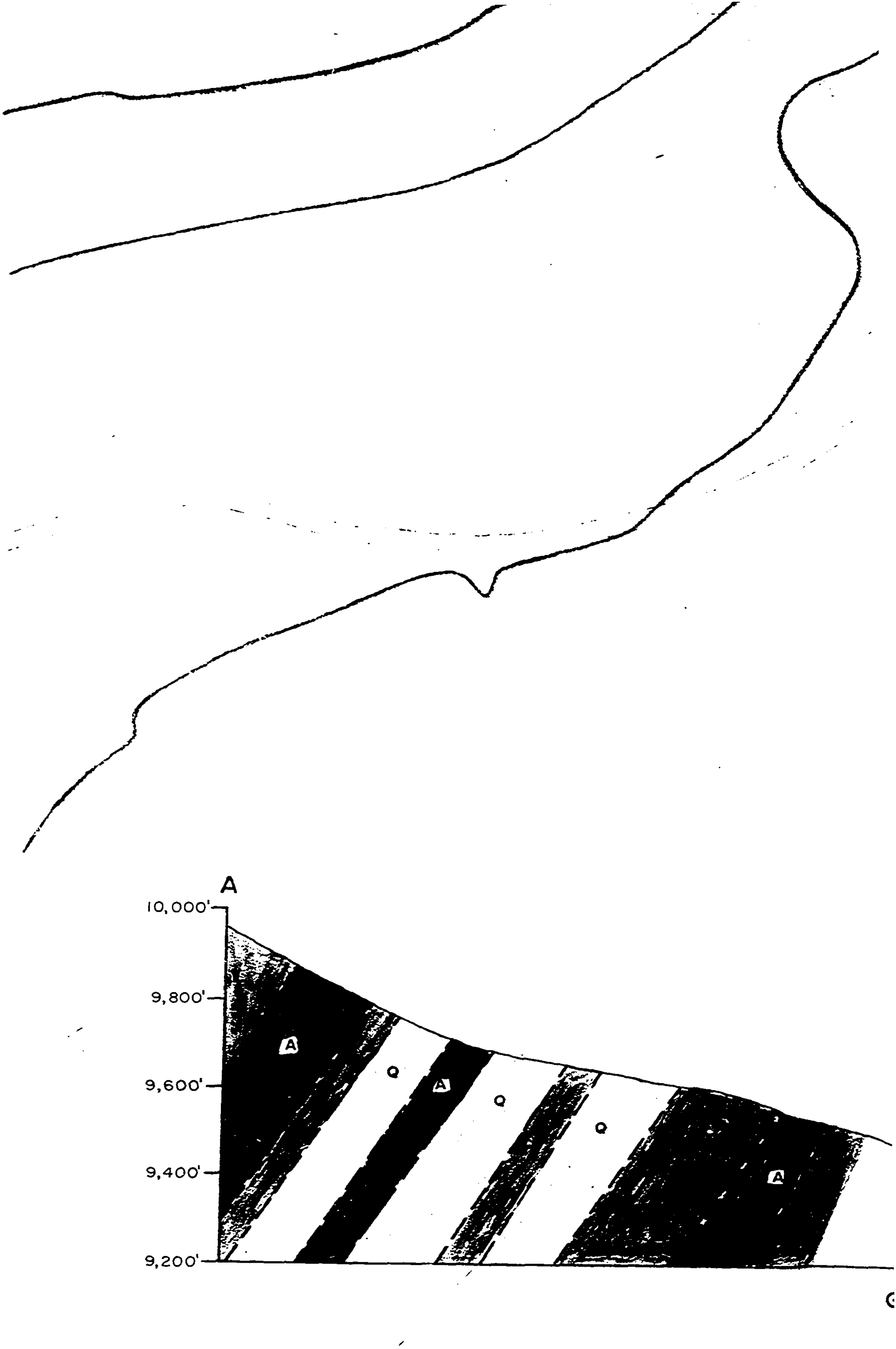
A
10,000'
9,800'
9,600'
9,400'
9,200'
A
Q
A
Q
Q
A

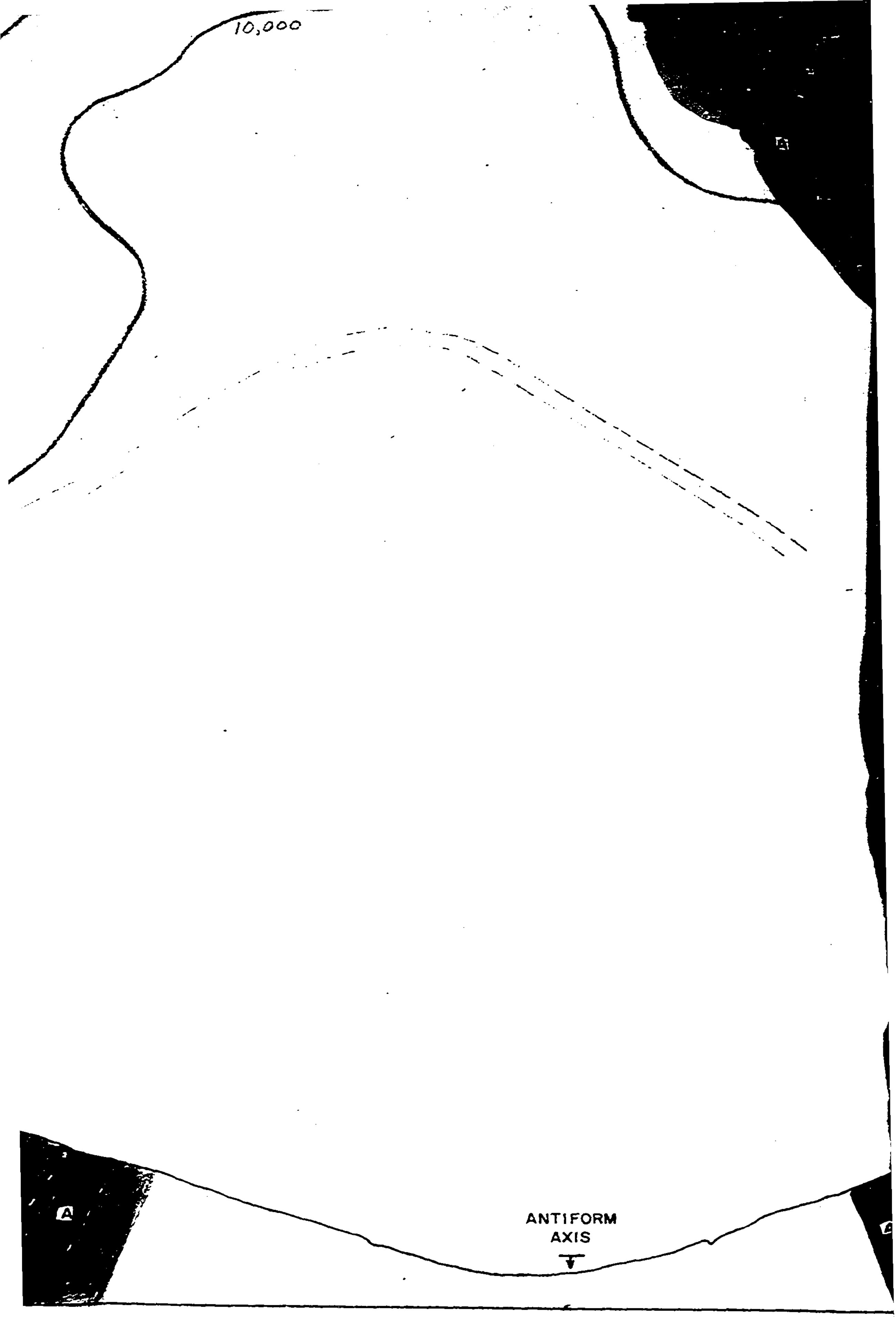

GENERALIZED CROSS-SECTION A-A'

GENERALIZED CROSS-SECTION A-A'

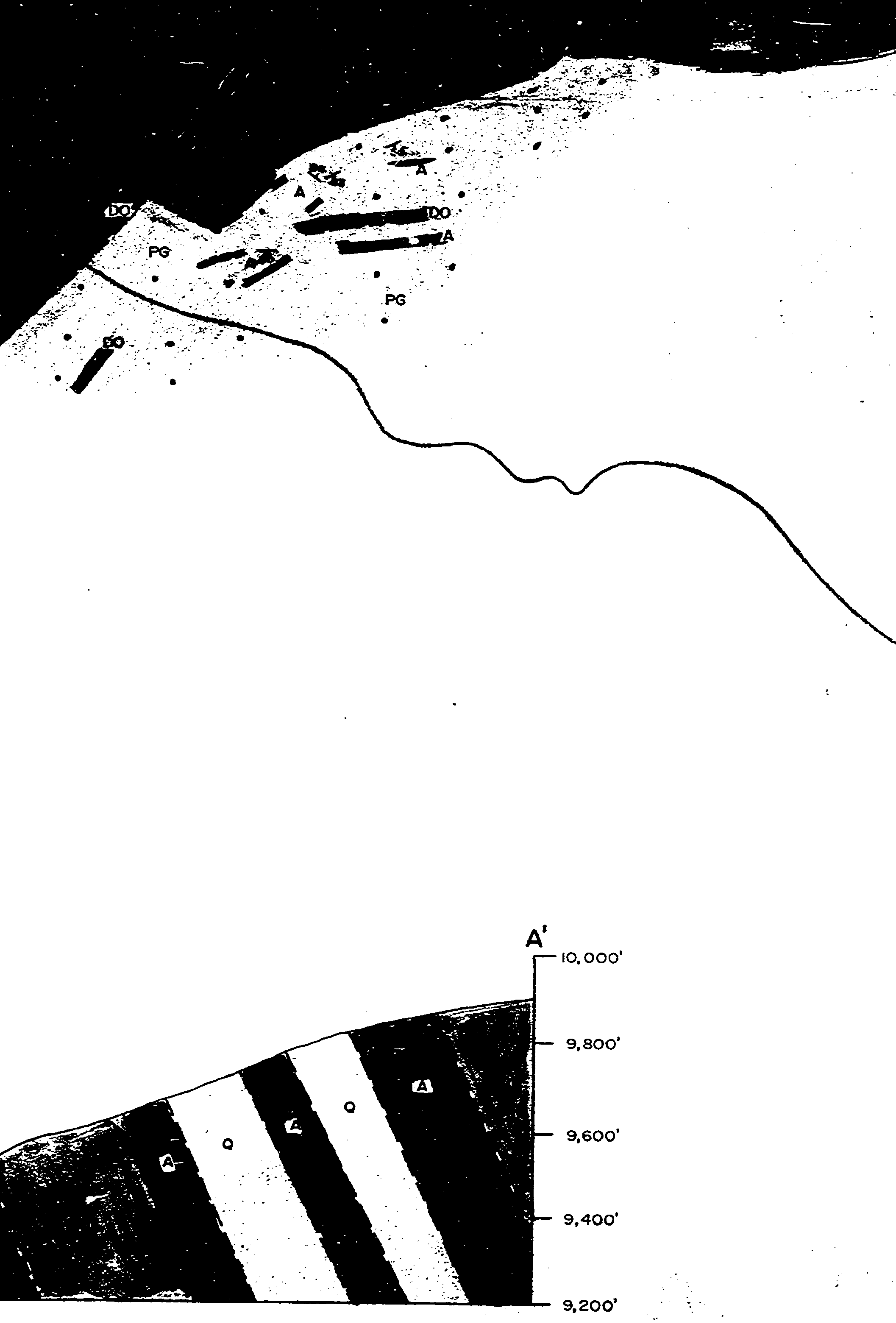
DO
A
A
DO
A
PG
PG
DO
A'
10,000'
9,800'
9,600'
9,400'
9,200'
A
Q
A
Q
A

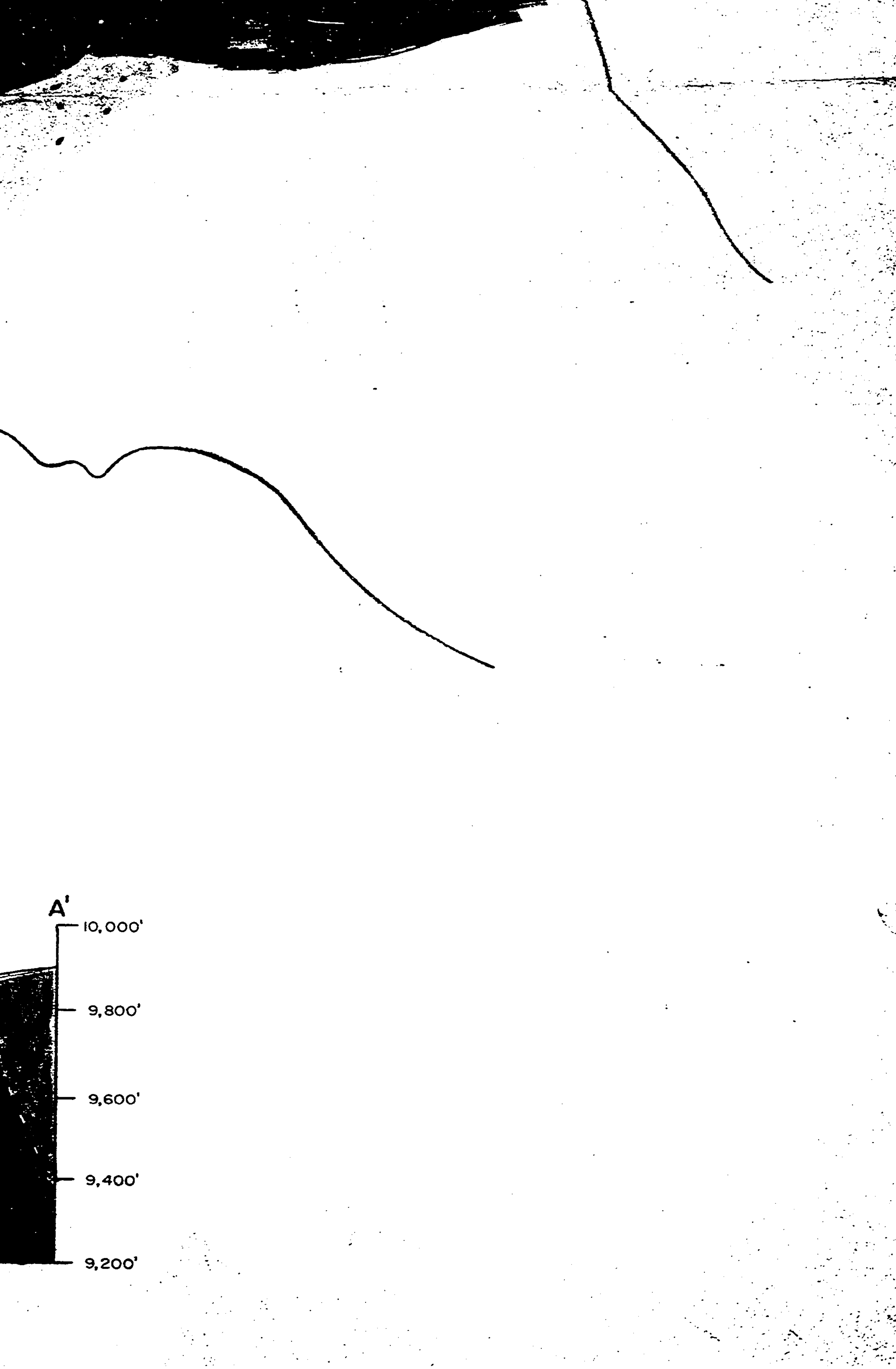
A'
10,000'
9,800'
9,600'
9,400'
9,200'

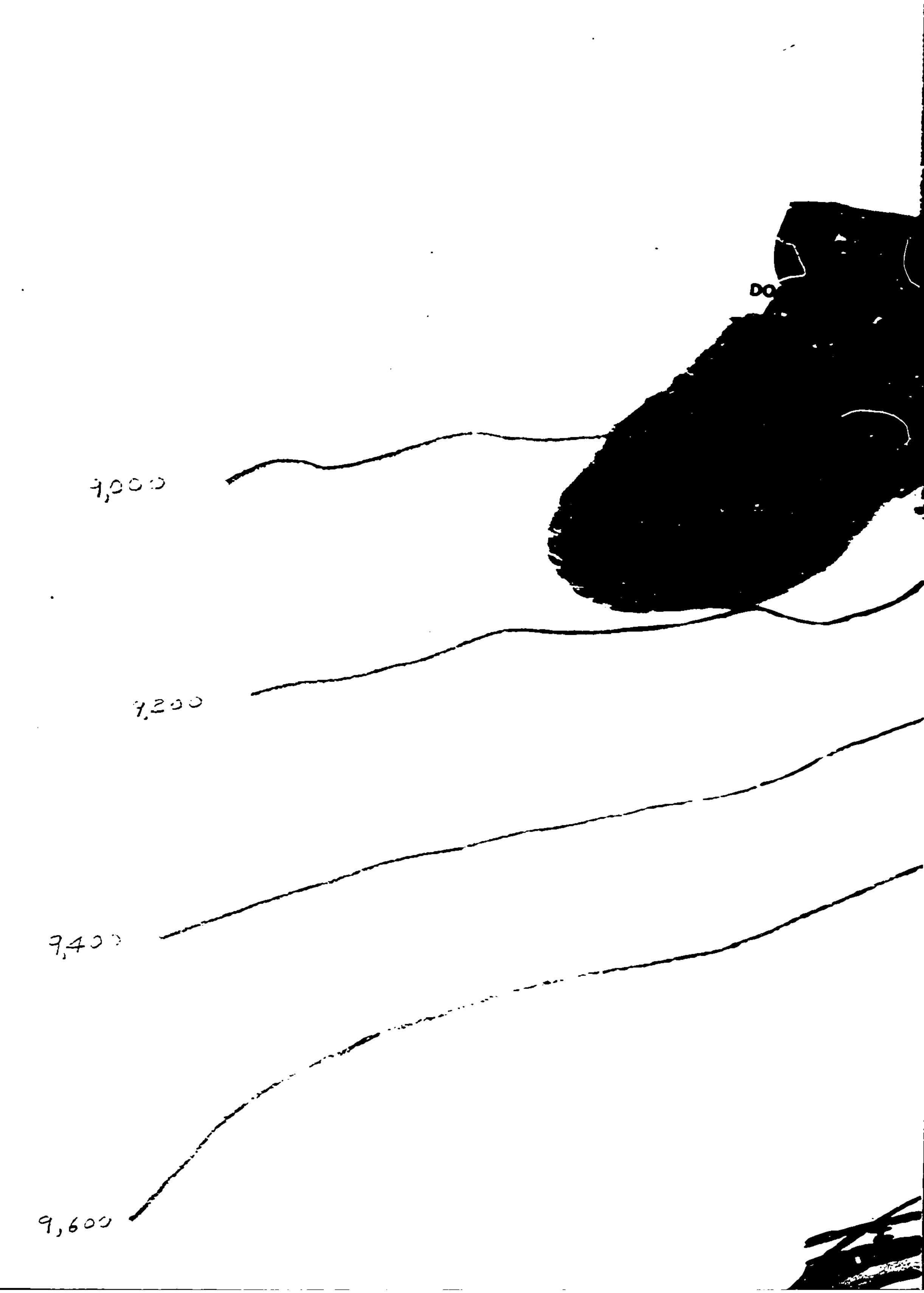
9,000
9,200
9,400
9,600

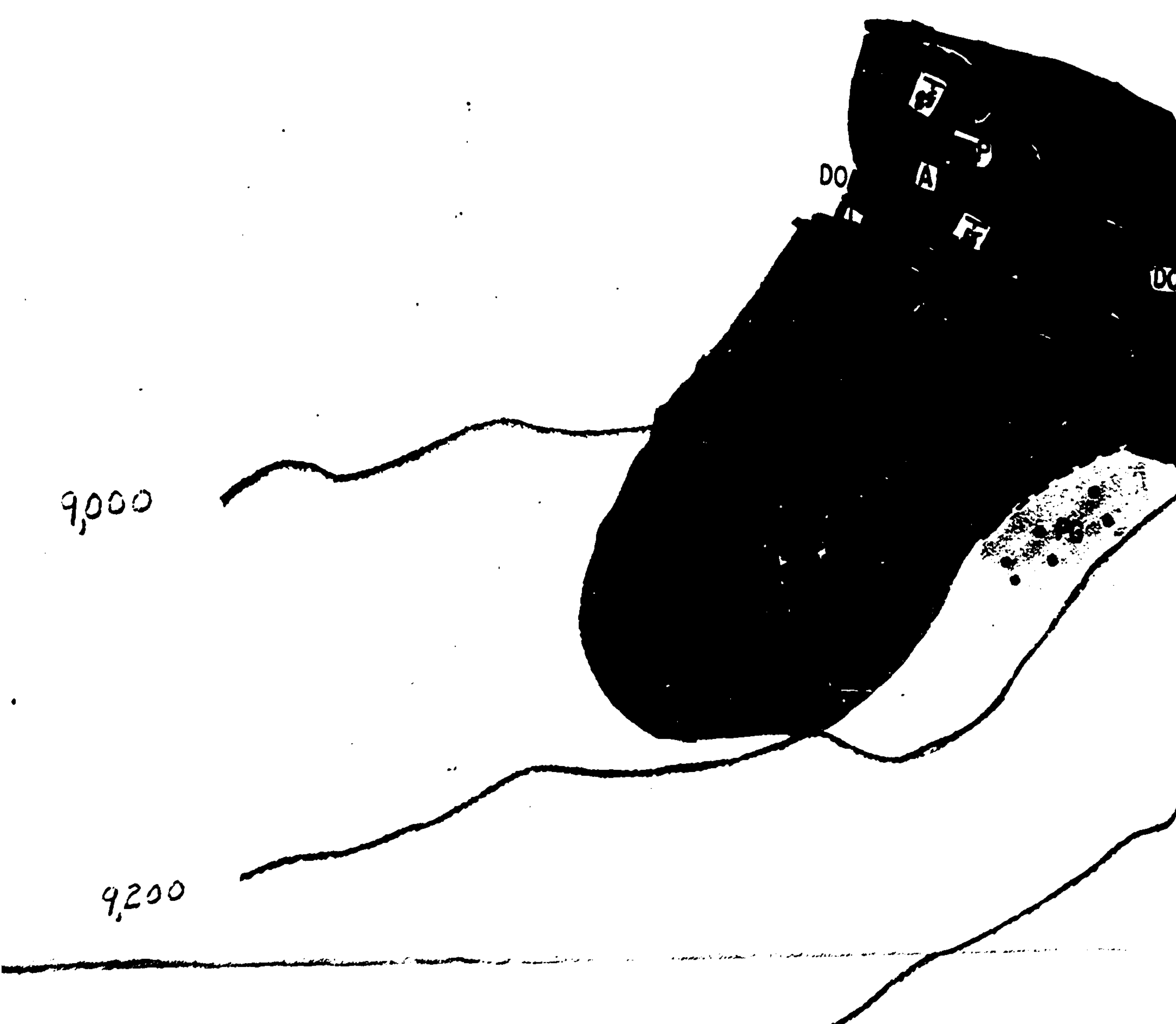
DO
A
DO
9,000
9,200

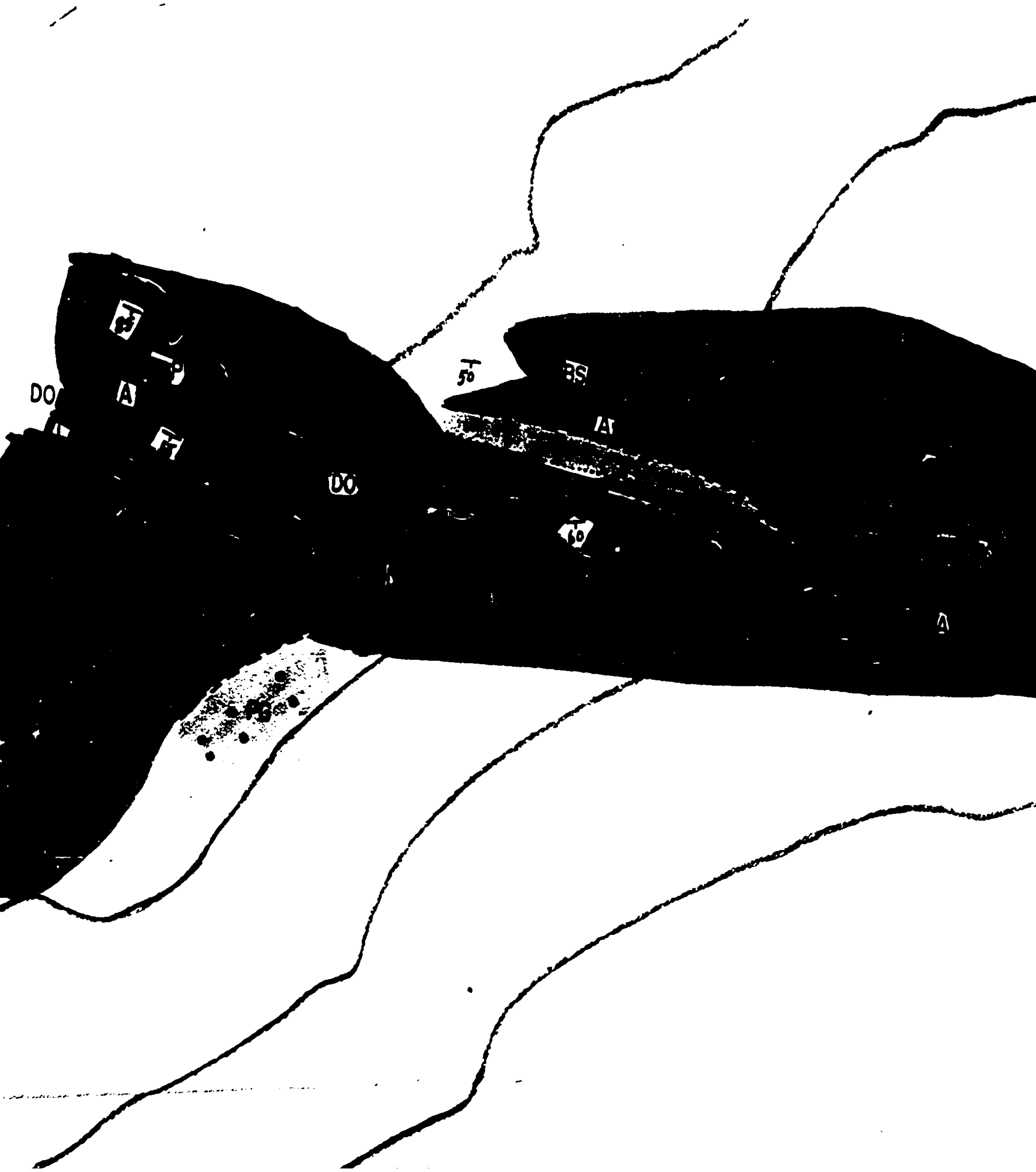
DO
A
50
BS
A
DO
60
A

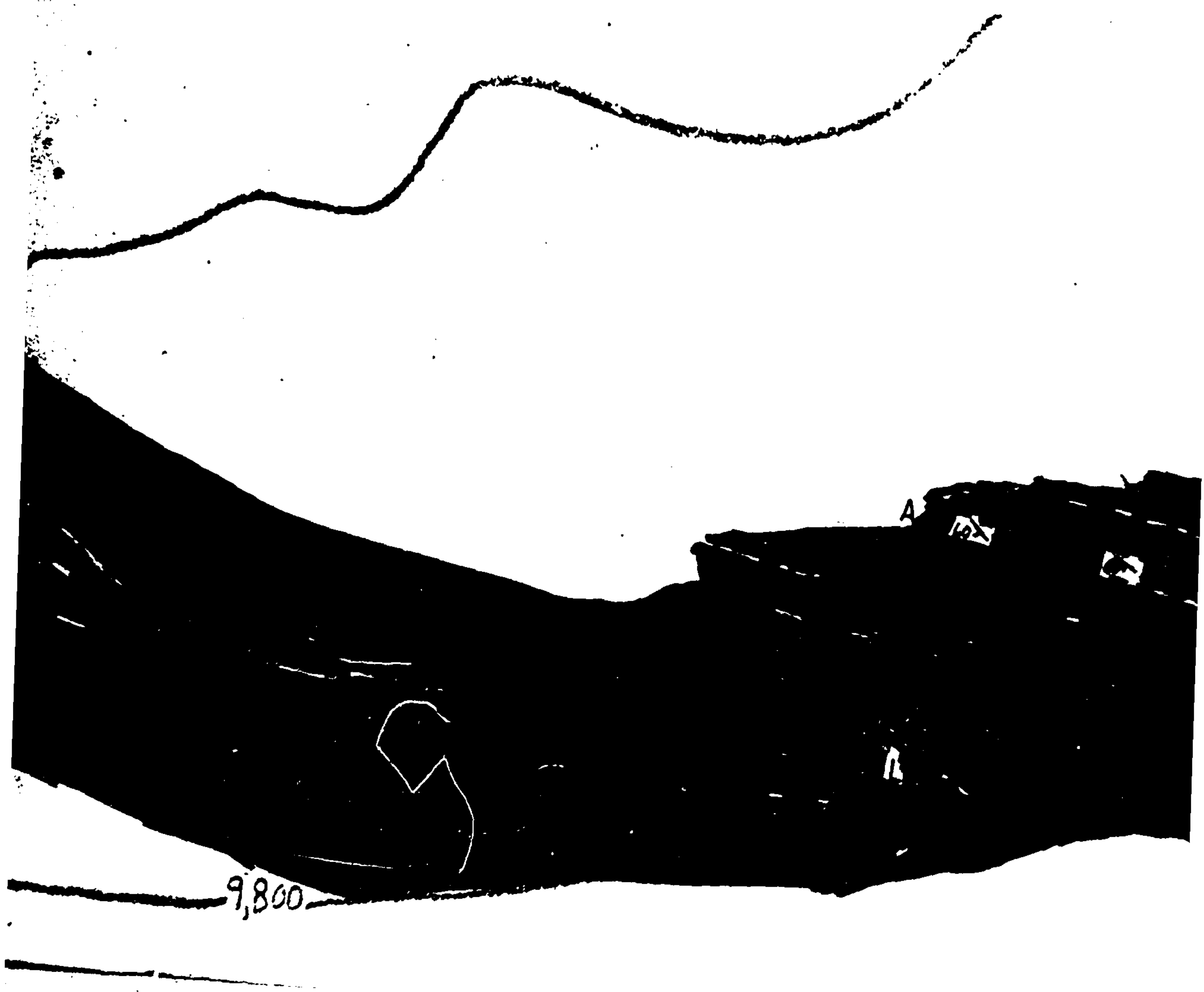
A
9,800

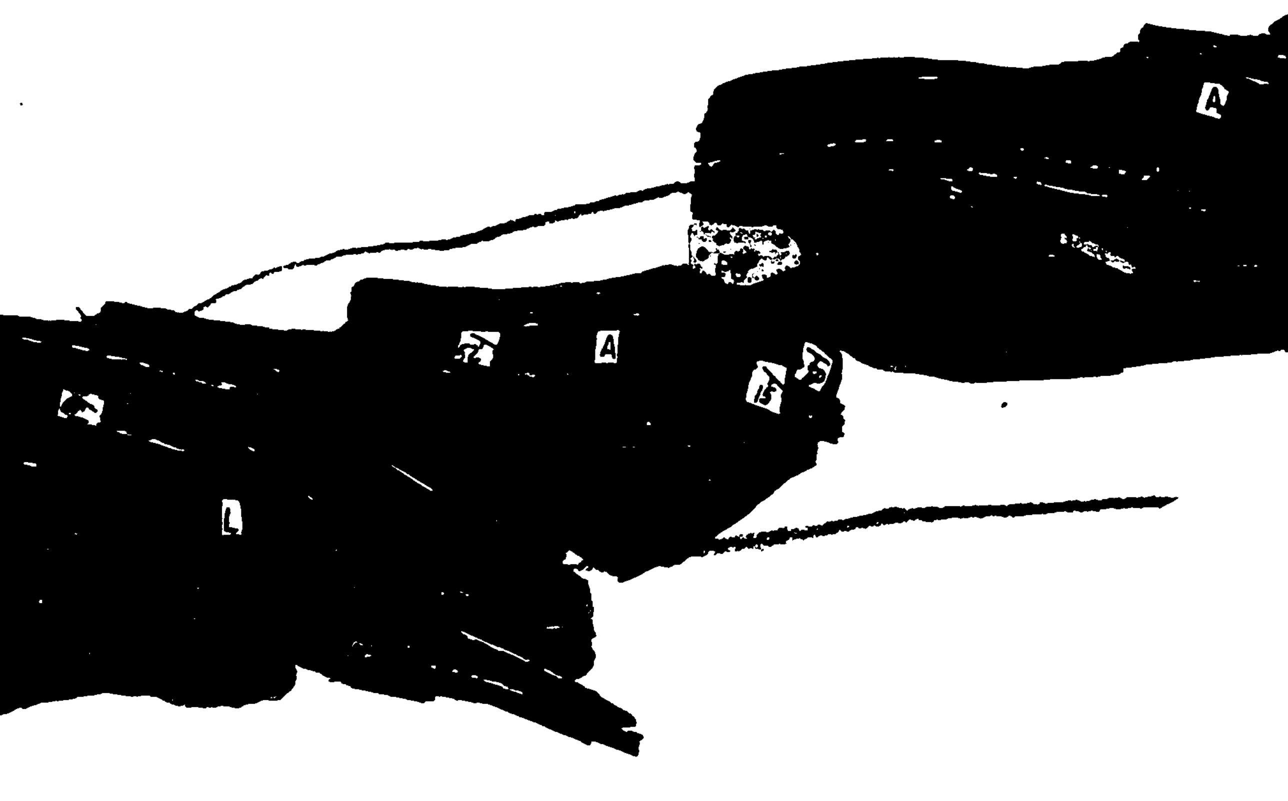
A
A
L


A
A
A
A


9,200
9,400
9,600
A
U
GG
Q


DO
DO
A
Q
A
GG
Q

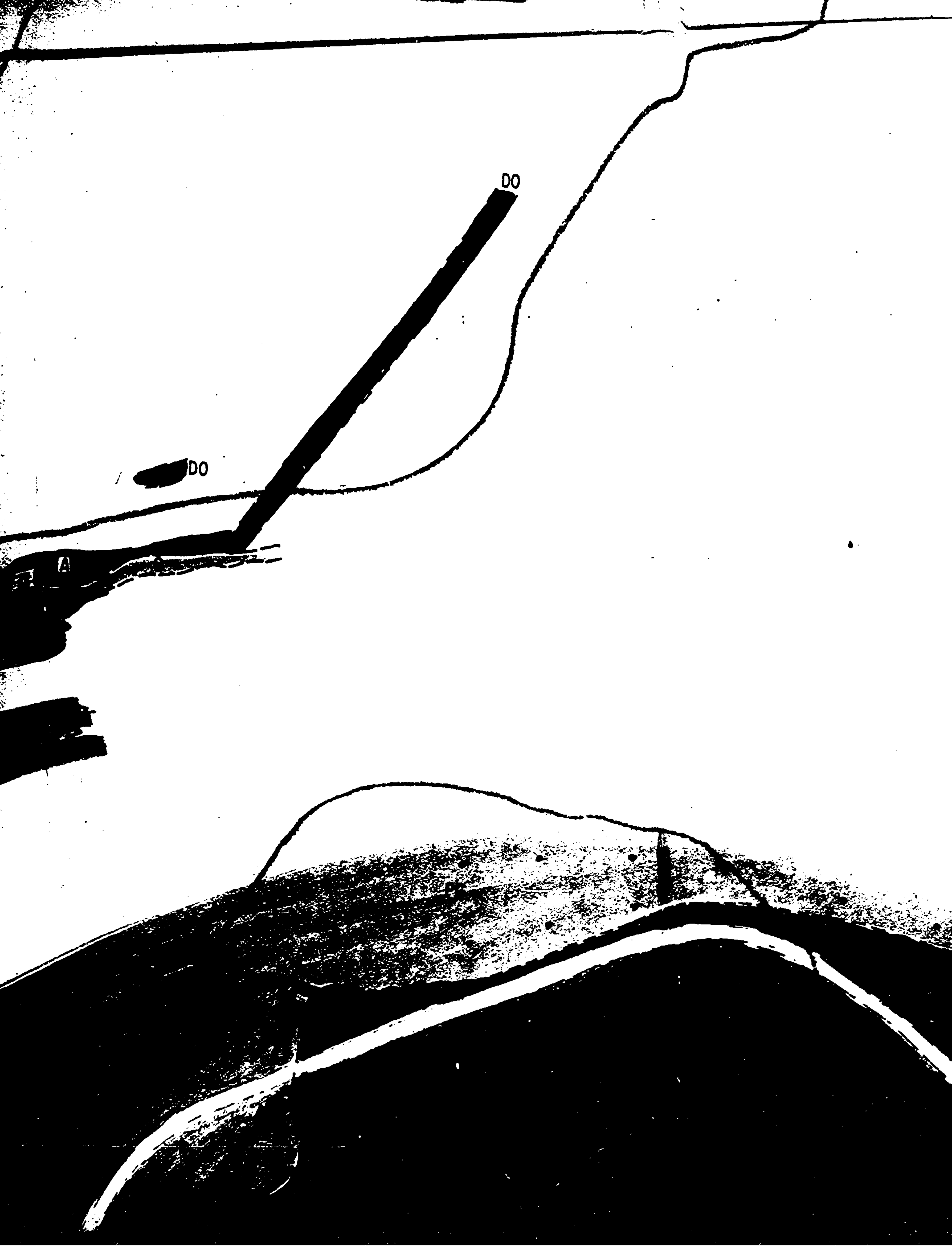
DO
DO
A

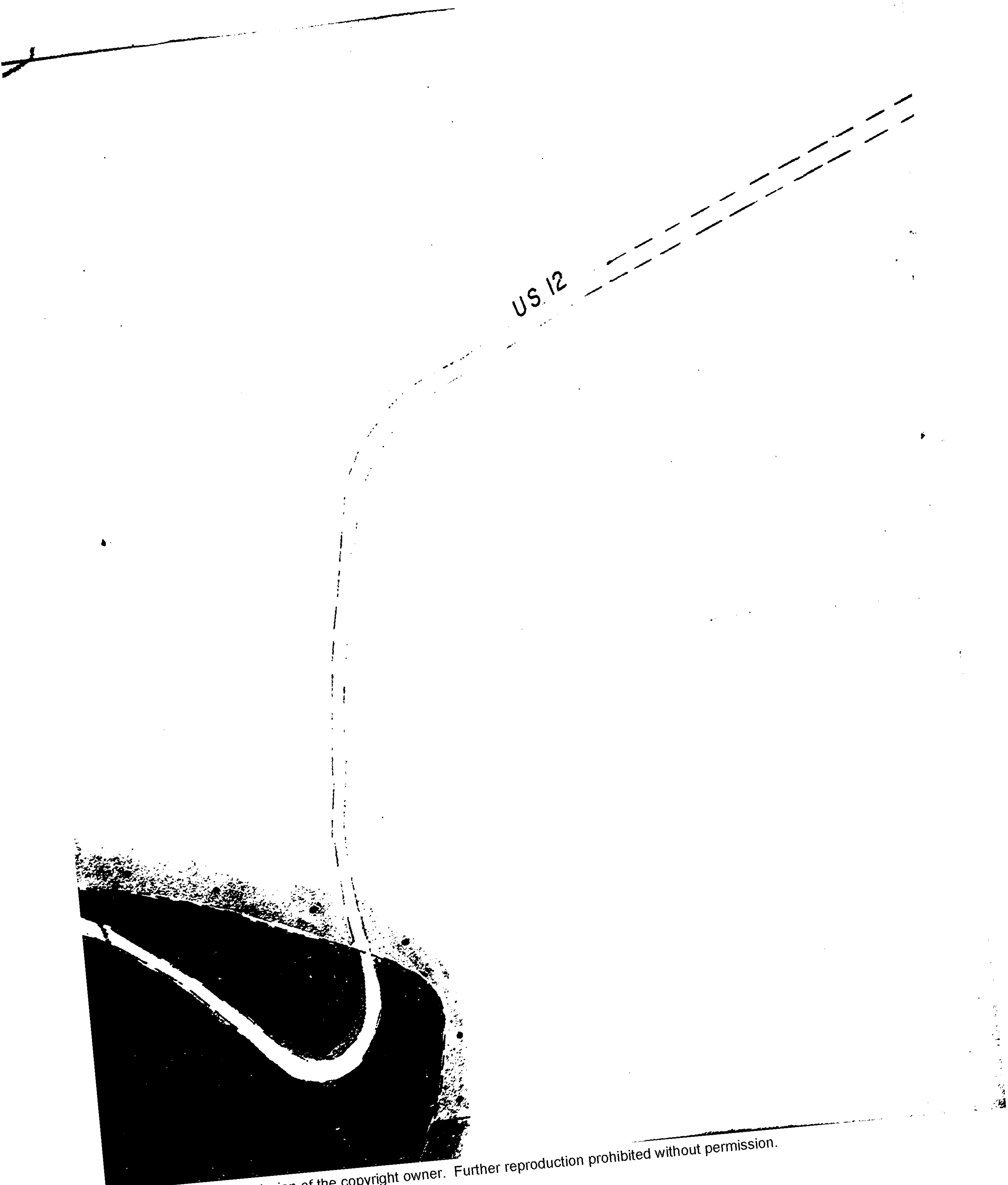
US 12


9,600
9,400
Q
GG
A
PG
BS


PG
PG

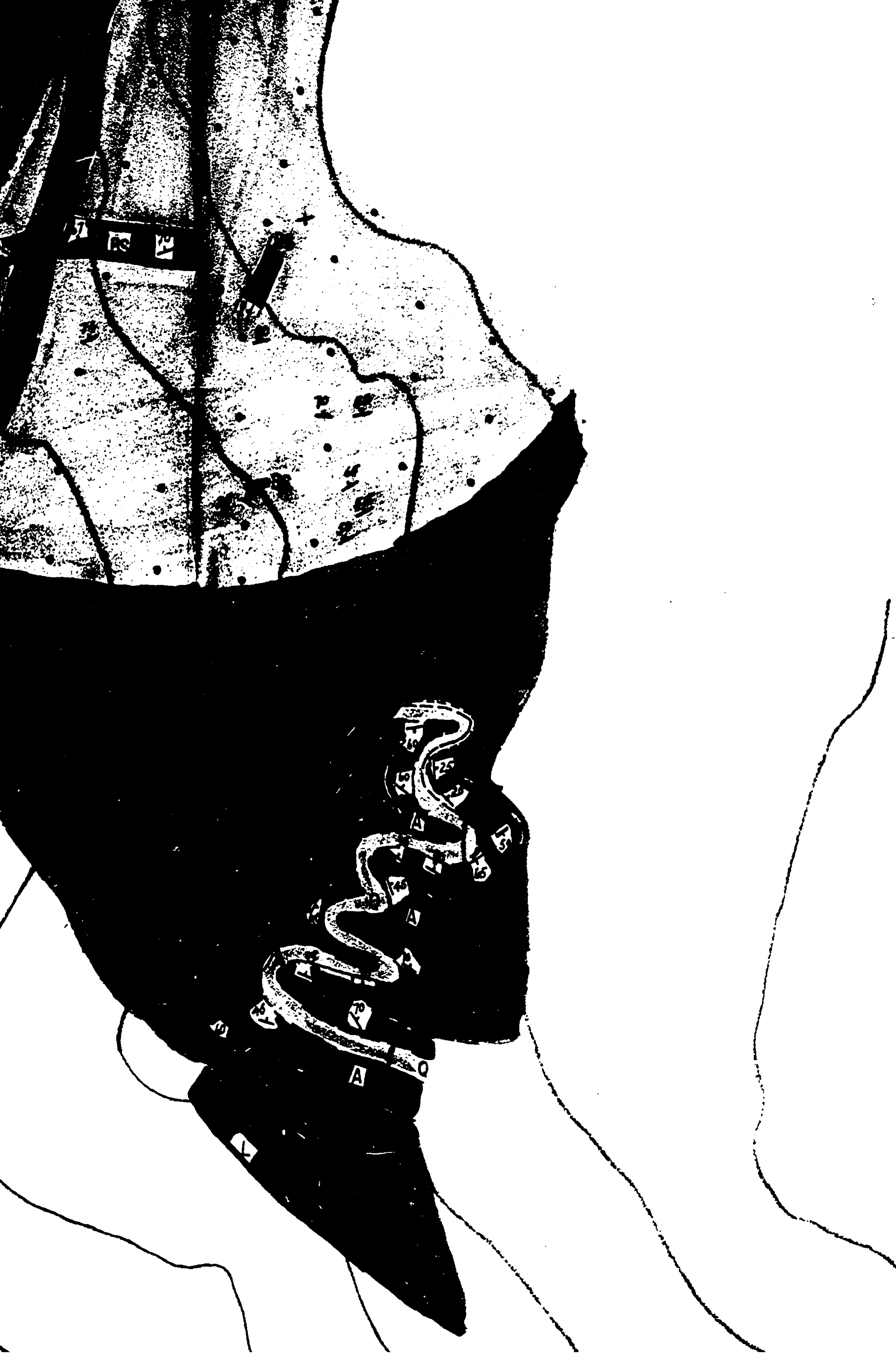
A
Q

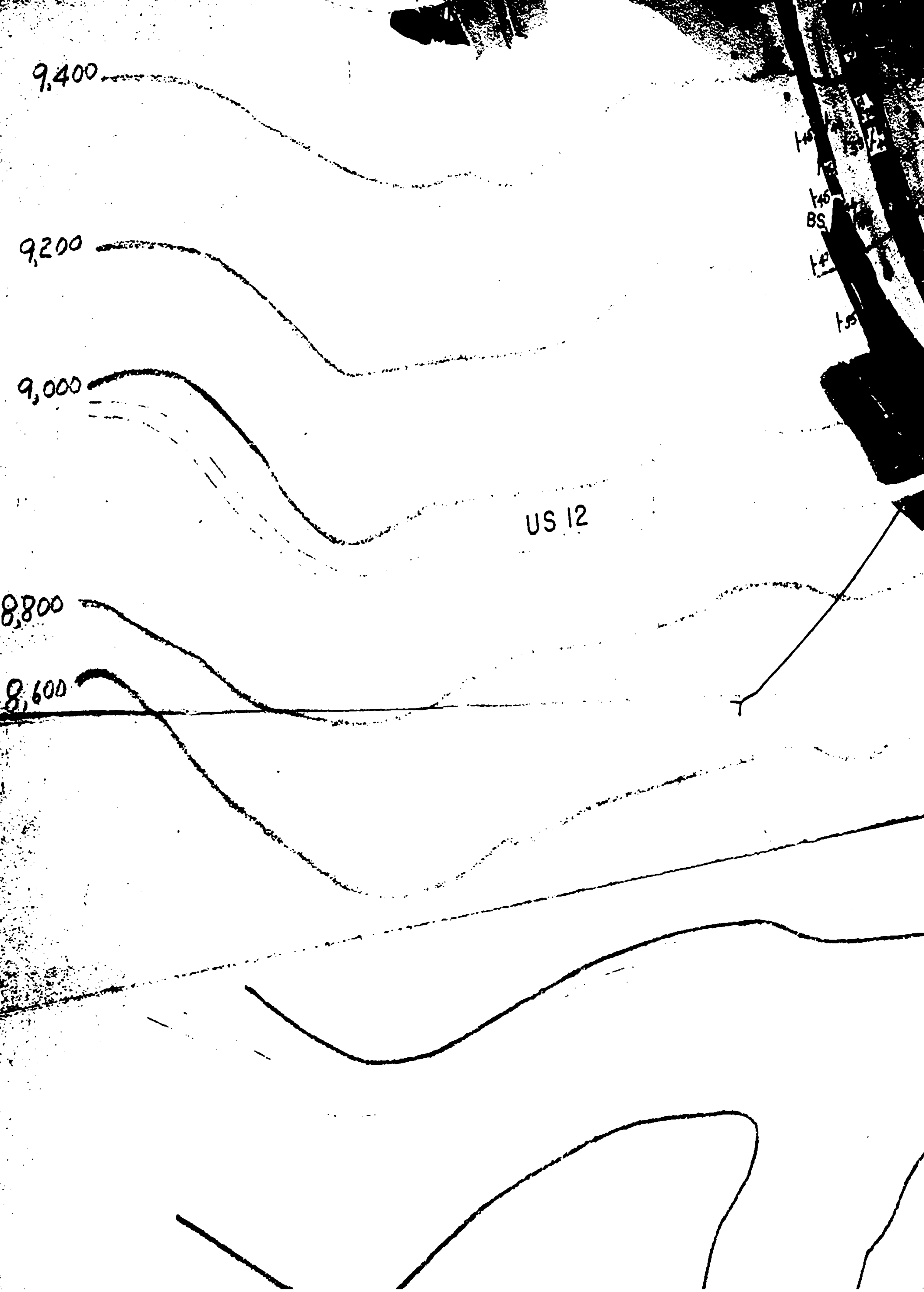
9,400
9,200
9,000
US 12
8,800
8,600
BS

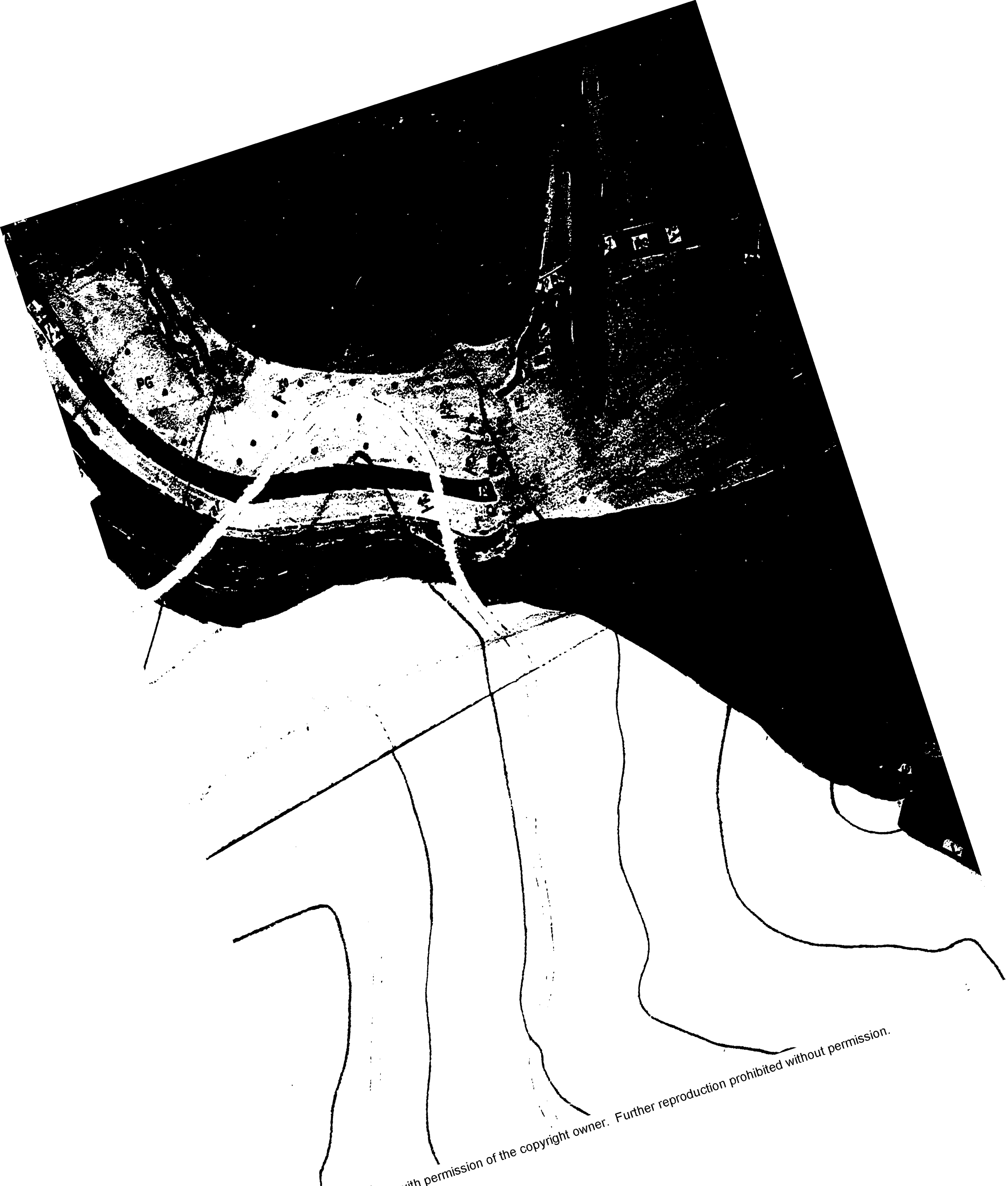

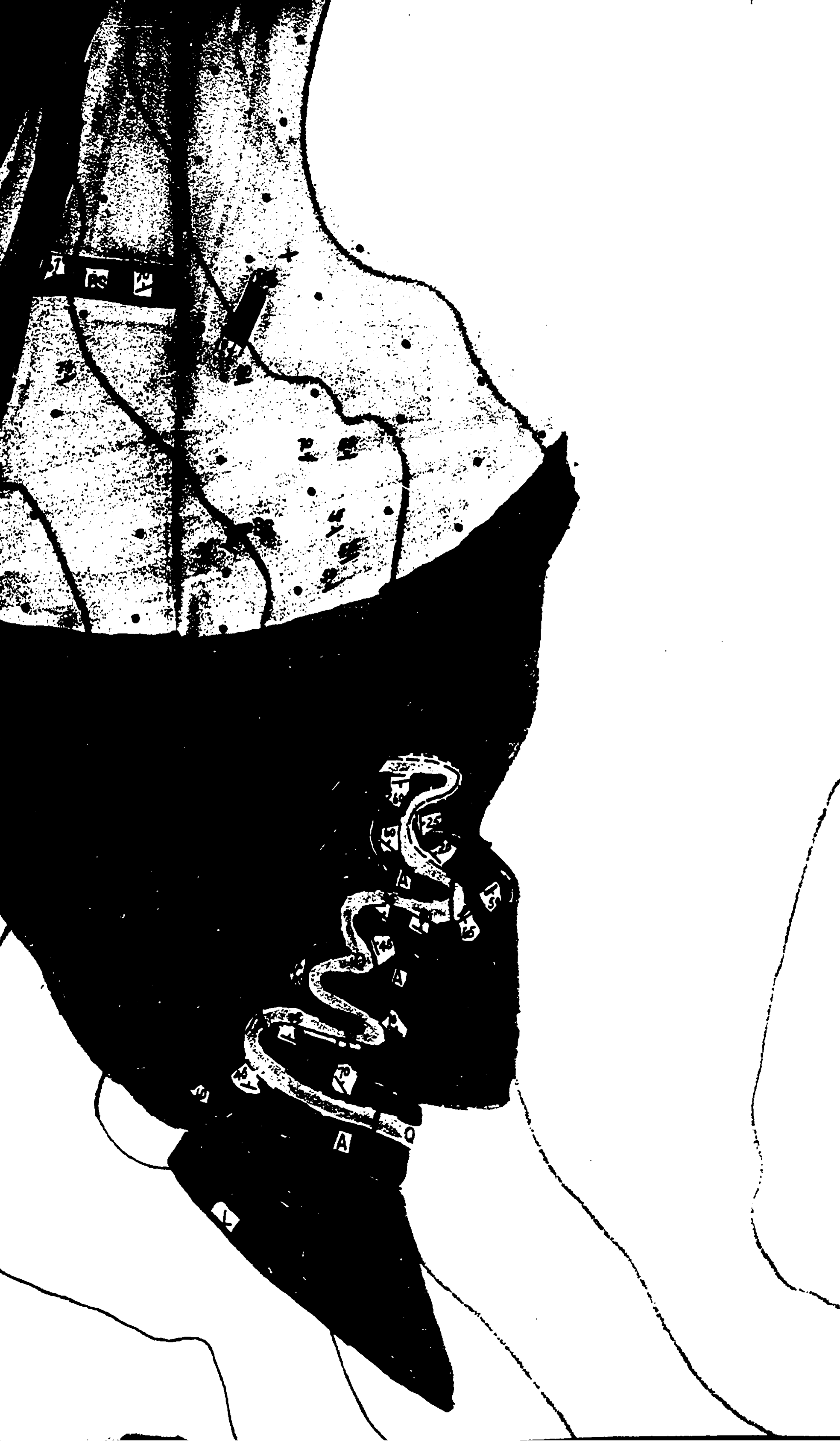

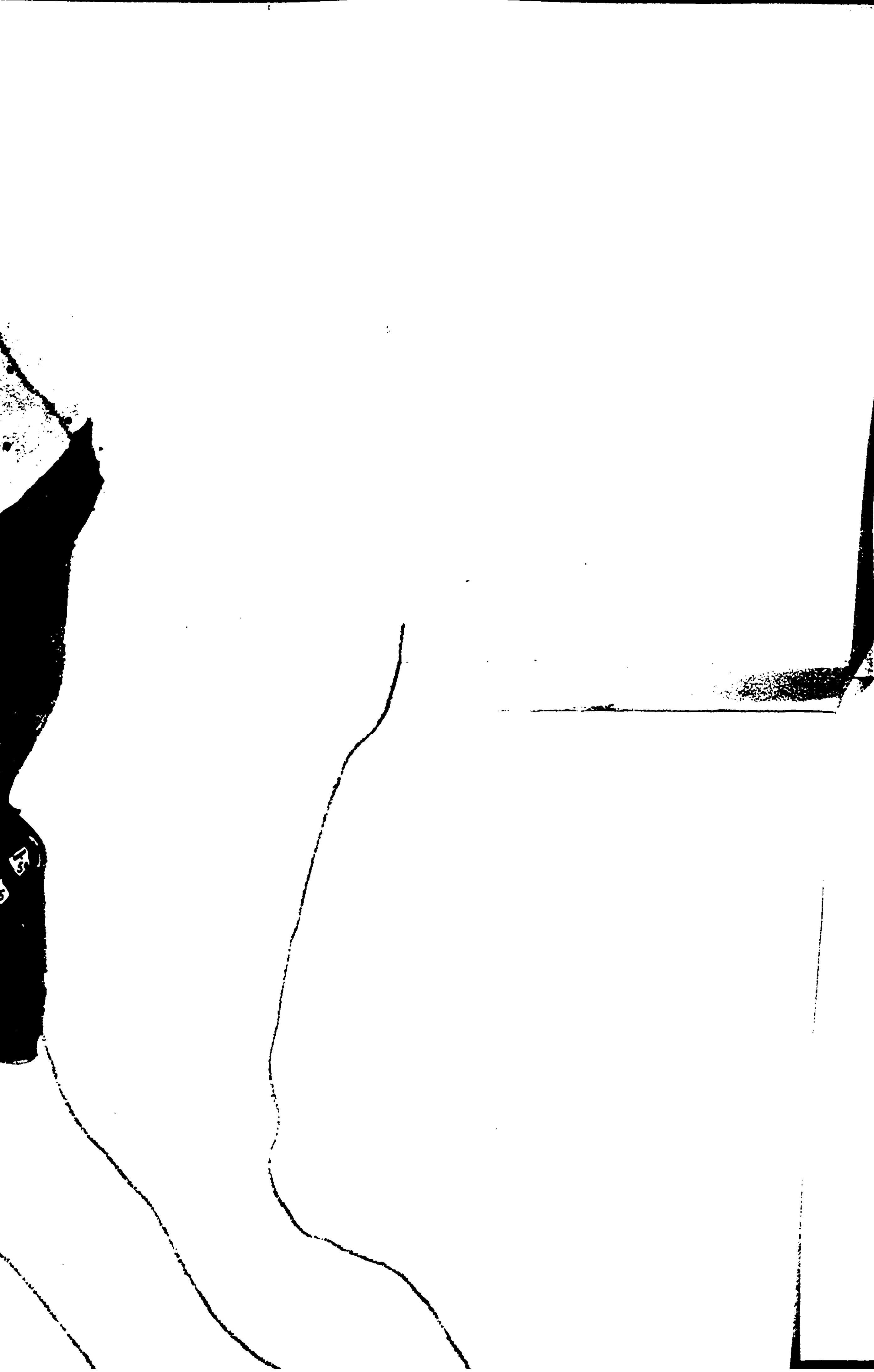


9,000
9,200
8,800

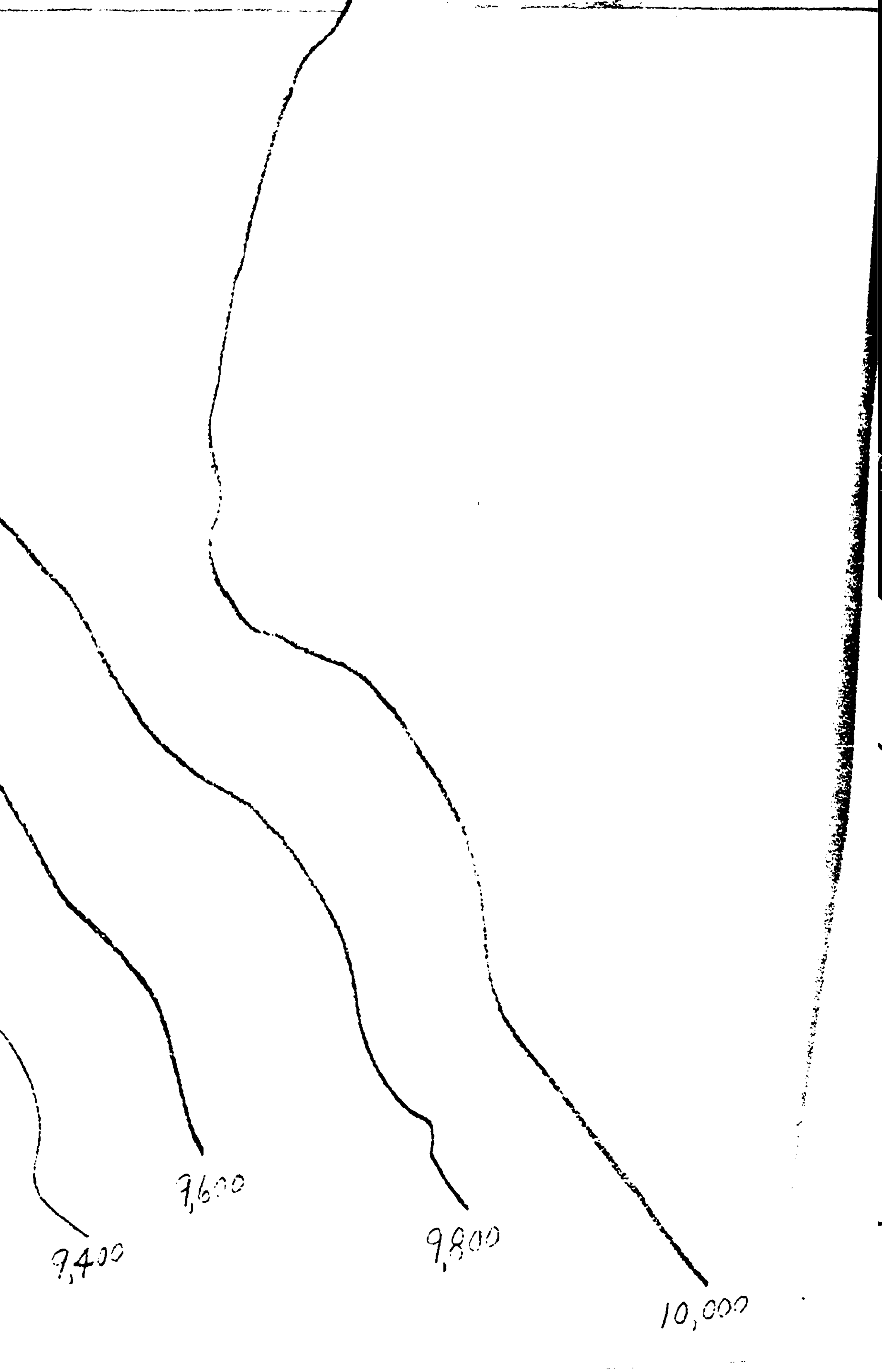
9,600
9,400
9,800
10,000

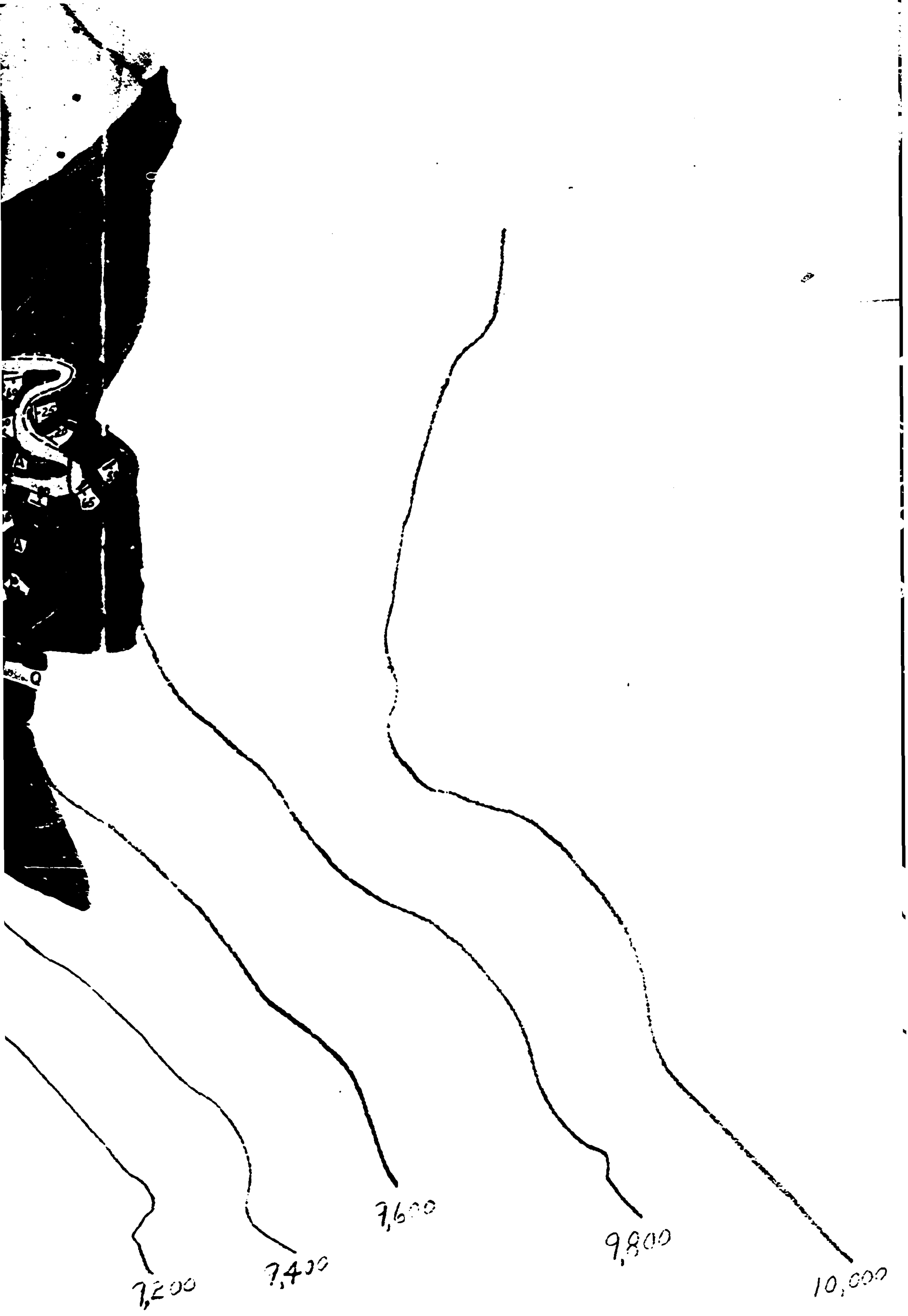
7,200
7,400
7,600
9,800
10,000

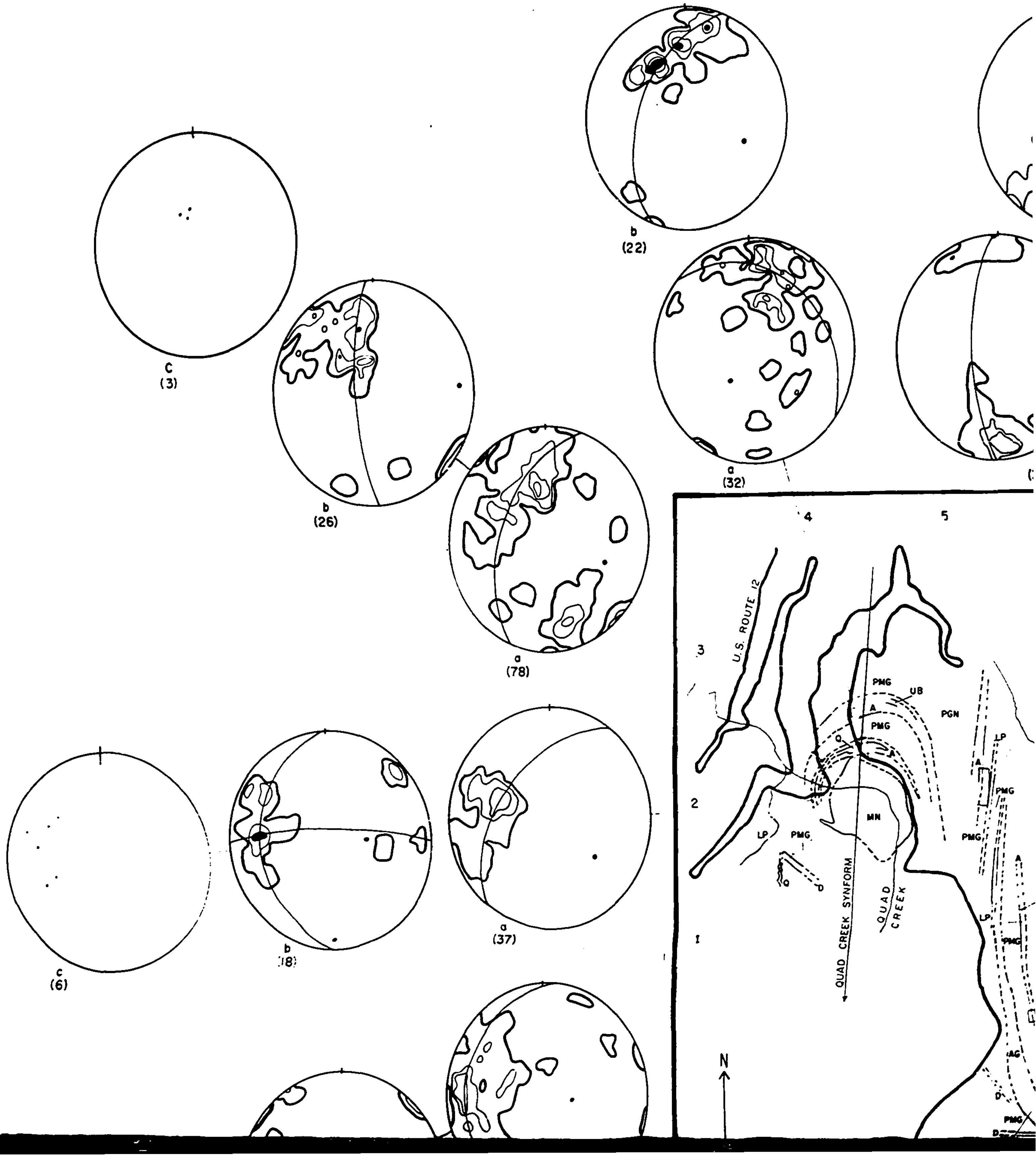
b
(22)
c
(3)
b
(26)
a
(32)
a
(78)
4
5
3
U.S. ROUTE 12
PMG
UB
A
PGN
PMG
Q
LP
2
MN
PMG
LP
QUAD CREEK SYNFORM
QUAD CREEK
Q
D
c
(6)
b
(18)
a
(37)
1
N
AG
D

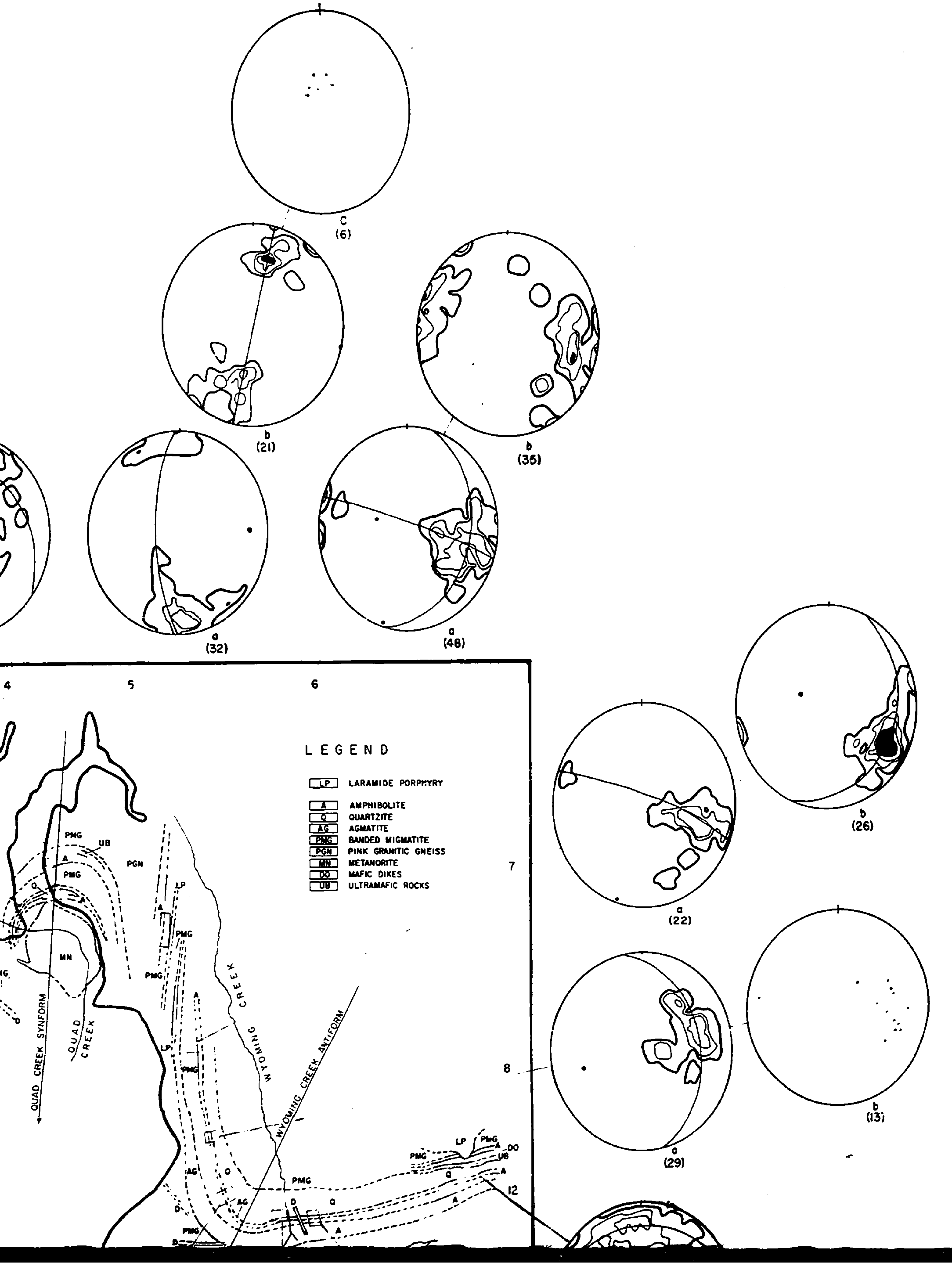
c
(6)
b
(21)
b
(35)
a
(32)
a
(48)
b
(26)
a
(22)
a
(29)
b
(13)
4
5
6
7
8
12
LEGEND
LP LARAMIDE PORPHYRY
A AMPHIBOLITE
Q QUARTZITE
AG AGMATITE
PMG BANDED MIGMATITE
PGN PINK GRANITIC GNEISS
MN METANORITE
DO MAFIC DIKES
UB ULTRAMAFIC ROCKS
QUAD CREEK SYNFORM
QUAD CREEK
WYOMING CREEK
WYOMING CREEK ANTIFORM
PMG
UB
PGN
MN
LP
DO

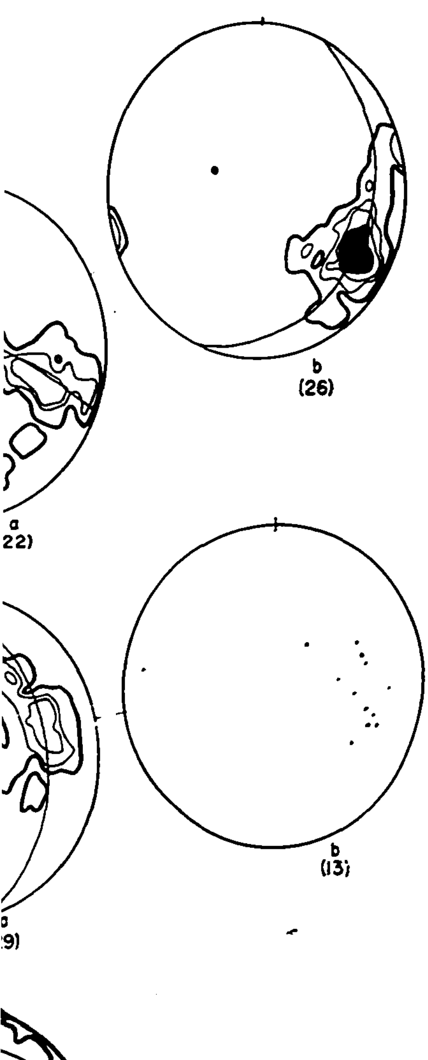

MAP 2a — FOLIATIONS MEASURED AT STRUCTURE STATIONS

(a) Compositional foliation, with contours at 1-5-10-15 % at Stations 3,9,10,11,12; 1-5-10 % at all other Stations.

(b) F_1 small fold axial planes, S_1, with contours at 1-10-18% at Sta. 11; 1-5-10% at Stas. 1,2,3,5; 1-5-10-15% at all other Stations.

(c) F_2 small fold axial planes, S_2, uncontoured.

Bracketed numbers are the number of measurements.

⊙ Indicates constructed β axes.

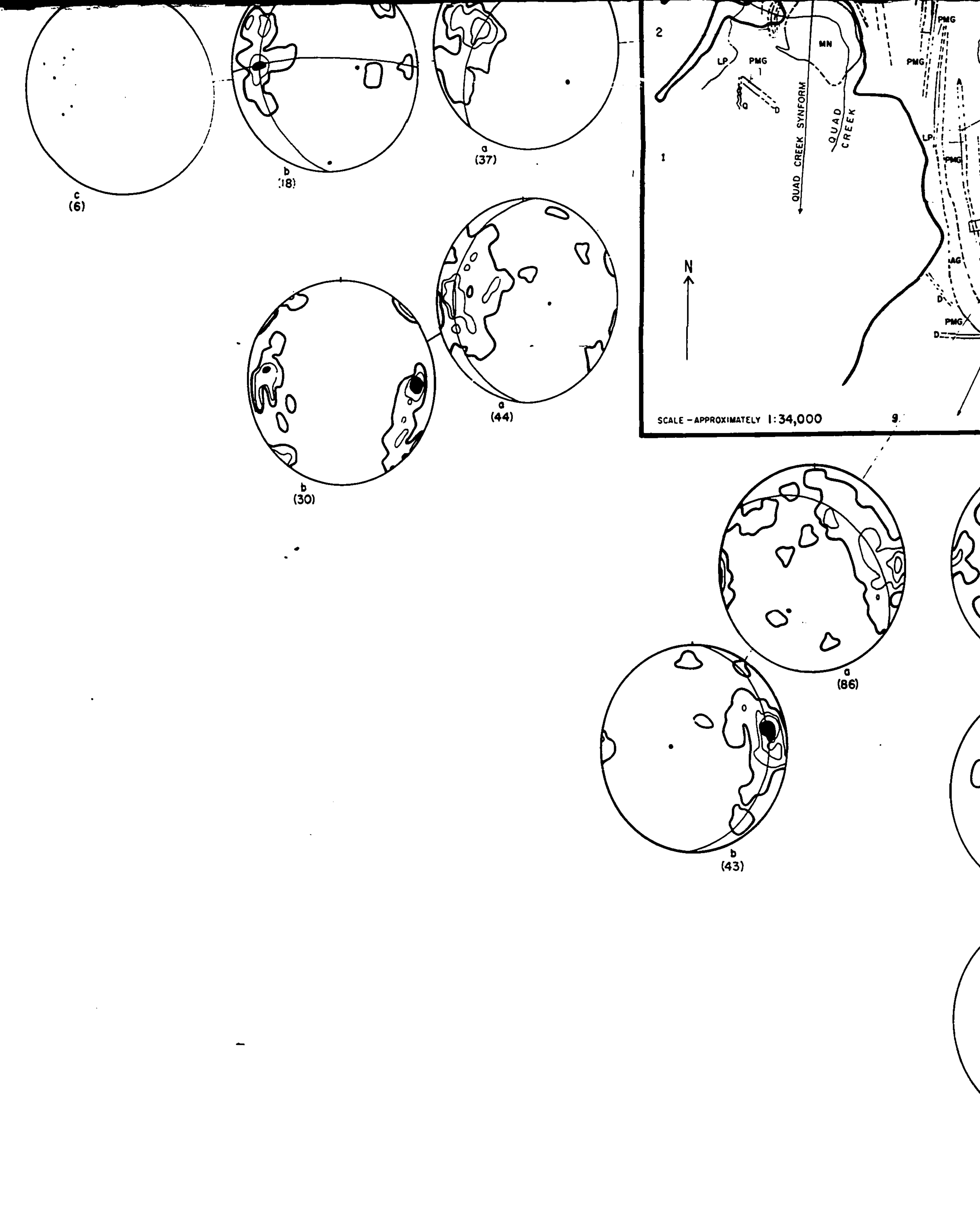
c
(6)
b
(18)
a
(37)
b
(30)
a
(44)
a
(86)
b
(43)
2
1
LP
PMG
MN
QUAD CREEK SYNFORM
QUAD CREEK
AG
N
SCALE – APPROXIMATELY 1:34,000
9

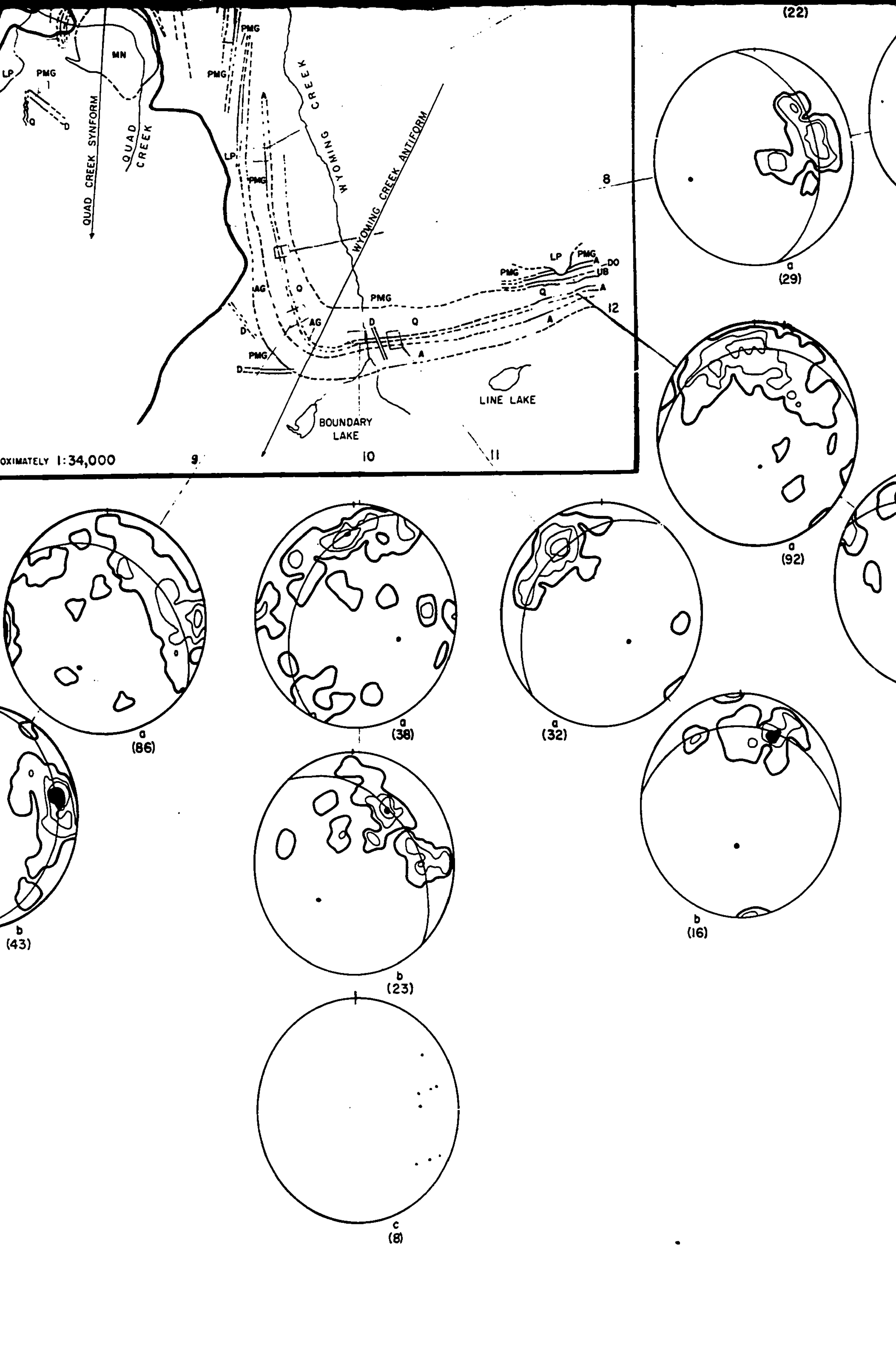

LP
PMG
MN
QUAD CREEK SYNFORM
QUAD CREEK
WYOMING CREEK
WYOMING CREEK ANTIFORM
AG
Q
D
A
UB
DO
LINE LAKE
BOUNDARY LAKE
OXIMATELY 1:34,000
8
9
10
11
12
a (22)
a (29)
a (92)
a (86)
a (38)
a (32)
b (43)
b (23)
b (16)
c (8)

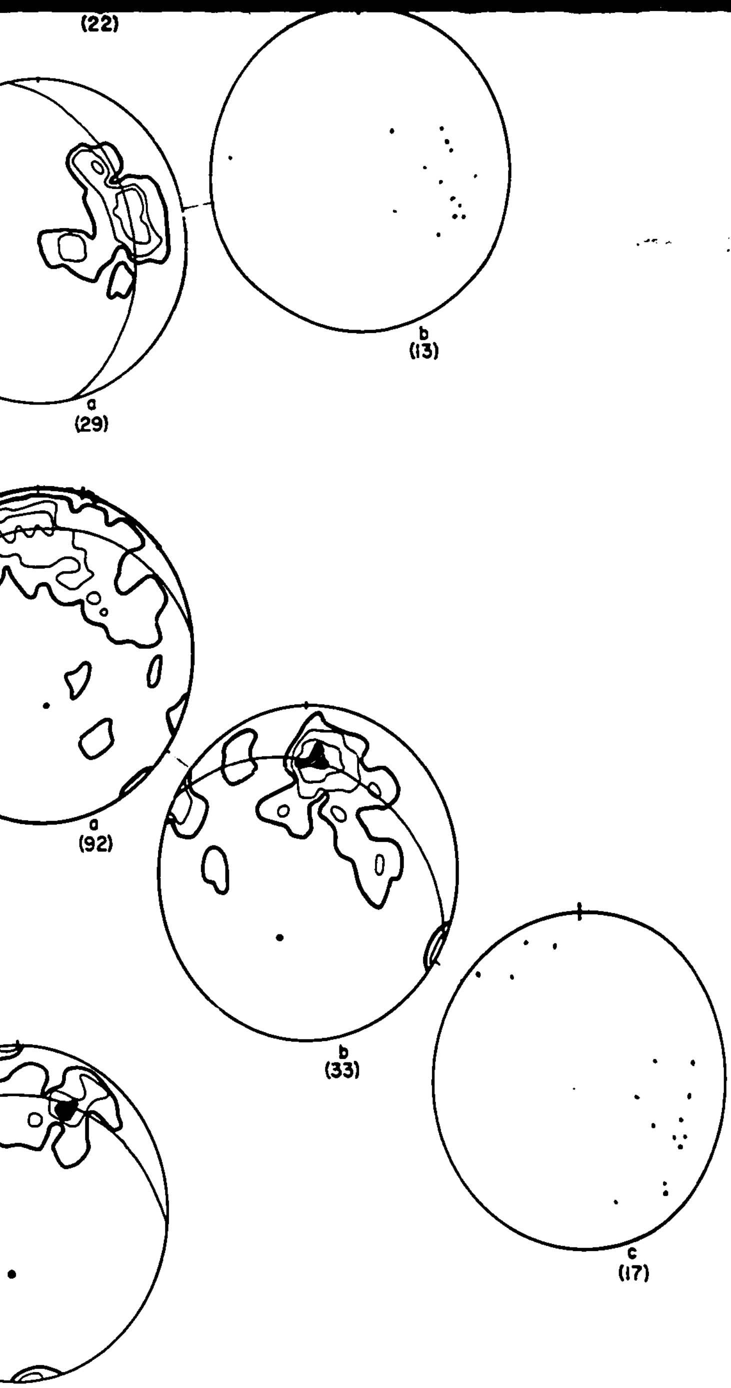
(22)
a
(29)
b
(13)
a
(92)
b
(33)
c
(17)

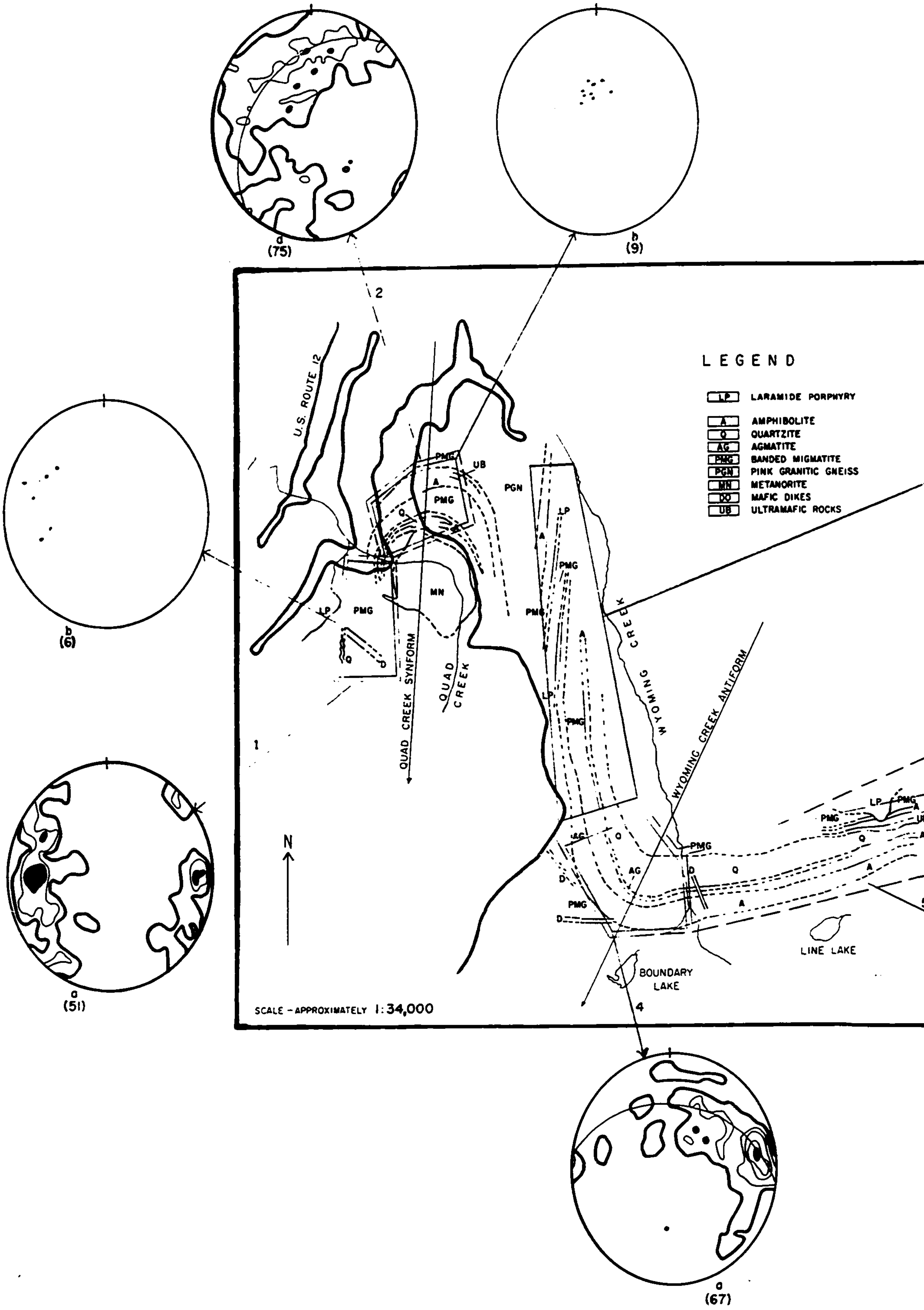
a
(75)
b
(9)
b
(6)
a
(51)
a
(67)
LEGEND
LP LARAMIDE PORPHYRY
A AMPHIBOLITE
Q QUARTZITE
AG AGMATITE
PMG BANDED MIGMATITE
PGN PINK GRANITIC GNEISS
MN METANORITE
DD MAFIC DIKES
UB ULTRAMAFIC ROCKS
U.S. ROUTE 12
QUAD CREEK SYNFORM
QUAD CREEK
WYOMING CREEK
WYOMING CREEK ANTIFORM
BOUNDARY LAKE
LINE LAKE
N
SCALE - APPROXIMATELY 1:34,000

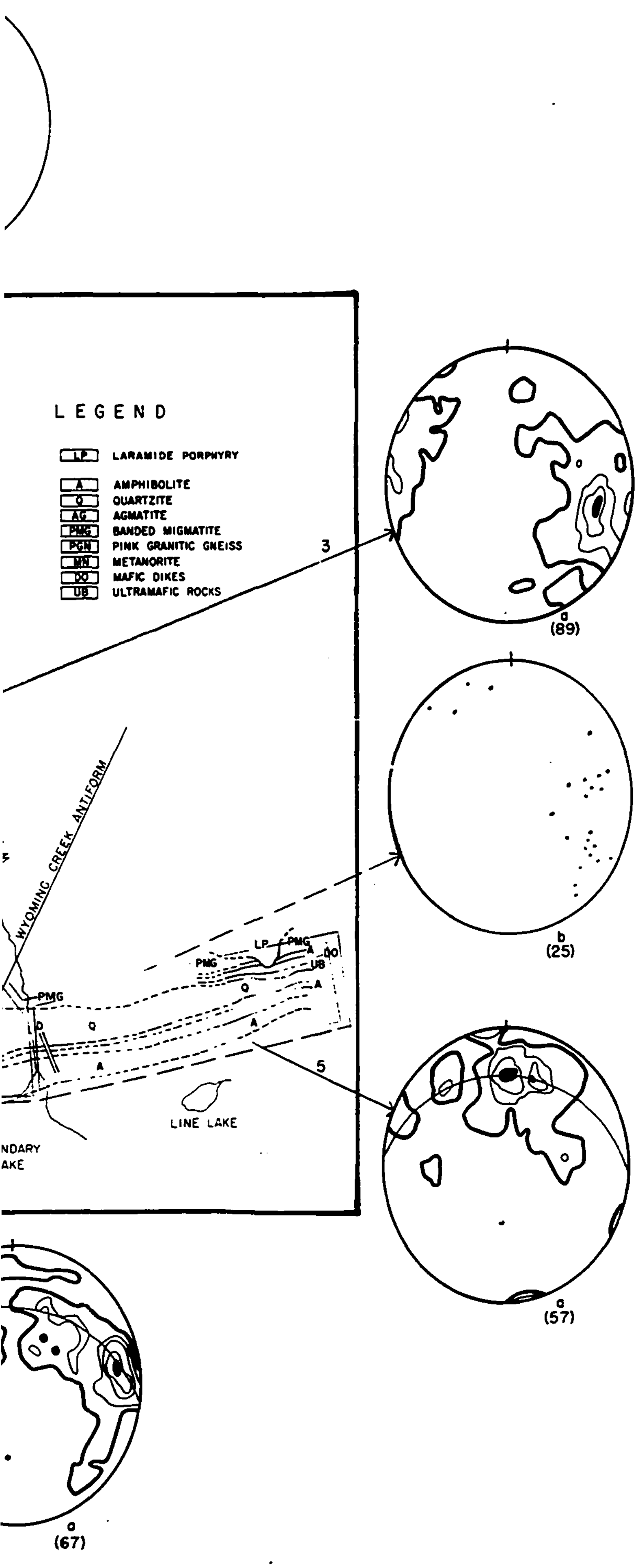

MAP 3a — FOLIATION IN SUBAREAS.

(a) F_1 small fold axial planes, S_1, with contours at 1-4-8% in Subareas 1 and 2; 1-4-8-12 % in Subareas 3 and 5; 1-4-8-12-16 % in Subarea 4.

(b) F_2 small fold axial planes, S_2, uncontoured.

Boundary symbols:

S_2 ———

S_1 - - - - -

⊙ Indicates constructed β axes

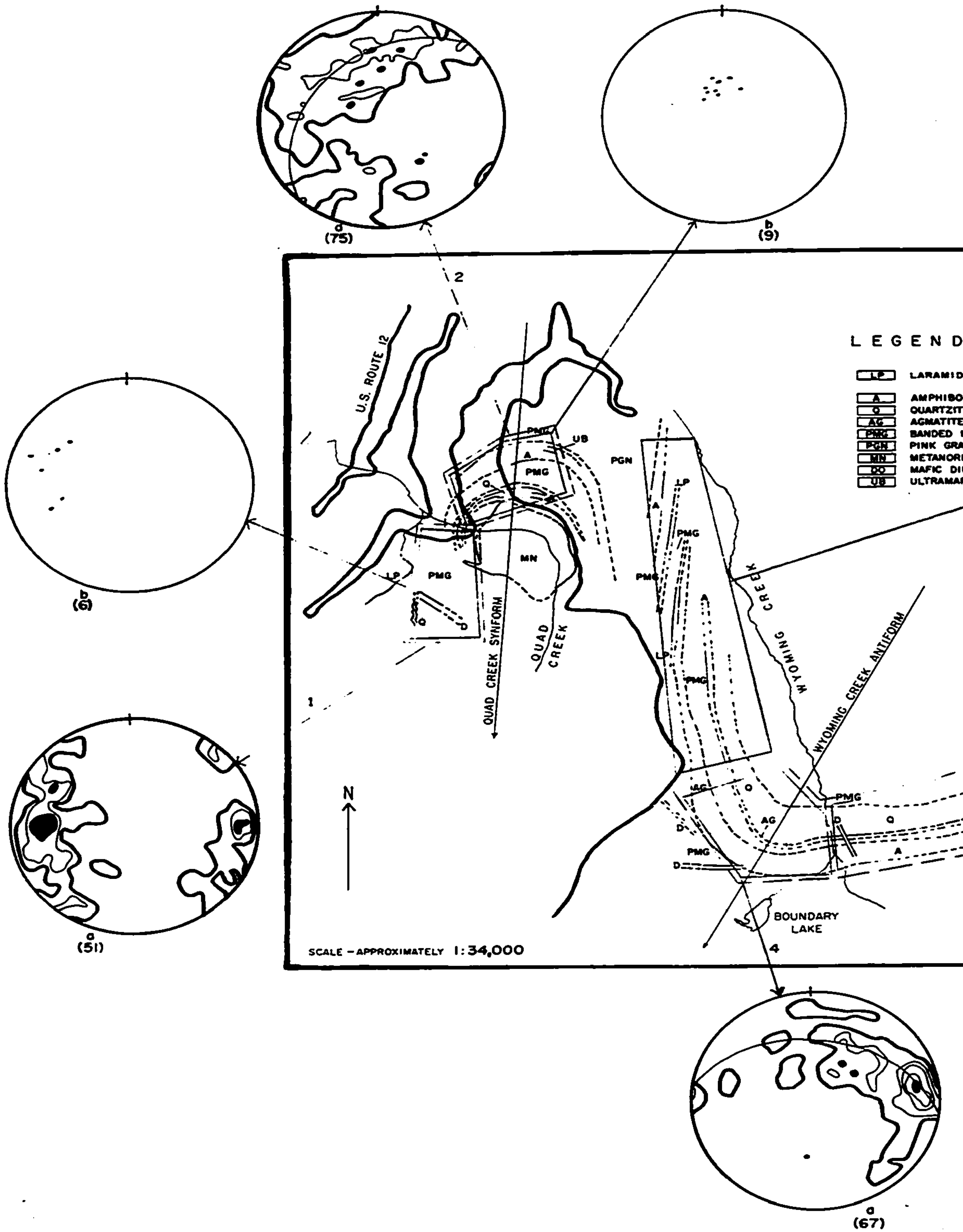

a
(75)
b
(9)
b
(6)
a
(51)
a
(67)
2
1
4
U.S. ROUTE 12
QUAD CREEK SYNFORM
QUAD CREEK
WYOMING CREEK
WYOMING CREEK ANTIFORM
BOUNDARY LAKE
PMG
UB
PGN
MN
LP
PMG
AG
Q
A
D
N
SCALE - APPROXIMATELY 1:34,000
LEGEND

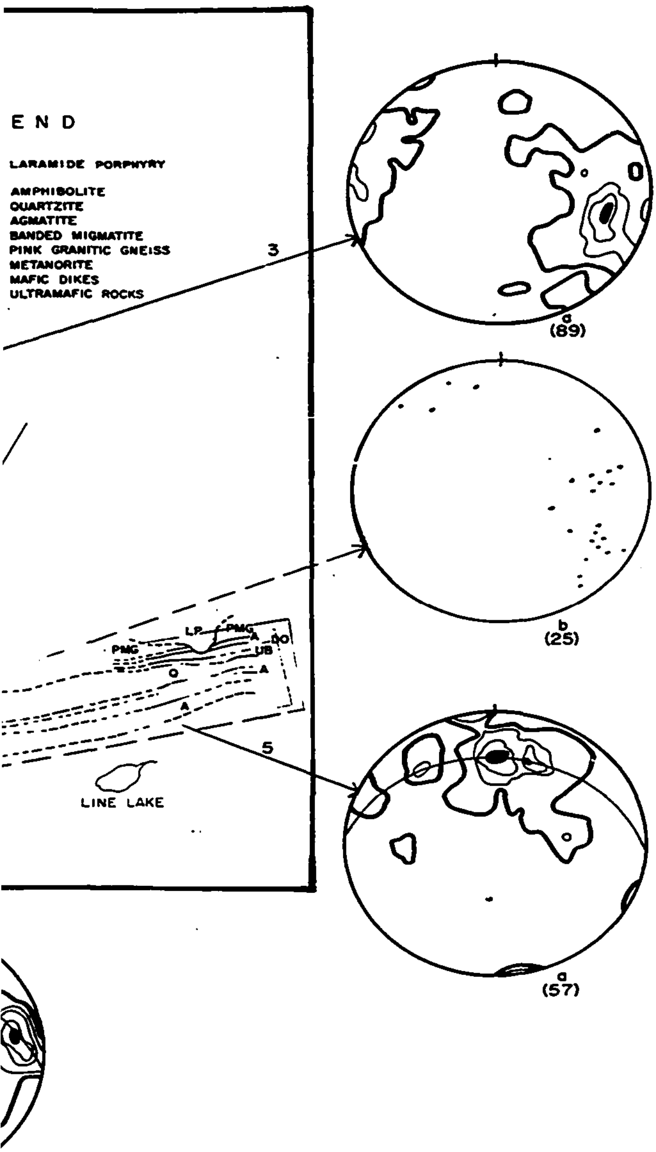

MAP 3a — FOLIATION IN SUBAREAS.

(a) F_1 small fold axial planes, S_1, with contours at 1–4–8% in Subareas 1 and 2; 1–4–8–12 % in Subareas 3 and 5; 1–4–8–12–16 % in Subarea 4.

(b) F_2 small fold axial planes, S_2, uncontoured.

Boundary symbols:

S_2 ———

S_1 - - - - -

⊙ Indicates constructed β axes

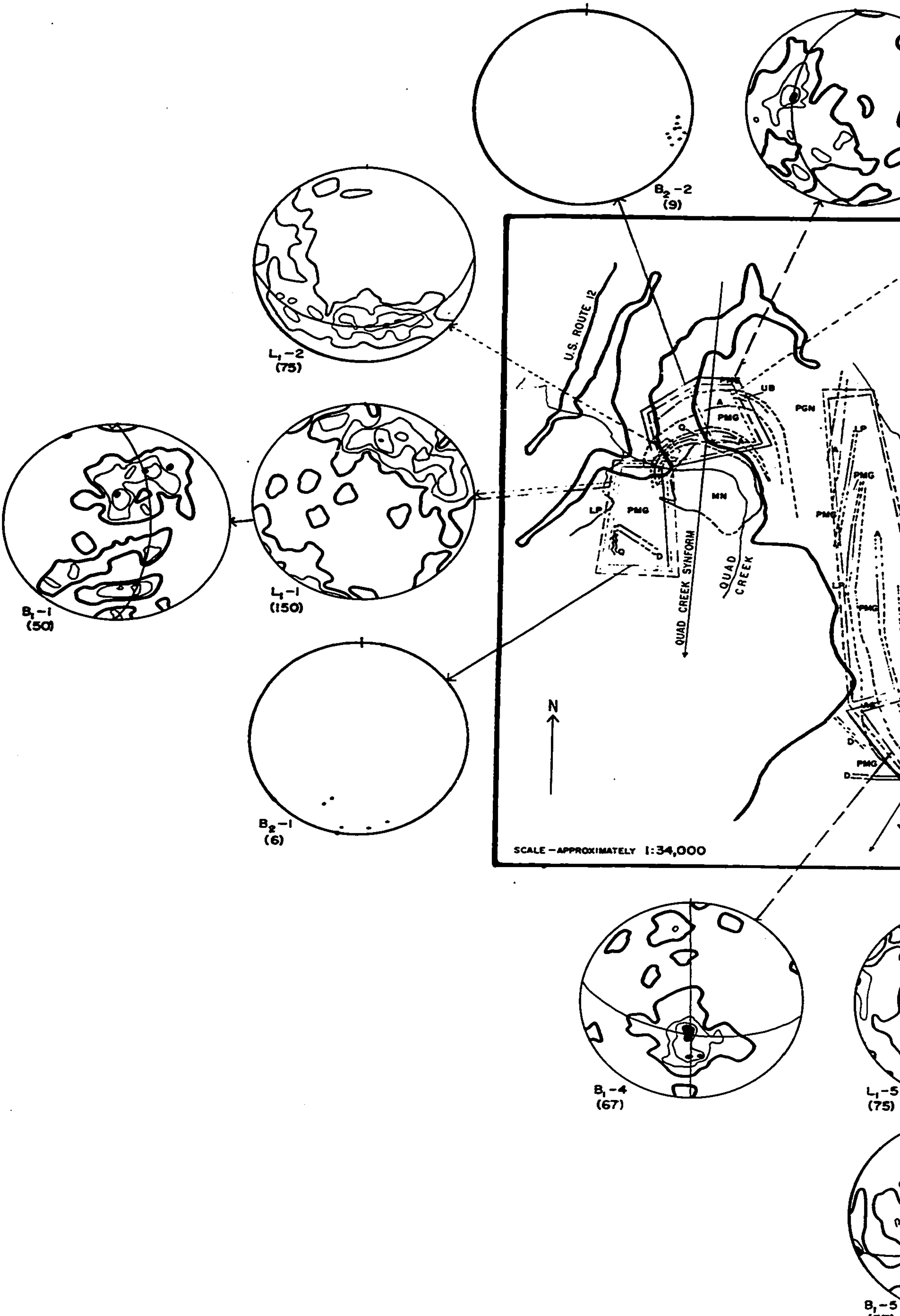

B_2-2
(9)
L_1-2
(75)
B_1-1
(50)
L_1-1
(150)
B_2-1
(6)
U.S. ROUTE 12
PMG
PGN
UB
A
Q
MN
LP
D
QUAD CREEK SYNFORM
QUAD CREEK
N
SCALE — APPROXIMATELY 1:34,000
B_1-4
(67)
L_1-5
(75)
B_1-5
(57)

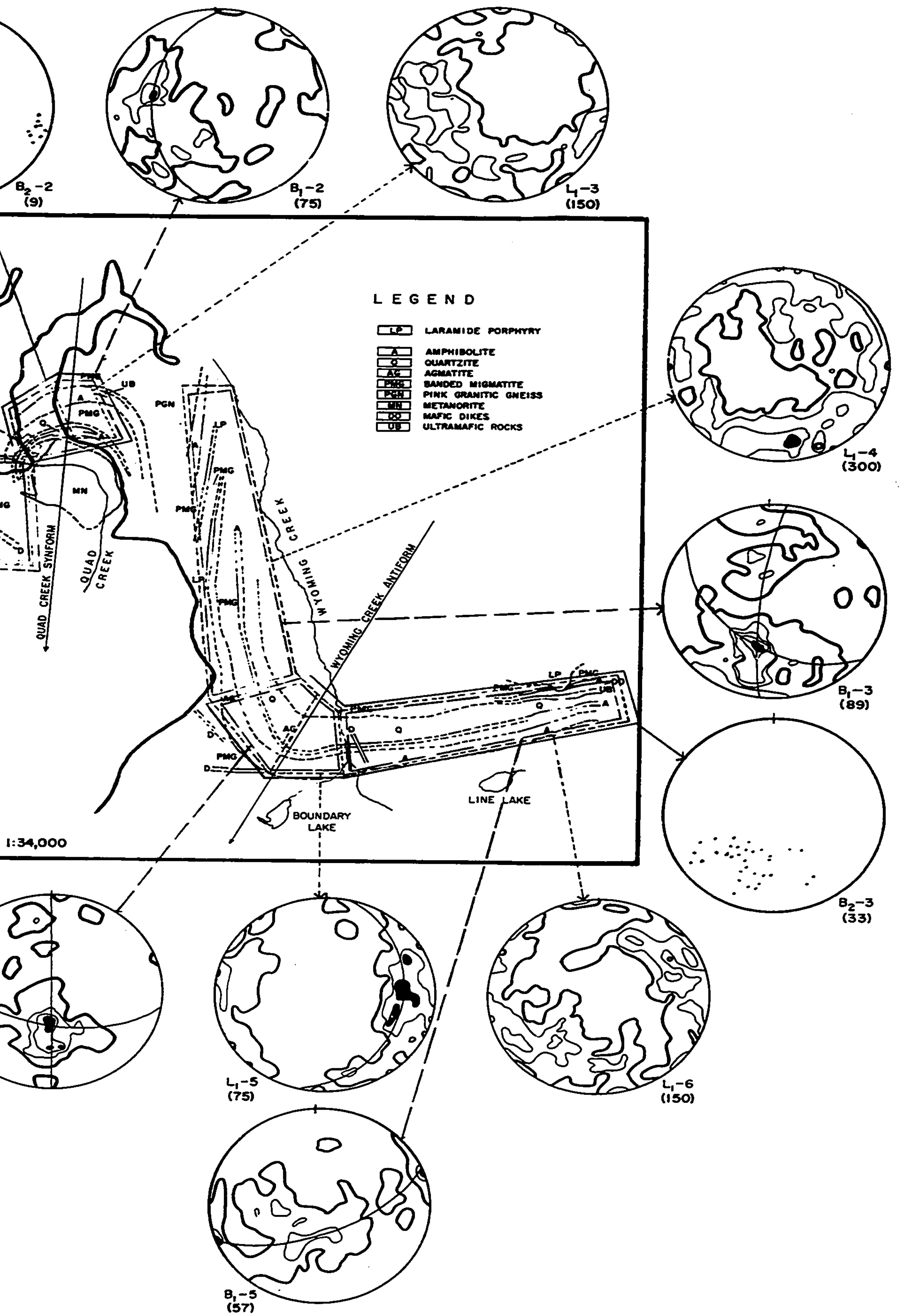

LEGEND
LP LARAMIDE PORPHYRY
A AMPHIBOLITE
Q QUARTZITE
AG AGMATITE
PMG BANDED MIGMATITE
PGN PINK GRANITIC GNEISS
MN METANORITE
DD MAFIC DIKES
UB ULTRAMAFIC ROCKS
QUAD CREEK SYNFORM
QUAD CREEK
WYOMING CREEK
WYOMING CREEK ANTIFORM
BOUNDARY LAKE
LINE LAKE
1:34,000
B_2-2 (9)
B_1-2 (75)
L_1-3 (150)
L_1-4 (300)
B_1-3 (89)
B_2-3 (33)
L_1-5 (75)
L_1-6 (150)
B_1-5 (57)

MAP 3b — LINEATIONS IN SUBAREAS.

L_1 Contours at 0.66 – 2.0 – 4.0 – 6.0 % in Subareas 1, 3, 6; 1–4–8 % in Subarea 5; 1–4–8–12 % in Subarea 2; 1–3–5–7 % in Subarea 4.

B_1 Contours at 1–4–8 % in Subarea 5; 1–4–8–12 % in Subareas 1, 2, 3, 4.

B_2 Uncontoured.

Numbers following lineation symbols are Subarea numbers.

Bracketed numbers are the number of measurements.

Boundary symbols:

L_1 -------

B_1 — — —

B_2 ———

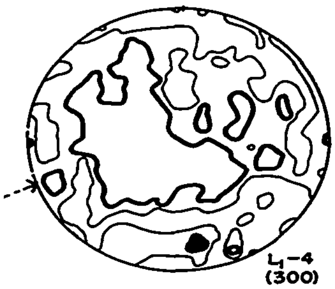

L_1–4
(300)

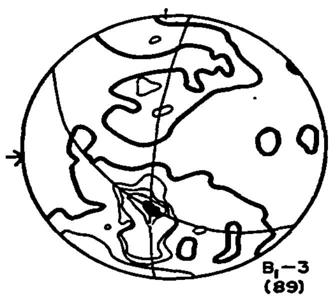

B_1–3
(89)

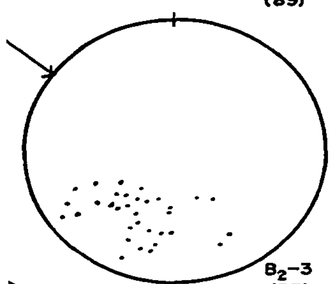

B_2–3
(33)

L_1–6
(150)